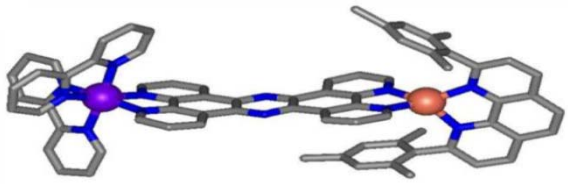

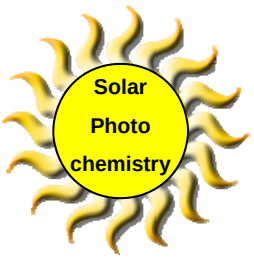

Marriott Washingtonian Center
Gaithersburg, Maryland June 6 - June 9, 2016

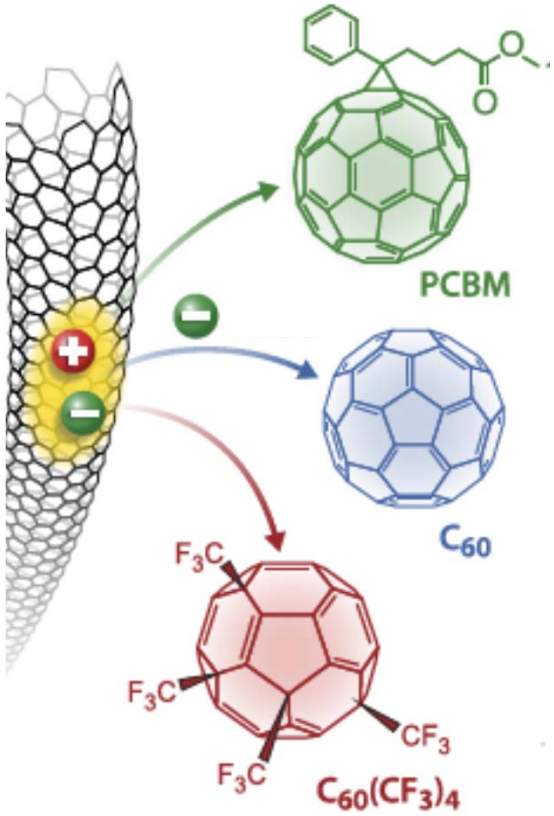

Proceedings of the

Thirty-Eighth DOE Solar Photochemistry P. I. Meeting

Sponsored by:

Chemical Sciences, Geosciences, and Biosciences Division
U.S. Department of Energy

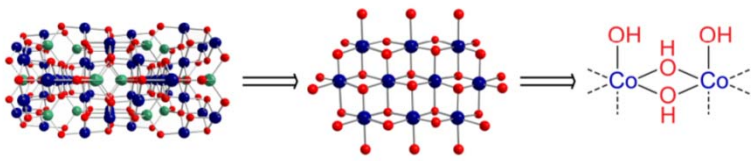

Program and Abstracts

Solar Photochemistry
P.I. Meeting

Marriott Washingtonian Center
Gaithersburg, Maryland
June 6-9, 2016

Chemical Sciences, Geosciences, and Biosciences Division
Office of Basic Energy Sciences
Office of Science
U.S. Department of Energy

Cover Graphics:
The cover figures are drawn from the abstracts of this meeting. One represents the crystal structure of a phenazine-linked bimetallic Ru(II)—Cu(I) chromophore for directional photoinduced electron transfer (Mulfort et al., p. 48). Another depicts the influence of driving force and reorganization energy on interfacial exciton dissociation in SWCNT/fullerene heterojunctions (Blackburn et al., p. 51). A third shows the dicobalt edge site in the dimensionally reduced active site of Co_3O_4 and Co-OEC. (Nocera et al. p. 150).

FOREWORD

The 38th Department of Energy Solar Photochemistry P.I. Meeting, sponsored by the Chemical Sciences, Geosciences, and Biosciences Division of the Office of Basic Energy Sciences, is being held June 6-9, 2016 at the Marriott Washingtonian Center in Gaithersburg, Maryland. These proceedings include the meeting agenda, abstracts of the formal presentations, posters of the conference, and an address list for the participants.

This Conference is the annual meeting of the grantees who perform research in solar photochemical energy conversion with the support of the Chemical Sciences, Geosciences, and Biosciences Division. This gathering is intended to enable the exchange of new ideas and research concepts between attendees and to further the collaboration and cooperation required for progress in such a difficult field.

Our special guest speaker this year for the opening session is Professor James Durrant of Imperial College in London, United Kingdom. He will discuss problems in charge carrier dynamics in polymer/fullerene blends in organic solar cells and in organohalide lead perovskite based devices, as well as in other systems for solar driven fuel synthesis. In addition, as part of the Solar Photochemistry's trajectory in **Supra Photosynthesis**, the program features two invited speakers from our sibling BES Program in Physical Biosciences. They will give presentations on model biochemical structures and reactions beyond the primary photo-driven electron transfer chain in the thylakoid membrane. Professor Cheryl Kerfeld of the Michigan State University Plant Research Laboratory will lecture on the dissociation of the complexity of photosynthetic processes into semi-autonomous functional modules. Professor Russ Hille will talk on unique air-stable enzymes for reduction reactions in the bio-transformation of energy-relevant, one carbon compounds.

We would like to express our appreciation to Diane Marceau of the Division of Chemical Sciences, Geosciences, and Biosciences, and Connie Lansdon of the Oak Ridge Institute of Science and Education for their assistance with the coordination of the logistics of this meeting. We must also thank all of the researchers whose enthusiasm, energy, and dedication to scientific inquiry have enabled these advances in solar photoconversion and made this meeting possible.

Mark T. Spitler
Chris Fecko
Chemical Sciences, Geosciences,
and Biosciences Division
Office of Basic Energy Sciences

Solar Photochemistry P.I. Meeting Overview

Time	Monday, June 6	Tuesday, June 7	Wednesday, June 8	Thursday, June 9	Time
7:30 AM		BREAKFAST	BREAKFAST	BREAKFAST	7:30 AM
7:45 AM		7:15 - 8:15	7:15 - 8:15	7:15 - 8:30	7:45 AM
8:00 AM					8:00 AM
8:15 AM					8:15 AM
8:30 AM		Session III	Session VI		8:30 AM
8:45 AM					8:45 AM
9:00 AM			Molecular Catalysis	*Session IX*	9:00 AM
9:15 AM		Interfacial behavior			9:15 AM
9:30 AM			*INVITED SPEAKER*	Heterogeneous	9:30 AM
9:45 AM		BREAK		Water Splitting	9:45 AM
10:00 AM		9:45 - 10:15	BREAK		10:00 AM
10:15 AM			10:00 - 10:30	BREAK	10:15 AM
10:30 AM		Session IV		10:15 - 10:45	10:30 AM
10:45 AM			Session VII		10:45 AM
11:00 AM				Session X	11:00 AM
11:15 AM		*Dye Redox Reactions*	*Inorganic Catalysis*	Photosystems	11:15 AM
11:30 AM			*of Water Splitting*	for Fuel Production	11:30 AM
11:45 AM					11:45 AM
12:00 PM				DOE Closing Comments	12:00 PM
12:15 PM		LUNCH	LUNCH		12:15 PM
12:30 PM		12:00 - 1:00	12:00 - 1:00		12:30 PM
12:45 PM					12:45 PM
1:00 PM					1:00 PM
1:15 PM					1:15 PM
1:30 PM					1:30 PM
1:45 PM		Open time	Open time		1:45 PM
2:00 PM		1:00 - 4:00	1:00 - 4:00		2:00 PM
2:15 PM					2:15 PM
2:30 PM					2:30 PM
2:45 PM					2:45 PM
3:00 PM					3:00 PM
3:15 PM	Registration				3:15 PM
3:30 PM	3:00 - 6:00 PM				3:30 PM
3:45 PM					3:45 PM
4:00 PM					4:00 PM
4:15 PM		Session V	*Session VIII*		4:15 PM
4:30 PM					4:30 PM
4:45 PM	Session I	Natural and Biomimetic	*Far From Equilibrium*		4:45 PM
5:00 PM		Energy transduction			5:00 PM
5:15 PM	Opening Session				5:15 PM
5:30 PM		*INVITED SPEAKER*			5:30 PM
5:45 PM	*INVITED SPEAKER*				5:45 PM
6:00 PM					6:00 PM
6:15 PM		DINNER			6:15 PM
6:30 PM	DINNER	5:45 - 7:30	DINNER		6:30 PM
6:45 PM	6:00 - 7:30	(on the town)	6:00 - 7:30		6:45 PM
7:00 PM					7:00 PM
7:15 PM					7:15 PM
7:30 PM					7:30 PM
7:45 PM	Session II				7:45 PM
8:00 PM		POSTERS	POSTERS		8:00 PM
8:15 PM	Photoelectrochemistry	odd numbers	even numbers		8:15 PM
8:30 PM					8:30 PM
8:45 PM					8:45 PM
9:00 PM					9:00 PM
9:15 PM	No-Host Reception				9:15 PM
9:30 PM	9:00 - 10:00	7:30 - 10:00	7:30 - 10:00		9:30 PM
9:45 PM					9:45 PM

Table of Contents

TABLE OF CONTENTS

Foreword iii

Overview iv

Program xvii

Abstracts of Oral Presentations

Session I – Opening Session

Charge Carrier Dynamics for Solar Energy Conversion
James R Durrant, Imperial College, U.K. 3

Session II – Photoelectrochemistry

Liquid Junction Perovskite Solar Cells and Charge Carrier Transport in Metal Oxides
Allen J. Bard and C. Buddie Mullins, University of Texas 5

Electrochemical Synthesis of Polycrystalline Semiconductor Electrodes with Optimum Compositions and Morphologies for Use in Solar Fuel Production
Kyoung-Shin Choi, University of Wisconsin-Madison 11

Photoelectrochemical hydrogen production: Catalysis, Stability and MEG
Jing Gu, Yong Yan, Jeffery A. Aguiar, Suzanne Ferrere, K. Xerxes Steirer, Chuanxiao Xiao, James L. Young, Boris D. Chernomordik, Andrew Norman, Gregory Pach, Ryan Crisp, Nathan R. Neale, Matthew C. Beard and **John A. Turner**, National Renewable Energy Laboratory 14

Session III –Interfacial Behavior

Semiconductor Interfacial Carrier Dynamics by Time-Resolving the Internal Electric Field and Observation of Hot-Phonon Bottleneck using Transient Absorption Spectroscopy
Ye Yang, Jing Gu, Elisa M. Miller, Kai Zhu, Joseph M. Luther, Nathan R. Neale, Jao van de Lagemaat, John A. Turner, **Matthew C. Beard**
National Renewable Energy Laboratory 19

Electron Transfer Processes in Catalyzed Photoelectrodes for Solar Water Splitting
Shannon Boettcher, Mike Nellist, Forest Laskowski, Teddy Huang, Fuding Lin, T.J. Mills, University of Oregon 23

Molecular and Structural Probes of Defect States in Quantum Dots for Solar Photoconversion
Robert J. Stewart, Adam Rimshaw, Christopher Grieco, Grayson Doucette, and **John B. Asbury**, The Pennsylvania State University 26

Session IV – Dye Redox Reactions in the Excited State

Oxomanganese Catalysts for Solar Fuel Production
Gary W. Brudvig, **Victor S. Batista**, Robert H. Crabtree and Charles A. Schmuttenmaer, Yale University, ... 31

Model Dyes for the Study of Molecule/Metal Oxide Semiconductor Interfaces and Electron Transfer Processes
E. Galoppini, R. A. Bartynski, L. Gundlach, A. Batarseh, H. Fan, S. Rangan, J. Nieto-Pescador, B. Abraham, Rutgers University-Newark 36

Electron Transfer and Transport by Delocalized Charges
T. Mani, M.J. Bird, A.R. Cook, L. Zaikowski, R. Holroyd, M.D. Newton, D.C. Grills, J. Bakalis, G. Mauro, X. Li., G. Rumbles, J. Blackburn, O.G. Reid and **J.R. Miller**, Brookhaven National Laboratory 39

Session V – Natural and Biomimetic Energy Transduction

Fundamental Studies and Engineering of Biological Modules Involved in Photosynthetic Energy Capture and Conversion
Cheryl A. Kerfeld, MSU-DOE Plant Research Laboratory, Michigan State University 45

Modular Homogeneous and Framework Photocatalyst Assemblies
Karen L. Mulfort, Oleg G. Poluektov, Lin X. Chen, Lisa M. Utschig, David M. Tiede Argonne National Laboratory 48

Long-Lived Charge Generation in Semiconducting Single-Walled Carbon Nanotubes
Jeff Blackburn, Rachelle Ihly, Andrew Ferguson, Obadiah Reid, Anne-Marie Dowgiallo, Kevin Mistry, Jaehong Park, Tyler Clikeman, Bryon Larson, Olga Boltalina, Steven Strauss, Philip Schulz, Joseph Berry, Justin Johnson, Garry Rumbles, National Renewable Energy Laboratory 51

Session VI – Molecular Catalysis – Natural and Not

A Tale of Two Enzymes: CO Dehydrogenase and Formate Dehydrogenase
Stephanie Dingwall, Jarett Wilcoxen, Dimitri Niks and **Russ Hille**, University of California, Riverside 57

Formation and Reactivity of Hydride Donors in Water
Dmitry E. Polyansky, Javier Concepcion, David Grills, Etsuko Fujita and James T. Muckerman, Brookhaven National Laboratory 59

The Development of Polypyridine Transition Metal Complexes as Homogeneous Catalysts for Water Decomposition
Ruifa Zong, Lars Kohler, Lianpeng Tong, Lanka Wickramasinghe, Debashis Basu, Husain Kagalwala, Andrew Kopecky, Rongwei Zhou, and **Randolph Thummel,** University of Houston 63

Session VII – Inorganic Catalysis of Water Splitting

Making the O-O Bond in Water Oxidation Catalysis: Single-Site vs O-O Coupling
David W. Shaffer, Yan Xie, Gerald F. Manbeck, David J. Szalda, **Javier J. Concepcion**, Brookhaven National Laboratory 69

Spectroscopic Analysis of Ru-Based Catalysts under Water Oxidizing Conditions **Yulia Pushkar**, Purdue University 72

Resolving Structures In-Situ for Solar-Driven Water-Oxidation Catalysts Using High Energy X-ray Scattering
David M. Tiede, Gihan Kwon, Alex B. F. Martinson, Karen L. Mulfort, Lisa M. Utschig, Oleg G. Poluektov, Lin X. Chen, Argonne National Laboratory 75

Session VIII – Far From Equilibrium

Understanding Roles of Ultrafast and Coherent Electronic and Atomic Motions in Photochemical Reactions
L. X. Chen, X. Li, R. D. Schaller, F. N. Castellano, K. L. Mulfort, M. A. Ratner, G. C. Schatz, T. Seideman, D. M. Tiede, et al.
Argonne National Laboratory, Northwestern University, University of Washington 81

Time-Domain Atomistic Studies of Far-from-Equilibrium Dynamics at Nanoscale Interfaces for Solar Energy Harvesting
Oleg V. Prezhdo, University of Southern California 84

Characterizing Singlet Fission in the Context of Exciton Migration and Dissociation
Justin Johnson, Dylan Arias, Natalie Pace, Joe Ryerson, Niels Damrauer, Garry Rumbles
National Renewable Energy Laboratory 89

Session IX – Heterogeneous Water Splitting

Modular Nanoscale and Biomimetic Systems for Photocatalytic Hydrogen Generation
Kara L. Bren, Richard Eisenberg, Todd D. Krauss, University of Rochester 95

Solar Energy-Driven Multi-Electron-Transfer Catalysts for Water Splitting: Robust and Carbon-Free Nano-Triads
Craig L. Hill, Tianquan Lian, Djamaladdin G. Musaev, Emory University 98

Observing Nanoscale Photochemical Charge Separation with Surface Photovoltage Spectroscopy
Frank Osterloh, University of California, Davis 102

Session X – Photosystems for Fuel Production

Components of an Artificial Photosynthetic Solar Fuel System
Devens Gust, Ana L. Moore, and Thomas A. Moore, Arizona State University 105

Nanostructured Photocatalytic Water Splitting Systems
Nicholas S. McCool, Nella M. Vargas-Barbosa, Timothy P. Saunders, Pengtao Xu, Tyler J. Milstein, Yuguang C. Li, Christopher Gray, Zhifei Yan, and **Thomas E. Mallouk,** Pennsylvania State University 109

Poster Abstracts (by poster number)

1. Excess Electron and Holes in Aliphatic Room Temperature Ionic Liquids
Francesc Molins, Domenech, Andrew T. Healy, Meghan Knutzon and David A. Blank 115

2. Carbon Dioxide Reduction to Organics in an Aqueous Photoelectrochemical Environment
James E. Park, Tao Zhang, Jessica J. Frick, Jason W. Krizan, Yuan Hu, Yong Yan, Jing Gu, Michael T. Kelly, Robert J. Cava and Andrew B. Bocarsly 116

3. Fundamental Studies of Energy- and Hole/Electron Transfer in Hydroporphyrin Architectures
David F. Bocian, Dewey Holten, Christine Kirmaier and Jonathan S. Lindsey 117

4. Extending Excited State Lifetimes in Cu(I) MLCT Excited States for Photochemical Upconversion
Catherine E. McCusker, Peter D. Crapps, and Felix N. Castellano 118

5. Can Cd chalcogenide clusters be covalently connected with other electron acceptor nanoparticles? And the relation between structure and electron dynamics in a series of substitutionally doped TiO and Cd-chalcogenide clusters
Philip Coppens, Yang Chen, Krishnayan Basuroy and Luis Velarde. 119

6. Twisted Amides and their Relevance to Linker Design for Solar Applications
Robert H. Crabtree, Subhajyoti Chaudhuri, Brandon Q. Mercado, Victor S. Batista, Charles A. Schmuttenmaer and Gary W. Brudvig 120

7. Linear Free Energy Relationships in the Proton Transfer Steps Underpinning H_2 Evolution
Jillian L. Dempsey, Noémie Elgrishi, Daniel J. Martin, Brian D. McCarthy, and Eric S. Rountree 121

8. Two-Dimensional Electronic-Vibrational Spectroscopy of Light Harvesting Complexes
NHC Lewis, T.A.A. Oliver, N. Gruenke, Roberto Bassi, M. Ballattori and Graham R. Fleming 122

9. Probing the Nature of Trap States Controlling Electron Diffusion in Nanostructured Films
Peter T. Erslev, Julio Villanueva-Cab, Song-Rim Jang, Kai Zhu, and Arthur J. Frank 123

10. Charge Transport Across Molecular Wires embedded in Ultrathin Silica Separation Membrane
Eran Edri, Dirk Guldi, and Heinz Frei 124

11. Do Bases in the Second Coordination Sphere Aid CO_2 Reduction?
Etsuko Fujita, Mehmed Z. Ertem and James T. Muckerman 125

12. Photoelectrochemical, Photophysical and Binding Studies of Chromophore-Linker-Anchor Compounds: the Influence of Interfacial Dipoles
E. Galoppini, R. A. Bartynski, L. Gundlach, J. Rochforde, A. Batarseh, H. Fan S. Rangan, J. Nieto-Pescador, and B. Abrahamd, K. Ngo 126

13. Controlling Pathways of CO_2 Reduction with Manganese Precatalysts: Electrochemical and Transient Spectroscopic Investigations
David C. Grills 127

14. Ultrafast Microscopy of Methylammonium Lead Iodide Perovskite Thin-Films: Heterogeneity of Excited State Spatial and Temporal Evolution
Andrew H. Hill, Eric S. Massaro, Kori E. Smyser, and Erik M. Grumstrup 128

15. Photoanode Energetics and Rate Limiting Processes in Dye-Sensitized Solar Cells with Cobalt-Based Redox Shuttles
Josh Baillargeon, Dhritabrata Mandal, Yuling Xie, and Thomas W. Hamann 129

16. Understanding and Controlling Light Harvesting, Energy Transport, and Charge Transport within Chromophoric, Metal-Organic Framework based Electrode Films
Joseph T. Hupp 130

17. Optical Inhomogeneity from 2D Spectra vs. TEM Size Dispersion in PbSe Nanocrystals
Samuel D. Park, Dmitry Baranov, Jisu Ryu, and David M. Jonas 131

18. Bandgap Versus Sub-Bandgap Excitations in Cu-Deficient $CuInS_2$ Quantum Dots
Danilo H. Jara, Kevin G. Stamplecoskie, and Prashant V. Kamat 132

19. Hot Hole Photochemistry of CdSe Quantum Dots
Youhong Zeng, Ke Gong and David F. Kelley 133

20. Establishing the Role of the Electrode Surface in Solar-Driven Pyridine-Catalyzed CO_2 Reduction
Coleman X. Kronawitter, Peng Zhao, Zhu Chen, and Bruce E. Koel 134

21. The Fate of Excitons in Single Walled Carbon Nanotubes
Amanda Amori, Zhentao Hou, Nicole M. B. Cogan, and Todd D. Krauss 135

22. Dynamics of the Injection and Transport of Electrons in DNA
Frederick D. Lewis 136

23. Efficient Hot Electron Transer by a Plasmon Induced Interfacial Charge Transfer Transition in CdSe-Au Nanorod Heterostructures
Kaifeng Wu, Jinquan Chen, James B McBride and Tianquan Lian 137

24. Electron/Hole Selectivity in Organic Semiconductors for Solar Energy Conversion
Chris Weber, Colin Bradley, D. Westley Miller, and Mark C. Lonergan 138

25. Gains and Losses in PbS Quantum Dot Solar Cells with Submicron Periodic Grating Structures
Yukihiro Hara, Abay Gadisa, Yulan Fu, Timothy Garvey, Kristina T. Vrouwenvelder, Chris W. Miller, Jillian L. Dempsey, and Rene Lopez 139

26. Preparation of High Surface Area p-GaP Photocathodes and Covalent Attachment of Dyes on p-GaP(111)A: Towards a High Efficiency Sensitized Photocathode
Stephen Maldonado 140

27. Stiff and Soft Solvent Environments Result in Anomalous Dynamics in Ionic Liquids and Conventional Solvent Mixtures
J. C. Araque, J. Hettige, S. K. Yadav, M. Shadeck, M. Maroncelli, and C. J. Margulis 141

28. Synthesis and Spectroscopy of Transition Metal-based Chromophores: Tailoring First-row Photophysics for Applications in Solar Energy Conversion
Monica Carey, Jonathan Yarranton, Sara Adelman, and James K. McCusker 142

29. Electron Transfer Dynamics in Efficient Molecular Solar Cells
Ryan M. O'Donnell, Tim Barr, Brian DiMarco and Gerald J. Meyer 143

30. Self-Assembled Molecular p/n Junctions on Mesoporous nano ITO Electrodes
Byron H. Farnum, Kyung-Ryang Wee, Bing Shan, and Thomas J. Meyer 144

31. Singlet Fission
Josef Michl, Thomas F. Magnera, Paul I. Dron, Eric A. Buchanan, Jin Wen, and Zdeněk Havlas 145

32. Molecular Photoelectrocatalysts for Hydrogen Evolution
Matthew B. Chambers, Catherine L. Pitman, and Alexander J. M. Miller 146

33. Toward Photochemical Water Oxidation in Metal Organic Frameworks
Maza, William A, Lin, Shaoyang, Ahrenholtz, S.R.; Zhu, J., Usov, P.,
and Morris, A.J. 147

34. Photocatalytic Water Oxidation at the Semiconductor-Aqueous Interface and Beyond…
James T. Muckerman 148

35. Unified Treatment of Electron Transfer Energetics and Coupling in Terms of Electron Detachment and Attachment
Marshall D. Newton 149

36. Unifying Heterogeneous and Homogeneous OER and ORR Catalysis
Casey Brodsky, Andrew M. Ullman and Daniel G. Nocera 150

37. Design Principles for Colloidal Semiconductor Nanocrystals through Surface Chemistry Modification
Daniel M. Kroupa, Márton Vörös, Elisa M. Miller, Brett McNichols, Nicholas Brawand, Greg Pach, Alan Sellinger, Giulia Galli, Arthur J. Nozik,
and Matthew C. Beard 151

38. Photosensitization of Natural and Synthetic SnO_2 and ZnO Crystals with Dyes and Quantum Dots
Laurie A. King, Qian Yang, Michael L. Grossett, Zbigniew Galazka, Reinhard Uecker
and B. A. Parkinson 152

39. Electronic Structure of Charge Separated States in Organic Bulk-Heterojunctions: A Combined EPR and DFT Study
Oleg G. Poluektov, Jens Niklas, Lisa M. Utschig, Karen L. Mulfort, David M. Tiede
and Kristy L. Mardis 153

40. Interfacial Processes at H_2O/III-V Semiconductor Surfaces under Operando Conditions
Xueqiang Zhang and Sylwia Ptasinska 154

41. Effect of Carrier Delocalization on Long-lived Free Carriers in Conjugated Polymers and Single-Walled Carbon Nanotubes
Garry Rumbles, Natalie Pace, Jessica Ramirez, Jaehong Park, Rachelle Ihly, Jeff Blackburn Jesse Bergkamp, Devens Gust, and Obadiah Reid 155

42. Studying Carrier Dynamics and Solar Energy Conversion using THz Spectroscopy
Charles A. Schmuttenmaer, Kevin P. Regan, Coleen T. Nemes, Christopher Koenigsmann, Victor S. Batista, Robert H. Crabtree, and Gary W. Brudvig 156

43. Ultrafast Photo-Induced Electron Transfer Seen via Vibrationally Coherent Wavepackets
Shahnawaz Rafiq, Marius Koch, Gregory D. Scholes 157

44. A Multi-Functional Biphasic Water Splitting Catalyst Tailored for Integration with High Performance Semiconductor Photoanodes
Jinhui Yang, Adam Schwartzberg, Francesca M. Toma, Jason K. Cooper,
Marco Favaro, Ethan Crumlin, Christian Kisielowski, and Ian D. Sharp 158

45. The Synthesis and Chemistry of Molybdenum Complexes that Contain a Trianionic Calix[6]azacryptand Ligand Derived from 1,3,5-Trismethoxy-Calix[6]arene
Richard R. Schrock and Lasantha A. Wickramasinghe 159

46. Photo-Induced Hole and Electron Transfer Reactions in Well-Defined Nanoscale Objects that Feature Electronically Homogeneous Single-Walled Carbon Nanotubes Wrapped by Redox Active Polymers
Jean-Hubert Olivier, Jaehong Park, Mary Glesner, Yusong Bai
and Michael J. Therien 160

47. Photocatalysts for H_2 Evolution: Combination of the Light Absorbing Unit and Catalytic Center in a Single Molecule
Travis A. White, Suzanne E. Witt, Tyler J. Whittemore, Ryan P. Coll, Kim R. Dunbar,
and Claudia Turro 161

48. Size Dependence of the Band Energetics of Coupled PbS Quantum Dot Films
Elisa M. Miller, Daniel M. Kroupa, Jianbing Zhang, Philip Schulz, Ashley R. Marshall,
Antoine Kahn, Stephan Lany, Joseph M. Luther, Matthew C. Beard, Craig L. Perkins,
and Jao van de Lagemaat 162

49. A Concerted Synthetic, Spectroscopic, and Computational Approach towards Water Splitting by Homo- and Hetero-Metallic Complexes
Claudio Verani, H. Bernhard Schlegel, and John Endicott 163

50. Enabling Singlet Fission by Controlling Intramolecular Charge Transfer
E. A. Margulies, C. E. Miller, Y. Wu, L. Ma, G. C. Schatz, R. M. Young,
and M. R. Wasielewski 164

51. Photoinduced Radical Generation, Cage Escape and Recombination in Ionic Liquids
James F. Wishart and Koji Osawa 165

52. Building a Toolbox of Singlet Fission Molecules for Solar Energy Conversion
Xiaoyang Zhu, and Colin Nuckolls 166

53. Chemical Control Over the Electrical Properties of GaAs and Group VI Dichalcogenide Semiconductor Surfaces and Photoelectrodes
Fan Yang, Joshua D. Wiensch, Ellen Yan and Nathan S. Lewis 167

54. Organic Macromolecular Materials for Long-Range and Efficient Transport Properties in Light Energy Conversion Applications
Goodson III, T. 169

LIST OF PARTICIPANTS 173

P.I. AUTHOR INDEX 183

Program

38th DOE SOLAR PHOTOCHEMISTRY
P.I. MEETING

June 6-9, 2016

Washingtonian Marriott Center
Gaithersburg, MD

PROGRAM

Monday, June 6

3:00 – 6:00 p.m. Registration

Monday Afternoon, June 6

SESSION I
Opening Session
Mark T. Spitler, Chair

4:30 p.m. Opening Remarks
Gail McLean and **Mark Spitler**, Department of Energy

5:00 p.m. **Opening Lecture**.
Charge Carrier Dynamics for Solar Energy Conversion
James R Durrant, Imperial College, U.K**.**

6:00 p.m. Dinner

Monday Evening, June 6

SESSION II
Photoelectrochemistry
Stephen Maldonado, Chair

7:30 p.m. Liquid Junction Perovskite Solar Cells and Charge Carrier Transport in Metal Oxides
Allen J. Bard, **Buddie Mullins**, University of Texas

8:00 p.m. Electrochemical Synthesis of Polycrystalline Semiconductor Electrodes with Optimum Compositions and Morphologies for Use in Solar Fuel Production
Kyoung-Shin Choi, University of Wisconsin-Madison

8:30 p.m. Photoelectrochemical Hydrogen Production: Catalysis, Stability and MEG
John A. Turner, National Renewable Energy Laboratory

9:00 p.m. No Host Reception

Tuesday Morning, June 7

7:15 a.m. Continental Breakfast

SESSION III
Interfacial Behavior
David Kelley, Chair

8:15 a.m. Semiconductor Interfacial Carrier Dynamics by Time-Resolving the Internal Electric Field and Observation of Hot-Phonon Bottleneck using Transient Absorption Spectroscopy
Matthew C. Beard, National Renewable Energy Laboratory

8:45 a.m. Electron Transfer Processes in Catalyzed Photoelectrodes for Solar Water Splitting
Shannon Boettcher, University of Oregon

9:15 a.m. Molecular and Structural Probes of Defect States in Quantum Dots for Solar Photoconversion
John B. Asbury, Pennsylvania State University

9:45 – 10:15 a.m. Break

SESSION IV
Dye Redox Reactions in the Excited State
Gerald Meyer, Chair

10:15 a.m. Oxomanganese Catalysts for Solar Fuel Production
Gary W. Brudvig, **Victor S. Batista**, Yale University

11:00 a.m. Model Dyes for the Study of Molecule/Metal Oxide Semiconductor Interfaces and Electron Transfer Processes
E. Galoppini, Rutgers University-Newark

11:30 a.m. Electron Transfer and Transport by Delocalized Charges
J.R. Miller, Brookhaven National Laboratory

12:00 p.m. Lunch

Tuesday Afternoon, June 7

SESSION V
Natural and Biomimetic Energy Transduction
Christine Kirmaier, Chair

4:00 p.m. Fundamental Studies and Engineering of Biological Modules Involved in Photosynthetic Energy Capture and Conversion
Cheryl A. Kerfeld, MSU-DOE Plant Research Laboratory, Michigan State University

4:45 p.m. Modular Homogeneous and Framework Photocatalyst Assemblies
Karen L. Mulfort, Argonne National Laboratory

5:15 p.m. Long-Lived Charge Generation in Semiconducting Single-Walled Carbon Nanotubes
Jeff Blackburn, National Renewable Energy Laboratory

Tuesday Evening, June 7

5:45 – 7:30 p.m. Dinner (on the Town)

7:30-10:00 p.m. Posters (Odd numbers)

Wednesday Morning, June 8

7:15 a.m. Continental Breakfast

SESSION VI
Molecular Photocatalysis – Natural and Not
Michael Wasielewski, Chair

8:15 a.m. A Tale of Two Enzymes: CO Dehydrogenase and Formate Dehydrogenase
Russ Hille, University of California, Riverside

9:00 a.m. Formation and Reactivity of Hydride Donors in Water

Dmitry E. Polyansky, Brookhaven National Laboratory

9:30 a.m. The Development of Polypyridine Transition Metal Complexes as Homogeneous Catalysts for Water Decomposition
Randolph Thummel, University of Houston

10:00 – 10:30 a.m. Break

SESSION VII
Inorganic Catalysis of Water Splitting
Claudio Verani, Chair

10:30 a.m. Making the O-O Bond in Water Oxidation Catalysis: Single-Site vs O-O Coupling
Javier J. Concepcion, Brookhaven National Laboratory

11:00 a.m. Spectroscopic Analysis of Ru-Based Catalysts under Water Oxidizing Conditions
Yulia Pushkar, Purdue University

11:30 a.m. Resolving Structures In-Situ for Solar-Driven Water-Oxidation Catalysts Using High Energy X-ray Scattering
David M. Tiede, Argonne National Laboratory

12:00 p.m. Lunch

Wednesday Afternoon, June 8

Session VIII
Far From Equilibrium
Michael Therien, Chair

4:00 p.m. Understanding Roles of Ultrafast and Coherent Electronic and Atomic Motions in Photochemical Reactions
L. X. Chen, **X. Li**, **R. D. Schaller**, Argonne National Laboratory, Northwestern University, University of Washington

4:45 p.m. Time-Domain Atomistic Studies of Far-from-Equilibrium Dynamics at Nanoscale Interfaces for Solar Energy Harvesting
Oleg V. Prezhdo, University of Southern California

5:15 p.m. Characterizing Singlet Fission in the Context of Exciton Migration and Dissociation
Justin Johnson, National Renewable Energy Laboratory

Wednesday Evening, June 8

6:00 p.m. Dinner

7:30-10:00 p.m. Posters (Even numbers)

Thursday Morning, June 9

7:15 a.m. Continental Breakfast

Session IX
Heterogeneous Water Splitting
Amanda Morris, Chair

8:30 a.m. Modular Nanoscale and Biomimetic Systems for Photocatalytic Hydrogen Generation
Kara L. Bren, **Richard Eisenberg**, **Todd D. Krauss**, University of Rochester

9:15 a.m. Solar Energy-Driven Multi-Electron-Transfer Catalysts for Water Splitting: Robust and Carbon-Free Nano-Triads
Craig L. Hill, **Tianquan Lian**, **Djamaladdin G. Musaev**, Emory University

10:00 a.m. Observing Nanoscale Photochemical Charge Separation with Surface Photovoltage Spectroscopy
Frank Osterloh, University of California, Davis

10:15 – 10:45 a.m. Break

Session X
Photosystems for Fuel Production
Bruce Parkinson, Chair

10:45 a.m. Components of an Artificial Photosynthetic Solar Fuel System

Devens Gust, **Ana L. Moore**, **and Thomas A. Moore**, Arizona State University

11:30 a.m. Nanostructured Photocatalytic Water Splitting Systems
Thomas E. Mallouk, Pennsylvania State University

12:00 p.m. Closing Remarks
Mark Spitler, U.S. Department of Energy

Session I

Opening Session

Charge carrier dynamics for solar energy conversion

James R Durrant

Department of Chemistry, Imperial College London, London SW7 2AZ, U.K.
and SPECIFIC IKC, College of Engineering, University of Swansea, Swansea, U.K.
Email: j.durrant@imperial.ac.uk

The development of low cost, stable and efficient materials for solar energy conversion is a key scientific challenge for addressing global sustainability and energy supply. My talk will address focus on the charge carrier dynamics which play a key role in determining the efficiency of many of the developing solar energy technologies. I will focus materials and devices relevant to two solar cell technologies – organic solar cells based on polymer / fullerene blends and organohallide lead perovskite based devices, as well as a range of metal oxide nanoparticles and photoelectodes for solar driven fuel synthesis. In my talk, I will also draw upon lessons we can learn from our understanding of the processes of charge separation and utilization in natural photosynthesis.

For organic solar cells, I focus on the processes of photoinduced charge separation and recombination between donor polymers and acceptor small molecules, and how these processes can be controlled through materials design, and their impact upon device performance.[1,2] These studies will be extended to perovskite solar cells, addressing in particular the role of material energetics in determining cell voltage. For the metal oxides, I will address the timescales of charge separation and recombination, and in particular the kinetics of water splitting into molecular hydrogen and oxygen at the metal oxide / electrolyte interface.[3,4] Parallels will be made with alternative photocatalytic systems, including dye sensitized approaches, the use of molecular catalysts and 2-D nanostructures. A particular focus will be on the timescales and reaction orders for the processes of water oxidation and reduction, and the extent to which metal oxides surfaces can catalysis this multi-electron redox chemistry.[5]

1. Dimitrov, S. D., and Durrant, J. R. (2014) Materials Design Considerations for Charge Generation in Organic Solar Cells, Chemistry of Materials 26, 616-630.

2. Dimitrov, S. D., Wheeler, S., Niedzialek, D., Schroeder, B. C., Utzat, H., Frost, J. M., Yao, J. Z., Gillett, A., Tuladhar, P. S., McCulloch, I., Nelson, J., and Durrant, J. R. (2015) Polaron pair mediated triplet generation in polymer/fullerene blends, Nature Communications 6.

3. Barroso, M., Pendlebury, S. R., Cowan, A. J., and Durrant, J. R. (2013) Charge carrier trapping, recombination and transfer in hematite (alpha-Fe2O3) water splitting photoanodes, Chemical Science 4, 2724-2734.

4. Tachibana, Y., Vayssieres, L., and Durrant, J. R. (2012) Artificial photosynthesis for solar water-splitting, Nature Photonics 6, 511-518.

5. Le Formal, F., Pastor, E., Tilley, S. D., Mesa, C. A., Pendlebury, S. R., Gratzel, M., and Durrant, J. R. (2015) Rate Law Analysis of Water Oxidation on a Hematite Surface, Journal of the American Chemical Society 137, 6629-6637.

Session II

Photoelectrochemistry

Liquid Junction Perovskite Solar Cells and Charge Carrier Transport in Metal Oxides

Allen J. Bard and C. Buddie Mullins
Departments of Chemistry and Chemical Engineering
University of Texas at Austin
Austin, Texas 78712

Liquid Junction Perovskite Solar Cells

A liquid junction photoelectrochemical (PEC) solar cell based on p-type methylammonium lead iodide (p-$MeNH_3PbI_3$) perovskite with a large open-circuit voltage has been developed. $MeNH_3PbI_3$ perovskite is readily soluble or decomposed in many common solvents. However, the solvent dichloromethane (CH_2Cl_2) can be employed to form stable liquid junctions. These were characterized with photoelectrochemical cells with several redox couples, including I_3^-/I^-, Fc/Fc^+, $DMFc/DMFc^+$, and $BQ/BQ^{\bullet -}$ (where Fc is ferrocene, DMFc is decamethylferrocene, BQ is benzoquinone) in CH_2Cl_2. The solution-processed $MeNH_3PbI_3$ shows cathodic photocurrents and hence p-type behavior. The difference between the photocurrent onset potential and the standard potential for $BQ/BQ^{\bullet -}$ is 1.25 V, which is especially large for a semiconductor with a band gap of 1.55 eV. A PEC photovoltaic cell, with a configuration of p-$MeNH_3PbI_3/CH_2Cl_2$, BQ (2 mM), $BQ^{\bullet -}$ (2 mM)/carbon, shows an opencircuit photovoltage of 1.05 V and a short-circuit current density of 7.8 mA/cm^2 under 100 mW/cm^2 irradiation. The overall optical-to-electrical energy conversion efficiency is 6.1%. The PEC solar cell shows good stability for 5 h under irradiation.

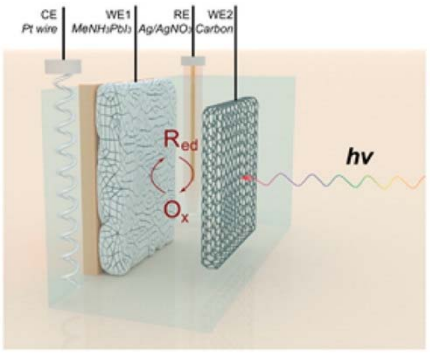

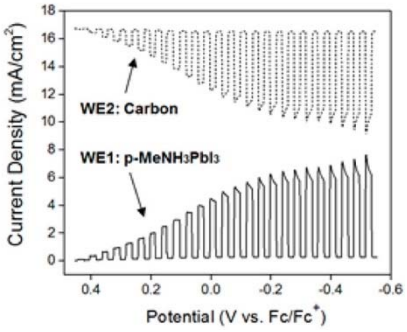

Additional details concerning this research can be found in *J. Am. Chem. Soc.* **137**, 14758–14764 (2015). http://dx.doi.org/10.1021/jacs.5b09758

Small-Polaron Transport in Metal Oxide Photoelectrodes

Transition-metal oxides are a promising class of semiconductors for the oxidation of water, a process that underpins both photoelectrochemical water splitting and electrochemical carbon dioxide reduction. However, these materials are limited by very slow charge transport. This is because, unlike conventional semiconductors, material aspects of metal oxides favor the formation of slow moving, self-trapped charge carriers: small polarons. We have conducted a few studies seeking to understand the salient features of small-polaron transport in metal oxides, so that we can offer guidelines for their experimental characterization. In particular we have examined two prototypical oxide photoanodes: tungsten-doped monoclinic bismuth vanadate ($W:BiVO_4$) and titanium-doped hematite ($Si:\alpha-Fe_2O_3$). Analysis shows conduction in both materials is well described by the adiabatic small-polaron model, with electron drift mobility (distinct from the Hall mobility) values on the order of 10^{-4} and 10^{-2} $cm^2\ V^{-1}\ s^{-1}$ respectively. Future directions to build a

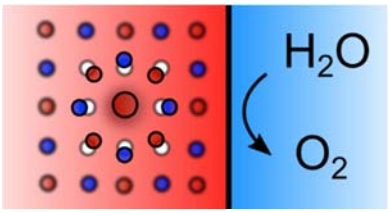

full picture of charge transport in this family of materials have been seriously considered. A more complete description of the points brought up in this paragraph can be found in *J. Phys. Chem. Lett.* **7**, 471-479 (2016): http://dx.doi.org/10.1021/acs.jpclett.5b02143.

Small-Polaron Hopping in W:BiVO$_4$: DC electrical conductivity, Seebeck and Hall coefficients are measured between 300 and 450K on single crystals of monoclinic bismuth vanadate that are doped n-type with 0.3% tungsten donors (W:BiVO4). Strongly activated small-polaron hopping is implied by the activation energies of the Arrhenius conductivities (about 300 meV) greatly exceeding the energies characterizing the falls of the Seebeck coefficients' magnitudes with increasing temperature (about 50meV). Small-polaron hopping is further evidenced by the measured Hall mobility in the ab-plane (10^{-1}cm^{2}V^{-1} s^{-1} at 300K) being larger and much less strongly activated than the deduced drift mobility (about 5×10^{-5}cm^{2}V^{-1} s^{-1} at 300K). The conductivity and n-type Seebeck coefficient is found to be anisotropic with the conductivity larger and the Seebeck coefficient's magnitude smaller and less temperature dependent for motion within the ab-plane than that in the c-direction. These anisotropies are addressed by considering highly anisotropic next-nearest-neighbor (~5Å) transfers in addition to the somewhat shorter (~4 Å), nearly isotropic nearest-neighbor transfers. This study built upon earlier findings that we published: *J. Am. Chem.* Soc. **135**, 11389-11396 (2013). http://dx.doi.org/10.1021/ja405550k. A more complete description of the science discussed in this paragraph can be found in *Appl. Phys. Lett.* **106**, 022106 (2015): http://dx.doi/org/10.1063/1.4905786.

Transport Properties of Si:α-Fe$_2$O$_3$: We also studied the synthesis (via chemical vapor transport) and electronic properties of silicon-doped hematite (Si:α-Fe_2O_3) single crystals, with Si incorporation on the order of 10^{19} cm^{-3}. The conductivity, Seebeck and Hall effect were measured in the basal plane between 200 and 400 K. Distinct differences in electron transport were observed above and below the magnetic transition temperature of hematite at ~265 K (the Morin transition, T_M). Above 265 K, transport was found to agree with the adiabatic small-polaron model, the conductivity was characterized by an activation energy of ~100 meV and the Hall effect was dominated by the weak ferromagnetism of the material. A room temperature electron drift mobility of ~10^{-1} cm^{2}V^{-1} s^{-1} was estimated. Below T_M, the activation energy increased to ~160 meV and a conventional Hall coefficient could be determined. In this regime, the Hall coefficient was negative and the corresponding Hall mobility was temperature-independent with a value of ~10^{-1} cm^{2}V^{-1} s^{-1}. Seebeck coefficient measurements indicated that the silicon donors were fully ionized in the temperature range studied. Finally, we observed a broad infrared absorption upon doping and tentatively assign the feature at ~0.8 eV to photon-assisted small-polaron hops. Additional details regarding this work can be found in *J. Mater. Chem. C* **4**, 559-567 (2016): http://dx.doi.org/10.1039/C5TC03368C.

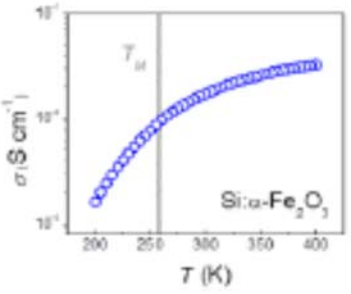

DOE Sponsored Publications 2013-2016 (Allen J. Bard and C. Buddie Mullins)

1. Son Hoang, Sean P. Berglund, Raymond R. Fullon, Ryan L. Minter, and C. Buddie Mullins, "Chemical bath deposition of vertically aligned TiO_2 nanoplatelet arrays for solar energy conversion applications," *J. Mater. Chem. A.* **1**, 4307-4315 (2013). http://dx.doi.org/10.1039/C3TA01384G

2. Sean P. Berglund, Heung Chan Lee, Paul D. Nunez, Allen J. Bard, and C. Buddie Mullins, "Screening of transition and post-transition metals to incorporate into copper oxide and copper bismuth oxide for photoelectrochemical hydrogen evolution," *Phys. Chem. Chem. Phys.* ***15****, 4554-4565 (2013).* http://dx.doi.org/10.1039/C3CP50540E

3. Son Hoang, Thong Q. Ngo, Sean P. Berglund, Raymond R. Fullon, John G. Ekerdt, and C. Buddie Mullins, "Improvement of solar energy conversion with Nb-incorporated TiO_2 hierarchical microspheres," *ChemPhysChem* **14**, 2270-2276 (2013). http://dx.doi.org/10.1002/cphc.201201092

4. Alexander J. E. Rettie, Heung-Chan Lee, Luke G. Marshall, Jung-Fu Lin, Cigdem Capan, Jeffrey Lindemuth, John S. McCloy, Jianshi Zhou, Allen J. Bard, and C. Buddie Mullins, "Combined charge carrier transport and photoelectrochemical characterization of $BiVO_4$ single crystals: Intrinsic behavior of a complex metal oxide," *J. Am. Chem. Soc*. **135**, 11389-11396 (2013). http://dx.doi.org/10.1021/ja405550k

5. Huichao He, Sean P. Berglund, Peng Xiao, William D. Chemelewski, Yunhuai Zhang, and C. Buddie Mullins, "Nanostructured Bi_2S_3/WO_3 heterojunction films exhibiting enhanced photoelectrochemical performance," *J. Mater. Chem. A.* **1**, 12826-12834 (2013). http://dx.doi.org/10.1039/C3TA13239K

6. Sean P. Berglund, Son Hoang, Ryan L. Minter, Raymond R. Fullon, and C. Buddie Mullins, "Investigation of 35 elements as single metal oxides, mixed metal oxides, or dopants for titanium dioxide for dye-sensitized solar cells," *J. Phys. Chem. C*. **117**, 25248-25258 (2013). http://dx.doi.org/10.1021/jp4073747

7. M. M. Najafpour, K. C. Leonard, F.-R. F. Fan, M. A. Tabrizi, A. J. Bard, C. K. King'ondu, S. L. Suib, B. Haghighia, S. I. Allakhverdiev "Nano-Size Layered Manganese–Calcium Oxide as an Efficient and Biomimetic Catalyst for Water Oxidation under Acidic Conditions: Comparable to Platinum" *Dalton Trans. 42,* 5085-5091 (2013). http://pubs.rsc.org/en/content/articlelanding/2013/dt/c3dt32864c#!divAbstract

8. C. Bhattacharya, H. C. Lee, A. J. Bard "Rapid Screening by Scanning Electrochemical Microscopy (SECM) of Dopants for Bi_2WO_6 Improved Photocatalytic Water Oxidation with Zn Doping" *J. Phys. Chem. C 117*, 9633−9640 (2013). http://pubs.acs.org/doi/abs/10.1021/jp308629q

9. H. S. Park, K. C. Leonard, A. J. Bard "Surface Interrogation Scanning Electrochemical Microscopy (SI-SECM) of Photoelectrochemistry at a W/Mo-$BiVO_4$ Semiconductor

Electrode: Quantification of Hydroxyl Radicals during Water Oxidation" *J. Phys. Chem. C 117*, 12093-12102 (2013). http://pubs.acs.org/doi/abs/10.1021/jp400478z

10. K. C. Leonard, K. M. Nam, H. C. Lee, S. H. Kang, H. S. Park, A. J. Bard "$ZnWO_4/WO_3$ Composite for Improving Photoelectrochemical Water Oxidation" *J. Phys. Chem. C 117*(31), 15901-15910 (2013). http://pubs.acs.org/doi/abs/10.1021/jp403506q

11. H. S. Park, H. C. Lee, K. C. Leonard, G. Liu, A. J. Bard "Unbiased Photoelectrochemical Water Splitting in Z-Scheme Device Using W/Mo-Doped $BiVO_4$ and $Zn_xCd_{1-x}Se$" *ChemPhysChem 14*(10), 2277-2287 (2013). http://onlinelibrary.wiley.com/doi/10.1002/cphc.201201044/abstract

12. K. M. Nam, H. S. Park, H. C. Lee, B. H. Meekins, K. C. Leonard, A. J. Bard "Compositional Screening of the Pb-Bi-Mo-O System. Spontaneous Formation of a Composite of p-$PbMoO_4$ and n-Bi_2O_3 with Improved Photoelectrochemical Efficiency and Stability" *J. Phys. Chem. Lett. 4*(16), 2707-2710 (2013). http://pubs.acs.org/doi/abs/10.1021/jz401334k

13. S. K. Cho, H. S. Park, H. C. Lee, K. M. Nam, A. J. Bard "Metal Doping of $BiVO_4$ by Composite Electrodeposition with Improved Photoelectrochemical Water Oxidation" *J. Phys. Chem. C 117*, 23048-23056 (2013). http://pubs.acs.org/doi/abs/10.1021/jp408619u

14. K. C. Leonard, A. J. Bard "Pattern Recognition Correlating Materials Properties of the Elements to Their Kinetics for the Hydrogen Evolution Reaction" *J. Am. Chem. Soc. 135*(42), 15885-15889 (2013). http://pubs.acs.org/doi/abs/10.1021/ja407394q

15. Hyun S. Park, Hyung-Wook Ha, Rodney S. Ruoff, Allen J. Bard, "On the improvement of photoelectrochemical performance and finite element analysis of reduced graphene oxide-$BiVO_4$ composite electrodes," *J. Electroanalytical Chem.* **716**, 8-15 (2014). http://www.sciencedirect.com/science/article/pii/S1572665713003962

16. Sean P. Berglund, Huichao He, William D. Chemelewski, Hugo Celio, and C. Buddie Mullins, "p-Si/W_2C and p-Si/W_2C/Pt photocathodes for the hydrogen evolution reaction," *J. Am. Chem. Soc*. **136**, 1535-1544 (2014). http://dx.doi.org/10.1021/ja411604k

17. William C. Chemelewski, Heung-Chan Lee, Allen J. Bard, and C. Buddie Mullins, "Amorphous FeOOH Oxygen Evolution Reaction Catalyst for Photoelectrochemical Water Splitting," *J. Am. Chem. Soc.* **136**, 2843-2850 (2014). http://dx.doi.org/10.1021/ja411835a

18. Alexander J. E. Rettie, Kyle C. Klavetter, Jung-Fu Lin, Andrei Dolocan, Hugo Celio, Ashioma Ishiekwene, Heather L. Bolton, Kristen N. Pearson, Nathan T. Hahn, and C. Buddie Mullins, "Improved visible light harvesting of WO_3 by incorporation of sulfur or iodine: A tale of two impurities," *Chem. Mater*. **26**, 1670-1677 (2014). http://dx.doi.org/10.1021/cm403969r

19. Yiqing Sun, William D. Chemelewski, Sean P. Berglund, Chun Li, Huichao He, Gaoquan Shi, and C. Buddie Mullins, "Antimony doped tin oxide nanorods as a transparent conducting electrode for enhancing photoelectrochemical oxidation of water by hematite," *ACS Appl. Mater. Interfaces* ***6****, 5494-5499 (2014).* http://dx.doi.org/10.1039/C4TA01167H

20. Xinsheng Zhang, Huicheng Li, Shijun Wang, Fu-Ren F. Fan, and Allen J Bard, "Improvement of Hematite as Photocatalyst by Doping with Tantalum," *J. Phys. Chem. C* **118**, 16842–16850 (2014). http://pubs.acs.org/doi/abs/10.1021/jp500395a

21. Huichao He, Sean P. Berglund, Alexander J. E. Rettie, William D. Chemelewski, Peng Xiao, Yunhuai Zhang, and C. Buddie Mullins, "Synthesis of $BiVO_4$ nanoflake array films for photoelectrochemical water oxidation," *J. Mater. Chem. A.* **2**, 9371-9379 (2014). http://dx.doi.org/10.1039/C4TA00895B

22. William D. Chemelewski, Jacob R. Rosenstock, and C. Buddie Mullins, "Electrodeposition of Ni-doped FeOOH oxygen evolution reaction catalyst for photoelectrochemical water splitting," *J. Mater. Chem. A* ***2****, 14957-14962 (2014).* http://dx.doi.org/10.1039/c4ta03078h

23. Alexander J. E. Rettie, Shirin Mozaffari, Martin D. McDaniel, Kristen N. Pearson, John G. Ekerdt, John T. Markert, and C. Buddie Mullins, "Pulsed laser deposition of epitaxial and polycrystalline bismuth vanadate thin films," *J. Phys. Chem. C*. **118**, 26543-26550 (2014). http://pubs.acs.org/doi/abs/10.1021/jp5082824

24. Hoang X. Dang, Alex J. E. Rettie, and C. Buddie Mullins, "Visible light-active NiV_2O_6 films for photoelectrochemical water oxidation," *J. Phys. Chem. C*. **119**, 14524-14531 (2015). http://pubs.acs.org/doi/abs/10.1021/jp508349g

25. Alexander J. E. Rettie, William D. Chemelewski, Jeffrey Lindemuth, John S. McCloy, Luke G. Marshall, Jianshi Zhou, David Emin and C. Buddie Mullins, "Anisotropic Small-Polaron Hopping in W:$BiVO_4$ Single Crystals," *Appl. Phys. Lett.* **106**, 022106 (2015). http://dx.doi.org/10.1063/1.4905786

26. K. M. Nam; E. A. Cheon; W. J. Shin; A. J. Bard, "Improved Photoelectrochemical Water Oxidation by WO_3/$CuWO_4$ Composite with Manganese Phosphate Electro-catalyst" *Langmuir* **2015**, 31 (39), 10897–10903. http://dx.doi.org/10.1021/acs.langmuir.5b01780

27. V. Jovic, J. Laverock, A. J. E. Rettie, J.-S. Zhou, C. B. Mullins, V. R. Singh, B. Lamoureux, D. Wilson, T.-Y Su, B. Jovic, H. Bluhm, T. Söhnel and K. E. Smith, "Soft X-Ray Spectroscopic Studies of the Electronic Structure in M-$BiVO_4$ (M = Mo or W) Single Crystals," *J. Mater. Chem. A* ***3****, 23743-23753 (2015).* http://dx.doi.org/10.1039/c5ta07898a

28. Hsien-Yi Hsu, Li Ji, Hyun S. Ahn, Ji Zhao, Edward T. Yu; A. J. Bard, "A Liquid Junction Photoelectrochemical Solar Cell Based on p-Type $MeNH_3PbI_3$ Perovskite with 1.05 V Open-Circuit Photovoltage" *J. Am. Chem. Soc.* **2015**, *137* (46), 14758–14764. http://dx.doi.org/10.1021/jacs.5b09758

29. William D. Chemelewski and C. Buddie Mullins, "SILAR growth of Ag_3VO_4 and characterization for photoelectrochemical water oxidation," *J. Phys. Chem. C*. **119**, 26803–26808 (2015). http://dx.doi.org/10.1021/acs.jpcc.5b06658

30. Wenlong Guo, William D. Chemelewski, Oluwaniyi Mabayoje, Alexander J. E. Rettie, Peng Xiao, Yunhuai Zhang, and C. Buddie Mullins, "Synthesis and characterization of CuV_2O_6 and $Cu_2V_2O_7$, two photoanode candidates for photoelectrochemical water oxidation," *J. Phys. Chem. C*. **119**, 27220-27227 (2015). http://dx.doi.org/10.1021/acs.jpcc.5b07219

31. William D. Chemelewski, Oluwaniyi Mabayoje, Ding Tang, Alexander J. E. Rettie, C. Buddie Mullins, "Bandgap engineering of Fe_2O_3 with Cr – Application to photoelectrochemical oxidation," *Phys. Chem. Chem. Phys*. **18**, 1644-1648 (2016). http://dx.doi.org/10.1039/C5CP05154A

32. Alexander J. E. Rettie, William D. Chemelewski, David Emin, and C. Buddie Mullins, "Unravelling small-polaron transport in metal oxide photoelectrodes," *J. Phys. Chem. Lett.* **7**, 471-479 (2016). http://dx.doi.org/10.1021/acs.jpclett.5b02143

33. Ding Tang, Alexander J. E. Rettie, Oluwaniyi (Niyi) Mabayoje, Yanqing Lai, Yexiang Liu, and C. Buddie Mullins, "Facile Growth of Porous $Fe_2V_4O_{13}$ Films for Photoelectrochemical Water Oxidation," *J. Mater. Chem. A.* **4**, 3034-3042 (2016). http://dx.doi.org/10.1039/C5TA07877F

34. Alexander J. E. Rettie, William D. Chemelewski, Bryan R. Wygant, Jeffrey Lindemuth, Jung-Fu Lin, David Eisenberg, Carolyn S. Brauer, Timothy J. Johnson, Toya N. Beiswenger, Richard D. Ash, Xiang Li, Jianshi Zhou, C. Buddie Mullins, "Synthesis, Electronic Transport and Optical Properties of Si:α-Fe_2O_3 Single Crystals," *J. Mater. Chem. C*. **4**, 559-567 (2016). http://dx.doi.org/10.1039/C5TC03368C

35. Bryan R. Wygant, Karalee A. Jarvis, William D. Chemelewski, Oluwaniyi Mabayoje, Hugo Celio, and C. Buddie Mullins, "Structural and Catalytic Effects of Iron- and Scandium-Doping on a Strontium Cobalt Oxide Electrocatalyst for Water Oxidation," *ACS Catalysis* **6**, 1122-1133 (2016). http://www.dx.doi.org/10.1021/acscatal.5b02429

36. Hsien-Yi Hsu, Li Ji, Minshu Du, Ji Zhao, Edward T. Yu and Allen J. Bard, "Optimization of PbI_2/$MeNH_3PbI_3$ Perovskite Composites by Scanning Electrochemical Microscopy," submitted.

Electrochemical Synthesis of Polycrystalline Semiconductor Electrodes with Optimum Compositions and Morphologies for Use in Solar Fuel Production

Kyoung-Shin Choi
Department of Chemistry
University of Wisconsin-Madison
Madison, WI 53706

The overall objective of our project is to bring about a marked advancement in the synthesis and understanding of polycrystalline photoelectrodes for use in solar fuel production. Identifying inexpensive and easily processable semiconductors that can achieve high solar energy conversion efficiencies and developing facile synthesis methods to produce them as high performance photoelectrodes are critical steps to considerably reduce the production cost of solar fuels. We achieve these goals by developing simple and practical electrochemical synthesis methods/conditions that can produce promising semiconductors as high quality photoelectrodes with systematically varying compositions and morphologies. During the past funding period, we focused on developing ternary oxide-based photocathodes. Our synthesis methods enabled us to accurately evaluate their photoelectrochemical properties and develop effective strategies to address their primary limitations. The most significant achievements made during the past funding period are summarized below.

A new series of photocathodes, $LnFeO_3$ (Ln: lanthanides). $LnFeO_3$ is a family of compounds having a perovskite structure, which are reported to be p-type with a bandgap of 2.0 – 2.1 eV. Most p-type oxides contain Cu (e.g. CuO, Cu_2O, $CuFeO_2$), but the presence of Cu is often responsible for their photoinstability. Therefore, $LnFeO_3$ is of great interest as it may provide a series of stable oxide-based photocathodes that can utilize visible light. We have established electrodeposition conditions to prepare $LnFeO_3$ (Ln: La and Sm) electrodes. Their photoelectrochemical properties were investigated using photoreduction of O_2 and water. (Photoreduction of O_2 is thermodynamically and kinetically easier than photoreduction of water on the oxide surface). The results show that their flatband potentials are more positive than 1 V vs. RHE. As a result, they can achieve a photovoltage (i.e. the difference between the thermodynamic reduction potential of water and the photocurrent onset potential) greater than 1 V for H_2 evolution (Figure 1a). Furthermore, our preliminary results suggest that $LaFeO_3$ electrodes appear not to suffer from photocorrosion (Figure 1b), which is very exciting. The major advantage of $LnFeO_3$ as a photocathode is that its bandgap can be easily lowered to 1.6 eV by substitutionally replacing Ln^{3+} with monovalent or divalent ions. In these doped samples, the charge compensation is achieved partially by converting Fe^{3+} to Fe^{4+} and partially by generating oxygen vacancies. The presence of Fe^{4+} (smaller than Fe^{3+}) causes a distortion on

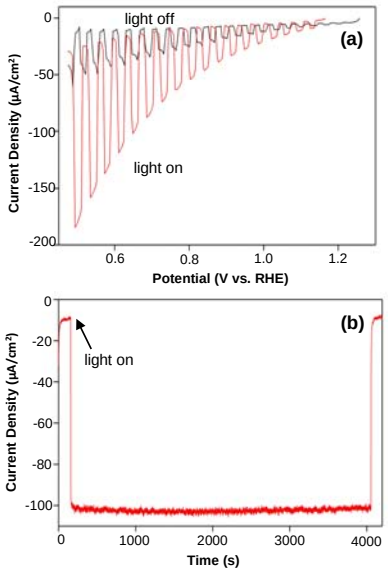

Figure 1. (a) *J-V* plots (scan rate = 10 mV/s) of $LaFeO_3$ for O_2 reduction (red) and water reduction (black) in 0.1 M NaOH. (b) *J-t* plot of $LaFeO_3$ for O_2 reduction at 0.6 V vs. RHE in 0.1 M NaOH (AM 1.5G illumination).

FeO_6 units and their connectivity (e.g. corner sharing FeO_6 framework). It is this distortion that is directly responsible for the change in electronic band structure and the bandgap energy of $LnFeO_3$. We believe that our investigation into the $LnFeO_3$ series will generate exciting new sets of results and will enable us to discover highly promising photocathodes with easily tunable bandgaps and charge transport properties.

$CuBi_2O_4$ and Ag-doped $CuBi_2O_4$ photocathodes. $CuBi_2O_4$ is a p-type semiconductor that possesses a band gap of 1.5 – 1.8 eV. Its conduction band minimum (CBM) is estimated to be at a more negative potential than the thermodynamic potential for water reduction. Furthermore, its flatband potential is located at a much more positive potential (> 1.0 V vs. RHE) than those of p-type Si and p-type Cu_2O, which are currently considered the most promising photocathodes. We developed electrochemical synthesis conditions to produce high quality $CuBi_2O_4$ photoelectrodes. The major advantage of our method compared to previously reported methods is that it allowed for the formation of $CuBi_2O_4$ films that achieve high surface coverage and high surface areas (Figure 2a inset). We were also able to prepare Ag-doped $CuBi_2O_4$ with the same morphology as undoped $CuBi_2O_4$ films, enabling us to unambiguously investigate the effect of Ag doping. In the Ag-doped $CuBi_2O_4$, Ag^+ ions substitutionally replaced Bi^{3+} ions and increased the hole concentration in $CuBi_2O_4$. As a result, photocurrent enhancements for both O_2 reduction (Figure 2a) and water reduction were achieved. Furthermore, while undoped $CuBi_2O_4$ electrodes suffered from anodic photocorrosion during O_2 reduction due to poor hole transport, Ag-doped $CuBiO_4$ effectively suppressed anodic photocorrosion (Figure 2b). The thermodynamic feasibility of photoexcited electrons in the conduction band of $CuBi_2O_4$ to reduce water was also confirmed by detection of H_2 during photocurrent generation. The observation that stable photocurrent could be generated by Ag-doped $CuBi_2O_4$ for O_2 reduction showed that it is possible to kinetically suppress both cathodic and anodic photocorrosion of $CuBi_2O_4$. If the rate of electron injection for water reduction is improved to the level of that for O_2 reduction and the hole transport does not limit photocurrent generation, stable photocurrent generation by $CuBi_2O_4$ for water reduction may be achieved.

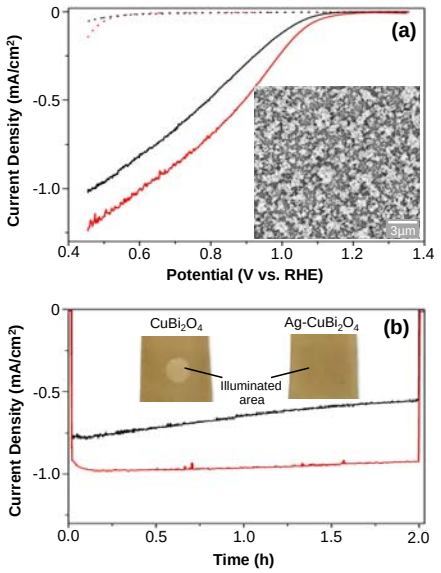

Figure 2. (a) *J-V* plots and (b) J-t plots (at 0.6 V vs. RHE) of $CuBi_2O_4$ (black) and Ag-doped $CuBi_2O_4$ (red) measured in 0.1 M NaOH solution (pH 12.8) saturated with O_2 under AM 1.5G (100 mW/cm^2) illumination. The inset in (a) shows an SEM image of $CuBi_2O_4$ while the inset in (b) shows photographs of $CuBi_2O_4$ and Ag-doped $CuBi_2O_4$ after 2 hours of *J-t* measurement for O_2 reduction.

In the next funding period, in addition to continuing to work on the promising oxide systems we identified, we plan to extend our expertise in electrochemical synthesis to III-V photoelectrodes. III-V photocathodes generally have smaller bandgaps and better charge transport properties than oxides, but their extremely high production costs have been the major limitation for their utilization as photoelectrodes. Our synthesis methods will allow for the production of highly efficient III-V photoelectrodes with lower costs.

DOE Sponsored Publications 2013-2016

1. Hill, J. C.; Choi, K.-S. "Synthesis and Characterization of High Surface Area $CuWO_4$ and Bi_2WO_6 Electrodes for use as Photoanodes for Solar Water Oxidation" *J. Mat. Chem.* A **2013**, *1*, 5006–5014.

2. Maijenburg, A.; Hattori, A.; De Respinis, M.; McShane, C.; Choi, K.-S.; Dam, B.; Tanaka, H.; ten Elshof, A. "Ni and p-Cu_2O nanocubes with a small size distribution by templated electrodeposition, and their characterization by photocurrent measurement" *ACS Appl. Mater. Interfaces*, **2013**, *5*, 10938–10945.

3. Park, Y.; Kang, D. H.; Choi, K.-S. "Marked Enhancement in Electron-Hole Separation Achieved in the Low Bias Region by Electrochemically Prepared Mo-Doped $BiVO_4$ Photoanodes" *Phys. Chem. Chem. Phys.* **2014**, *16*, 1238–1246.

4. Maijenburg, A. W.; Regis, M.; Hattori, A.; Tanaka, H.; Choi, K.-S.; ten Elshof, J. "MoS_2 nanocube structures as catalysts for electrochemical H_2 evolution from acidic aqueous solutions" ACS *Appl. Mater. Interfaces* **2014**, *6*, 2003–2010.

5. Kang, D.; Park, Y.; Hill, J. C.; Choi, K.-S. **"**Preparation of Bi-Based Ternary Oxide Photoanodes $BiVO_4$, Bi_2WO_6, and $Bi_2Mo_3O_{12}$ Using Dendritic Bi Metal Electrodes" *J. Phys. Chem. Lett.*, **2014**, *5*, 2994–2999.

6. Cha, H. G.; Choi, K.-S. "Combined Biomass Valorization and Hydrogen Production in a Photoelectrochemical Cell" *Nat. Chemistry*, **2015**, 7, 328–333.

7. Papa, C. M.; Cesnik, A. J.; Evans, T. C.; Choi, K.-S. "Electrochemical Synthesis of Binary and Ternary Niobium-Containing Oxide Electrodes Using the p-Benzoquinone/Hydroquinone Redox Couple" *Langmuir*, **2015**, *31*, 9502–9510.

8. Kang, D.; Kim, T. W.; Kubota, S.; Cardiel, A.; Cha, H. G.; Choi, K.-S. "Electrochemical Synthesis of Photoelectrodes and Catalysts for Use in Solar Water Splitting" *Chem. Rev.* **2015**, *115*, 12839–12887.

9. Kim, T. W.; Choi K.-S. "Improving Photoelectrochemical Performance and Stability of $BiVO_4$ in Basic Media by Adding a $ZnFe_2O_4$ Layer" *J. Phys. Chem. Lett.* **2016**, *7*, 447–451.

10. Roylance, J. J.; Kim, T. W.; Choi K.-S., "Efficient and Selective Electrochemical and Photoelectrochemical Reduction of 5-hydroxymethylfurfural to 2,5-bis(hydroxymethyl)furan Using Water as the Hydrogen Source" *ACS Catalysis*, **2016**, 6, 1840–1847.

11. Kang, D.; Choi, K.-S. "Enhancing Photoelectrochemical Properties and Photostability of p-type $CuBi_2O_4$ Photoelectrodes" **2016**, Submitted to *Chem. Mater.*

12. Kang, D.; Choi, K.-S. "Electrochemical Synthesis of Highly Oriented, Transparent, and Pinhole-free ZnO and Al-doped ZnO Films and Their Use in Heterojunction Solar Cells." **2016**, To be submitted.

13. Wheeler, G. P.; Choi, K.-S. "P-type $LaFeO_3$ as a Photocathode for a Photoelectrochemical Water Splitting Cell" **2016**, To be submitted.

Photoelectrochemical hydrogen production: Catalysis, Stability and MEG

Jing Gu, Yong Yan, Jeffery A. Aguiar, Suzanne Ferrere, K. Xerxes Steirer, Chuanxiao Xiao, James L. Young, Boris D. Chernomordik, Andrew Norman, Gregory Pach, Ryan Crisp, Nathan R. Neale, Matthew C. Beard and John A. Turner
Chemical and Nanoscience Center
National Renewable Energy Laboratory
Golden, CO, 80401

The use of sunlight to drive the conversion of water into H_2 and O_2 via a photoelectrochemical (PEC) reactor provides a strategy for storing solar energy, providing an energy carrier for transportation and a feedstock for ammonia production. High photoconversion efficiency is an important criterion as is the stability of the semiconductor electrolyte interface.

High efficiency semiconductor materials such as III-Vs are a clear choice as light harvesters, however other approaches to high efficiency such as multiple exciton generation (MEG) can also be explored. This talk will cover both approaches. While these are separate paths, the goal is the same: maximize the number of excited carriers that are converted into chemical fuels.

Graded $MoS_x/MoO_x/TiO_2$ interfacial layer for catalysis and interface stabilization. Although tandem cells based on III-V materials sets have shown the ability to reach high efficiencies, the catalytic activity and long-term stability of the interface still remains a significant challenge. Previously we showed that a combination of an ALD TiO_2 layer coupled with a homogeneous catalyst could not only provide high catalytic activity but impart some increased stability over a Pt catalyzed surface (1). Optimizing both the catalytic activity and stability of the interface requires an understanding of the interfacial charge transfer processes between the semiconductor and the TiO_2 layer. Therefor in conjunction with the effort on the TiO_2-CobaltOxime scheme, a time-resolved spectroscopic probe was developed. Termed transient photoreflectance this tool can directly monitor carrier dynamics within and across such junctions (2). This unique approach is well-suited for the study of

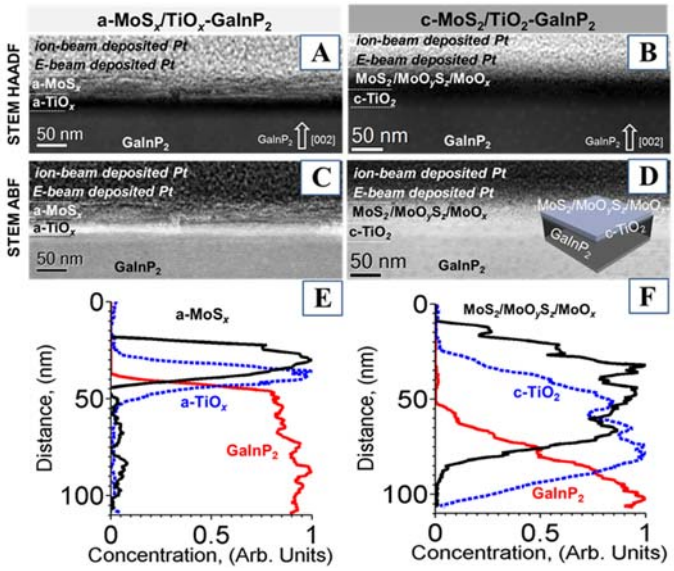

Figure 1. (A) Cross-sectional of high-angle annular dark field (HAADF) and (C) annular bright-field (ABF) STEM image of MoS_x/TiO_x-$GaInP_2$ before annealing. (E) STEM EDS line profiling coupled with spectral component matching showing the individual layer thickness (MoS_x, black; TiO_x, blue; $GaInP_2$, red) and interface abruptness before annealing. (B) Cross-sectional of HAADF and (D) ABF STEM image of MoS_2/TiO_2-$GaInP_2$ after annealing. (F) STEM EDS line profiling coupled with spectral component matching showing the individual layer thickness (MoS_2, black; TiO_2, blue; $GaInP_2$, red) and evidence of interdiffusion between layers after annealing.

*Joint with the Center for Advanced Solar Photophysics (CASP)

highly reflective surfaces such as we have here with the epitaxial $GaInP_2$.

We have developed a new strategy for stabilizing a p-$GaInP_2$ photocathode using a robust and catalytically active interfacial layer based on $MoS_x/MoO_x/TiO_2$. We find that annealing a bilayer of amorphous titanium dioxide (TiO_x) and amorphous molybdenum sulfide (MoS_x) deposited onto $GaInP_2$ results in the $MoS_x/MoO_x/TiO_2$ coating that provides the $GaInP_2$ photocathode with good efficiency (current density of 11 mA/cm^2 at a potential of 0 V vs. RHE under 1 sun illumination) and stability (retains 80% of its initial photocurrent density over a 20 h period) for the hydrogen evolution reaction in strong acid solution compared with traditional surface-deposited platinum-ruthenium cocatalysts on a $GaInP_2$ photocathode. We explore the composition and phase of the interfacial layer using transmission electron microscopy (TEM), scanning transmission electron microscopy (STEM), energy dispersive x-ray spectroscopy (EDS), electron energy loss spectroscopy (EELS), and x-ray photoelectron spectroscopy (XPS) before and after annealing (Figure 1). These studies reveal that annealing results in a graded $MoS_x/MoO_x/TiO_2$ layer that retains much of the high catalytic activity of amorphous MoS_x but with stability similar to crystalline MoS_2.

Quantum yield exceeding unity for PEC hydrogen via MEG*. Multiple exciton generation has been shown for quantum dots (QDs) in solution and in quantum dot solar cells. We have found that a lead sulfide QD photoelectrochemical cell is able to drive the hydrogen evolution reaction with an external quantum efficiency (EQE) of over 100%, up to an EQE of 114±1.3%. QD photoelectrodes with bandgap energies (E_g) of 0.85, 0.92 and 1.08 eV all demonstrated clear MEG in a PEC cell. The absorption of a photon with at least 2.7xE_g began to produce more than one electron-hole pair per absorbed photon (Figure 2), as determined by both current measurement and hydrogen production. This shows that under the appropriate conditions the external quantum efficiency can be over unity for photoelectrochemical hydrogen generation. This result is interesting for the future design and development of PEC systems where MEG may be utilized to photo-split water to generate hydrogen fuels with the goal of surpassing the Shockley-Queisser limit. We note that effective water oxidation as counter reaction is undeniably another non-trivial step to investigate. This effort shows that photon-to-hydrogen quantum efficiency can pass unity via MEG and demonstrates a possible new direction for exploring high efficiency approaches to generate solar fuels.

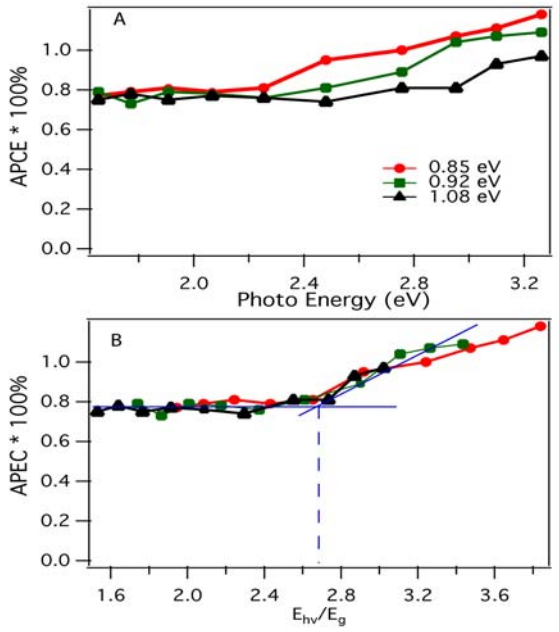

Figure 2. A) Absorbed Photon-to-Current Efficiency (APCE) as function of absolute incident photo energy, *hv*. B) Absorbed Photon-to-Current Efficiency (APCE) as function of incident photo energy divided by QD band gap energy, or multiples of the band gap.

*Joint with the Center for Advanced Solar Photophysics (CASP)

DOE Sponsored Publications 2013-2016

1. "Water reduction by a p-$GaInP_2$ photoelectrode stabilized by an amorphous TiO_2 coating and a molecular cobalt catalyst", Jing Gu, Yong Yan, James L. Young, K. Xerxes Steirer, Nathan R. Neale & John A. Turner, *Nature Materials* 15, 456–460 **2016** doi:10.1038/nmat4511
2. "Semiconductor interfacial carrier dynamics via photoinduced electric fields", Ye Yang, Jing Gu, James L. Young, Elisa M. Miller, John A. Turner, Nathan R. Neale, Matthew C. Beard, *Science*, Vol. 350, Issue 6264, pp. 1061-1065 **2015** doi:10.1126/science.aad3459
3. "Proton Reduction using a Hydrogenase-Modified Nanoporous Black Silicon Photoelectrode," Yixin Zhao, Nicholas C. Anderson, Michael W. Ratzloff, David W. Mulder, Kai Zhu, John A. Turner, Nathan R. Neale, Paul W. King, and Howard M. Branz, *ACS Appl. Mater. Inter.*, *under revision* **2016**
4. "Quantum Yield Exceeding 100% For Photoelectrochemical Hydrogen Evolution Reaction", Yong Yan, Ryan Crisp, Jing Gu, Boris D. Chernomordik, Gregory Pach, John A. Turner, Matthew C. Beard, *submitted* **2016**
5. "Stabilizing Water-Splitting Photoelectrodes Using a Graded $MoS_x/MoO_x/TiO_2$ Interfacial Layer," Jing Gu, Jeffery A. Aguiar, Suzanne Ferrere, K. Xerxes Steirer, Yong Yan, Chuanxiao Xiao, James L. Young, Andrew Norman, Heli Wang, Nathan R. Neale, John A. Turner, *in preparation* **2016**.

*Joint with the Center for Advanced Solar Photophysics (CASP)

Session III

Solar Photoconversion at Semiconductor Surfaces

Semiconductor Interfacial Carrier Dynamics by Time-Resolving the Internal Electric Field and Observation of Hot-Phonon Bottleneck using Transient Absorption Spectroscopy

Ye Yang, Jing Gu, Elisa M. Miller, Kai Zhu, Joseph M. Luther, Nathan R. Neale, Jao van de Lagemaat, John A. Turner, Matthew C. Beard
Chemical and Nanoscience Center
National Renewable Energy Laboratory
Golden, CO 80401

Solar photoconversion in semiconductors is driven by charge separation at the interface of the semiconductor and contacting layers. Junctions that form between a semiconductor surface and a contacting layer are the key to that charge separation. Equilibration of chemical potential at such junctions creates an internal electric field (built-in field) and establishes a region where mobile charges are driven away (depletion region). Absorption of light produces electrons and holes within the depletion region where the charges are separated. Photogenerated electrons (holes) cross the interface to participate in a reduction (oxidation) reaction while holes (electrons) are transported to the counter electrode for the oxidation (reduction) reaction. However, photocarriers can also recombine across the same interface, and such recombination reduces the energy conversion efficiency. Thus, the carrier dynamics – charge separation and recombination across junctions – represent a key-determining factor in the PEC performance.

Isolating spectral signatures and/or the carrier dynamics that are specific to junctions and not just the interface or bulk is challenging. We developed transient photoreflectance (TPR) as an innovative time-resolved spectroscopic probe that can directly monitor carrier dynamics within and across such junctions. In the TPR method, the change in reflectance (ΔR) of a broadband probe from a specific interface is monitored as a function of pump-probe delay (Fig. 1). The reflectance can be modulated by either photogenerated free-carriers due to band filling, and/or by transient fields due to electro-optic effects when charges are separated. The spectral nature of the reflected beam provides quantitative information about the built-in field; thus, TPR is a non-contact probe of the electric field at that interface.

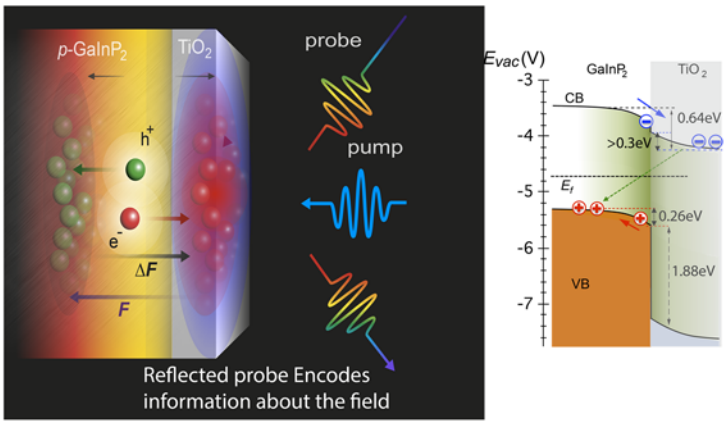

Figure 1. A broadband probe pulse spanning the semiconductor bandgap is reflected off an interface of interest. An above-bandgap monochromatic pump pulse modulates the reflectance. (right) details of *p-n* (*p*-$GaInP_2$/TiO_2) junction deduced from TPR and XPS. Charge recombination is slowed by the *p-n* nature of the junction.

We applied TPR to study charge transfer at *p*-type gallium-indium phosphide (*p*-$GaInP_2$) and *n*-type gallium-arsenide (*n*-GaAs) interfaces. We monitored the formation and decay of transient electric fields that form upon photoexcitation within bare *p*-$GaInP_2$, *p*-

$GaInP_2$/platinum (Pt), and *p*-$GaInP_2$/amorphous titania (TiO_2) interfaces. A field at both the *p*-$GaInP_2$/Pt and *p*-$GaInP_2$/TiO_2 interfaces forms that drives charge separation, however, recombination at the *p*-$GaInP_2$/TiO_2 interface is significantly reduced compared the *p*-$GaInP_2$/Pt interface. On the other hand, *n*-GaAs forms an ohmic contact with TiO_2 while only a small field forms at the n-GaAs/NiO interface that promotes hole transfer to nickel oxide (NiO).

Hot-phonon bottleneck in Pb-iodide Perovskite. New PV technologies should have the potential not only to reduce module costs, but also to achieve power conversion efficiencies (PCE) beyond ~33%. Charge carriers with excess kinetic energy (hot-carriers) are generated when a semiconductor absorbs photons with energy larger than that of the bandgap. In a typical semiconductor, the excess kinetic energy is quickly dissipated as hot carriers lose excess energy by heating the lattice and this process accounts for ~50% of the free-energy loss in current solar energy conversion strategies. Gaining control and preventing such thermalization could result in a doubling of the limiting efficiencies (33% to 66%). One approach to slowing carrier thermalization is via a hot-phonon bottleneck. In this approach, a non-equilibrium population of LO-phonons is generated and not allowed to dissipate and results in efficient re-absorption of phonons by the carrier population. Past studies showed that efficient hot-phonon bottlenecks could be produced in highly engineered multiple quantum well structures. Here we find an efficient hot-phonon bottleneck in solution processed Pb-iodide perovskite thin films.

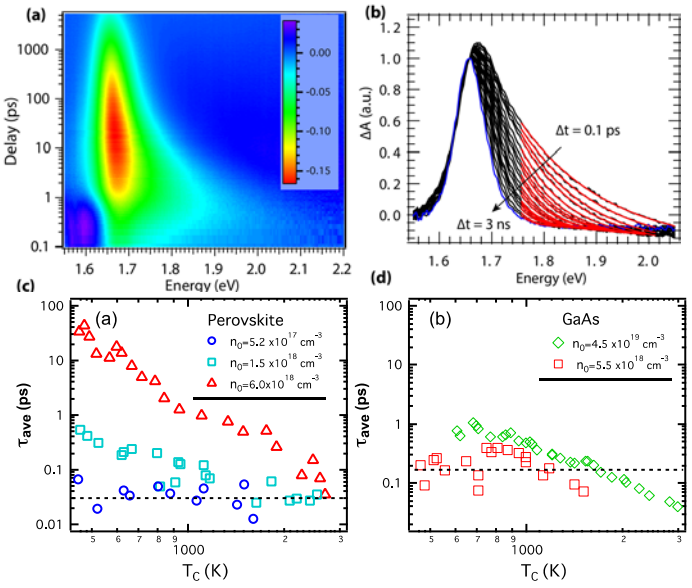

Figure 2. (a) Pseudocolor representation and (b) normalized perovskite TA spectra for n_0 of 6.0×10^{18} cm^{-3} and $\hbar\omega_{pump}$ of 3.10 eV. Panel (a) depicts the τ_{ave} of perovskites for three different n_0 as a function of T_e. The dashed line is a constant τ_{ave} = 30 fs. Panel (b) depicts the τ_{ave} of GaAs for two different n_0 as a function of T_e. The dashed line is a constant τ_{ave} = 200

We studied the carrier dynamics in planar methyl ammonium lead iodide perovskite films using broadband transient absorption (TA) spectroscopy. We fully characterize the TA-spectrum by free-carrier induced bleaching of the exciton transition, quasi-Fermi energy, carrier-temperature and bandgap renormalization constant. The photo-induced carrier temperature is extracted from the TA spectra and monitored as a function of delay time for different excitation wavelengths and photon fluences. We find an efficient hot-phonon bottleneck that slows down cooling of hot carriers by 3-4 orders of magnitude in time above a critical injection carrier density of ~5×10^{17} cm^{-3}. Compared to molecular beam epitaxially (MBE) grown GaAs the critical density is an order of magnitude lower and the relaxation time is ~3 orders of magnitude longer.

DOE Sponsored Publications 2013-2016

1. Y. Yang, D. Ostrowski, R. France, K. Zhu, J. van de Lagemaat, J.M. Luther, M.C. Beard, "Observation of a Hot-Phonon Bottleneck in Lead Iodide Perovskites", *Nature Photonics*, 10, 53-59, **2016** doi: 10.1038/nphoton.2015.213

2. M. R. Bergren, P.B. Palomaki, N.R. Neale, T.E. Furtak, M.C. Beard, "Size-Dependent Hot-Carrier Relaxation and Exciton-Dynamics in Colloidal Silicon Quantum Dots", *ACS Nano*, 10, 2316-2323, **2016,** doi: 10.1021/acsnano.5b07073

3. L.M. Wheeler, A.W. Nichols, B.D. Chernomordik, N. C. Anderson, M.C. Beard, N.R. Neale, "All-Inorganic Germanium Nanocrystal Films by Cationic Ligand Exchange", N*ano Letters*, 16(3), 1949-1954, **2016,** doi: 10.1021/acs.nanolett.5b05192

4. B.G. Lee, L.W. Luo, N.R. Neale, M.C. Beard, D. Hiller, M. Zacharias, P. Stradins, A. Zunger, "Quasi-Direct Optical Transitions in Silicon Nanocrystals with intensity exceeding the bulk", *Nano Letters*, 16, 1583, **2016,** doi: 10.1021/acs.nanolett.5b04256

5. S. Boriskina, M.A. Green, K. Catchpole, E. Yablonovitch, M.C. Beard, Y. Okada, S. Lany, T. Gershon, A. Zakutayev, M. Tahersima, V. J. Sorger, M. Naughton, K. Kempa, M. Dagenais, Y. Yao, L. Xu, X. Shing, N. D. Bronstein, J. A. Rogers, A. P. Alivisatos, R. G. Nuzzo, J. M. Gordon, D. M. Wu, M. D. Wisser, A. Salleo, J. Dionne, P. Bermel, J.J. Greffet, I. Celanovic, M. Soljacic, A. Manor, C. Rotschild, A. Raman, L. Shu, S. Fan, G. Chen "Roadmap for Optical Energy Conversion:", *J. of Optics*, in press, **2016**

6. E.M. Miller, D. Kroupa, J. Zhang, P. Schulz, A. Khan, J. M. Luther, M.C. Beard, C.L. Perkins, J. van de Lagemaat, "Re-visiting the Size-dependent Valence and Conduction Bands of PbS QDs: Photoelectron and Inverse Photoelectron Spectroscopy", *ACS Nano*, 10, 3302-3311, **2016,** doi: 10.1021/acsnano.5b06833

7. Y. Yang, J. Gu, J.L. Young, E.M. Miller, J. Turner, N. Neale, M.C. Beard, "Semiconductor interfacial carrier dynamics via photo-induced electric fields", *Science*, 350, 1061-1065, **2015** doi: 10.1126/science.aad3459

8. Y. Yang, M. Yang, Z. Li, R.W. Crisp, K. Zhu, M.C. Beard "Comparison of Recombination Dynamics in $CH_3NH_3PbBr_3$ and $CH_3NH_3PbI_3$ Perovskite Films: Influence of Exciton Binding Energy", *J. Phys. Chem. Lett.*,6, 4688-4692, **2015** doi: 10.1021/acs.jpclett.5b02290

9. S. Kim, A.R. Marshall, E.M. Miller, D.M. Kroupa, J.M. Luther, S. Jeong, M.C. Beard, "Air Stable and Efficient PbSe Quantum Dots Solar Cells Based Upon Cation Exchange from ZnSe Quantum Dots", *ACS Nano*, 9, 8157-8164, **2015** doi: 10.1021/acsnano.5b02326

10. J. Zhang, B. D. Chernomordik, R.W. Crisp, D. Kroupa, J.M. Luther, E.M. Miller, J. Gao, M.C. Beard, "Preparation of Cd/Pb Chalcogenide Heterostructured Janus Particles via Controllable Cation Exchange", *ACS Nano*, 9, 77151-7163, **2015** doi: 10.1021/acsnano.5b01859

11. Y. Yang, Y. Yan, M. Yang, S. Choi, K. Zhu, J. M. Luther, M.C. Beard, "Low Surface Recombination Velocity in Solution-Grown $CH_3HN_3PbBr_3$ Perovskite Single Crystal", *Nature Comm.*, 6, 7961, **2015,** doi: 10.1038/ncomms8961

12. J. Zhang, R.W. Crisp, J. Gao, D.M. Kroupa, M.C. Beard, J.M. Luther "Synthetic Conditions for high-accuracy size control of PbS Quantum Dots ", *J. Phys. Chem. Lett.*, 6, 1830-1833, **2015,** doi: 10.1021/acs.jpclett.5b00689

13. M.C. Beard, J.C. Johnson, J.M. Luther, A. J. Nozik, "Multiple Exciton Generation in Quantum Dots vs. Singlet Fission in Molecular Chromophores for Solar Photon Conversion", *Philosophical Transactions A*, 373, 40412, **2015,** doi: 10.1098/rsta.2014.0412

14. D.M. Sagar, J. Atkin, P.B. Palomaki, N.R. Neale, J.L. Blackburn, J.C. Johnson, A.J. Nozik, M. Raschke, M.C. Beard, "Quantum confined electron-phonon interaction in silicon nanocrystals" *Nano Letters*, 15 (3), 1511-1516, **2015,** doi: 10.1021/nl503671n

16. B. K. Hughes, J.L. Blackburn, A. Shabeav, S.C. Erwin, A.L. Efros, A.J. Nozik, J.M. Luther, M.C. Beard, "Synthesis and Spectroscopy of PbSe QD-QD Fused Dimer Structures", *JACS*, 136, 4670, **2014**, doi: 10.1021/ja413026h

17. M.R. Bergren, C. E. Kendrick, N.R. Neale, J.M. Redwing, R.T. Collins, T.E. Furtak, M.C. Beard, "Ultrafast Electrical Measurements of Isolated Silicon Nanowires and Nanocrystals", *J. Phys. Chem. Lett.*, 5, 2050-2057, **2014,** doi: 10.1021/jz500863a

18. M.C. Beard, J.M. Luther, A.J. Nozik, "Promise and Challenge of Nanostructured Solar Cells", *Nature Nanotechnology*, 9(12), 951-954, **2014,** doi: 10.1038/nnano.2014.292

19. M.R. Bergren, B.J. Simonds, B. Yan, G. Yue, R. Ahrenkeil, T.E. Furtak, R. T. Collins, P.C. Taylor, M.C. Beard, "Direct Observation of Electron Transfer in Nanocrystalline Silicon", *Phys. Rev. B.*, **2013,** 87, 081391(R) doi: 10.1103/PhysRevB.87.081301

15. M.C. Beard, J.M. Luther, O.E. Semonin, A.J. Nozik, "Third Generation Photovoltaics based on Multiple Exciton Generation in Quantum Confined Semiconductors", *Accounts of Chemical Research*, **2013**, 46**,** 1252-1260**,** doi:10.1021/ar3001958

20. A.G. Midgett, J.M. Luther, J.T. Stewart, D.K. Smith, L.A. Padilha, V.I. Klimov, A.J. Nozik, M.C. Beard, "Size and Composition Dependent Multiple Exciton Generation Efficiency in PbS, PbSe and PbSSe Alloyed Quantum Dots", *Nano Letters*, **2013**, 13, 3078-3085, doi: 10.1021/nl4009748

21. R.W. Crisp, J.N. Schrauben, M.C. Beard, J.M. Luther, J.C. Johnson, "Coherent exciton delocalization in strongly coupled quantum dot arrays", *Nano Letters*, 13, 4862-4869, **2013,** doi: 10.1021/nl402725m

Electron Transfer Processes in Catalyzed Photoelectrodes for Solar Water Splitting

Shannon Boettcher[1], Mike Nellist[1], Forest Laskowski[1], Teddy Huang[2], Fuding Lin[1], T.J. Mills[1]
[1]Department of Chemistry and Biochemistry
University of Oregon, Eugene, OR 97403
[2]Bruker Atomic Force Microscopes
Santa Barbara CA, 93106

Light-absorbing semiconductor electrodes coated with electrocatalysts are key components of photoelectrochemical energy conversion and storage systems. Efforts to optimize these systems have been slowed by an inadequate understanding of the semiconductor-electrocatalyst interface. The semiconductor-electrocatalyst interface is important because it separates and collects photoexcited charge carriers from the semiconductor. The photovoltage generated across the interface drives "uphill" photochemical reactions, such as water splitting to form hydrogen fuel. In this presentation I will describe our progress using new experimental approaches and simulations to understand the microscopic processes and materials parameters governing interfacial electron transfer between light-absorbing semiconductors, electrocatalysts, and solution (Figure 1).

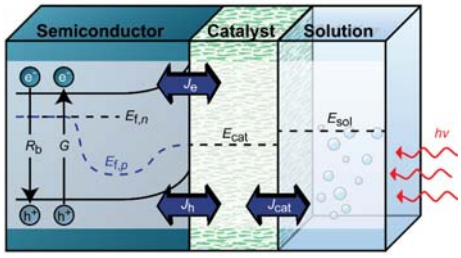

Figure 1. Key electronic processes occuring in catalyzed photoelectrodes.

In the first stage of this project we developed an experimental technique, dual-working-electrode (DWE) photoelectrochemistry, allowing for direct electrical measurement of the semiconductor-electrocatalyst interface *in situ*. We also developed the first theory of the semiconductor-electrocatalyst interface and applied the theory through numerical simulation to explain the measured interfacial charge-transfer properties. We discovered that porous, electrolyte-permeable, redox-active catalysts such as Ni-(Fe) oxyhydroxides form so-called "adaptive" junctions where the effective interfacial barrier height for electron transfer depends on the charge state of the catalyst. This is in sharp contrast to interface properties of dense ion-impermeable catalysts, which we found form buried junctions that could be described by simple equivalent electrical circuits. These results elucidated a design principle for catalyzed photoelectrodes - high-performance photoelectrodes with direct semiconductor-electrocatalyst junctions use soft deposition techniques that yield electrolyte-permeable catalysts. In this talk I will present our experimental and theoretical progress aiming to address key limitations identified in our initial work.

While our first studies focused on single-crystal model systems (e.g. *n*-TiO_2), practical systems must have smaller band gaps to absorb visible light. We are applying DWE and traditional photoelectrochemistry techniques to uncover the extent to which our interface models apply to both idealized small band-gap catalyzed semiconductor photoelectrodes, such as Ni(Fe)OOH on *n*-Si, as well as defective semiconductors such as Fe_2O_3 hematite that have a high density of surface states. For *n*-Si/Ni(Fe)OOH we find evidence that the performance of the photoelectrode is directly correlated with the extent of conversion of the catalyst to an electrolyte-permeable electrocatalyst phase (and an adaptive junction) but that systems that completely convert are unstable to Si oxidation (Figure 2). We also show how the catalyst

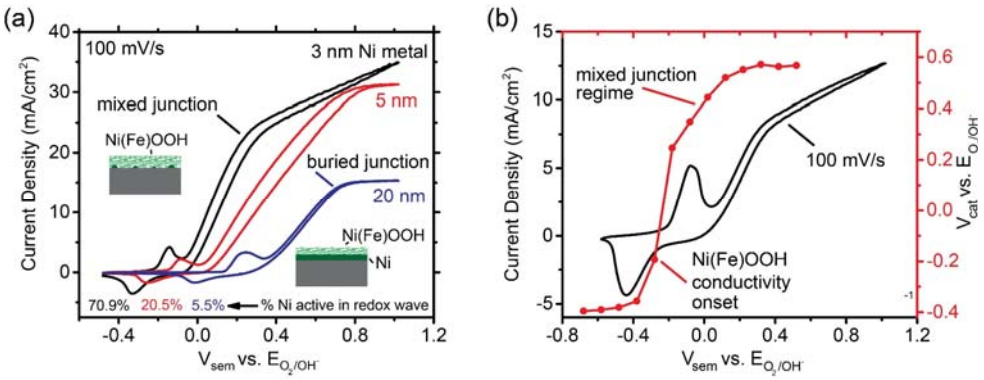

Figure 2. (a) *J-E* response of *n*-Si photoelectrodes with different amouints of Ni metal catalyst deposited. Thin layers convert to Ni(Fe)OOH phases where-as thick layers do not completely convert. (b) DWE measurements showing that even thin Ni layers that primarily convert to Ni(Fe)OOH do not show semiconductor/catalyst junctions that operate in the adaptive limit suggesting incomplete electrolyte permeability in the catalyst and consistent with the moderate protective layer effect.

activity is thus a strong driver on the apparent photocurrent onset potential on n-Si, in contrast to that observed for TiO_2. For Fe_2O_3, we will discuss how the DWE technique allows for observation and quantification of surface states responsible for Fermi-level pinning in the measured semiconductor-electrocatalyst junction properties. To quantitatively understand such phenomena, we have developed a model describing semiconductor photoelectrodes with both catalyst layers and surface states. Simulations show how catalyst activity affects the charge stored in the surface states and hence the response of the photoelectrode.

In the final portion of the talk I will describe our progress on developing a nanoscale DWE PEC technique by combining an electrochemical atomic force microscope with optical excitation and bipotentiostat electronics. The new technique will be used to map spatially dependent interface and charge-transport processes in electrocatalyst-modified photoelectrodes *in situ.* It should provide a major advantage over our previous method as it allows for high spatial resolution and does not require fabrication of metallized (and short-free) sample-test architectures. Preliminary work in collaboration with Dr. Teddy Huang at Bruker has successfully demonstrated that potentials and currents can be directly measured on model catalyzed semiconductor surfaces (Pt/Si) in liquid (Figure 3).

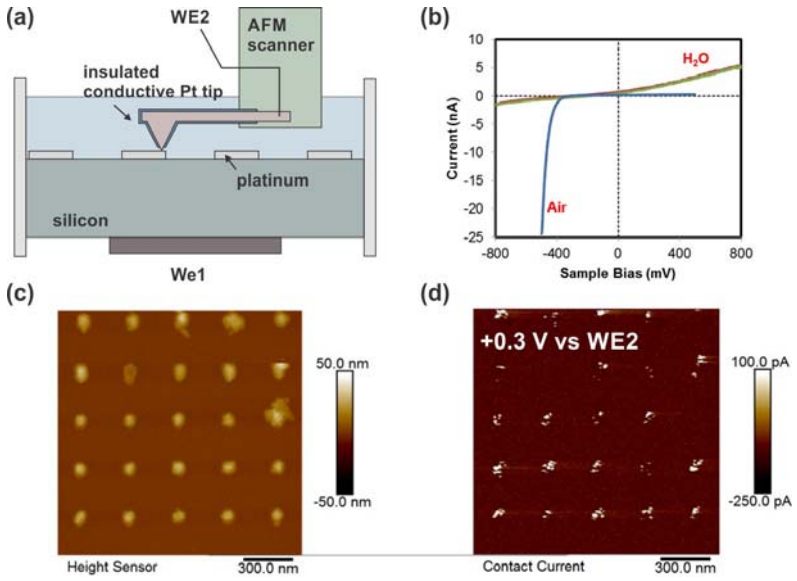

Figure 3. (a) schematic of electrical/electrochemical AFM in liquids, (b) current-voltage curves of Pt nanodots on Si in liquid and air, (c) AFM height image of Pt dots on Si, (d) current map in liquid showing high currents correlated with the Pt nano-catalysts islands.

DOE Sponsored Publications 2013-2016

1. Nellist, M. R.; Laskowski, F. A. L.; Lin, F.; Mills, T. J.; Boettcher, S. W. Semiconductor - Electrocatalyst Interfaces: Theory, Experiment, and Applications in Photoelectrochemical Water Splitting. *Acc. Chem. Res.* **2016**, ASAP.

2. Lin, F.; Boettcher, S. W. Advanced Photoelectrochemical Characterization: Principles and applications of dual-working-electrode photoelectrochemistry. In *Photoelectrochemical Solar Fuel Production: From Basic Principles to Advanced Devices*; Bisquert, J., Gimenez, S., Eds.; Springer: **2016**.

3. Lin, F.; Bachman, B. F.; Boettcher, S. W. Impact of Electrocatalyst Activity and Ion Permeability on Water-Splitting Photoanodes. *J. Phys. Chem. Lett.* **2015**, *6*, 2427.

4. Mills, T. J.; Lin, F.; Boettcher, S. W. Theory and simulations of electrocatalyst-coated semiconductor electrodes for solar water splitting. *Phys. Rev. Lett.* **2014**, *112*, 148304.

5. Lin, F.; Boettcher, S. W. Adaptive semiconductor-electrocatalyst junctions in water splitting photoanodes. *Nat. Mater.* **2014**, *13*, 81-86.

6. Trotochaud, L.; Mills, T.J.; Boettcher, S. W. An Opto-catalytic Model for Semiconductor-catalyst Water-Splitting Photoelectrodes Based on in-situ Optical Measurements on Operational Catalysts. *J. Phys. Chem. Let.* **2013**, 4, 931-935.

Molecular and Structural Probes of Defect States in Quantum Dots for Solar Photoconversion

Robert J. Stewart, Adam Rimshaw, Christopher Grieco, Grayson Doucette, and John B. Asbury
Department of Chemistry
The Pennsylvania State University
University Park, PA 16802

The objective of this research is to develop new electro-optical spectroscopic techniques that allow a direct correlation of molecular structural information about ligand-nanocrystal interactions with the corresponding density and energetic distribution of surface defects and the influence that these defects have on charge transport and recombination in quantum confined nanocrystalline arrays. The insight that is gained will provide a molecular basis for the rational development of novel pathways for the of use quantum dots in systems for solar energy transduction. This presentation serves as a progress report toward development of two electro-optical techniques that will enable this molecular-level correlation with electronic structure: 1) photocurrent detected infrared (PDIR) spectroscopy and 2) infrared detected admittance spectroscopy (IRAS).

The ultrafast PDIR technique is designed to directly correlate molecular structural information about interactions of ligands and quantum dot surfaces with the corresponding density and energetic distribution of defects together with the impact the defects have on charge transport and recombination in quantum confined nanocrystalline thin films. The technique enables these capabilities by coupling a photocurrent measurement to ultrafast and time-resolved vibrational spectroscopy methods that provide structural information about molecules giving rise to defects through their vibrational spectra.

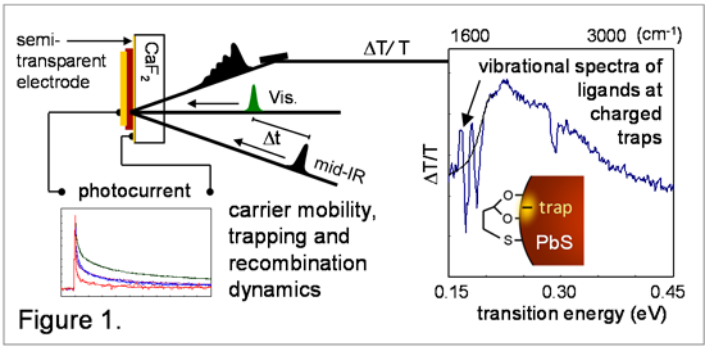

Figure 1.

We have made substantial progress toward development of the PDIR technique, which has required making advances in three areas jointly and simultaneously: i) adaptation of ultrafast spectroscopy to study functional electrical devices in a cryostat with an attached electrode package; ii) fabrication of functional electrical devices that can be electrically addressed in a cryostat and that survive for periods of days during which ultrafast experiments are conducted; and iii) development of low noise electrical circuitry capable of detecting small signals from functional devices that are excited by sufficiently low pulse energy that they survive for days of exposure. The foremost challenge we have overcome in this effort has been the much lower damage threshold of photoactive layers in functional electrical circuits in comparison to the same layers on insulating optical flats. This has led us to work with excitation densities in the 10 nJ/cm^2 range, roughly two orders lower than typically used in transient absorption experiments. The technological advances that have enabled these measurements to be as 'routine' as ultrafast spectroscopy experiments will be described along with next steps to fully utilize the combined spectroscopic and electrical transport capabilities to study colloidal quantum dot nanocrystalline arrays.

The IRAS technique provides another means to directly correlate molecular structural information about interactions of ligands and quantum dot surfaces with the corresponding density and energetic distribution of defects – but without the dynamics that come from ultrafast spectroscopy. In this regard, the technique is more limited but also more robust – more of an analytical tool. The technique uses principles from admittance spectroscopy to control the population of charge traps whose occupation is modulated by a bias potential at frequency ω. Modulation of the potential V(ω) (1) at frequencies low enough for charges to be trapped and released within a single cycle enables measurement of the vibrational features of the ligands that are perturbed by being closely associated with those traps using FTIR spectroscopy (2). Temperature dependent measurements of the rates for charges to be trapped and released, determined through frequency dependent capacitance measurements (3) provide direct links between charge trap structural information from vibrational spectroscopy and their corresponding density and energetic distribution. Key advances and insights from development of the technique will be described.

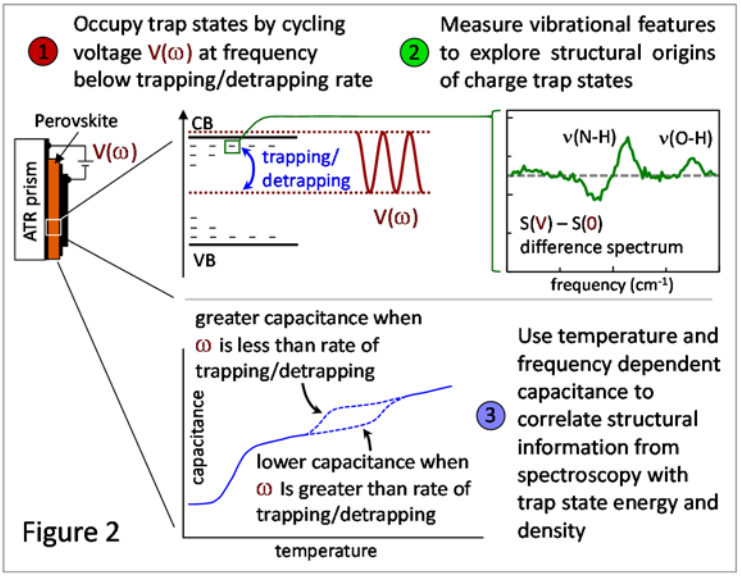

Figure 2

Finally, a brief discussion of recent insights about how ligand nanocrystal interactions at organo-halide perovskites surfaces determine their overall electronic structure will be given. While perovskites are not the focus of the project, the work addresses similar fundamental questions at a molecular level and enables us to validate the techniques under development. Key insights from this work include the realization that much of the dependence of perovskite material and device properties on processing conditions and morphology may be explained by how these affect the surface chemistry of the perovskite crystals. Furthermore, surface passivation of nanocrystalline perovskite films provides a pathway to realize bulk-like carrier dynamics without having to grow macroscopic single crystals. These findings further suggest that surface passivation may provide a means to decouple the electronic properties of organo-halide perovskites from the processing conditions used to deposit the films. Furthermore, iodoplumbate species that preform in solution survive the film formation process and lead to charge recombination centers in the solid state. We hypothesize that it is the moderate temperatures at which perovskite absorbers are annealed that allow these species to survive the film formation process. Finally, the ability of a variety of ligands of different Lewis basicity to passivate organo-halide perovskite surfaces will be explored and discussed as a means to gain insight about the chemistry of ligand binding and the nature of the surface states that serve as charge recombination centers before passivation.

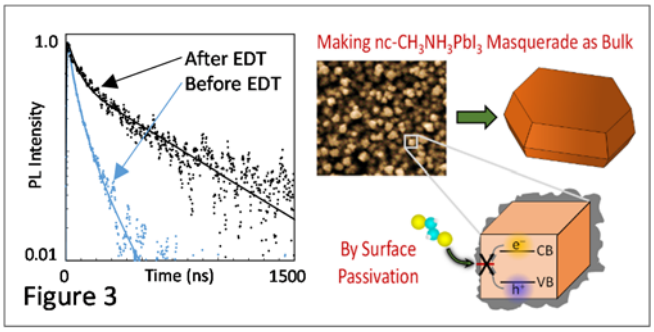

Figure 3

DOE Sponsored Publications 2013-2016

1. “Note: Using Fast Digitizer Acquisition and Flexible Resolution in Enhance Noise Cancellation for High Performance Nanosecond Transient Absorption Spectroscopy,” A. Rimshaw, C. Grieco, and J. B. Asbury, *Rev. Sci. Inst*. (2015) **86**, 066107(3).

2. “High Sensitivity Nanosecond Mid-Infrared Transient Absorption Spectrometer Enabling Low Excitation Density Measurements of Electronic Materials,” A. Rimshaw, C. Grieco, and J. B. Asbury, *Appl. Spec*. (2016) **70**, ASAP.

3. “Approaching Bulk Carrier Dynamics in Organo-Halide Perovskite Nanocrystalline Films by Surface Passivation,” R. J. Stewart, C. Grieco, A. V. Larsen, J. J. Maier, and J. B. Asbury, *J. Phys. Chem. Lett*. (2016) **7**, 1148-1153.

4. “Molecular Origins of Defects in Organo-Halide Perovskites and Their Influence on Charge Carrier Dynamics,” R. J. Stewart, C. Grieco, A. V. Larsen, G. S. Doucette, and J. B. Asbury, *J. Phys. Chem. C* (2016) submitted.

Session IV

Dye Redox Reactions in the Excited State

Oxomanganese Catalysts for Solar Fuel Production

Gary W. Brudvig, Victor S. Batista, Robert H. Crabtree and Charles A. Schmuttenmaer
Department of Chemistry, Yale University, New Haven, CT 06520-8107

The goal of this project is to construct solar-driven water-splitting photocatalytic cells, based on our own water-oxidation catalysts and sensitized metal oxide nanoparticles (NPs). Four research groups in the Chemistry Department at Yale University are working together to synthesize metal oxide NPs and anchor-linker-catalyst conjugates, develop new methods for surface attachment of catalysts using oxidation-resistant anchors and linkers that are stable in water, develop and apply computational methods to analyze interfacial electron transfer and characterize catalytic water-oxidation complexes, and use spectroscopic methods to characterize the photochemistry. See also posters by Crabtree and Schmuttenmaer.

Functioning Photoelectrochemical (PEC) Devices Studied with Time-resolved Terahertz (THz) Spectroscopy: THz spectroscopy has been used to study carrier dynamics in many semiconductor materials utilized in PEC cells. However, due to low transmission of far-IR radiation through conductive films, thin layers of material deposited on non-conducting substrates have been investigated rather than inside actual devices. To address this shortcoming, we photolithographically etched fluorine-doped tin oxide (FTO) coatings to produce a pattern analogous to a wire-grid THz polarizer, and measured a nearly 260-fold increase in percent power transmitted at 1 THz through patterned electrodes (15 μm wire width, 20 μm wire period) relative to continuous FTO films. We employed them to probe the carrier dynamics of dye-sensitized solar cells under an applied bias and with background illumination using time-resolved THz spectroscopy. We found that the electron injection efficiency and carrier trapping time both increase as the magnitude of the bias voltage is increased.

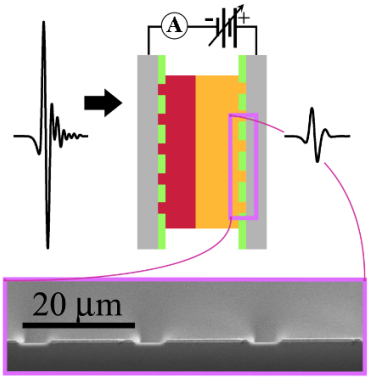

Figure 1. Schematic illustration of photoelectrochemical cell utilizing patterned FTO electrodes (SEM image shown at bottom). This design allows high THz transparency and also the ability to apply a bias voltage while making the measurements.

Computational Design of Molecular Rectifiers. We have performed a systematic computational search of molecular frameworks for intrinsic rectification of electron transport. The screening of molecular rectifiers included 52 molecules and conformers spanning over 9 series of structural motifs (Figure 2). N-phenylbenzamide was found to be a promising framework with both

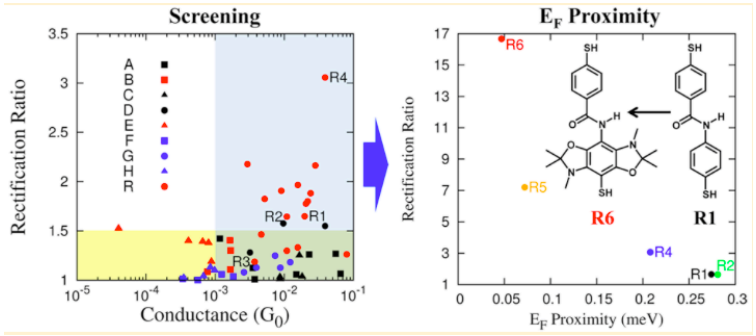

Figure 2: Calculated rectification ratios (left panel) versus conductance on a semilog scale for 52 synthetically plausible molecular candidates and conformers spanning the structural motifs shown in the right panel.

suitable conductance and rectification properties. A targeted screening performed on 30 additional derivatives and conformers of N-phenylbenzamide yielded enhanced rectification based on asymmetric functionalization. We demonstrated that electron-donating substituents that maintain an asymmetric distribution of charge in the dominant transport channel (e.g., HOMO) enhance rectification by raising the channel closer to the Fermi level. These findings are particularly valuable for the design of molecular assemblies that could ensure directionality of electron transport in a wide range of applications, from molecular electronics to solar catalytic reactions.

Stable Iridium(IV) Complexes of an Oxidation-Resistant Pyridine-Alkoxide Ligand: Highly Divergent Redox Properties Depending on the Isomeric Form Adopted. We have prepared and characterized a series of reversibly oxidizable $Ir^{III/IV}$ complexes based on an oxidation-resistant LX-type pyridine-alkoxide ligand. As an extremely strong donor, the alkoxide group favors high metal oxidation states while the large donicity difference between the two ligand arms leads to a dramatic influence on the $Ir^{III/IV}$ couple based on isomer geometry. A ligand field theory rationalization, supported by DFT calculations, accounts for the phenomenon in terms of differential distribution of the ligand field effects among the metal valence orbitals. We demonstrate that incorporation of alkoxide groups in ligand sets can stabilize high oxidation states, allowing for the isolation of species that would otherwise be transient or too unstable. In addition, it is made evident that ligand arrangement, not just ligand identity, needs to be taken into account when designing homogeneous catalysts, especially ones with highly disparate ligand types. This is particularly relevant for organometallic compounds, where it is not uncommon for ligands spanning the entire gamut of donicity to be found on the same metal atom.

Plans. Ongoing work is exploring the application of silatrane anchors for

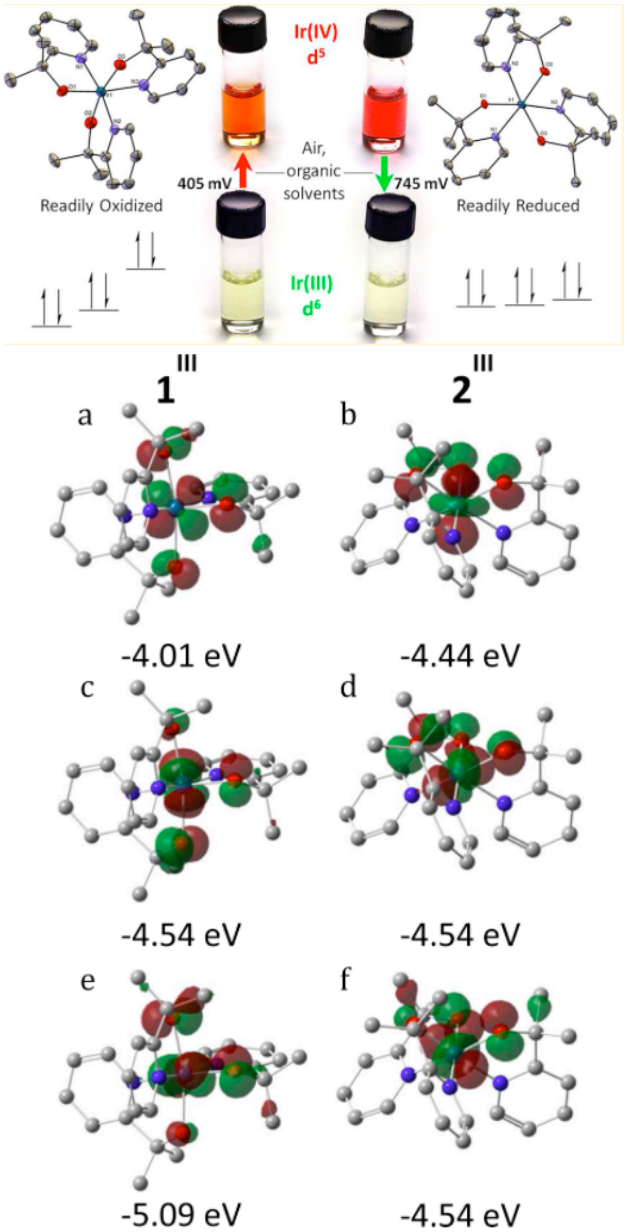

Figure 3: Top: reversibly oxidizable $Ir^{III/IV}$ complexes based on an oxidation-resistant LX-type pyridine-alkoxide ligand. DFT t_{2g} orbital energies and isosurfaces for 1^{III} (a, c, e) and 2^{III} (b, d, f) (lower panel) showing the dramatic effect of isomerism.

attachment of water-oxidation catalysts to metal oxide surfaces, hole-hopping antenna and molecular rectifiers in the design of TiO_2 photoanodes functionalized with water-oxidation catalysts, and high-potential porphyrin dyes for light-driven water oxidation.

DOE Sponsored Solar Photochemistry Publications 2013-2016

1. "Cp* Iridium Precatalysts for Selective C−H Oxidation with Sodium Periodate as the Terminal Oxidant", Meng Zhou, Ulrich Hintermair, Brian G. Hashiguchi, Alexander R. Parent, Sara M. Hashmi, Menachem Elimelech, Roy A. Periana, Gary W. Brudvig and Robert H. Crabtree (2013) *Organometallics* **32**, 957-965.
2. "Comparison of Primary Oxidants for Water-Oxidation Catalysis", Alexander R. Parent, Robert H. Crabtree and Gary W. Brudvig (2013) *Chem. Soc. Rev.* **42**, 2247-2252.
3. "Artificial Photosynthesis as a Frontier Technology for Energy Sustainability", Thomas Faunce, Stenbjörn Styring, Michael R. Wasielewski, Gary W. Brudvig, A. William Rutherford, Johannes Messinger, Adam F. Lee, Craig L. Hill, Huub deGroot, Marc Fontecave, Douglas R. MacFarlane, Ben Hankamer, Daniel G. Nocera, David M. Tiede, Holger Dau, Warwick Hillier, Lianzhou Wang and Rose Amal (2013) *Energy & Environ. Science* **6**, 1074-1076.
4. "Computational Studies of Natural and Artificial Photosynthesis", Ivan Rivalta, Gary W. Brudvig and Victor S. Batista (2013) *ACS Sym. Ser.* **1133**, 203-215.
5. "Hydroxamate Anchors for Improved Photoconversion in Dye-Sensitized Solar Cells", T. P. Brewster, S. J. Konezny, S. W. Sheehan, L. A. Martini, C. A. Schmuttenmaer, V. S. Batista, and R. H. Crabtree (2013) *Inorg. Chem.* **52**, 6752–6764.
6. "An Anionic N-donor Ligand Promotes Manganese-catalyzed Water Oxidation", Karin J. Young, Michael K. Takase and Gary W. Brudvig (2013) *Inorg. Chem.* **52**, 7615-7622.
7. "Modular assembly of high-potential Zn-porphyrin photosensitizers attached to TiO_2 with a series of anchoring groups", Lauren A. Martini, Gary F. Moore, Rebecca L. Milot, Lawrence Z. Cai, Stafford W. Sheehan, Charles A. Schmuttenmaer, Gary W. Brudvig, and Robert H. Crabtree (2013) *J. Phys. Chem. C* **117**, 14526–14533.
8. "Precursor Transformation during Molecular Oxidation Catalysis with Organometallic Iridium Complexes", Ulrich Hintermair, Stafford W. Sheehan, Alexander R. Parent, Daniel H. Ess, David T. Richens, Patrick H. Vaccaro, Gary W. Brudvig and Robert H. Crabtree (2013) *J. Am. Chem. Soc.* **135**, 10837-10851.
9. "Electron Injection Dynamics from Photoexcited Porphyrin Dyes into SnO_2 and TiO_2 Nanoparticles", Rebecca L. Milot, Gary F. Moore, Robert H. Crabtree, Gary W. Brudvig, and Charles A. Schmuttenmaer (2013) *J. Phys. Chem. C* **117**, 21662-21670.
10. "Efficiency of Interfacial Electron Transfer from Zn-Porphyrin Dyes into TiO_2 Correlated to the Linker Single Molecule Conductance", Christian F. A. Negre, Rebecca L. Milot, Lauren A. Martini, Wendu Ding, Robert H. Crabtree, Charles A. Schmuttenmaer, and Victor S. Batista (2013) *J. Phys. Chem. C* **117**, 24462-24470.
11. "Photoelectrochemical Oxidation of a Turn-On Fluorescent Probe Mediated by a Surface Mn^{II} Catalyst Covalently Attached to TiO_2 Nanoparticles", Alec C. Durrell, Gonghu Li, Matthieu Koepf, Karin J. Young, Christian F. A. Negre, Laura J. Allen, William R. McNamara, Hee-eun Song, Victor S. Batista, Robert H. Crabtree and Gary W. Brudvig (2014) *J. Catal.* **310**, 37-44.
12. "Ultrafast Carrier Dynamics in Nanostructures for Solar Fuels", Jason B. Baxter, Christiaan Richter, and Charles A. Schmuttenmaer (2014) *Ann. Rev. Phys. Chem.* **65**, 423-447.

13. "Organosilatrane Building Blocks", Bradley J. Brennan, Devens Gust and Gary W. Brudvig (2014) *Tetrahedron Lett.* **55**, 1062-1064.
14. "Linker Rectifiers for Covalent Attachment of Transition Metal Catalysts to Metal-Oxide Surfaces", Wendu Ding, Christian F. A. Negre, Julio L. Palma, Alec C. Durrell, Laura J. Allen, Karin J. Young, Rebecca L. Milot, Charles A. Schmuttenmaer, Gary W. Brudvig, Robert H. Crabtree and Victor S. Batista (2014) *ChemPhysChem* **15**, 1138-1147.
15. "High Conductance Conformers in Histograms of Single-Molecule Current-Voltage Characteristics", Wendu Ding, Christian F. A. Negre, Leslie L. Vogt and Victor S. Batista (2014) *J. Phys. Chem. C* **118**, 8316-8321.
16. "Substitution of a Hydroxamic Acid Anchor into the MK-2 Dye for Enhanced Photovoltaic Performance and Water Stability in a DSSC", Christopher Koenigsmann, Teresa S. Ripolles, Bradley J. Brennan, Christian F. A. Negre, Matthieu Koepf, Alec C. Durrell, Rebecca L. Milot, Jose A. Torre, Robert H. Crabtree, Victor S. Batista, Gary W. Brudvig, Juan Bisquert and Charles A. Schmuttenmaer (2014) *Phys. Chem. Chem. Phys.* **16**, 16629-16641.
17. "Structural Studies of Oxomanganese Complexes for Water Oxidation Catalysis", Ivan Rivalta, Gary W. Brudvig and Victor S. Batista (2014) in: "Molecular Water Oxidation Catalysts: A Key Topic for New Sustainable Energy Conversion Schemes" (A. Llobet, ed.) John Wiley & Sons, Ltd., pp. 1-14.
18. "Co(II), a Catalyst for Selective Conversion of Phenyl Rings to Carboxylic Acid Groups", Shashi Bhushan Sinha, Jesús Campos, Gary W. Brudvig and Robert H. Crabtree (2014) *RSC Adv.* **4**, 49395-49399.
19. "Photoelectrochemical Hole Injection Revealed in Polyoxotitanate Nanocrystals Functionalized with Organic Adsorbates", Christian F. A. Negre, Karin J. Young, Ma. Belén Oviedo, Laura J. Allen, Cristián G. Sánchez, Katarzyna N. Jarzembska, Jason B. Benedict, Robert H. Crabtree, Philip Coppens, Gary W. Brudvig and Victor S. Batista (2014) *J. Am. Chem. Soc.* **136**, 16420-16429.
20. "Interfacial Electron Transfer in Photoanodes Based on Phosphorus(V) Porphyrin Sensitizers Co-deposited on SnO_2 with the $Ir^{III}Cp^*$ Water Oxidation Precatalyst" Prashanth K. Poddutoori, Julianne M. Thomsen, Rebecca L. Milot, Stafford W. Sheehan, Christian F. A. Negre, Venkata K. R. Garapati, Charles A. Schmuttenmaer, Victor S. Batista, Gary W. Brudvig, Art van der Est (2015) *J. Mat. Chem. A* **3**, 3868-3879.
21. "Facet-Dependent Photoelectrochemical Performance of TiO_2 Nanostructures: An Experimental and Computational Study" Chuanhao Li, Christopher Koenigsmann, Wendu Ding, Benjamin Rudshteyn, Ke R. Yang, Kevin P. Regan, Steven J. Konezny, Victor S. Batista, Gary W. Brudvig, Charles A. Schmuttenmaer and Jae-Hong Kim (2015) *J. Am. Chem. Soc*. **137**, 1520-1529.
22. "Electron Injection Dynamics in High-Potential Porphyrin Photoanodes" Rebecca L. Milot and Charles A. Schmuttenmaer, (2015) *Acc. Chem. Res.* **48**, 1423-1431.
23. "A Molecular Catalyst for Water Oxidation that Binds to Metal Oxide Surfaces", Stafford W. Sheehan, Julianne M. Thomsen, Ulrich Hintermair, Robert H. Crabtree, Gary W. Brudvig and Charles A. Schmuttenmaer (2015) *Nature Comm.* **6**, 6469.
24. "Photosynthetic Water Oxidation: Insights from Manganese Model Chemistry", Karin J. Young, Bradley J. Brennan, Ranitendranath Tagore and Gary W. Brudvig (2015) *Accts. Chem. Res.* **48**, 567-574.
25. "Functioning Photoelectrochemical Devices Studied with Time-Resolved Terahertz

Spectroscopy", Coleen T. Nemes, Christopher Koenigsmann, and Charles A. Schmuttenmaer (2015) *J. Chem. Phys. Lett.*, **6** 3257-3262.

26. "Towards Multielectron Photocatalysis: A Porphyrin Array for Lateral Hole Transfer and Capture on a Metal Oxide Surface", Bradley J. Brennan, Alec C. Durrell, Matthieu Koepf, Robert H. Crabtree and Gary W. Brudvig (2015) *Phys. Chem. Chem. Phys.* **17**, 12728-12734.
27. "Photoelectrochemical Cells Utilizing Tunable Corroles", Bradley J. Brennan, Yick Chong Lam, Paul M. Kim, Xing Zhang and Gary W. Brudvig (2015) *ACS Appl. Mater. Interfaces* **7**, 16124-16130.
28. "Surfactant-Mediated Electrodeposition of a Water-Oxidizing Manganese Oxide", Wojciech T. Osowiecki, Stafford W. Sheehan, Karin J. Young, Alec C. Durrell, Brandon Q. Mercado and Gary W. Brudvig (2015) *Dalton Trans.* **44**, 16873-16881.
29. "Preparation of Halogenated Fluorescent Diaminophenazine Building Blocks", Matthieu Koepf, Shin Hee Lee, Bradley J. Brennan, Dalvin D. Méndez-Hernández, Victor S. Batista, Gary W. Brudvig and Robert H. Crabtree (2015) *J. Org. Chem.* **80**, 9881-9888.
30. "Silatranes for Binding Inorganic Complexes to Metal Oxide Surfaces", Kelly L. Materna, Bradley J. Brennan and Gary W. Brudvig (2015) *Dalton Trans.* **44**, 20312-20315.
31. "Computational Design of Intrinsic Molecular Rectifiers Based on Asymmetric Functionalization of N-phenylbenzamide", W. Ding, M. Koepf, C. Koenigsmann, A. Batra, L. Venkataraman, C. F. A. Negre, G. W. Brudvig, R. H. Crabtree, C. A. Schmuttenmaer and V. S. Batista (2015) *J. Chem. Theory Comput.* **11**, 5888-5896.
32. "Molecular Catalysts for Water Oxidation", James D. Blakemore, Robert H. Crabtree and Gary W. Brudvig (2015) *Chem. Rev.* **115**, 12974-13005.
33. "A Stable Coordination Complex of Rh(IV) in an N,O-donor Environment", Shashi B. Sinha, Dimitar Y. Shopov, Liam S. Sharninghausen, David J. Vinyard, Brandon Q. Mercado, Gary W. Brudvig and Robert H. Crabtree (2015) *J. Am. Chem. Soc.* **137**, 15692-15695.
34. "A New Method for the Synthesis of β-Cyano Substituted Porphyrins and Their Use as Sensitizers in Photoelectrochemical Devices", Antaeres Antoniuk-Pablant, Yuichi Terazono, Bradley J. Brennan, Benjamin D. Sherman, Jackson D. Megiatto, Jr., Gary W. Brudvig, Ana L. Moore, Thomas A. Moore and Devens Gust (2016) *J. Mater. Chem. A* **4**, 2976-2985.
35. "Ultrafast Electron Injection Dynamics of Photoanodes for Water-Splitting Dye-Sensitized Photoelectrochemical Cells", Swierk, J. R.; McCool, N. S.; Nemes, C. T.; Mallouk, T. E.; Schmuttenmaer, C. A. (2016) *J. Phys. Chem. C* **120**, 5940-5948.
36. "Structure-Function Relationships in Single-Molecule Rectification by *N*-phenylbenzamide Derivatives", Christopher Koenigsmann, Wendu Ding, Matthieu Koepf, Arunabh Batra, Latha Venkataraman, Christian F. A. Negre, Gary W. Brudvig, Robert H. Crabtree, Victor S. Batista and Charles A. Schmuttenmaer (2016) *New J. Chem.* **40**, submitted.
37. "Heme Biomolecule as Redox Mediator and Oxygen Shuttle for Efficient Charging of Lithium-Oxygen Batteries", Won-Hee Ryu, Forrest S. Gittleson, Julianne Thomsen, Jinyang Li, Mark Schwab, Gary Brudvig and André D. Taylor (2016) *Nature Comm.* **7**, submitted.
38. "In-situ Deprotection of THP-Protected Hydroxamic Acids on Titania", B. J. Brennan, C. Koenigsmann, K. L. Materna, P. M. Kim, M. Koepf, R. H. Crabtree, C. A. Schmuttenmaer and G. W. Brudvig (2016) *J. Phys. Chem. C* **120**, submitted.
39. "Light-Induced Water Oxidation Catalyzed by an Oxo-Bridged Trinuclear Ruthenium Complex", Yuta Tsubonouchi, Shu Lin, Alexander R. Parent, Gary W. Brudvig and Ken Sakai (2016) *Chem. Comm.* **53**, submitted.

Model Dyes for the Study of Molecule/Metal Oxide Semiconductor Interfaces and Electron Transfer Processes

E. Galoppini,[a] R. A. Bartynski,[b] L. Gundlach,[c,d]
A. Batarseh,[a] H. Fan,[a] S. Rangan,[b] J. Nieto-Pescador[c], B. Abraham[d]

[a]Chemistry Department, Rutgers University-Newark, Newark, NJ 07102; [b]Department of Physics and Astronomy, Rutgers University-New Brunswick, Piscataway, NJ 08854
[c]Department of Physics and Astronomy, University of Delaware, Newark, DE 19716
[d]Department of Chemistry and Biochemistry, University of Delaware, Newark, DE 19716

The interface between nanostructured metal oxide semiconductors, primarily TiO_2 and ZnO, and chromophoric compounds is important in solar photochemical energy conversion and photocatalysis. Despite the fact that such hybrid organic-inorganic systems have been studied for decades, a molecular-level understanding of heterogeneous charge transfer processes and the ability to control electron injection and recombination remain, to a large extent, elusive.

As part of our interest in using molecular design to study molecules/semiconductor interfaces, and tune important parameters that influence charge transfer, we have started addressing the role played by interface dipoles. On transition metal oxide semiconductors, the adsorption of structurally simple molecules that form polar layers was found to shift the position of the semiconductor conduction band, and the change in dipole moment accompanying sensitizer oxidation has been reported to influence the open-circuit photovoltage in dye-sensitized solar cells.

To study this effect, porphyrin-bridge-anchor compounds with a dipole in the bridge that, when bound to TiO_2 or ZnO is aligned parallel or antiparallel to the semiconductor surface normal, were synthesized. The dipole in the bridge, introduced using NMe_2 (electron donor) and NO_2 (electron acceptor) groups enabled us to probe the dipole influence on the energy level alignment between the semiconductor and the chromophore. Compounds **1** and **3** formed a monolayer and an electrostatic potential that shifted the HOMO and LUMO of the porphyrin chromophore by (±) ~100 meV with respect to the band edges of the ZnO(11$\bar{2}$0) surface, when compared with **2**, as in **Fig.1**.

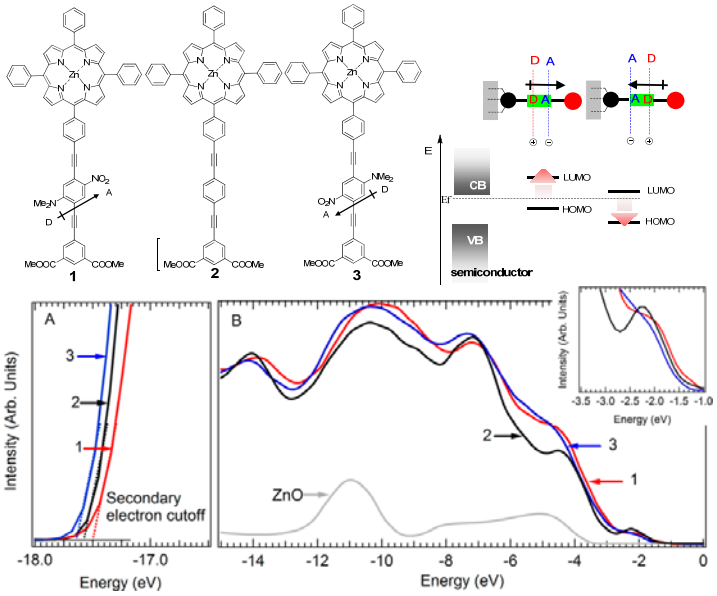

Fig. 1. *Top.* The compounds and schematic representation of energy level shifts. UPS spectra of the pristine ZnO(11−20) surface (gray), and of the same surface functionalized with 1 (red), 2 (black) or 3 (blue). (**A**) Secondary electron cutoff. (**B**) Valence band region; inset: zoomed-in plot of the position of the molecular HOMO.

When the direction of the dipole in the linker was reversed, the shift direction was reversed by the same amount.

Electron injection for **1**, **2**, and **3** bound to nanostructured TiO_2 films was studied by femtosecond transient absorption spectroscopy in solution and adsorbed on a TiO_2 nanostructured film in a vacuum, to probe whether the dipole influences charge transfer. In solution, a slow relaxation pathway competing with S_2–S_1 internal conversion was attributed to energy transfer from the photoexcited porphyrin to the *p*-nitro aniline group in the linker. On the TiO_2 film, heterogeneous electron injection from the S_2 state was found to occur in 80 fs, much faster than all intramolecular pathways. Despite a difference of 200 meV in level alignment of the excited state with respect to the semiconductor conduction band, identical electron-transfer times were measured for **1** and **3, Fig. 2**. This result, consistent with a previously published theoretical and experimental work for heterogeneous electron transfer, suggests the formation of a transient transition state during the first tens of femtoseconds of the reaction that is different from the surface density of states found from equilibrium calculations. This short-lived configuration governs the density of acceptor states and, consequently, the dynamics. Our progress towards compounds with different chromophores, and with stronger, better aligned bridge dipoles, will be discussed.

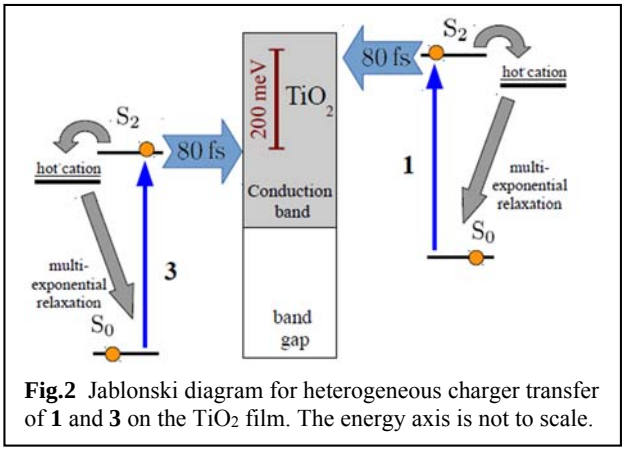

Fig.2 Jablonski diagram for heterogeneous charger transfer of **1** and **3** on the TiO_2 film. The energy axis is not to scale.

To increase the dipole effect we started exploring a "mixed layer" approach where molecules with chromophoric head groups are co-deposited with closely packed dipoles (**Fig. 3**). We have tested this approach synthesizing dipole-linkers with $Si(Me)_3$ head groups so that the dipole-induced shifts can be monitored via energy shifts of the Si 1s core level. Initial results using valence band photoemission show encouraging agreement between the measured and calculated densities of state of the molecules.

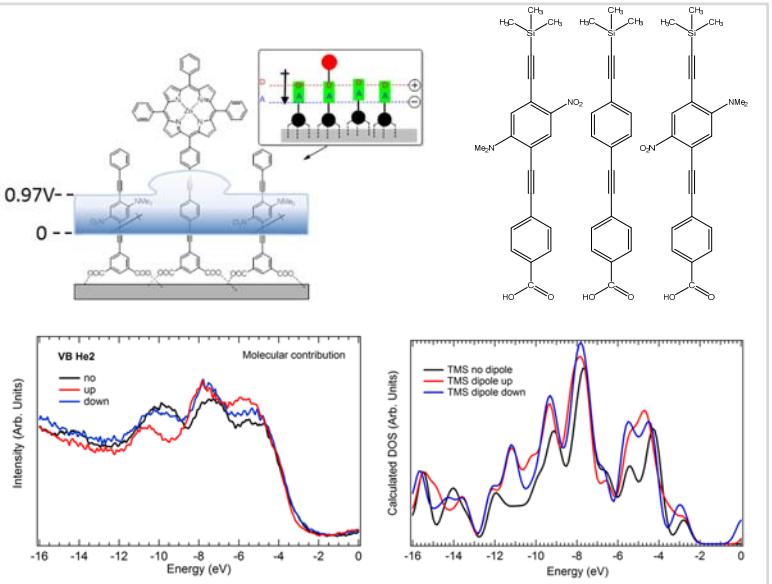

Fig. 3 (***Upper Left***) Illustration of the mixed layer approach. Shaded region illustrates that the electrostatic potential change across the molecular layer is realized at the chromophore. (***Upper Right***) HLAs with trimethylsilyl head groups used in initial tests of the mixed approach. Measured (***Lower Left***) and calculated (***Lower Right***) DOS for these molecules deposited on the TiO_2(110) surface.

DOE Sponsored Publications 2013-2016

1. *Heterogeneous Electron Transfer Dynamics via Dipole-Bridge Groups* Nieto-Pescador, Jesus; Abraham, Baxter; Li, Jingjing; Batarseh, Alberto; Bartynski, Robert; Galoppini, Elena; Gundlach, Lars *J. Phys. Chem. C*, **2016**, *120,* 48-55. DOI: 10.1021/acs.jpcc.5b09463.
2. *Photoelectrochemical Properties of Porphyrin Dyes with a Molecular Dipole in the Linker* K.T. Ngo, J. Rochford, H. Fan, A. Batarseh, K. Chitre, S. Rangan, R. A. Bartynski, E. Galoppini *Faraday Discussions,* **2015***, 185,* 497-506. DOI: 10.1039/c5fd00082c.
3. *Synthesis of Zinc Tetraphenylporphyrin Rigid-Rods with a Built-in Dipole* K. Chitre, A. Batarseh, A. Kopecky, H. Tang, R. Lalancette, R. A. Bartynski, E. Galoppini **Miller/Newton JPC Festschrift**, *J. Phys. Chem. B*, **2015**, *119*, 7522-7530 http://dx.doi.org/10.1021/jp5112982
4. *Tuning Energy Level Alignment At Organic/Semiconductor Interfaces Using a Built-In Dipole in Chromophore–Bridge–Anchor Compounds* S. Rangan, A. Batarseh, K. P. Chitre, A. Kopecky, E. Galoppini, R. A. Bartynski *J. Phys. Chem. C* **2014**, *118*, 12923-12928 DOI: 10.1021/jp502917c
5. *Energy Level Alignment of Polythiophene/ZnO Hybrid Solar Cells* Feng, W.; Rangan, S.; Cao, Y.; Galoppini, E.; Bartynski, R.; Garfunkel R. *J. Mater. Chem. A* **2014**, *2*, 7034-7044. DOI: 10.1039/C4TA00937A.
6. *Homoleptic "Star" Ru(II) Polypyridyl Complexes: Shielded Chromophores to Study Charge-Transfer at the Sensitizer-TiO_2 Interface*, P.G. Johansson, Y. Zhang, G.J. Meyer and E. Galoppini, *Inorg. Chem.,* **2013**, *52* , 7947-7957 DOI: 10.1021/ic4004565
7. *Distance Dependent Electron Transfer at TiO_2 Interfaces Sensitized with Phenylene Ethynylene Bridged RuII-Isothiocyanate Compounds* P. G. Johansson, A. Kopecky, E. Galoppini, G. J. Meyer *J. Am. Chem. Soc.*, **2013**, *135*, 8331-8341. DOI: 10.1021/ja402193f
8. *A sensitized Nb_2O_5 photoanode for hydrogen production in a dye sensitized photoelectrosynthesis cell* H.L. Luo, W.J. Song, P.G. Hoertz, K. Hanson, R. Ghosh, S. Rangan, M.K. Brennaman, J.J. Concepcion, R.A. Binstead, Robert Allen Bartynski, R. Lopez, and T.J. Meyer, Chem. Mater. **2013***, 25,* 122-131. DOI: 10.1021/cm3027972

Related Publications (non-DOE sponsored)

News&Views Commentary *Strike While the Iron is Cold* E. Galoppini *Nature Chemistry* **2015**, *7*, 861-862. DOI: 10.1038/nchem.2373

Chemical Interaction, Space-Charge Layer, and Molecule Charging Energy for a TiO_2/TCNQ Interface, J. I. Martínez, F. Flores, J. Ortega, S. Rangan, C. Ruggieri, and R.A. Bartynski, *J. Phys Chem. C* **2015**, *119*, 22086. DOI: 10.1021/acs.jpcc.5b07045.

Densely Packed ZnTPPs Monolayer on a Rutile TiO_2(110) surface: Adsorption Behavior and Energy Level Alignment, S. Rangan, C. Ruggieri, and R.A. Bartynski, J. I. Martínez, F. Flores, J. Ortega, *J. Phys Chem. C* **2016***, 120*, 4430. DOI: 10.1021/acs.jpcc.5b12736

Electron Transfer and Transport by Delocalized Charges

T. Mani, M.J. Bird, A.R. Cook, L. Zaikowski, R. Holroyd, M.D. Newton, D.C. Grills, J. Bakalis, G. Mauro, X. Li., G. Rumbles, J. Blackburn, O.G. Reid and J.R. Miller

Chemistry Department
Brookhaven National Laboratory
Upton, NY 11973

Delocalization is a key concept in light-driven energy capture. We will argue that delocalization can regulate electron transfer rates and transport of electrons and holes along conjugated chains and in solid films. We further suggest its potential for huge impacts in enhancing escape of electrons and holes from each other by a) reducing Coulomb attraction and b) making the Marcus inverted effect a more powerful regulator of highly exoergic charge recombination.

Delocalization of DA Polymers Donor-Acceptor or "push-pull" conjugated polymers are widely used to obtain red-absorbing, wide bandgap polymers for organic photovoltaics (OPV). DA structures are widely believed to promote localization of charges, which could have the undesirable effect of reducing their mobilities. We added electrons or holes to the DA polymer F8BT in a variety of environments. In THF solution $F8BT^{\bullet-}$ created by chemical doping was localized to one repeat unit, and the optical spectrum did not contain the strong "P_1" band characteristic of delocalized charges, but a weak transition identified as a charge transfer (CT) transition to neighboring BT groups. The Na^+ counter-ion, which played a role in the localization, so slightly more delocalized charges were seen with Na^+ encapsulated in a cryptand or without a counter-ion. $F8BT^{\bullet+}$ had more delocalized charges and a reasonably strong P_1 band. Holes created on F8BT in benzene by pulse radiolysis showed transient microwave conductivity (Figure 1) signals nearly as large as those in delocalized conjugated polymers like polyfluorenes. The signals for electrons were smaller, but by less than a factor of three. These measurements show that intrachain charge transport can be substantial in DA polymers, but the nature of medium is critical.

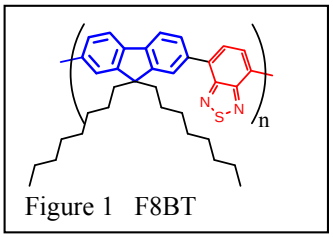

Figure 1 F8BT

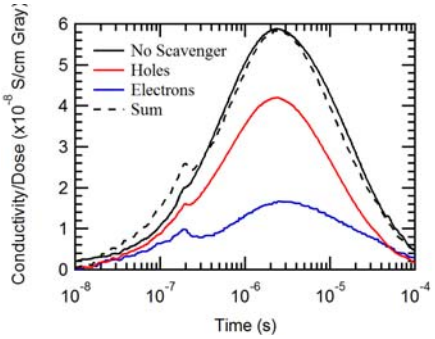

Figure 2 Transient microwave conductivity in benzene solution for for electron, holes and both in F8BT compared to the sum of electron and hole signals.

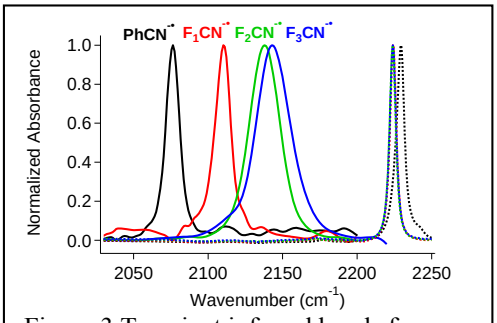

Figure 3 Transient infrared bands from radical anions of benzonitrile and fluorene-nitriles, F_nCN (n=1-3) compared to the nitrile bands in the neutrals (right).

Probing Localization/Delocalization by Vibrational Spectroscopy Figure 3 shows infrared absorption bands measured by transient IR (TRIR) of nitriles which shift

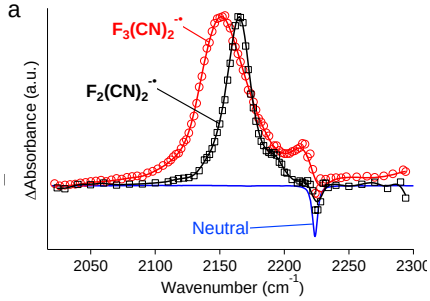

Figure 4 Transient infrared bands from radical anions of fluorene oligomers containing nitrile groups at opposite ends.

upon addition of an electron by an amount that reflects electron density on the CN group. In $F_n(CN)_2$ (n=1-3) which have two CN groups at opposite ends of oligomers of 1-3 fluorenes TRIR of the anions displays two nitrile absorption bands (Figure 4), along with the bleach of the CN neutral. This result shows that relaxation breaks the symmetry of the molecules creating one CN with a larger electron density than the other.

Effect of Dihedral Angles on Barriers to Charge and Exciton Transport The possibility that dihedrals may limit transport due to higher barriers for singlets point to triplet transport as an interesting and potentially important subject to enable basic understanding of transport. Fortunately pulse radiolysis offers abilities to rapidly create triplets in molecules having low triplet quantum yields. That ability, including fast creation of triplets, possibly without singlet precursors, is under investigation in another part of our program. While it is only partly understood, it enabled observations that triplets in (pF) chains completely span pF chains with lengths to >100 repeat units. Although the method could say only that this transport occurred in <1 μs, earlier results found transport in <40 ns, and current results suggest it may be much faster. New methods will perform measurements with high time resolution, and will seek to couple understanding of exciton transport with charge transport. The current results on triplets showed that defects were rare in the pF chains and measured of the completeness of end capping by acceptor groups.

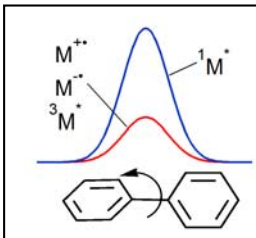

Figure 5 Barrier heights for holes, electrons and excitons.

Outracing the Diffusion-Controlled Limit for Electron Transfer Radiation chemistry methods also observe the inverted region for bimolecular electron transfer reactions, where the free energy change can be continuously adjusted over a range of ~300 meV. The rate vs. ΔG° relation is free from the effects of the diffusion-controlled limit due to the very high mobilities of the electrons in these fluids.

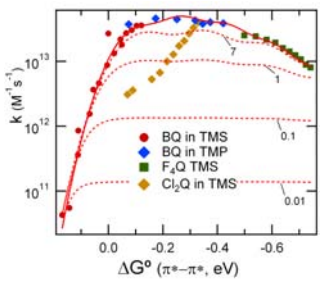

Figure 6 Rate constants for bimolecular electron to benzoquinone (BQ) and derivatives in (TMS) tetramethylsilane and (TMP) 2,2,4-trimethylpentane.

Ion Pairing and Redox Potentials Without Electrolyte

We propose that understanding of ion pairing can be the key to a long-sought goal to determine redox potentials in the absence of electrolyte. Redox potentials are of tremendous value for determination of energetics of electron transfer in photosynthesis, dye-sensitized solar cells and organic photovoltaics, although none of those energy conversion systems contain the high concentrations of electrolytes needed for the electrochemical measurements. While essential, we know that the electrolytes substantially alter the measured values in ways that are imperfectly understood, so substantial efforts have sought to determine what their effect is, but closure to obtain well-defined potentials with no electrolyte has been fraught with difficulties.

Here we employ the technique of pulse radiolysis which can add electrons or holes to molecules in media ranging from water to non-polar liquids like alkanes. A principal method determines equilibrium constants for electron transfer, $D^{\bullet-} + A \rightleftharpoons D + A^{\bullet-}$, in the presence of electrolyte at concentrations from 100 mM to a few μM to zero.

DOE Sponsored Publications 2013-2016

1. Hack, J.; Grills, D. C.; Miller, J. R.; Mani, T. "Identification of Ion-Pair Structures in Solution by Vibrational Stark Effects", *J. Phys. Chem. B,* **2016**, *120*, 1149-1157.
2. Zaikowski, L.; Mauro, G.; Bird, M.; Karten, B.; Asaoka, S.; Wu, Q.; Cook, A. R.; Miller, J. R. "Charge Transfer Fluorescence and 34 nm Exciton Diffusion Length in Polymers with Electron Acceptor End Traps", *J. Phys. Chem. B,* **2015**, *119*, 7231-7241.
3. Sanders, S. N.; Kumarasamy, E.; Pun, A. B.; Trinh, M. T.; Choi, B.; Xia, J.; Taffet, E. J.; Low, J. Z.; Miller, J. R.; Roy, X.; Zhu, X. Y.; Steigerwald, M. L.; Sfeir, M. Y.; Campos, L. M. "Quantitative Intramolecular Singlet Fission in Bipentacenes", *J. Am. Chem. Soc.,* **2015**, *137*, 8965-8972.
4. Mani, T.; Grills, D. C.; Newton, M. D.; Miller, J. R. "Electron Localization of Anions Probed by Nitrile Vibrations", *J. Am. Chem. Soc.,* **2015**, *137*, 10979-10991.
5. Mani, T.; Grills, D. C.; Miller, J. R. "Vibrational Stark Effects to Identify Ion Pairing and Determine Reduction Potentials in Electrolyte-Free Environments", *J. Am. Chem. Soc.,* **2015**, *137*, 1136-1140.
6. Li, X.; Bird, M.; Mauro, G.; Asaoka, S.; Cook, A. R.; Chen, H.-C.; Miller, J. R. "Transport of Triplet Excitons Along Continuous 100 nm Polyfluorene Chains", *J. Phys. Chem. B,* **2015**, *119*, 7210-7218.
7. Busby, E.; Xia, J.; Wu, Q.; Low, J. Z.; Song, R.; Miller, J. R.; Zhu, X. Y.; Campos, L. M.; Sfeir, M. Y. "A Design Strategy for Intramolecular Singlet Fission Mediated by Charge-Transfer States in Donor-Acceptor Organic Materials", *Nat. Mater.,* **2015**, *14*, 426-433.
8. Bird, M.; Mauro, G.; Zaikowski, L.; Li, X.; Reid, O.; Karten, B.; Asaoka, S.; Chen, H.-C.; Cook, A. R.; Rumbles, G.; Miller, J. R. In *Physical Chemistry of Interfaces and Nanomaterials Xiv*; Hayes, S. C., Bittner, E. R., Eds. 2015; Vol. 9549.
9. Miller, J. R. "Electron Transfer Lower Tunnel Barriers", *Nature Chemistry,* **2014**, *6*, 854-855.
10. Mani, T.; Miller, J. R. "Role of Bad Dihedral Angles: Methylfluorenes Act as Energy Barriers for Excitons and Polarons of Oligofluorenes", *J. Phys. Chem. A,* **2014**, *118*, 9451-9459.
11. Holroyd, R.; Miller, J. R.; Cook, A. R.; Nishikawa, M. "Pressure Tuning of Electron Attachment to Benzoquinones in Nonpolar Fluids: Continuous Adjustment of Free Energy Changes", *J. Phys. Chem. B,* **2014**, *118*, 2164-2171.
12. Bird, M. J.; Reid, O. G.; Cook, A. R.; Asaoka, S.; Shibano, Y.; Imahori, H.; Rumbles, G.; Miller, J. R. "Mobility of Holes in Oligo- and Polyfluorenes of Defined Lengths", *J. Phys. Chem. C,* **2014**, *118*, 6100-6109.
13. Bakalis, J.; Cook, A. R.; Asaoka, S.; Forster, M.; Scherf, U.; Miller, J. R. "Polarons, Compressed Polarons, and Bipolarons in Conjugated Polymers", *J. Phys. Chem. C,* **2014**, *118*, 114-125.
14. Zamadar, M.; Cook, A. R.; Lewandowska-Andralojc, A.; Holroyd, R.; Jiang, Y.; Bikalis, J.; Miller, J. R. "Electron Transfer by Excited Benzoquinone Anions: Slow Rates for Two-Electron Transitions", *J. Phys. Chem. A,* **2013**, *117*, 8360-8367.
15. Zamadar, M.; Asaoka, S.; Grills, D. C.; Miller, J. R. "Giant Infrared Absorption Bands of Electrons and Holes in Conjugated Molecules", *Nature Comm.,* **2013**, *4*.
16. Johnson, J. C.; Akdag, A.; Zamadar, M.; Chen, X.; Schwerin, A. F.; Paci, I.; Smith, M. B.; Havlas, Z.; Miller, J. R.; Ratner, M. A.; Nozik, A. J.; Michl, J. "Toward Designed Singlet Fission: Solution Photophysics of Two Indirectly Coupled Covalent Dimers of 1,3-Diphenylisobenzofuran", *J. Phys. Chem. B,* **2013**, *117*, 4680-4695.
17. Cook, A. R.; Bird, M. J.; Asaoka, S.; Miller, J. R. "Rapid "Step Capture" of Holes in Chloroform During Pulse Radiolysis", *J. Phys. Chem. A,* **2013**, *117*, 7712-7720.
18. Bao, J.; Yu, Z.; Gundlach, L.; Benedict, J. B.; Coppens, P.; Chen, H. C.; Miller, J. R.; Piotrowiak, P. "Excitons and Excess Electrons in Nanometer Size Molecular Polyoxotitanate Clusters: Electronic Spectra, Exciton Dynamics, and Surface States", *J. Phys. Chem. B,* **2013**, *117*, 4422-4430.

Session V

Natural and Biomimetic Energy Transduction

Fundamental Studies and Engineering of Biological Modules Involved in Photosynthetic Energy Capture and Conversion

Cheryl A. Kerfeld
MSU-DOE Plant Research Laboratory and Department of Biochemistry and Molecular Biology, Michigan State University, East Lansing MI 48824 and Molecular Biophysics and Integrated Bioimaging Division, Lawrence Berkeley National Laboratory, Berkeley, CA,

Dissociating the complexity of photosynthetic processes into modules is a shift in perspective from the single gene/gene product to discrete functional and evolutionary units (1). Modules can be defined as semi-autonomous functional units, with relatively strong intramodule functional connectivity among components and weaker, yet important, inter-module connections. Modules are generally components or subsystems of a larger system and can be combined with other modules to give rise to new functions. When viewing the levels of biological organization through this conceptual lens, modules are found across the continuum: domains within proteins, co-regulated groups of functionally associated genes, operons, metabolic pathways, and (sub)cellular compartments. By virtue of their potential for "plug and play" into new contexts, modules can be viewed as units of both evolution and engineering, including the re-purposing for new functions. By coupling modular thinking with the technical advances that have made large scale DNA fabrication affordable, the prospects of engineering organisms by installing new functional modules becomes attainable. Two different biological processes, the control of photoprotection by a modular carotenoid binding protein and spatial compartmentalization of carbon fixation will be used to as illustrations.

The conversion of solar into chemical energy by plants and cyanobacteria is essential to life on earth. However when the amount of light energy exceeds the capacity of the photosystems, widespread cellular damage results. Photoprotective mechanisms play a crucial role in the ecophysiology of cyanobacteria which inhabit a range of environments where stresses like extreme temperature fluctuations, salinity and drought exacerbate the threat of photodamage. The soluble Orange Carotenoid Protein (OCP) and the Fluorescence Recovery Protein (FRP) function together as the on/off switch for photoprotection in cyanobacteria. The OCP is the only known photoactive protein that uses a carotenoid as the photoreceptor. The OCP is a modular protein; the C-terminal domain functions as a sensor/regulatory domain, responding to light or to the FRP whereas the N-terminal domain is the effector, dissipating excess energy at the level of the antenna (2,3). Bioinformatically we have identified multiple clades of the discretely encoded effector and sensor domains (Melnicki et al., submitted); we posit that different combinations of protein domains and carotenoids allow for a tunable switch for a dynamic range of photoprotective responses. We have recently determined the crystal structure of the isolated N-terminal domain which is a constitutively active quencher (4). Remarkably, in comparison to the resting form of the protein, the carotenoid has shifted position by more than 12Å. By dissecting out the intramolecular structural determinants for light perception (e.g. pigment-protein interactions) and the intermolecular interactions that govern energy flow from the antenna in response to interaction with the OCP, we are learning mechanistic principles that can be used, for example, to develop light regulated switches for optogenetic applications.

Bacterial microcompartments (BMCs) such as carboxysomes illustrate biological modularity at

another scale, that of a multienzyme-containing proteinaceous organelle. The carboxysome is a self-assembling metabolic module for CO_2 fixation found in all cyanobacteria. These large (~100-500 nm) polyhedral bodies sequester Carbonic Anhydrase and RuBisCO within a protein shell, thereby concentrating substrates and protecting RuBisCO from oxygen generated by the light reactions.

Because carboxysomes and other BMCs function to organize reactions that require special conditions for optimization, including the sequestration of substrates, cofactors, or toxic intermediates and the protection of oxygen sensitive enzymes, they have received considerable attention as templates for synthetic nanoreactors in bioengineering (5). There are two central challenges to building bespoke protein-based nanoreactors, design and assembly of multi-enzyme cores and engineering of the shell proteins to serve as a selectively permeable barrier, the interface between the cytosol and the encapsulated reactions.

We have recently demonstrated proof-of-concept for an approach to engineering BMC catalytic cores. To engineer the carboxysome, its catalytic core can be viewed as a collection of interacting protein domains. Using knowledge of the sequence of protein domain interactions in the course of carboxysome biogenesis, a single chimeric protein was designed that functionally replaces four different gene products in carboxysome assembly (6). Only a subset of the native complement of protein domains in the carboxysome core was selected and their coding sequences fused together in a specific order to create a synthetic gene. Notably, the design of the synthetic core protein rendered some of the native protein domains dispensable, thereby reducing the amount of DNA needed. Moreover, it reduced the number of genes necessary to form a carboxysomes core from four to one. The resulting streamlined carboxysomes were shown to support photosynthesis in cyanobacteria. This approach can be broadly applied to the development of diverse multienzyme nanoreactor cores. Given that protein domains are the structural, functional and evolutionary units of proteins, we propose that (re)engineering BMCs and other large multi-protein macromolecular assemblies may be more readily tractable by focusing on domain structures and interactions rather than genes, leveraging the inherent modularity of proteins for building new subcellular architectures.

Successful designs for metabolic nanocompartments also require a selectively permeable protein shell that provides both a barrier to and an interface with the rest of the cellular environment. Naturally occurring BMC shells are thought to be passive barriers to the bulk cytosol. We recently engineered functionality into a shell protein, inserting an FeS cluster binding site to allow electrons to be conducted across the shell. The conversion of a passive barrier into a redox active membrane represents a major advance in the construction of tailor-made nanoreactors for biotechnological applications that can be connected via electron reactions with the rest of metabolism.

DOE Sponsored Publications 2014-2016

1. Kerfeld, C.A. Plug and Play for Improving Primary Productivity. American Journal of Botany 102: 1949-50, 2015.

2. Leverenz, R.L., Jallet, D., Li, M., Mathies, R.A., Kirilovsky, D. and Kerfeld, C.A. Structural and Functional Modularity of the Orange Carotenoid Protein: Distinct Roles for the N- and C-

terminal Domains in Cyanobacterial Photoprotection. Plant Cell 26: 426-437, 2014.

3. Gupta, S., Guttman, M., Leverenz, R.L., Zhumadilova, K., Pawlowski, E.G., Petzold, C.J., Lee, K.K., Ralston, C. and Kerfeld, C.A. Local and Global Structural Drivers for the Photoactivation of the Orange Carotenoid Protein. Proceedings of the National Academy of Sciences, USA 112: E5567-5574, 2015.

4. Leverenz, R.L., Sutter, M. Wilson, A., Gupta, S., Thurotte, A., Bouncier de Carbon, C. Perreau, F., Petzold, C.J., Ralston, C., Kirilovsky, D. and Kerfeld, C.A. A carotenoid translocation activates photoprotection in cyanobacteria. Science 348: 1463-1466, 2015.

5. Gonzalez-Esquer, C.R., Newnham, S.E. and Kerfeld, C.A. Bacterial Microcompartments as Metabolic Modules for Plant Synthetic Biology. Plant Journal, in press.

6. Gonzalez-Esquer, C.R., Shubitowski, T.B. and Kerfeld, CA. Streamlined construction of the cyanobacterial CO2-fixing organelle via protein domain fusions for use in plant synthetic biology. Plant Cell 27: 2637-2644, 2015.

7. Aussignargues, C., Pandelia, M-E., Sutter, M., Plegaria, J.S., Zarzycki, J., Turmo, A., Huang, J., Ducat, D.C., Hegg, E.L., Gibney, B.R. and Kerfeld, C.A. Structure and function of a bacterial microcompartment shell protein engineered to bind a [4Fe-4S] cluster. Journal of the American Chemical Society in press.

Modular homogeneous and framework photocatalyst assemblies

Karen L. Mulfort, Oleg G. Poluektov, Lin X. Chen, Lisa M. Utschig, David M. Tiede
Division of Chemical Sciences and Engineering
Argonne National Laboratory
Argonne, IL 60439

This program investigates the self-assembly of molecular chromophores and catalysts into complex architectures which are capable of coupling one-electron photoinduced excited states to multi-electron charge accumulation and ultimately, multi-electron redox catalysis. A modular approach enables the integration of molecular components into different types of self-assembled structures and a unique comparison of how the linking chemistry and environment impacts the primary steps required for solar energy conversion. This talk will specifically focus on the integration and characterization of chromophore and catalyst molecular modules in 1) homogeneous supramolecular assemblies and 2) metal-organic frameworks. A highlight of this program is the close interaction of targeted synthesis with high-resolution physical characterization of the ground and excited states using techniques including transient optical spectroscopy, multi-frequency EPR, X-ray absorption spectroscopy, and X-ray scattering. We anticipate that these studies will inform the design of advanced photocatalyst architectures based on molecular modules.

Supramolecular photocatalyst assemblies. We have focused on the use of $[Ru(bpy)_3]^{2+}$ and cobaloximes as chromophore and catalyst modules in the design of homogeneous supramolecular photocatalyst assemblies (Figure 1). Previous work from our group and others has demonstrated that chromophore coordination directly to the cobalt center of the catalyst module leads to fast back electron transfer and provides no significant increase in photocatalytic efficiency as compared to multimolecular photocatalyst systems. A new linked photocatalyst design which features Co(II)-templated assembly does in fact show ultrafast charge separation from the chromophore to catalyst module, although it is rather short-lived to initiate proton reduction. Work is in progress to incorporate modifications to the chromophore-catalyst link which will continue to facilitate photoinduced electron transfer and also stabilize the Co(I) state long enough for diffusional interaction with protons in solution.

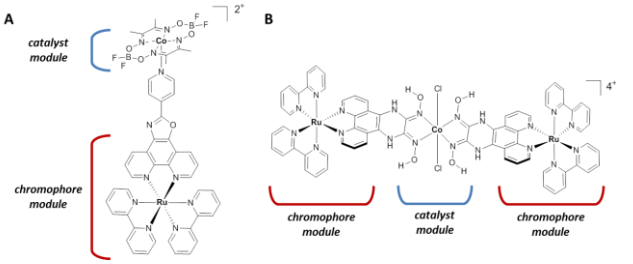

Figure 1. Structures of $[Ru(bpy)_3]^{2+}$-cobaloxime based assemblies using (A) axial coordination to Co(II) and (B) equatorial coordination through glyoxime ligand.

In efforts to incorporate earth-abundant chromophore modules into new photocatalyst assemblies, we have synthesized a series of heteroleptic Cu(I)bis(phenanthroline) chromophores and fully characterized their ground and

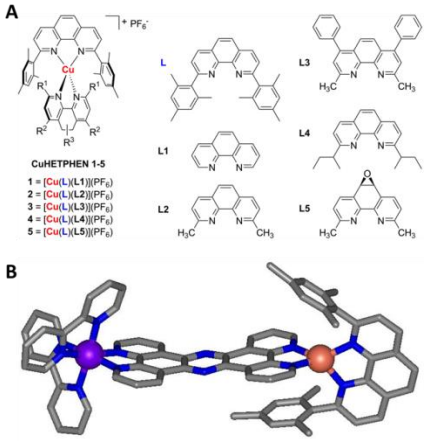

Figure 2. A) Chemical structures of model heteroleptic Cu(I) chromophores. B) Crystal structure of phenazine-linked bimetallic Ru(II)—Cu(I) chromophore for directional photoinduced electron transfer.

excited states (Figure 2A). The excited state lifetime can be tuned over two orders of magnitude, up to 74 ns in acetonitrile, by modification of the phenanthroline ligand sterics adjacent to the Cu(I) center. Preliminary work in linking these heteroleptic Cu(I) chromophores to catalyst modules as well as to modules with complimentary excited state properties to drive directional electron transfer (Figure 2B) will be presented.

Photo-active metal-organic frameworks. Because of their chemical diversity and crystallinity, MOFs present an important opportunity to study photoinduced electron transfer and charge separation in an extended array of chromophore and catalyst modules with atomic-level precision. In order to understand the impact of structural factors unique to MOFs on light-driven electron transfer and charge separation, there is a need to develop new structures which feature the same modules in various coordination geometries. Recent work from our lab demonstrates how MOF synthesis conditions can be used to manipulate the spatial organization of potential chromophore and catalyst modules. Two new bimetallic MOFs were obtained from the self-assembly of $[Ru_3(\mu_3\text{-}O)(OAc)_6(pyCOOH)]^+$ (pyCOOH = isonicotinic acid) with Co(II) under typical synthesis conditions (Figure 3). **RuCo-1** features two dimensional sheets of $[Ru_3O(OAc)_6(pyCOO)_3]^{2-}$ coordinated through carboxylate groups to a linear Co_3 node formed *in situ*. A slight increase in synthesis temperature yields **RuCo-2**, a three-dimensional structure with the same Co_3 nodes as **RuCo-1**, but the increased temperature has resulted in Ru_3O ligand scrambling and formation of a new extended strut composed of a central Ru_3O coordinated to six additional Ru_3O modules. This unit in particular is potentially very important in supporting sequential and accumulative charge separation given its multiple accessible oxidation states and demonstrated mixed valency in analogous homogeneous supramolecular assemblies.

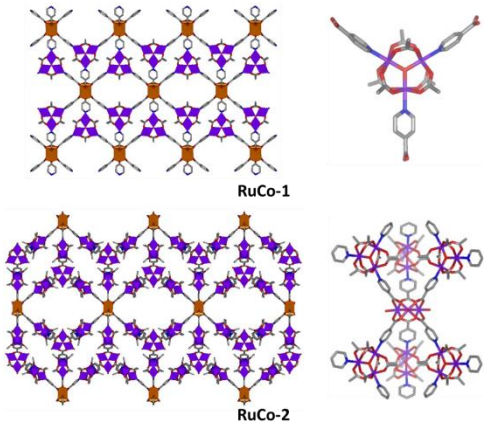

Figure 3. Crystal structure packing diagram of bimetallic MOFs (left) and detail of Ru_3O strut connectivity (right).

Preliminary work has yielded the incorporation of the well-studied molecular electron donor-acceptor modules $[Ru(bpy)_3]^{2+}$ and diquat (DQ^{2+}) into an Al(III)-based MOF (Figure 4). Stepwise post-synthetic modification was used to generate a core-shell MOF structure with $[Ru(bpy)_3]^{2+}$ chromophores decorating the exterior struts of the crystallites and diquat (DQ^{2+}) lining the core. The structure was confirmed by a number of techniques including UV-Vis, ICP, PXRD, and X-ray absorption spectroscopy. Room temperature X-band EPR of the core-shell MOF under visible illumination demonstrates that charge separation from Ru* to DQ^{2+} persists on the order of seconds. We are currently investigating pathways for coupling this long-lived multi-electron charge accumulation to multi-electron redox catalysis.

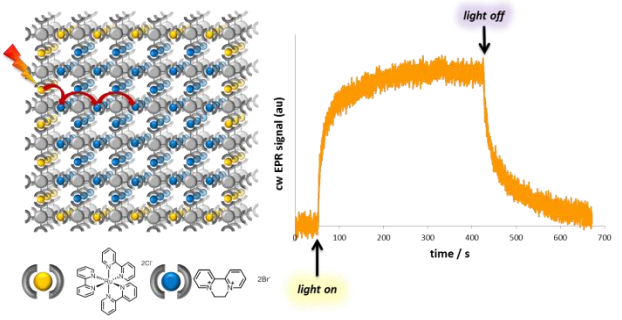

Figure 4. Left: depiction of core-shell MOF with $[Ru(bpy)_3]^{2+}$ struts lining the exterior struts and DQ^{2+} core struts. Right: X-band EPR time plot of $DQ^{\cdot+}$ signal in response to visible excitation.

DOE Sponsored Publications 2013-2016

1. K. L. Mulfort, A. Mukherjee, O. Kokhan, P. Du, D. M. Tiede. Structure-based analyses of solar fuels catalysts using in situ X-ray scattering, *Chem. Soc. Rev.*, **2013**, *42*, 2215-2227. *Inside cover.*

2. A. Mukherjee, O. Kokhan, J. Huang, J. Niklas, L. X. Chen, D. M. Tiede, K. L. Mulfort. Detection of a charge-separated catalyst precursor state in a linked photosensitizer-catalyst assembly, *Phys. Chem. Chem. Phys.*, **2013**, *15*, 21070-21076. Selected as a HOT article on PCCP blog, 18 November 2013.

3. S. Li, Y.-S. Chen, K. L. Mulfort. Synthetic control over structure in bimetallic Ru(III)-Co(II) metal-organic frameworks, *CrystEngComm*, **2015**, *17*, 1005-1009.

4. S. R. Soltau, J. Niklas, P. D. Dahlberg, D. M. Tiede, O. G. Poluektov, K. L. Mulfort, L. M. Utschig. Aqueous light-driven hydrogen production by a Ru-Ferredoxin-Co biohybrid, *Chem. Commun*., **2015**, *51*, 10628-10631.

5. O. Kokhan, N. Ponomarenko, R. Pokkuluri, M. Schiffer, K. L. Mulfort, D. M. Tiede. Characterizing photoinduced electron transfer in Ruthenium(II)-tris-bipyridyl modified PpcA, a multi-heme c-type cytochrome from Geobactor sulfurreducens, *J. Phys. Chem. B*, **2015**, *119*, 7612-7624 (John R. Miller and Marshall D. Newton Festschrift).

6. J. Huang, Y. Tang, K. L. Mulfort, X. Zhang. The direct observation of charge separation dynamics in CdSe quantum dots/cobaloxime hybrids, *Phys. Chem. Chem. Phys*., **2016**, *18*, 4300-4303.

7. L. Kohler, D. Hayes, J. Hong, T. J. Carter, M. L. Shelby, K. A. Fransted, L. X. Chen, K. L. Mulfort. Synthesis, structure, ultrafast kinetics, and light-induced dynamics of CuHETPHEN chromophores, *Dalton Trans*., **2016**, DOI: 10.1039/C6DT00324A. (Invitation to special issue for New Talent: Americas)

8. K. L. Mulfort. Interrogation of cobaloxime-based supramolecular photocatalyst architectures, *Comptes Rendus Chimie*, **2016**, DOI: 10.1016/j.crci.2015.12.010. (Invitation to special issue on Artificial Photosynthesis)

9. K. L. Mulfort, L. M. Utschig. Modular homogeneous chromophore-catalyst assemblies, *Acc. Chem. Res*., **2016**, *accepted*.

Long-lived Charge Generation in Semiconducting Single-walled Carbon Nanotubes

Jeff Blackburn, Rachelle Ihly, Andrew Ferguson, Obadiah Reid, Anne-Marie Dowgiallo, Kevin Mistry, Jaehong Park, Tyler Clikeman, Bryon Larson, Olga Boltalina, Steven Strauss, Philip Schulz, Joseph Berry, Justin Johnson, Garry Rumbles
Chemistry and Nanoscience Center
National Renewable Energy Laboratory
Golden, CO 80401

Semiconducting single-walled carbon nanotubes (s-SWCNTs) are attractive absorbers for use in solar energy harvesting schemes because of their strong and energetically tunable optical absorption, and high charge carrier mobilities due to the delocalized π-electron system. Beyond their technological potential, s-SWCNTs offer attractive properties for fundamental studies of charge generation in strongly confined nanoscale systems and photoinduced electron transfer (PET) processes. For example, strong quantum confinement and low dielectric screening impart single-walled carbon nanotubes with exciton-binding energies substantially exceeding k_BT at room temperature. Despite these large binding energies, reported luminescence quantum yields are typically low and some studies suggest that photoexcitation of SWCNT excitonic transitions can produce free charge carriers. Additionally, s-SWCNTs are unique organic semiconductors, in that they are relatively stiff pi-conjugated molecules with highly delocalized charge carriers (in contrast with typical semiconducting polymers that are dominated by polaron transport). These attributes imply that charges on s-SWCNTs should cause minor perturbations to bond lengths, making s-SWCNTs a model system to search for low PET reorganization energies. Finally, the energetically narrow and distinct spectroscopic signatures for excitons and charges within s-SWCNT thin films enables the unambiguous temporal tracking of fundamental photophysical processes occuring at important photoactive heterojunctions designed for charge separation. In this presentation, we discuss a number of studies that probe the generation and recombination of long-lived charges in samples consisting of s-SWCNTs with well-defined electronic structure. We focus on three distinct studies, with an emphasis on how important parameters influence charge separation and recombination, such as (1) the energetics of well-defined s-SWCNT interfaces, and (2) the high degree of carrier delocalization within s-SWCNTs.

Spontaneous Free Carrier Generation in s-SWCNTs in a low dielectric solvent

I will briefly discuss a study in which we use solution-phase time-resolved microwave conductivity to directly measure the generation of long-lived free charge carriers in chirality-pure (7,5) s-SWCNTs in a low dielectric solvent. The conditions of the microwave conductivity measurement allow us to avoid the complications of most previous measurements of nanotube free-carrier generation, including tube–tube/tube–electrode contact, dielectric screening by nearby excitons, and many-body interactions. The carrier-generation quantum yield under S_2 excitation is about three times higher than that under S_1 excitation, and the carriers are long-lived (hundreds of nanoseconds) irrespective of the excitonic level from which they originate.

Tuning the Driving Force for Exciton Dissociation at SWCNT Heterojunctions

In this study, we investigate the influence of the thermodynamic driving force for photoinduced electron transfer (PET) between s-SWCNTs and fullerene derivatives by employing time-resolved microwave conductivity as a sensitive probe of interfacial exciton dissociation. We

observe an apparent Marcus inverted regime and quantify low reorganization energies ($\lambda \approx 130–140$ meV, most of which likely arises from fullerenes) for SWCNT/fullerene donor/acceptor systems. The small measured reorganization energies indicate these systems may enable charge extraction with relatively low carrier energy loss, relative to some polymer/fullerene systems that exhibit much larger reorganization energies. The reorganization energy strongly depends on the extent of carrier localization, with delocalized carriers leading to lower perturbation of individual bonds, thus contributing to small λ. SWCNTs display increased rigidity and significantly higher carrier mobility relative to most conjugated polymers and enable a higher degree of carrier delocalization than fullerenes. As such, we suggest that charges in SWCNTs exhibit less polaronic character and hence less charge-induced lattice distortion, ultimately resulting in smaller reorganization energy than both typical conjugated polymers and fullerenes.

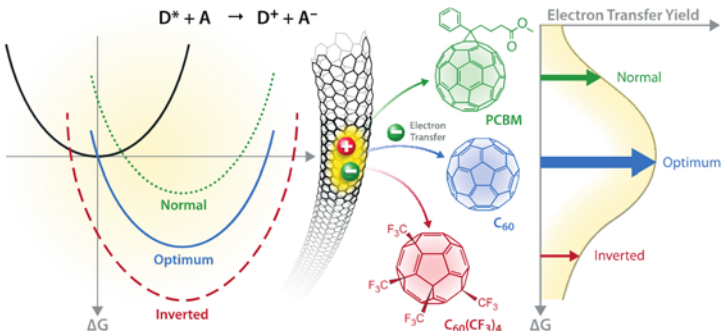

Figure 1. Schematic depicting the influence of driving force and reorganization energy on interfacial exciton dissociation in SWCNT/fullerene heterojunctions

Efficient Charge Extraction and Slow Recombination at Junctions Between Hybrid Perovskites and s-SWCNTs

Metal-halide based perovskite solar cells have rapidly emerged as a promising alternative to traditional inorganic and thin-film photovoltaics. Although charge transport layers are used on either side of perovskite absorber layers to extract photogenerated electrons and holes, the time scales for charge extraction and recombination are poorly understood. An important contributing factor to this uncertainty is the lack of *specific and narrow* spectral signatures for charges in traditional charge extraction layers. Here, we use time-resolved spectroscopy over many decades of time to demonstrate that highly enriched s-SWCNT thin films enable rapid (sub-picosecond) hole extraction from a prototypical perovskite absorber layer and extremely slow back-transfer and recombination (hundreds of microseconds). Photoelectron spectroscopy measurements suggest that the very slow loss of holes from the s-SWCNT layer results from an appreciable energetic barrier to back-transfer. The efficient hole extraction by the s-SWCNT layer also improves electron extraction by the compact titanium dioxide electron transport layer, which should reduce charge accumulation at each critical interface. Thus, these studies demonstrate that s-SWCNT layers can serve two important roles for fundamental perovskite interfacial studies: (i) they provide a material-specific spectroscopic signature to follow important processes, such as charge diffusion, extraction, and recombination and (ii) they enable the long-lived charge separation needed to improve solar energy harvesting.

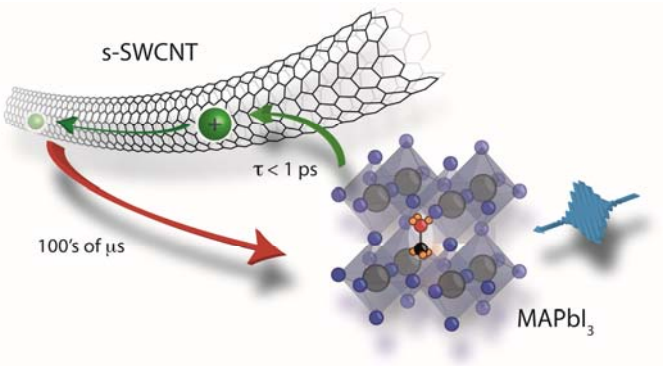

Figure 2. Schematic depicting rapid charge extraction and slow recombination in SWCNT/perovskite heterojunctions.

DOE Sponsored Publications 2013-2016

1. Ihly, R., Mistry, K.S., Ferguson, A.J., Clikeman, T.T., Larson, B.W., Boltalina, O.V., Strauss, S.H., Rumbles, G., Blackburn, J.L. Tuning the Driving Force for Exciton Dissociation in Single-walled Carbon Nanotube Heterojunctions. *Nature Chemistry*, **2016**, *In Press*.
2. Dowgiallo, A-M, Mistry, K.S., Johnson, J.C., Ferguson, A.J., Reid, O.G., Blackburn, J.L. Probing Exciton Diffusion and Dissociation in Single-walled Carbon Nanotube-C_{60} Heterojunctions. *J. Phys. Chem. Lett.*, **2016**, *In Press.*
3. Ihly, R., Dowgiallo, A-M, Yang, M., Schulz, P., Stanton, N.J., Reid, O.G., Ferguson, A.J., Zhu, K., Berry, J.J., Blackburn, J.L. Efficient Charge Extraction and Slow Recombination in Organic-Inorganic Perovskites Capped with Semiconducting Single-walled Carbon Nanotubes. *Energy & Environmental Science*, **2016**, *Advance Article*, **DOI:** 10.1039/C5EE03806E.
4. Schulz, P., Dowgiallo, A-M, Yang, M., Zhu, K., Blackburn, J.L., Berry, J. Charge Transfer Dynamics between Carbon Nanotubes and Hybrid Organic Metal Halide Perovskite Films. *J. Phys. Chem. Lett*. **2016***, 7,* 418.
5. Avery, A.D., Zhou, B.H., Lee, J.H., Lee, E-S, Miller, E.M., Ihly, R., Wesenberg, D., Mistry, K.S., Guillot, S.L., Zink, B.L., Kim, Y-H, Blackburn, J.L., Ferguson, A.J. Tailored Semiconducting Carbon Nanotube Networks with Enhanced Thermoelectric Properties. *Nature Energy,* **2016**, *1*, 16033, DOI: 10.1038/nenergy.2016.33.
6. Park, J., Reid, O.G., Blackburn, J.L., Rumbles, G. Photoinduced Spontaneous Free-Carrier Generation of (7,5)-Chirality Enriched Single-Walled Carbon Nanotubes in a Low Dielectric Solvent. *Nature Communications,* **2015**, *6,* 8809, **DOI**: 10.1038/ncomms9809.
7. Bodiou, L., Gu, Q., Guezo, M., Delcourt, E., Batte, T., Lemaitre, J., Lorrain, N., Guendouz, M., Folliot, H., Charrier, J., Mistry, K.S., Blackburn, J.L., Doualan, J-L, Braud, A., Camy, P. Guided Photoluminescence from Integrated Carbon Nanotubes-Based Optical Waveguides. *Advanced Materials*, **2015**, *27*, 6181, **DOI**: 10.1002/adma.201502536.
8. Wheeler, L., Anderson, N.C., Palomaki, P.K.B., Blackburn, J.L., Johnson, J., Neale, N. Silyl Radical Abstraction in the Functionalization of Plasma-Syntesized Silicon Nanocrystals. *Chemistry of Materials*, **2015**, *27*, 6689, **DOI**: 10.1021/acs.chemmater.5b03309.
9. Diao, S., Hong, G., Antaris, A.L., Blackburn, J.L., Cheng, K., Cheng, Z., Dai, H. Biological Imaging Without Autofluorescence in the Second Near-Infrared Window. *Nano Research*, **2015**, *8*, 3027. **DOI**: 10.1007/s12274-015-0808-9
10. Sarpkaya, I., Ahmadi, E., Shepard, G., Mistry, K.S., Blackburn, J.L., Strauf, S. Strong Acoustic Phonon Localization in Copolymer Wrapped Carbon Nanotubes. *ACS Nano*, **2015**, *9,* 6383. **DOI:** 10.1021/acsnano.5b01997
11. Ferguson, A., Bindl, D., Mistry, K.S., Dowgiallo, A-M., Reid, O.G., Kopidakis, N., Arnold, M., Blackburn, J.L. Trap-limited carrier recombination in single-walled carbon nanotube heterojunctions with fullerene acceptor layers. *Phys. Rev. B*, **2015**, *91*, 245311.
12. Fagan, J., Haroz, E., Ihly, R., Gui, H., Blackburn, J.L., Simpson, J., Lam, S., Hight Walker, A., Doorn, S., Zheng, M. Isolation of >1 nm Diameter Single-Wall Carbon

Nanotubes Species using Aqueous Two-Phase Extraction. *ACS Nano*, **2015**, *9***,** 5377. **DOI:** 10.1021/acsnano.5b01123

13. D. M. Sagar, Joanna M. Atkin, Peter K. B. Palomaki, Nathan R. Neale, Jeffrey L. Blackburn, Justin C. Johnson, Arthur J. Nozik, Markus B. Raschke, and Matthew C. Beard. Quantum Confined Electron-Phonon Interaction in Silicon Nanocrystals. *Nano Lett.*, **2015**, *15*, 1511.
14. Subbaiyan, N., Para-Vasquez, A.N., Cambre´, S., Santiago-Cordoba, M., Yalcin, S., Hamilton, C., Mack, N. Blackburn, J.L., Doorn, S., Duque, J.G. Benchtop Extraction of Isolated Individual Single-Walled Carbon Nanotubes. *Nano Research*, **2015**, *8*, 1755. DOI 10.1007/s12274-014-0680-z.
15. Dowgiallo, A-M., Mistry, K.S., Johnson, J.C., Blackburn, J.L. Ultrafast Spectroscopic Signature of Charge Transfer Between Single-Walled Carbon Nanotubes and C_{60}. *ACS Nano*, **2014**, *8*, 8573.
16. Barbara K. Hughes, Jeffrey L. Blackburn, Daniel Kroupa, Andrew Shabaev, Steven C. Erwin, Alexander L. Efros, Arthur J. Nozik, Joseph M. Luther, and Matthew C. Beard. Synthesis and Spectroscopy of PbSe Fused Quantum-Dot Dimers. *J. Am. Chem. Soc.* **2014**, *136*, 4670.
17. Niklas, J., Holt, J.M., Mistry, K., Rumbles, G., Blackburn, J.L., Poluektov, O.G. Charge Separation in P3HT:SWCNT Blends Studied by EPR: Spin Signature of the Photoinduced Charged State in SWCNT. *J. Phys. Chem. Lett.*, **2014**, *5*, 601.
18. Bindl, D., Ferguson, A., Wu, M.Y., Kopidakis, N., Blackburn, J.L., Arnold, M. Free Carrier Generation and Recombination in Polymer Wrapped Semiconducting Carbon Nanotube Films and Heterojunctions. *J. Phys. Chem. Lett.*, **2013**, *4,* 3350.
19. Arnold, M.S., Blackburn, J.L., Crochet, J.J., Doorn, S.K., Duque, J.G., Mohite, A., Telg, H. Recent Developments in the Photophysics of Single-walled Carbon Nanotubes for Their Use as Active and Passive Material Elements in Thin Film Photovoltaics. *Phys. Chem. Chem. Phys.*, **2013**, *15*, 14896 (invited perspective).
20. Mistry, K.S., Larsen, B.A., Blackburn, J.L. High-Yield Dispersions of Large-Diameter Semiconducting Single-Walled Carbon Nanotubes with Tunable Narrow Chirality Distributions. *ACS Nano*, **2013**, *7*, 2231.
21. Ferguson, A.J., Blackburn, J.L., Kopidakis, N. Fullerenes and Carbon Nanotubes as Acceptor Materials in Organic Photovoltaics. *Materials Letters*, **2013,** 90, 115. (invited perspective)

Session VI

Molecular Catalysis – Natural and Not

A Tale of Two Enzymes: CO Dehydrogenase and Formate Dehydrogenase

Stephanie Dingwall, Jarett Wilcoxen, Dimitri Niks and Russ Hille
Department of Biochemistry
University of California, Riverside
Riverside, CA 92521

We report on two air-stable enzymes involved in the biotransformation energy-relevant one-carbon compounds, the Mo- and Cu-containing CO dehydrogenase from *Oligotropha carboxidovorans* and the Mo-containing formate dehydrogenase from *Ralstonia eiutropha* (also known as *Cupriavidus necator*). The first of these enzymes catalyzes the oxidation of CO to CO_2, with reducing equivalents thus obtained being transferred to the quinone pool. We present ENDOR evidence that the reaction proceeds by nucleophilic attack on an activated Cu•carbonyl complex,[1] taking advantage of the highly delocalized redox-active orbital of the binuclear metal center.[2] Interestingly, when silver is substituted for copper in the active site, the enzyme retains activity, albeit reacting some five-fold slower with substrate than native enzyme, consistent with the weaker backbonding capacity of Ag relative to Cu.[3] In addition to CO, the native enzyme is also able to oxidize H_2, again a reflection of the reactivity of the highly delocalized redox-active orbital.[4] Proposed reaction mechanisms for the oxidation of CO and H_2 are shown in Figure 1.[1,4]

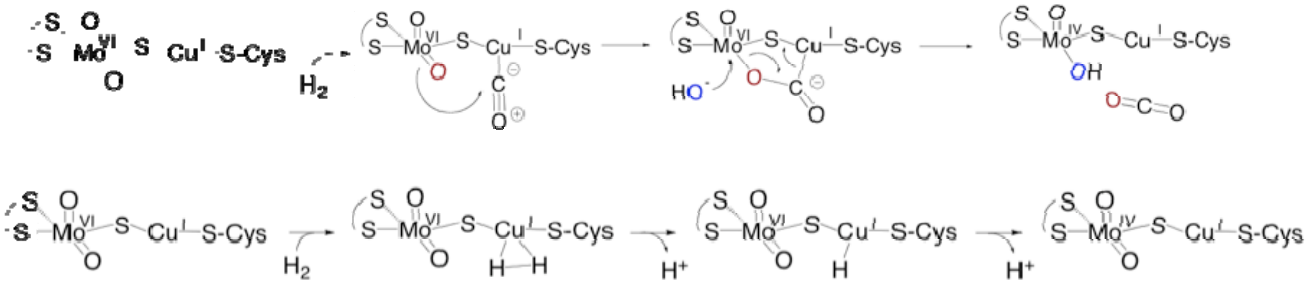

Figure 1. *Proposed mechansims for the oxidation of CO and H_2 by O. carboxidovorans CO dehydrogenase.*

The *R. eutropha* formate dehydrogenase (FdsABG) is a heterotrimeric, cytosolic enzyme containing a molybdenum center, seven iron-sulfur clusters and FMN. Based on sequence similarities, the enzyme structure is expected to closely resemble that of NADH dehydrogenase (which, although lacking the molybdenum center and one of the iron-sulfur clusters, retains the protein domains in which these are found in the formate dehydrogenase).[5] The active site molybdenum center of FdsABG has two equivalents of the pyranopterin cofactor found in all mononuclear molybdenum (and tungesten) enzymes coordinated to the molybdenum by an enedithiolate side chain, with Mo=S and cysteine ligands completing the metal coordination sphere.[6] Unlike most selenocystein-containing formate dehydrogenases, the *R. eutropha* FdsABG enzym is air-stable. We have identified four, possibly, five, EPR signals attributable to the iron-sulfur centers of the enzyme.[7] One of these is magnetically coupled to the molybdenum center in the Mo(V) valence state, and is assigned to the proximal [4Fe-4S] cluster in the protein structure. We have also demonstrated direct hydrogen transfer from the C_α of substrate to the molybdenum center, and propose a reaction mechanism predicated on hydride transfer from substrate to the Mo^{VI}=S, yielding Mo^{IV}-SH as shown in Figure 2.[7]

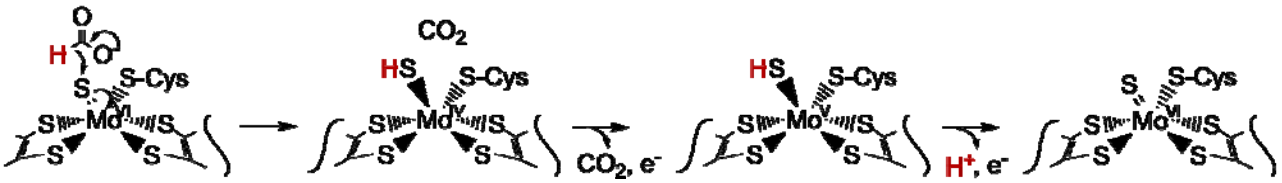

Figure 2. A proposed reaction mechansim for the enzyme involving hydride transfer from substrate to the active site molybdenum center.

Literature Cited

1. See #1 below in Publications 2013-2016
2. Gourlay, C.; Nielsen, D. J.; White, J. M.; Knottenbelt, S. Z.; Kirk, M. L.; Young, C. G. J. *Am. Chem. Soc.* **2006**, 128, 2164.
3. Wilcoxen, J., Snider, S., & Hille, R. (2011) Substitution of silver for copper in the binuclear Mo/Cu cluster of CO dehydrogenase leads to partial retention of catalytic power. *J. Am. Chem. Soc.*, **133**, 12934-12936.
4. See #2 below in Publications 2013-2016.
5. Sazanov, L. A., and Hinchliffe, P. (2006) Structure of the hydrophilic domain of respiratory complex I from *Thermus thermophilus*. *Science* **311**, 1430–1436
6. Schrapers, P., Hartmann, T., Kositzki, R., Dau, H., Reschke, S., Schulzke, C., Leimkühler, S., and Haumann, M. (2015) Sulfido and cysteine ligation changes at the molybdenum cofactor during substrate conversion by formate dehydrogenase (FDH) from Rhodobacter capsulatus. *Inorg. Chem.* **54**, 3260–3271
7. See #10 below in Publications 2013-2016

DOE Sponsored Publications 2013-2016

1. Shanmugam, M., Wilcoxen, J., Habel-Rodriguez, D., Kirk, M.L., Hoffman, B.M. Hille, R. (2013) ^{13}C and $^{63,65}Cu$ ENDOR studies of CO dehydrogenase from *O. carboxidovorans*. Experimental evidence in support of a copper-carbonyl intermediate. *J. Am. Chem. Soc.* **135**, 17775-17782.
2. Wilcoxen, J., Hille, R. (2013) The hydrogenase activity of CO dehydrogenase from *Oligotropha carboxidovorans*. *J. Biol. Chem.* **288**, 36052-36060.
3. Appel, A.M., Bercaw, J.E., Bocarsly, A.B., Dobbek, H., Dubuis, M., Dubois, D., Ferry, J.G., Fujita, E., Hille, R., Kenis, P.J.A., Kerfeld, C.A., Morris, R.H., Peden, C.H.F., Portis, A.R., Ragsdale, S.J., Rauchfuss, T.B., Reek, J.N.H., Seefeldt, L., Thauer, R.K., Waldrop, G.L. (2013) Frontiers, Opportunities, and Challenges in Biochemical and Chemical Catalysis of CO_2 Fixation. *Chem. Rev.* **113**, 6621-6658.
4. Cao, H., Hall, J., & Hille, R. (2014) Crystal structures of xanthine oxidoreductase complexed with guanine and indole-3-aldehyde. *Biochemistry* **53**, 533-541.
5. Anderson, R.F., Shinde, S.S, Hille, R, Rothery, R.A., Weiner, J.H., Rajagukguk, S., Maklashina, E. & Cecchini, G. (2014) Efficient Electron Transfer to the Heme in Complex II Involves the [3Fe-4S] and Quinone Sites of the Enzyme. *Biochemistry* **53**, 1637-1646.
6. Hall, J., Reschke, S., Cao, H., Leimkühler, S. & Hille, R. (2014) The reaction mechanism of xanthine dehydrogenase from *R. capsulatus*. *J. Biol. Chem.* **289**, 32121-32130.
7. Wang, J., Krizowski, S., Fischer, K, Niks, D., Tejero, J., Wang, L., Sparacino-Watkins, C., Ragireddy, P., Frizzell, S., Kelley, E., Shiva, S., Zhang, Y., Hille, R., Basu, P., Schwarz, G., Gladwin, M.T. (2015) Sulfite oxidase catalyzes single electron transfer reaction at its molybdenum domain to reduce nitrite to NO. *Antiox. Redox. Sign.* **23**, 283-294.
8. Hille, R., Hall, J., Basu, P. The mononuclear molybdenum enzymes. (2014) *Chem. Rev.* **114**, 3963-4038.
9. Hille, R., Dingwall, S., & Wilcoxen, J. (2015) The aerobic CO dehydrogenase from *Oligotropha carboxidovorans*. *J. Biol. Inorg. Chem.* **20**, 243-251145.
10. Niks, D, Duvvuru, J., Escalona, M. Hille, R. (2015) Spectrosccopic and kinetic studies of the soluble, NAD^+-dependent formate dehydrogenase from *Ralstonia eutropha*, *J. Biol. Chem.* **291**, 1162-1174.

Formation and Reactivity of Hydride Donors in Water

Dmitry E. Polyansky, Javier Concepcion, David Grills, Etsuko Fujita and James T. Muckerman
Chemistry Department
Brookhaven National Laboratory
Upton, NY 11973-5000

Artificial photosynthetic systems exploit a variety of photochemical transformations with the ultimate result of efficient storage of the energy of photons in a chemical form. The efficiency of these transformations strongly depends on how successfully proton-coupled electron transfer (PCET) processes are implemented. One of our program efforts aims at a mechanistic understanding of the role of PCET in: (1) ground and excited state chemistry of NAD^+-like transition metal complexes; (2) formation and reactivity of transition metal hydride species as intermediates in CO_2 or proton reduction catalysis; and (3) light-driven or electrochemical water oxidation catalyzed by transition metal complexes.

Hydride ion transfer (HIT) is a subset of PCET and it plays an important role in enabling low energy pathways in reductive catalysis such as proton or CO_2 reduction. HIT reactions are typically mediated by transition metal or organic hydride donors. We have found that while the production of organic hydride donors can be achieved photo- or electrochemically in reasonably high yields their reactivity towards carbon dioxide is limited by the unfavorable thermodynamics of the HIT reaction. On the other hand, metal hydride donors can rapidly react with CO_2 resulting in coordinated or un-coordinated formate species. However, regeneration of metal hydrides in water from protons and electrons remains a challenging task due to hydride reactivity towards proton sources resulting in efficient hydrogen evolution. Our work has been focused on investigating mechanistic pathways for the generation of metal hydride species relevant to hydrogen evolution or CO_2 reduction catalysis in water. Due to the transient nature of most critical intermediates we have employed the technique of pulse radiolysis in order to establish the identity of transient species and study their reactivity.

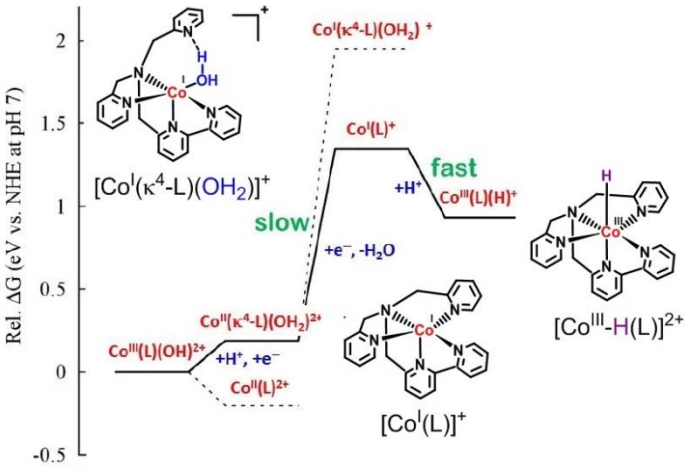

Figure 1. The proposed mechanism for the formation of [**Co^{III}**–H)]$^{2+}$ intermediate with pentadentate ligand L in water.

In one example, we investigated the proton reduction catalyst [(DPA-Bpy)Co(OH$_2$)]$^{2+}$ ([**Co**(OH$_2$)]$^{2+}$), and found that the reduction of a Co^{II} species leads to the loss of the aqua ligand and the formation of [**Co^{I}**–VS)]$^+$ (VS = vacant site). Both electrochemical and kinetic results indicate that the Co^{I} species must undergo some structural change prior to accepting the proton and this transformation represents the rate determining step (RDS) in the overall formation of

[**Co^{III}**–H)]$^{2+}$. We proposed that this RDS may originate from the slow removal of a solvent ligand in the intermediate [Co^{I}(κ^4-L)(OH$_2$)]$^{+}$ in addition to the significant structural reorganization of the metal complex and surrounding solvent resulting in a high free energy of activation (Fig. 1). The [**Co^{III}**–H)]$^{2+}$ intermediate has been produced in pulse radiolysis experiments and was originally observed using Uv-Vis spectroscopy (Fig. 2, left).

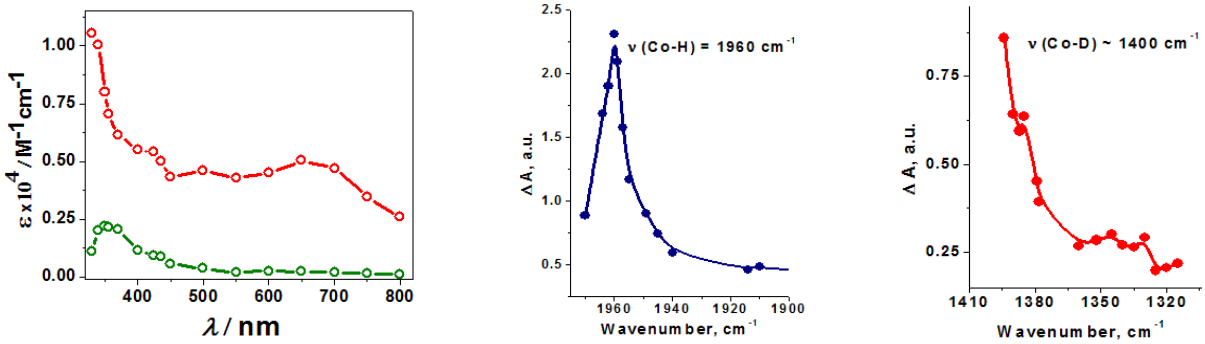

Figure 2. Pulse radiolysis reduction of [(DPA-Bpy)Co(OH$_2$)]$^{2+}$ in water. Left: UV-vis spectra of Co(I) (red) and [**Co^{III}**–H)]$^{2+}$ (green) species. Middle: IR spectrum of [**Co^{III}**–H)]$^{2+}$. Right: IR spectrum of [**Co^{III}**–D)]$^{2+}$ (measured in D$_2$O).The abrupt cutoff of the spectrum at 1390 cm^{-1} is due to the limited range of the IR source (our currently available quantum cascade laser) in this region.

Recently, we have conducted a series of experiments using the *unprecedented IR detection of transient species produced by pulse radiolysis in water*. The observed [**Co^{III}**–H)]$^{2+}$ stretching frequency at 1960 cm^{-1} (Fig. 2, middle) is in the typical region for metal hydride vibrations, and is close to the DFT predicted value of 1985 cm^{-1}. Moreover, the same species produced in D$_2$O exhibits an IR band around 1400 cm^{-1} (Fig. 2, right) which corresponds exactly to the isotopic shift of the Co–H stretching frequency (ν_H/ν_D = 1.4) predicted by a harmonic oscillator model. The results obtained from the IR spectroscopy allow unambiguous assignment of the transient species as [**Co^{III}**–H)]$^{2+}$.

In another example, we have investigated the formation of Ru hydride species in water starting with the solvent coordinated complex (e.g., [Ru^{II}(bpy)(tpy)(H$_2$O)]$^{2+}$. We found that contrary to their reduction in organic solvents, the one-electron reduced species lose the water ligand followed by their reaction with a proton and an electron resulting in [Ru^{II}(H)]$^{+}$ (Fig. 3, green path, Sol = water). This pathway requires less negative potential compared to, e.g., reduction in acetonitrile (Sol = CH$_3$CN), where two-electron reduction is needed to lose the coordinated solvent molecule (Fig. 3, red path).

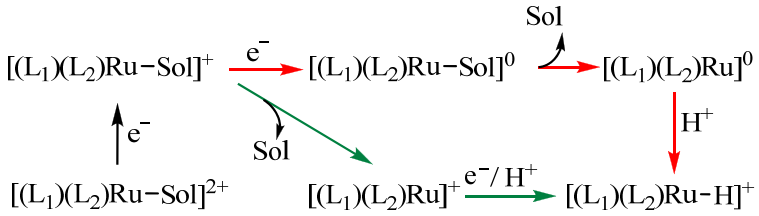

Figure 3. Formation of Ru hydride species from protons and electrons in acetonitrile (red) and water (greeen) solutions.

Our future directions include comprehensive mechanistic investigations of metal hydride chemistry in water, including the identification of reactive intermediates using the technique of pulse radiolysis with time-resolved mid-infrared detection.

Acknowledgements: We thank our collaborators S. D Senanayake, X. Zhao, R. P. Thummel and K. Tanaka.

DOE Sponsored Publications 2013-2016

1. Badiei, Y. M.; Polyansky, D. E.; Muckerman, J. T.; Szalda, D. J.; Haberdar, R.; Zong, R.; Thummel, R. P.; Fujita, E. "*Water Oxidation with Mononuclear Ruthenium(II) Polypyridine Complexes Involving a Direct Ru^{IV}=O Pathway in Neutral and Alkaline Media" Inorg. Chem.* **2013**, *52*, 8845-8850.
2. Doherty, M. D.; Grills, D. C.; Huang, K.-W.; Muckerman, J. T.; Polyansky, D. E.; van Eldik, R.; Fujita, E. "*Kinetics and Thermodynamics of Small Molecule Binding to Pincer-PCP Rhodium(I) Complexes" Inorg. Chem.* **2013**, *52*, 4160-4172.
3. Lewandowska-Andralojc, A.; Polyansky, D. E. "*Mechanism of the Quenching of the Tris(bipyridine)ruthenium(II) Emission by Persulfate: Implications for Photoinduced Oxidation Reactions" J. Phys. Chem. A* **2013**, *117*, 10311-10319.
4. Lewandowska-Andralojc, A.; Polyansky, D. E.; Zong, R. F.; Thummel, R. P.; Fujita, E. "*Enabling light-driven water oxidation via a low-energy Ru^{IV}=O intermediate" Phys. Chem. Chem. Phys.* **2013**, *15*, 14058-14068.
5. Zhong, D. K.; Zhao, S.; Polyansky, D. E.; Fujita, E. "*Diminished photoisomerization of active ruthenium water oxidation catalyst by anchoring to metal oxide electrodes" J. Catal.* **2013**, *307*, 140-147.
6. Lewandowska-Andralojc, A.; Polyansky, D. E.; Wang, C.-H.; Wang, W.-H.; Himeda, Y.; Fujita, E. "*Efficient water oxidation with organometallic iridium complexes as precatalysts" Phys. Chem. Chem. Phys.* **2014**, *16*, 11976-11987.
7. Matsubara, Y.; Hightower, S. E.; Chen, J.; Grills, D. C.; Polyansky, D. E.; Muckerman, J. T.; Tanaka, K.; Fujita, E. "*Reactivity of a fac-ReCl(α-diimine)$(CO)_3$ complex with an NAD^+ model ligand toward CO_2 reduction" Chem. Commun.* **2014**, *50*, 728-730.
8. Muckerman, J. T.; Kowalczyk, M.; Badiei, Y. M.; Polyansky, D. E.; Concepcion, J. J.; Zong, R.; Thummel, R. P.; Fujita, E. "*New Water Oxidation Chemistry of a Seven-Coordinate Ruthenium Complex with a Tetradentate Polypyridyl Ligand" Inorg. Chem.* **2014**, *53*, 6904-6913.
9. Polyansky, D. E. "*Electrocatalysis for Carbon Dioxide Reduction"* In *Encyclopedia of Applied Electrochemistry*; Kreysa G., Ota K., Savinell R., Eds.; Springer Science: New York, 2014; Vol. 1, p 431-436.
10. Polyansky, D. E.; Hurst, J. K.; Lymar, S. V. "*Application of Pulse Radiolysis to Mechanistic Investigations of Water Oxidation Catalysis" Eur. J. Inorg. Chem.* **2014**, 619-634.
11. Hsieh, Y.-C.; Senanayake, S. D.; Zhang, Y.; Xu, W.; Polyansky, D. E. "*The effect of chloride anions on the synthesis and enhanced catalytic activity of silver nano-coral electrodes for CO_2 electroreduction" ACS Catal.* **2015**.
12. Kunwar, N.; Sharma, S.; Benjamin, S.; Polyansky, D. E. "*Artificial Photosynthesis"* In *Solar Energy Conversion and Storage. Photochemical Modes*; Ameta, S. C., Ameta, R., Eds.; CRC Press: Boca Raton, 2015, p 187-218.
13. Lewandowska-Andralojc, A.; Baine, T.; Zhao, X.; Muckerman, J. T.; Fujita, E.; Polyansky, D. E. "*Mechanistic Studies of Hydrogen Evolution in Aqueous Solution Catalyzed by a Tertpyridine-Amine Cobalt Complex" Inorg. Chem.* **2015**, *54*, 4310-4321.
14. Luo, S.; Nguyen-Phan, T. D.; Johnston-Peck, A. C.; Barrio, L.; Sallis, S.; Arena, D. A.; Kundu, S.;

Xu, W. Q.; Piper, L. F. J.; Stach, E. A.; Polyansky, D. E.; Fujita, E.; Rodriguez, J. A.; Senanayake, S. D. "*Hierarchical Heterogeneity at the CeO_x-TiO_2 Interface: Electronic and Geometric Structural Influence on the Photocatalytic Activity of Oxide on Oxide Nanostructures" J. Phys. Chem. C* **2015**, *119*, 2669-2679

15. Musat, R. M.; Crowell, R. A.; Polyanskiy, D. E.; Thomas, M. F.; Wishart, J. F.; Katsumura, Y.; Takahashi, K. "*Ultrafast transient absorption spectrum of the room temperature Ionic liquid 1-hexyl-3-methylimidazolium bromide: Confounding effects of photo-degradation" Radiat. Phys. Chem.* **2015**, *117*, 78-82.

16. Nguyen-Phan, T. D.; Luo, S.; Liu, Z. Y.; Gamalski, A. D.; Tao, J.; Xu, W. Q.; Stach, E. A.; Polyansky, D. E.; Senanayake, S. D.; Fujita, E.; Rodriguez, J. A. "*Striving Toward Noble-Metal-Free Photocatalytic Water Splitting: The Hydrogenated-Graphene-TiO_2 Prototype" Chem. Mater.* **2015**, *27*, 6282-6296.

17. Nguyen-Phan, T. D.; Luo, S.; Voychok, D.; Llorca, J.; Graciani, J.; Sanz, J. F.; Sallis, S.; Xu, W. Q.; Bai, J. M.; Piper, L. F. J.; Polyansky, D. E.; Fujita, E.; Senanayake, S. D.; Stacchiola, D. J.; Rodriguez, J. A. "*Visible Light-Driven H_2 Production over Highly Dispersed Ruthenia on Rutile TiO_2 Nanorods" ACS Catal.* **2016**, *6*, 407-417.

18. Thuy-Duong, N.-P.; Liu, Z.; Luo, S.; Gamalski, A. D.; Vovchok, D.; Xu, W.; Stach, E. A.; Polyansky, D. E.; Fujita, E.; Rodriguez, J. A.; Senanayake, S. D. "*Unraveling the Hydrogenation of TiO_2 and Graphene Oxide/TiO_2 Composites in Real Time by in Situ Synchrotron X-ray Powder Diffraction and Pair Distribution Function Analysis" J. Phys. Chem. C* **2016**, *120*, 3472-3482.

19. Ward, W.; Kowalczyk, M.; Concepcion, J. J.; Polyansky, D. E. "*Production of strongly reducing metal hydride donors from protons and electrons: the effect of media and solvent coordination"* submitted.

The Development of Polypyridine Transition Metal Complexes as Homogeneous Catalysts for Water Decomposition

Ruifa Zong, Lars Kohler, Lianpeng Tong, Lanka Wickramasinghe, Debashis Basu, Husain Kagalwala, Andrew Kopecky, Rongwei Zhou, and Randolph Thummel
Department of Chemistry
University of Houston
Houston, Texas 77204-5003

The ultimate objective of this project is the discovery and development of a homogeneous molecular catalyst that will use the energy of sunlight to convert water into its elements. Early phases of the project focused mainly on dinuclear and mono-nuclear Ru^{II} complexes for water oxidation. The oxidations were driven by sacrificial reagents such as Ce^{IV} or photogenerated $[Ru(bpy)_3]^{3+}$. Careful consideration was given to the compatibility of the sensitizer (chromophore) and the catalyst. Sufficient thermodynamic driving force was required as well as selective light absorption by the chromophore. A detailed study of the complex $[Ru(dpp)(pic)_2]^{2+}$ (**1**, dpp = 2,9-di(pyrid-2'-yl)-1,10-phenanthroline, pic = 4-picoline) was carried out in conjunction with our Brookhaven collaborators.

Three important features of mononuclear Ru^{II}-based water oxidation catalysts have been identified. When Ru^{II} is bound to a tetradentate ligand such as dpp in complex **1**, the exterior N-Ru-N bond angle of 126° will allow a water molecule to attack an oxidized Ru center in the equatorial plane, expanding the coordination geometry to seven. Whereas dpp is a 5-5-5 chelator, the ligand 2-(pyrid-2'-yl)-8-(1",10"-phenanthrolin-2"-yl)-quinoline (ppq) contains an additional sp^2 carbon and thus is a 5-6-5 chelator. Complex **2** is not as accessible to water attack in the equatorial plane and therefore is much less reactive towards water oxidation.

A second important feature is that the axial ligands (picoline in the case of **1** and **2**) be aligned in a linear fashion to allow formation of the pentagonal bipyramid geometry demanded by hepta-coordination. The 5-5 chelator 2,2';6,2"-terpyridine (tpy) does not allow this linear orientation and is thus **3** is unreactive in the presence of Ce^{IV}. However the 6-5 chelator in complex **4** is more favorable to the requisite 7-coordinate geometry and is a relatively effective catalyst.

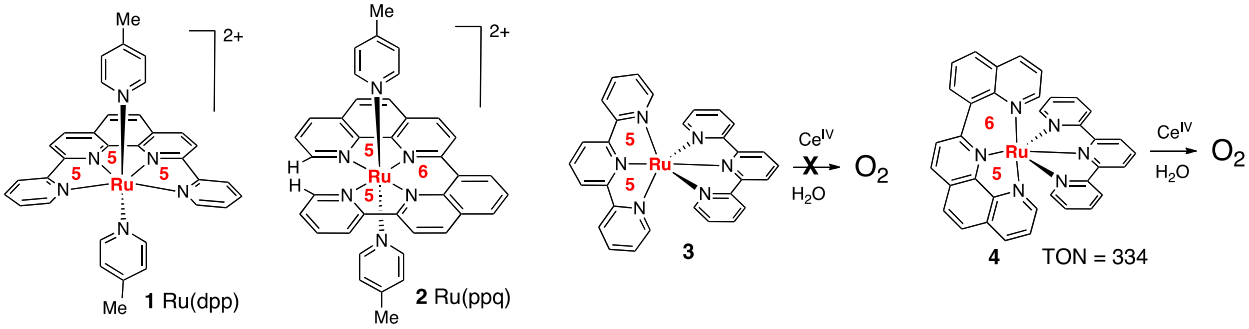

A third important feature for water oxidation is the impact of an anionic ligand which should help to stabilize the higher oxidation states of Ru involved in the catalytic cycle. This effect has been demonstrated by Sun and coworkers for systems involving carboxy-bpy and carboxy-phen. We have found that the phenoxyphen ligand in complex **5** shows enhanced reactivity. The form-

ation of **6** presents a clear example of the oxidation of a metal bound ligand accompanied by the evolution of CO_2. Both NMR and MS evidence are presented for the formation of **6**. Interestingly **6** is a 5-5 system but it shows better reactivity and stability than **5**.

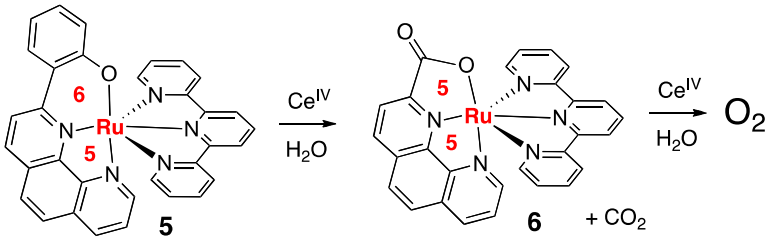

5 **6**

The smaller binding cavity of ppq can better accommodate first row transition metals that do not readily bind in a tetradentate fashion to ligands such as dpp. Thus Co^{II} binds to ppq to form the complex **7** that when irradiated by a blue LED in the presence of ascorbic acid as a sacrificial electron donor and $[Ru(bpy)_3]Cl_2$ as a photosensitizer evolves hydrogen with a TOF = 586 h^{-1}. It appears that bridging adjacent binding sites in the ligand also serves to increase the stability and thus the performance of the catalyst. For this reason the Co^{II} complex of ligand **10** is more reactive than the corresponding complexes of **8** and **9**.

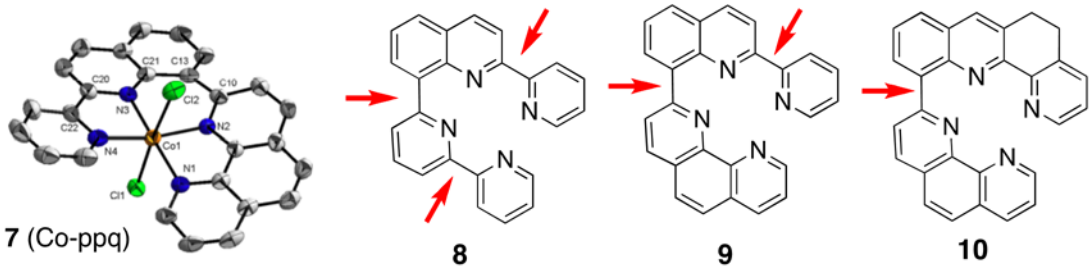

7 (Co-ppq) **8** **9** **10**

The same ppq ligand will bind to $FeCl_3$ to provide the oxo-bridged dimer **11**. In the presence of Ce^{IV} **11** proved to be an excellent water oxidation catalyst (TOF = 7920 h^{-1}). The ligand diphenanthrolinyl-N-isopentylamine (dpa) was prepared from 2-chlorophen and has a binding cavity similar to ppq. Due to the bulky isopentenyl group, the Fe complex **12** does not dimerize. Preliminary evidence for the parent ligand $(phen)_2NH$ indicates that the complex with Fe^{III} is a dimer and is about 10x less active than **11** as a water oxidation catalyst. Increasing evidence points to the importance of having a planar tetradentate ligand system with an approximate square planar arrangement of the four pyridine rings. Earlier this year, results from Alberto and coworkers demonstrated this for the Co complex of a cyclic bis-phenanthroline system (*Dalton Trans*, **2016**, *45*, 1737). We are currently focused on the synthesis of a cyclic analog of ppq.

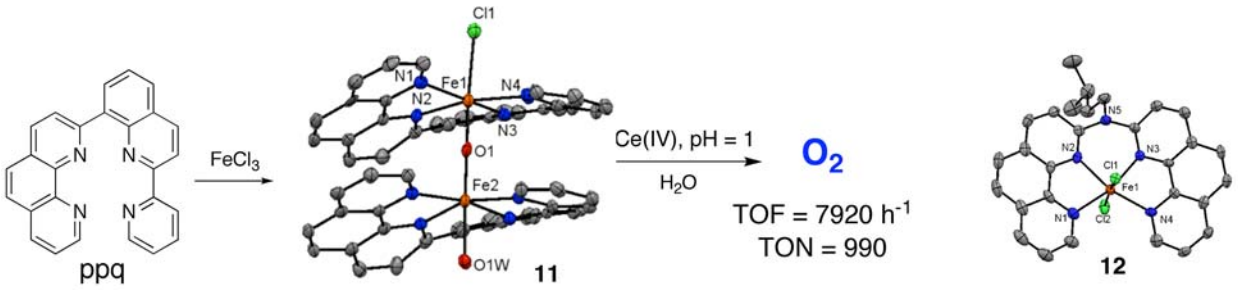

ppq **11** **12**

Publications Acknowledging DOE Support since 2013.

1. "Water Oxidation with Mononuclear Ruthenium (II) Polypyridine Complexes Involving a Direct Ru^{IV}=O Pathway in Neutral and Alkaline Media," Badiei, Y.; Polyansky, D. E.; Muckerman, J. T.; Szalda, D. J.; Haberdar, R.; Zong, R.; Thummel, R. P.; Fujita, E. *Inorg. Chem.* **2013**, *52,* 8845-8850.

2. "Enabling Light-Driven Water Oxidation via a Low-Energy Ru^{IV}=O Intermediate," Lewandowska-Andralojc, A.; Polyansky, D. E.; Zong, R.; Thummel; R. P.; Fujita, E. *Phys. Chem. Chem. Phys.* **2013**, *15,* 14058-14068.

3. "A Ru(II) Bis-terpyridine-like Complex that Catalyzes Water Oxidation: the influence of Steric Strain," Kaveevivitchai, N.; Kohler, L.; Zong, R.; El Ojaimi, M.; Mehta, N.; Thummel, R. P. *Inorg. Chem.* **2013**, *52,* 10615-10622.

4. "Component Analysis of Dyads Designed for Light-Driven Water Oxidation," Kohler, L.; Kaveevivitchai, N.; Zong, R.; Thummel, R. P. *Inorg. Chem.* **2014**, *53,* 912-921.

5. "Visible Light-driven Hydrogen Evolution from Water Catalyzed by A Molecular Cobalt Complex," Tong, L.; Zong, R.; Thummel, R. P. *J. Am. Chem. Soc.* **2014**, *136,* 4881-4884.

6. "New Water Oxidation Chemistry of Seven-Coordinate Ruthenium Complexes with Tetradentate Polypyridine-type Ligands," Muckerman, J. T.; Kowalczyk, M.; Badiei, Y.; Polyansky, D. E.; Yang, L.; Concepcion, J. J.; Zong, R.; Thummel, R.; Fujita, E. *Inorg. Chem.* **2014**, *53,* 6904-6913.

7. "Ultrafast Structural Dynamics of Cu(I)-Bicinchoninic Acid and Their Implications for Solar Energy Applications," Fransted, K.; Jackson, N.; Zong, R.; Mara, M.; Huang, J.; Harpham, M.; Shelby, M.; Thummel, R.; Chen, L. X. *J. Phys. Chem. A* **2014**, *118,* 10497-10506.

8. "Ruthenium Catalysts for Water Oxidation Involving Tetradentate Polypyridine-type Ligands," Tong, L.; Zong, R.; Zhou, R.; Kaveevivitchai, N.; Zhang, G.; Thummel, R. P. *Faraday Discussions* **2015**, *185,* 87-104.

9. "Light-driven Proton Reduction in Aqueous Medium Catalyzed by a Family of Cobalt Complexes with Tetradentate Polypyridine-type Ligands," Tong, L.; Kopecky, A.; Zong, R.; Gagnon, K. J.; Ahlquist, M. S. G.; Thummel, R. P. *Inorg. Chem.,* **2015**, *54,* 7873-7884.

10. "Iron Complexes of Square Planar Tetradentate Polypyridyl-type Ligands as Catalysts for Water Oxidation," Wickramasinghe, L. D.; Zhou, R.; Zong, R.; Vo, P.; Gagnon, K.; Thummel, R. P. *J. Am. Chem. Soc.* **2015**, *137,* 13260-13263.

Session VII

Inorganic Catalysis of Water Splitting

Making the O-O Bond in Water Oxidation Catalysis: Single-Site *vs* O-O Coupling

David W. Shaffer, Yan Xie, Gerald F. Manbeck, David J. Szalda, Javier J. Concepcion
Chemistry Division
Brookhaven National Laboratory
Upton, NY 11973-5000

Worldwide growth in energy consumption and anthropogenic damage to the global climate demand the development of clean and sustainable energy technologies. Artificial photosynthesis is anticipated to play a pivotal role in this transition and become our main source of energy, replacing fossil fuels with renewable solar fuels. Achieving this goal requires the development of integrated systems that combine light absorption, excited state quenching leading to charge separation, water oxidation and fuel production catalysis with proton management. We are developing new redox mediators/chromophores, new strategies for anchoring catalysts and chromophores to electrodes, as well as new families of water oxidation catalysts. In addition, we are exploring new mechanistic pathways to achieve CO_2 reduction beyond CO.

We will focus on two topics in this presentation: water oxidation with multifunctional ligands and CO_2 reduction with organic hydride donors. In the first topic, we will present a comparison between single-site and bimolecular catalysts in water oxidation. Multifunctionality is introduced by phosphonate groups as structural motifs in tetradentate ligands. These groups provide redox potential leveling through charge compensation and sigma donation allowing easy access to high oxidation states. In addition, the position of these groups allows them to act as proton shuttles, moving protons in and out of the catalytic site and reducing activation barriers. Ruthenium complexes with these multifunctional ligands display unique pH-dependent electrochemistry associated with deprotonation of the phosphonic acid groups. One of the families of complexes that will be presented constitutes the fastest single-site catalysts known to date. In the second topic, CO_2 reduction with organic hydride donors, a critical discussion of CO_2 reduction using this approach will be presented. It involves a combination of experimental results and DFT calculations that address erroneous reports in the literature. We also provide a detailed analysis of the kinetic and thermodynamic requirements for hydride transfer to CO_2 from potential organic hydride donors in the context of assessing the validity of this approach to CO_2 reduction. Finally, we explore methods for lowering the barrier of hydride transfer in these systems.

O-O bond formation is the key step in water oxidation catalysis. It accounts for ~70% of the free energy requirement for this energetically and mechanistically demanding half-reaction. Two competing mechanisms are generally invoked for this step, regardless of the nature of the catalyst (OEC, homogeneous, or heterogeneous): water nucleophilic attack on a high-valent metal-oxo (single-site) or O-O coupling between two high-valent metal-oxo moieties with significant oxyl radical character (two-site). These mechanisms can both operate with mono-nuclear or multi-nuclear catalysts. A detailed comparison between these two mechanisms will be presented for molecular ruthenium-based water oxidation catalysts. This study involves a combination of experimental results and DFT calculations. In the single-site pathway, a water molecule attacks an electron-deficient metal-oxo with simultaneous proton transfer to a hydrogen-bound proton acceptor, generating an intermediate metal-hydroperoxide, Figure 1. The

proton acceptor can be another water molecule, the basic form of a buffer, a strategically positioned base, or another nearby metal-oxo moiety (as is the case in the Ru blue dimer). Catalysts in this class typically display kinetic isotope effects if the O-O bond formation is rate-limiting and the overall rate of water oxidation is sensitive to both the nature (pK_a) and concentration of the buffer.

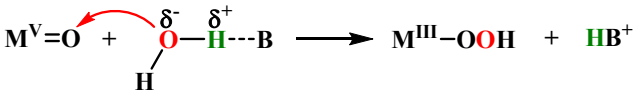

Figure 1. O-O bond formation *via* single-site pathway.

In the second class, two metal-oxyl radicals undergo O-O coupling to form a peroxo bridge between the two metal centers, Figure 2. These two metals can be a part of the same molecule in a multinuclear complex, a cluster or nanoparticle, or two independent molecules, as reported for [Ru (bda)(L)$_2$] by Sun and coworkers (bda is 6,6′-dicarboxylate-2,2′-bipyridine; L is a monodentate ligand). If the O-O bond formation is rate-limiting, catalysts in this class *should not* display kinetic isotope effects and the overall rate of water oxidation should be insensitive to both the nature and concentration of the buffer.

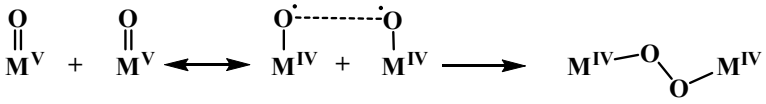

Figure 2. O-O bond formation *via* O-O radical coupling.

We will show evidence for low energy pathways for O-O bond formation via nucleophilic attack when coupled to proton transfer (Figure 3, left), by replacing the carboxylate groups in bda by phosphonate groups. Using this strategy we have prepared the fastest single-site water oxidation catalysts known to date.

TS single-site: $\Delta G^{\ddagger}$ = +13.5 kcal/mol **TS O-O coupling: $\Delta G^{\ddagger}$ = +31.9 kcal/mol**

Figure 3. Transition state (TS) structures and corresponding free energies of activation for O-O bond formation *via* single-site (left) and O-O radical coupling pathways for [Ru^{V}(bpa)(py)$_2$(O)]$^{2-}$ (bpa is 6,6′-diphosphonate-2,2′-bipyridine; py is pyridine).

We are applying this strategy to known and new water oxidation catalysts. For example, we have replaced one of the pyridines in tpy by a phosphonate group in [Ru^{II}(tpy)(bpy)(OH$_2$)]$^{2+}$ (a very inefficient water oxidation catalyst) and the new [Ru^{II}(bpy-PO(O)(OH))(bpy)(OH$_2$)]$^{+}$ complex displays one of the lowest overpotentials for water oxidation reported to date at pH 1 with $\Delta G^{\ddagger}$ = **+10.3 kcal/mol** for O-O bond formation. We are also exploring other functional groups as proton acceptors and we are beginning to incorporate these catalysts in chromophore-catalyst assemblies.

DOE Sponsored Publications 2013-2016

1. "Extremely Fast Water Oxidation Catalysts with Hybrid Phosphonate-Carboxylate Bipyridyl Ligands: Single-site *vs* O-O coupling", Shaffer, D. W.; Szalda, D. J.; Concepcion, J. J., in preparation.

2. "Manipulating the Rate-Limiting Step in Water Oxidation Catalysis by Ruthenium Bipyridine-Dicarboxylate Complexes", Shaffer, D. W.; Xie, Yan; Szalda, D. J.; Concepcion, J. J., *J. Am. Chem. Soc.*, submitted.

3. "A Strongly Coupled Tyrosine-Histidine Mimic of Photosystem II with Stepwise Oxidation and Concerted Reduction by Proton-Coupled Electron Transfer", Manbeck, G. F.; Fujita, E.; Concepcion, J. J., *J. Am. Chem. Soc.*, submitted.

4. "Water Oxidation by Ruthenium Complexes Incorporating Multifunctional Bipyridyl Diphosphonate Ligands", Xie, Yan; Shaffer, D. W.; Lewandowska-Andralojc, A.; Szalda, D. J.; Concepcion, J. J., *Angew. Chem., Int. Ed.* **2016**, accepted.

5. "Mechanism of Water Oxidation by [Ru(bda)(L)$_2$]: the Return of the "Blue Dimer"", Concepcion, J. J.; Zhong, D. K.; Szalda, D. J.; Muckerman, J. T.; Fujita, E. *Chem. Commun.* **2015**, *51*, 4105.

6. "New Water Oxidation Chemistry of a Seven-Coordinate Ruthenium Complex with a Tetradentate Polypyridyl Ligand", Muckerman, J. T.; Kowalczyk, M.; Badiei, Y. M.; Polyansky, D. E.; Concepcion, J. J.; Zong, R.; Thummel, R. P.; Fujita, E., *Inorg. Chem.* **2014**, *53*, 6904.

Spectroscopic analysis of Ru-based catalysts under water oxidizing conditions

Yulia Pushkar
Department of Physics
Purdue University
West Lafayette, Indiana 47907

Development of efficient catalysts for water splitting is one of the main challenges towards the future realization of energy production based on the concept of artificial photosynthesis. Our work has been focused on determining the structure and electronic configurations of the critical intermediates of water oxidation as well as the dynamic of their interconversion under catalytic conditions. Molecular-defined ruthenium catalysts are the best systems for mechanistic studies due to their relative simplicity and the possibility to control, via ligand design, their reactivity and stability. These catalysts can be integrated into functional electrodes for sunlight-to-fuel production. The best techniques to study *in situ* catalytic water oxidation are synchrotron-based X-ray spectroscopy, including X-ray absorption near edge structure (XANES), extended X-ray absorption fine structure (EXAFS) and X-ray emission spectroscopy (XES), electron paramagnetic resonance (EPR) and multiwavelength kinetic resonance Raman spectroscopy. These experimental techniques delivered information on the structure of the intermediates and their electronic configuration and evolution of molecules during the catalytic processes (see publications 2, 3, 5, 6, 9). Computational approaches were used to supplement experimental analysis (see publications 1, 2, 6).

Our recent efforts were focused on the *in situ* analysis of the electrodes functionalized with Ru-based molecular catalysts and electrochemical water oxidation cells with solution of catalyst. We accomplished the highly challenging plan and demonstrated *in situ* analysis of the single site Ru catalysts attached to the electrode surface. In spite of formidable experimental challenges we achieved Ru K-edge XANES of molecular water oxidation catalysts and demonstrated the presence of Ru^{IV} species under working conditions of water oxidation (+1.8 V vs. NHE), Figure 1. To achieve our results we synthetized $[Ru(bpy\text{-}2PO_3H_2)(tpy)H_2O]^{2+}$ with two anchoring -PO_3H_2 groups. These groups are currently the best available for the strongest binding of the Ru complex to the electrode surfaces of transparent conducting materials such as ITO and FTO. The $[Ru(bpy\text{-}2PO_3H_2)(tpy)H_2O]^{2+}$ compound was characterized by NMR, EPR and catalytic activity in O_2 evolution. Prepared electrodes showed catalytic currents as previously reported, however, under operational conditions they lost surface functionalization with Ru complexes faster (on a minute scale) than we could conduct measurements! To overcome the challenge of the complexes desorption from the

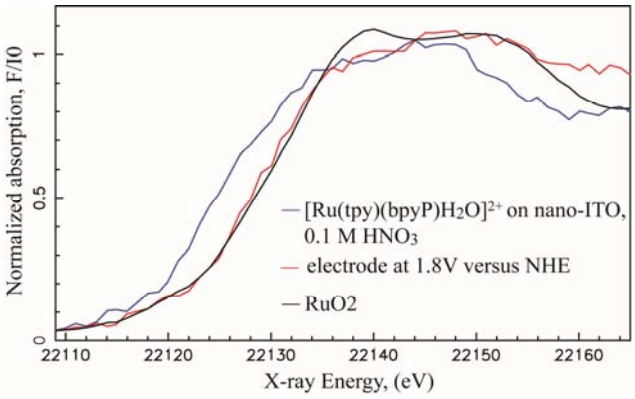

Figure 1. *In situ* Ru K-edge XANES of molecular catalyst chemically attached (via $-PO_3H_2$ groups) to electrode shows that Ru oxidation state does not exceed Ru^{IV} at +1.8 V (NHE) of applied potential.

electrodes under operational conditions, we used nano-ITO coating which increases overall complex loading, Figure 1. We are confident that molecular complexes have been analyzed and no RuO_2 formation took place during the experiment. Our *in situ* set up allows simple verification of it. When potential was cycled back to +0.2V all Ru species have been converted back to Ru^{II} which would not be the case if RuO_2 had formed under reaction condition. XANES analysis shows that the final oxidation state of the Ru center under catalytic conditions of water oxidation is Ru^{IV}. Production of advanced assemblies with stabilized surface species is required for future testing at different pH, buffer conditions and using Ru complexes with different catalytic activities. In the future we will explore potential of MOF assemblies which integrate molecular Ru catalysts in their framework.

We also conducted a detailed *in situ* analysis of the parent $[Ru(tpy)(bpy)H_2O]^{2+}$ complex under electrocatalytic conditions, Figure 2. *In situ* Ru K-edge XANES and EXAFS of $[Ru^{II}(bpy)(tpy)H_2O]^{2+}$ show that the onset of catalytic current under acidic and neutral conditions coincides with significant modification of the Ru ligand environment while oxidation to Ru^{V} has not been observed at any time. During *in situ* catalysis the oxidation state and key fragment of the majority species is Ru^{IV}=O (1.8 Å bond distance has been verified by EXAFS) at acidic conditions, Figure 2 while at neutral pH the contribution of the Ru^{III} species is significant (data not shown). Changes in the Ru oxidation state under *in situ* catalysis indicates the change of the water oxidation mechanism with pH suggesting that the Ru^{IV}=O species reacts faster with water under neutral pH depleting these species from solution. Much deeper theoretical analysis is needed to understand the underlying chemical principals. *In situ* resonance Raman will be conducted to better understand structural modifications in ligand environment under catalytic condition.

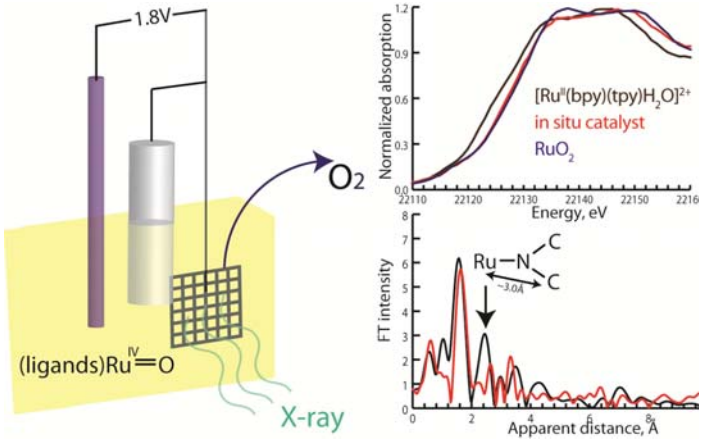

Figure 2. *In situ* XANES and EXAFS show presence of catalysts with Ru^{IV}=O fragment under catalytic condition of water oxidation, 0.1 M HNO_3. Significant modification of ligand environment occurs at the onset of catalytic current. Ru^{IV}=O bond distance of 1.80Å has been detected at pH=1 and 1.8 V (NHE).

In the future we will expand application of time resolved techniques to monitor the evolution of electronic states and bond formation dynamic during the water oxidation and light harvesting. Optical transient absorption spectroscopy and time resolved X-ray absorption spectroscopy will be used in conjunction with other techniques. We plan to uncover (i) factors controlling O-O bond formation in single site Ru complexes; (ii) the effects of integration into MOF framework on activity, stability and mechanism of action of molecular water oxidation catalysts; (iii) pathways of charge separation, electron transfer and catalytic activation in multifunctional assemblies. Analysis of intermediates reactive towards the O-O bond formation will allow to enhance reactions at low overpotentials resulting in better catalysts.

DOE Sponsored Publications 2013-2016

1. "Electronic structure assessment: Combined Density Functional Theory Calculations and Ru $L_{2,3}$-edge X-ray Absorption Near-edge Spectroscopy of Water Oxidation Catalyst" I. Alperovich, D. Moonshiram, J. Concepcion, and Y. Pushkar, **J. Phys. Chem. C**, 2013, *117* (37), pp 18994–19001.
2. "Experimental Demonstration of Radicaloid Character in a Ru^{V}=O Intermediate in Catalytic Water Oxidation" D. Moonshiram, I. Alperovich, J. Concepcion, T. Meyer, Y. Pushkar, **PNAS**, 2013, 110 (10) 3765-3770.
3. "Mechanism of Catalytic Water Oxidation by Ruthenium Blue dimer catalyst: comparative study in D_2O versus H_2O" D. Moonshiram, V. Purohit, J. Concepcion, T. Meyer, Y. Pushkar, **Materials**, 2013, 6 (2), pp 392-409.
4. "Kinetic modeling of the x-ray induced damage to a metalloprotein" K. M. Davis, I. Kosheleva, R. W. Henning, G. T. Seidler, Y. Pushkar, **J. Phys. Chem. B**, 2013, *117* (31), pp 9161–9169.
5. "A Mononuclear Nonheme Manganese(IV)-Oxo Complex Binding Redox-Inactive Metal Ions" J. Chen, Y.-M. Lee, K. Davis, X. Wu, M. S. Seo, K.B. Cho, H. Yoon, Y. J. Park, S. Fukuzumi, Y. Pushkar, W. Nam. **J. Am. Chem. Soc.,** 2013, *135* (17), pp 6388–6391. *This work was featured on JACS cover and selected as "one of the outstanding recent results" at Advanced Photon Source news letter.*
6. „Spectroscopic analysis of catalytic water oxidation by $Ru^{II}(bpy)(tpy)H_2O]^{2+}$ suggests that Ru^{V}=O is not a rate-limiting intermediate" Y. Pushkar, D. Moonshiram, V. Purohit, L. Yan, I. Alperovich, **J. Am. Chem. Soc.**, **2014,** *136* (34), pp 11938–11945.
7. "Serial Time-resolved crystallography of Photosystem II using a femtosecond X-ray laser" C. Kupitz, S. Basu, I. Grotjohann, R. Fromme, N. A. Zatsepin, K. N. Rendek, M. Hunter, R. L. Shoeman, T. A. White, D. Wang, D. James, J.-H. Yang, D. E Cobb, B. Reeder, R. G. Sierra, H. Liu , A. Barty, A. L. Aquila, D. Deponte, R. A. Kirian, S. Bari, J. J. Bergkamp, K. R. Beyerlein, M. J. Bogan, C. Caleman, T.-C. Chao, C. E. Conrad, K. M. Davis, H. Fleckenstein, L. Galli, S. P. Hau-Riege, S. Kassemeyer, H. Laksmono, M. Liang, L. Lomb, S. Marchesini, A. M. Martin, M. Messerschmidt, D. Milathianaki, K. Nass, A. Ros, S. Roy-Chowdhury, K. Schmidt, M. Seibert, J. Steinbrener, F. Stellato, L. Yan, C. Yoon, T. A. Moore, A. L. Moore, Y. Pushkar, G. J. Williams, S. Boutet, R. B. Doak, U. Weierstall, M. Frank, H. N. Chapman, J. C.H. Spence and P. Fromme, **Nature**, 2014, 513, pp 261-265.
8. „Triplet excited state energies and phosphorescence spectra of (bacterio)chlorophylls." D. A. Hartzler, D. M. Niedzwiedzki, D. A. Bryant, R. E. Blankenship, Y. Pushkar, S. Savikhin, **J. Phys. Chem. B**, **2014**, *118* (26), pp 7221–7232.
9. "Unexpected ligand lability in condition of water oxidation catalysis" L. Yan, R. Zong, Y. Pushkar, **J. Catal.**, 2015, V. 330, p. 255-260.

Resolving Structures *In-Situ* for Solar-Driven Water-Oxidation Catalysts Using High Energy X-ray Scattering

David M. Tiede[1], Gihan Kwon[1], Alex B. F. Martinson[2], Karen L. Mulfort[1], Lisa M. Utschig[1], Oleg G. Poluektov[1], Lin X. Chen[1]
[1]Chemical Sciences and Engineering and [2]Materials Sciences Divisions
Argonne National Laboratory
Argonne, IL, 60439

The program in solar photochemistry at the Argonne National Laboratory investigates fundamental mechanisms for coupling light-generated excited-states to multiple-electron, proton-coupled water-splitting and fuels catalysis. A key aspect of this program is the development advanced synchrotron X-ray, electron paramagnetic resonance, and ultrafast transient optical approaches for investigating structures and mechanisms at the atomic scale, and that are applied for the analysis of designed artificial and biomimetic systems for solar energy conversion. This presentation will discuss the development of high energy X-ray (60 keV) scattering and atomic pair distribution function (PDF) analyses for the resolution water-oxidation and solar fuel catalyst structures, with a goal of resolving structure, "one electron at a time", following successive, single-electron, photo-initiated electron transfers. The PDF technique offers an opportunity to resolve atomic pair correlations across the full inner and outer shell coordination spheres for transition metal complexes with 0.2 Å spatial resolution. This level of precision is sufficient to develop explicit coordinate models. We are developing PDF techniques as *in-situ* approaches for investigation of photochemical processes for both homogeneous and interfacial, electrode-supported, solar-driven water splitting and fuels catalysis.

1. Amorphous Metal Oxide Clusters as Biomimetic Water-Oxidation Catalysts. Amorphous thin film oxygen evolving catalysts (OECs) of first-row transition metals are of significant interest for applications in solar energy conversion as catalytic sub-systems in artificial photosynthesis. We have developed X-ray atomic pair distribution function analysis techniques for the characterization of the "molecular-dimensioned" domain structures within amorphous oxide water-oxidation catalyst films. We have extended the *in-situ* PDF technique by developing 3-D porous electrode architectures based on microchannel arrays ALD coated with conductive ITO layers that enable structural characterization of interfacial thin films of first row transition metal oxides during photo-electrochemical function. With these porous electrode architectures, we find that

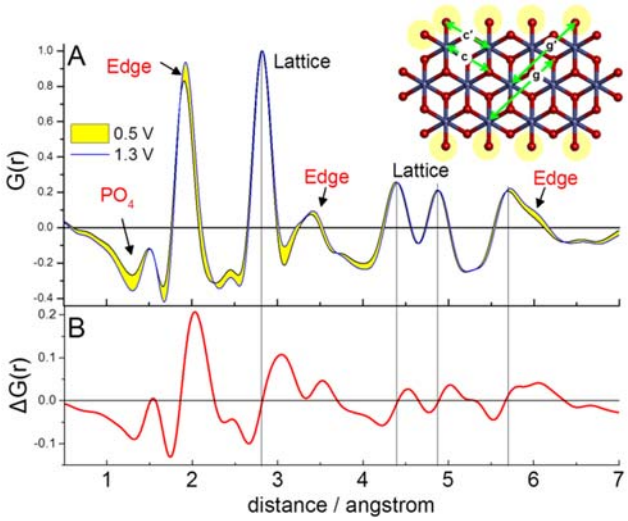

Figure 1. Oxidation-induced changes in PDF fine structure for the CoPi OEC amorphous thin film catalyst. Part A shows PDF for the CoPi held at 0.5 V (yellow) and 1.34 V (blue) vs. NHE. The shaded area highlights the areas of difference between these curves. The inset shows the edge-sharing cobaltate domain structure and highlights locations of atoms associated with the fine structure change. Part B shows the 0.5 V - 1.34 V difference PDF pattern.

are able to carry out high resolution PDF analysis for amorphous oxide catalyst thin films with thickness below 70 nm and under active electrochemical control.

For example, Figure 1 compares PDF patterns for the cobalt phosphate, CoPi, OEC poised at 0.5 V and 1.34 V vs NHE, that are understood to approximately correspond to the valence states $Co^{II}Co^{III}$ and $Co^{III}Co^{III}$, respectively, for redox-active cobalt atoms across di-μ-oxo units. The PDF for the CoPi OEC can be quantitatively modeled as an edge-sharing cobaltate domain from which each of the PDF peaks can be assigned. The redox-induced changes in PDF amplitudes associated with oxygen ligand coordination changes are found to be localized to sites at the domain edge, and involve only a subset of the terminal oxygen atoms. PDF peaks for atoms located within the lattice show no change in atom positions. In addition the PDF differences show changes in the background electron density that can be modelled to arise from oxidation-state driven PO_4 anion intercalation movement. These results provide the first direct "visualization" of the sites for structure changes linked to redox activity within the CoPi OEC. Further, we have discovered methods to generate a new amorphous cobaltate thin film OEC having a smaller domain and reduced edge-sharing motif, candidate structure **2**, compared to the CoPi OEC, structure **1**, Figure 2. Preliminary PDF-electrochemistry suggest that suggest this new Co-OEC has a higher proportion of redox-active atoms, potentially allowing more detailed resolution of structure changes linked to catalysis.

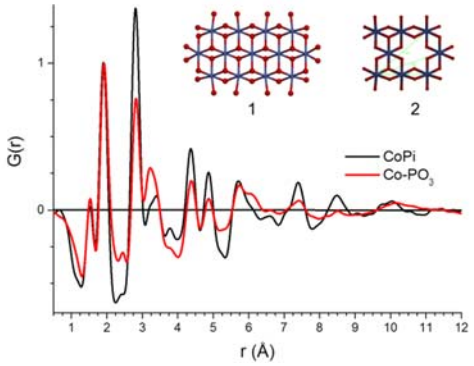

Figure 2. Comparison of the PDF for the CoPi OEC (black line) and a new Co-OEC (red line). Insets compare domain models **1** and **2** for the two OEC, respectively.

2. In-situ Structure-Function Analysis of Molecular Water Oxidation Catalysts. Building from the expertise gained from the *in-situ* analyses of amorphous oxide OECs, we are developing approaches for extending PDF for structure characterization of molecular OEC, both in solution and in electrode-supported photoelectrochemical cells. For example, Figure 3 shows the PDF pattern measured for the cobalt cubane, $Co_4O_4Ac_4Pyr_4$ (collaboration with C. Dismukes, Rutgers) in solution and compared to that calculated from the crystal structure. A good correspondence is found for the cubane core structure. Interestingly, the solution experiment shows missing outer sphere peaks that arise from the pyridine ligands. Modeling studies show that this type of selective peak attenuation can arise from rotational disorder in the pyridyl ligands, and demonstrates the opportunity to use *in-situ* PDF to resolve outer sphere ligand distances and dynamics linked to catalysis. On-going work is developing strategies for connecting photosensitizer-catalyst assemblies to electrodes and molecular electron sources and sinks, including "protein molecular wires" which we have found offer unique opportunities to investigate light-driven, multi-step photocatalysis in artificial systems by exploiting protein wire-enabled ultrafast secondary electrons transfer at cryogenic temperature.

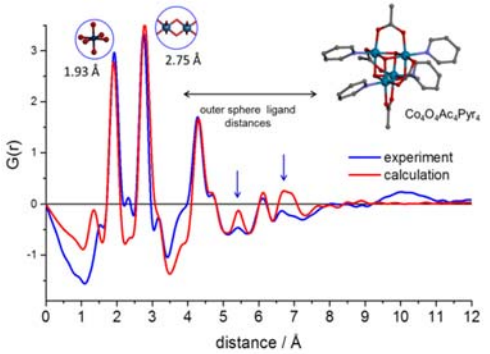

Figure 3. Comparison between experimental solution (blue) and crystal structure calculated (red) PDF for the cobalt cubane, $Co_4O_4Ac_4Pyr_4$.

DOE Sponsored Publications 2013-2016

1. Structures of Highly Active Ir Water Oxidation Catalysts from Density Functional Theory Combined with High-Energy X-Ray Scattering and EXAFS Spectroscopy. Ke R. Yang, Adam J. Matula, Gihan Kwon, Jiyun Hong, Julianne Thomsen, Gary W. Brudvig, Robert H. Crabtree, David M. Tiede, Lin X. Chen, and Victor S. Batista, (2016) J. Amer. Chem. Soc., *submitted*.

2. Oxyanion Induced Variations in Domain Structure for Amorphous Cobalt Oxide Oxygen Evolving Catalysts, Resolved by X-ray Pair Distribution Function Analysis. Gihan Kwon, Oleksandr Kokhan, Ali Han, Karena W. Chapman, Peter J. Chupas, Pingwu Du, and David M. Tiede*, (2015) *Acta Crystal. B, 71(6) Energy Materials Special Issue, 713-721*.

3. Aqueous light-driven hydrogen production by a Ru-Ferredoxin-Co biohybrid. Sarah R. Soltau, Jens Niklas, Peter D. Dahlberg, David M. Tiede, Oleg G. Poluektov, Karen L. Mulfort, and Lisa M. Utschig, (2015) *Chem. Comm., 51, 10628-10631*.

4. Bidirectional Photoinduced Electron Transfer in Ruthenium(II)- tris-bipyridyl Modified Multi-Heme c-Cytochromes from Geobacter sulfurreducens. O. Kokhan, N. Ponomarenko, A. Mukherjee, R. Pokkuluri, M. Schiffer, K. M. Mulfort, D.M. Tiede*, (2015) *Invited Article for the John R. Miller and Marshall D. Newton Festschrift in J. Phys. Chem. B,* 119, 7612-7624.

5. Nature-driven Photochemistry for Solar Hydrogen Production. L. M. Utschig, S.R. Soltau, D. M. Tiede, (2015) *Invited Article: Current Opinion in Chemical Biology, 25:1-8.*

6. Cobaloxime-Based Artificial Hydrogenases, Marine Bacchi, Gustav Berggren, Jens Niklas, Elias Veinberg, Michael W. Mara, Megan L. Shelby, Oleg G. Poluektov, Lin X. Chen, David M. Tiede, Christine Cavazza, Martin J. Field, Marc Fontecave, Vincent Artero, (2014) *Inorg. Chem.* 53(15): 8071-8082.

7. Multimerization of Solution-State Proteins by Tetrakis(4-Sulfonatophenyl) Porphyrin. Oleksandr Kokhan, Nina Ponomarenko, P. Raj Pokkuluri, Marianne Schiffer, and David M. Tiede*, (2014) *Biochemistry, 53(31): 5070-5079.*

8. Resolving the Domain Structure for the Amorphous Iridium-oxide Water Oxidation Catalyst by X-ray Pair Distribution Function Analysis, Jier Huang, James D. Blakemore, Oleksandr Kokhan, Nathan D. Schley, Robert H. Crabtree,* Gary W. Brudvig,* and David M. Tiede*, (2014) *Phys. Chem. Chem. Phys., 16(5): 1814-1819.*

9. Detection of a charge-separated catalyst precursor state in a linked photosensitizer-catalyst assembly, Anusree Mukherjee, Oleksandr Kokhan, Jier Huang, Jens Niklas, Lin X. Chen, David M. Tiede, Karen L. Mulfort* (2013) *Phys. Chem. Chem. Phys., **15**, 21070-21076.*

10. "Protein Delivery of a Ni Catalyst to Photosystem I for Light-Driven Hydrogen Production", Silver, S. C., Niklas, J., Du, P., Poluektov, O.G., Tiede, D.M., and Utschig, L.M, J. Amer. Chem. Soc., (2013) 135(36) 13246-13249.

11. Nanostructured TiO2/Polypyrrole for Visible Light Photocatalysis, Dimitrijevic, N. M.; Tepavcevic, S.; Liu, Y.; Rajh, T.; Silver, S. C.; Tiede, D. M. (2013) *J. Phys. Chem. C* **117**: 15540-15544.

12. Artificial Photosynthesis as a Frontier Technology for Energy Sustainability, T. Faunce, S. Styring, M. R Wasielewski, G. W. Brudvig, A. W. Rutherford, J. Messinger, A. F. Lee, C. L.

Hill, H. deGroot, M. Fontecave, D. R. MacFarlane, B. Hankamer, D. G Nocera , D. M. Tiede, H. Dau, W. Hillier, L. Wang (2013) *Energy Environ. Sci., 6, 1074–1076*

13. Characterization of an amorphous iridium water oxidation catalyst electrodeposited from organometallic precursors, J. D. Blakemore, M. W. Mara, M. N. Kushner-Lenhoff,† N. D. Schley, S.J. Konezny, I. Rivalta, C. F. A. Negre, R. C. Snoeberger, O. Huang, A. Stickrath, L. A. Tran, M. L. Parr, L. X. Chen,* D. M. Tiede,* V. S. Batista,* R. . Crabtree,* and G.W. Brudvig*, (2013) *Inorgan. Chem*. **52**: 1860-1871.

14. Structure-based analysis of solar fuels catalysts using *in-situ* X-ray scattering analyses, Karen L. Mulfort*, Anusree Mukherjee, Oleksandr Kokhan, Pingwu Du, David M. Tiede* (2013) *Chem. Soc. Rev*. ***42***, 2215-2227.

Session VIII

Far From Equilibrium

Understanding Roles of Ultrafast and Coherent Electronic and Atomic Motions in Photochemical Reactions

L. X. Chen,[1,2] X. Li,[3] R. D. Schaller,[1,2] F. N. Castellano,[4] K. L. Mulfort,[1] M. A. Ratner,[2] G. C. Schatz,[2] T. Seideman,[2] D. M. Tiede,[1] and their coworkers

[1]Chemical Sciences and Engineering Division, Argonne National Laboratory, Lemont, IL 60439;
[2]Department of Chemistry, Northwestern University, Evanston, IL 60208;
[3]Department of Chemistry, University of Washington, Seattle, WA 98195;
[4]Department of Chemistry, North Carolina State University, Raleigh, NC 27695

Understanding ultrafast quantum dynamics of molecular excited states prior to establishment of thermal equilibrium is an important area of solar energy harvesting and conversion. A collaborative team of nine PIs with synthesis, structural dynamics characterization and theoretical calculation has been formed since August 2014 with the aims of investigating the effects of coherent electronic or nuclear motions in the fundamental steps of photochemical reactions and energetic, structural and dynamic factors pertinent to these coherent motions. Three research foci include A) identifying, characterizing and computing functionally important coherent electronic and nuclear motions in the excited state properties of transition metal complexes (TMCs) with one or multiple metal centers. B) understanding and engineering ultrafast two-electron transfer reactions in chromophore-catalyst-chromophore supramolecular TMC assemblies and C) elucidating structure-function relationships between plasmonic structures and coherent ultrafast lattice "breathing modes" in gold nanoparticles and exploring their effects on the interfacial electron and energy transfer processes of TMC-nanoparticle hybrids.

Over the past 20 months, progress has been made in all three fronts. Several supramolecular systems with multiple chromophores have been synthesized with targeted structural modulations for altering coherent electronic and nuclear motions in these systems. A 2DES setup is being built in order to extract the dynamics of the coherences. Particularly exciting is the progress made in theoretical modeling in coherent electronic and nuclear motions in platinum dimer molecules with previously observed coherent structural dynamics, the theoretical treatment of double excitations, and inner shell excitation in the molecular excited states. More importantly, a cohesive and collaborative team with PIs and their students/postdocs has been formed through monthly meetings, the first annual meeting as well as frequent informal interactions. Here we will report two examples from our recent work: 1) coherent electronic dynamics in pyrazolate bridged di-platinum complexes (Li), and 2) coherent phonon dynamics in gold nano-double-pyramids (Schaller).

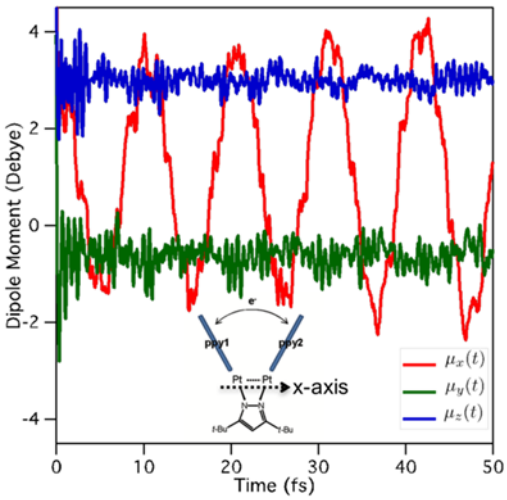

Figure 1. Calculated electronic coherence in one of the platinum pyrazolate dimer complexes, showing anisotropy of the electronic coherence.

Coherent electronic phenomena are responsible for some of the most efficient energy transfer pathways in

nature. Due to the unique potential for excited coherent states to direct the flow of energy/charge with minimal dissipation, coherently-evolving electronic excitations hold the potential to increase quantum yields in a variety of energy conversion materials. Recently, a periodic beating observed in the transient absorption anisotropy for a bi-nuclear platinum complex ([Pt(ppy)(μ-R_2pz)]$_2$, with R=tBu) was identified as a potential manifestation of a coherent, recurrent exciton motion between the two halves of the bi-chromophoric complex. To demonstrate the ability of this system, and several closely related analogues (R=phen, Me, and H), to support such electronic coherences at the experimentally-relevant excitation energies and pulse-widths, real-time time-dependent density functional theory was employed to simulate the electronic dynamics that would be initiated by a non-resonant, ultra-short laser pulse. Results indicate that at the crystal structure geometries, both the R=tBu and R=phen analogues give sufficiently short Pt-Pt distances to facilitate interactions that allow for efficient exciton transfer, while no such periodic charge oscillations were observed for the two analogues demonstrating longer interplatinum distances (R=H and R=Me). Future work will investigate the potential for electron-nuclear coherence in these system, inter-system crossings in the early-time excited state dynamics, and solvent influence on the decoherence mechanism.

We are also examining coherence in bipyramidal metal nanoparticles that exhibit especially narrow ensemble localized surface plasmon resonances (LSPRs). The small size dispersion that can be achieved in this morphology permits characterization of ensemble dynamical phenomena such as coherent phonons that interestingly induce periodic oscillations of the LSPR energy. We experimentally characterized the transient optical response of a large range of gold bipyramid sizes, as well as higher aspect ratio nanojavelin ensembles with specific attention to the lowest-order acoustic phonon mode of these nanoparticles. Nanojavelins behave similarly to nanobipyramids but offer separate control over LSPR energy and coherent phonon oscillation period. Via characterization of a large range of particle sizes for a systematic variation of excitation fluences, we have developed a new methodology for quantitatively determining the mechanical expansion caused by photo-generated coherent phonons. Using this method, we find a mode-specific particle elongation of approximately 1% per photon absorbed per unit cell and that particle expansion along the lowest frequency acoustic phonon mode is linearly proportional to excitation fluence for the range studied. Systematic variation with particle size or LSPR energy is not observed, which we attribute to finer details of particle morphology. These characterizations provide insight regarding means to manipulate phonon period and transient mechanical deformation. Ongoing work that we pursue in this area includes molecular functionalization of the surfaces of these structures with the aim of developing probes of hybridization between molecular orbitals and LSPRs. Here the goal is to determine how decoherence is impacted, as well as the extent to which hybridization is impacted by the shifts in LSPR energy.

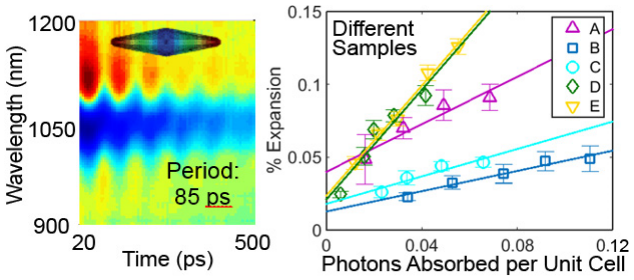

Figure 2. (left) Spectrally-resolved transient absorption data for an ensemble of gold nanoparticles following resonant excitation shows coherent phonon-induced oscillations of plasmon resonance energy, here with an 85 ps period. (right) Vibrational mode-specific percent expansion of several differently sized bipyramidal nanostructures as a function of excitation intensity.

DOE Sponsored Publications 2015-2016

1. Cobalt Kβ Valence-to-Core X-ray Emission Spectroscopy: A Sensitive Probe of Cobalt-Ligand Coordination, Katarina Schwalenstocker, Jaya Paudel, Alexander W. Kohn, Tao Yu, Chao Dong, Angelique Amado,1 George C. Schatz, Katherine M. Van Heuvelen, Erik R. Farquhar, Feifei Li, *Inorg. Chem.* Submitted (2016).

2. Transient Absorption Dynamics of Sterically Congested Cu(I) MLCT Excited States, Sofia Garakyaraghi, Evgeny O. Danilov, Catherine E. McCusker, and Felix N. Castellano, *J. Phys. Chem. A*. 119, 3181−3193 (2015).

3. Direct observation of triplet energy transfer from semiconductor nanocrystals, Cédric Mongin, Sofia Garakyaraghi, Natalia Razgoniaeva, Mikhail Zamkov, Felix N. Castellano, *Science* 351, 369 – 372 (2016).

4. Ultrafast Excited State Relaxation of a Metalloporphyrin Revealed by Femtosecond X-ray Absorption Spectroscopy, Megan L. Shelby, Patrick J. Lestrange, Nicholas E. Jackson, Kristoffer Haldrup, Michael W. Mara, Andrew B. Stickrath, Diling Zhu, Henrik Lemke, Matthieu Chollet, Brian M. Hoff-man, Xiaosong Li, Lin X. Chen, *J. Am. Chem. Soc.*, revision under review (2016).

5. Size Dependent Coherent Phonon Plasmon Modulation and Deformation Characterization in Gold Bipyramids and Nanojavelins, Matthew S. Kirschner, Clotilde M. Lethiec, Xiao-Min Lin, George C. Schatz, Lin X. Chen, and Richard D. Schaller, *ACS Photonics*, ASAP (2016).

6. Butterfly deformation modes in a photo-excited pyrazolate-bridged Pt-complex measured by time-resolved X-ray scattering in solution, Kristoffer Haldrup, Asmus Dohn, Megan L. Shelby, Michael W. Mara, Andrew B. Stickrath, Michael R. Harpham, Jier Huang, Xiaoyi Zhang, Klaus B. Møller, Arnab Chakraborty, Felix N. Castellano, David M. Tiede and Lin X. Chen, *J. Phys. Chem*. A. manuscript written to be submitted (2016).

7. Exploring the Unexplored, Double Excitations: Optical transitions and X-ray Absorption Near Edge Spectroscopy of Excited States using Time-dependent Density Functionals, Martin A. Mosquera, Lin X. Chen, Mark A. Ratner, George C. Schatz, *J. Chem. Phys.*, revision under review, (2016).

8. The Consequences of Improperly Describing Oscillator Strengths Beyond the Electric Dipole Approximation, P. J. Lestrange, F. Egidi, X. Li, *J. Chem. Phys.*, 143, 234103 (2015).

9. Energy-Specific Equation-of-Motion Coupled-Cluster Methods for High-Energy Excited States: Application to K-edge X-ray Absorption Spectroscopy, B. Peng, P. J. Lestrange, J. J. Goings, M. Caricato, X. Li, *J. Chem. Theory Comput.,* 11, 4146(2015).

10. Calibration of Energy-Specific TDDFT for Modeling K-edge XAS Spectra of Light Elements P. J. Lestrange, P. D. Nguyen, X. Li, *J. Chem. Theory Comput.,* 11, 2994 (2015).

Time-Domain Atomistic Studies of Far-from-Equilibrium Dynamics in Nanoscale Structures for Solar Energy Harvesting

Oleg V. Prezhdo
Department of Chemistry
University of Southern California
Los Angeles, CA 90089

Absorption of a photon from the visible part of the solar spectrum puts a light-harvesting system in a highly non-equilibrium state. The ensuing ultrafast dynamics determines whether the sun energy will be converted to electricity or fuel, or lost to heat. Multiple experimental groups study such dynamics using time-resolved spectroscopies. In close collaboration with experiment, we develop state-of-the-art methodologies combining non-adiabatic molecular dynamics and time-dependent density functional theory, and apply them to study specific systems and processes. The talk will cover several recent examples of atomistic modeling of ultrafast for-from-equilibrium dynamics in nanoscale materials for energy harvesting, including:

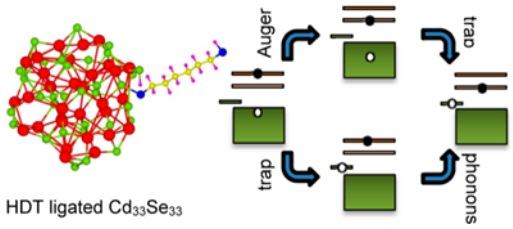

Auger-mediated electron relaxation. By slowing down electron-phonon relaxation in nanoscale materials, one can increase efficiencies of solar energy conversion via hot electron extraction, multiple exciton generation, and elimination of exciton trapping. The elusive phonon bottleneck is hard to achieve, in particular, due to Auger-type energy exchange between electrons and holes. The Auger channel can be suppressed by hole trapping. We showed that deep hole traps cannot fully eliminate the Auger channel. The simulations demonstrated that the hole-mediated electron relaxation is slowed down only by about 30%, which is in agreement with the recent experiments. The Auger energy exchange and hole relaxation to the trap state occur on similar time scales. Hole trapping is slow, because holes themselves experience a weak bottleneck effect. The study shows that more sophisticated hole trapping strategies, for example involving shell layers, are required in order to reduce electronic energy losses.

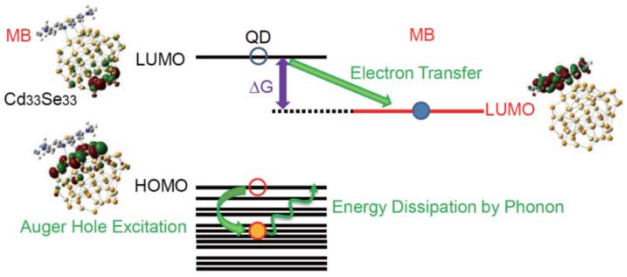

Auger-assisted electron transfer. Quantum confinement in nanoscale materials allows Auger-type electron−hole energy exchange. We showed by direct time-domain atomistic simulation and analytic theory that Auger processes give rise to a new mechanism of charge transfer (CT). Auger-assisted CT eliminates the Marcus inverted regime, rationalizing recent experiments on CT from quantum dots (QDs) to molecular adsorbates. The ab initio simulation reveals a complex interplay of the electron−hole and charge−phonon channels of energy exchange, demonstrating a variety of CT scenarios. The developed Marcus rate theory for Auger-assisted CT described, without adjustable parameters, the experimental plateau of the CT rate in the region of large donor-acceptor energy gap. The analytic theory and atomistic insights apply broadly to charge and energy transfer in nanoscale systems.

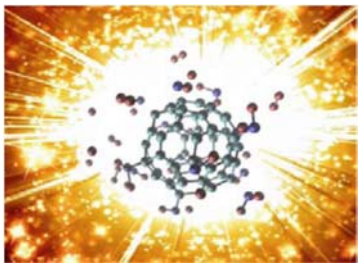

High energy buckyball. Nanoscale systems containing high density of energetic covalent bonds provide means to store the energy harvested from the sun. We investigated energy release from a nitro-fullerene. Upon initial heating, $C_{60}(NO_2)_{12}$ disintegrates, increasing temperature and pressure by thousands of Kelvins and bars within tens of picoseconds. The explosion starts with NO_2 group isomerization into C−O−N−O, followed by emission of NO molecules and formation of CO groups on the buckyball surface. NO oxidizes into NO_2, and C_{60} falls apart, liberating CO_2. At the highest temperatures, CO_2 gives rise to diatomic carbon. The study showed that the initiation temperature and released energy depend strongly on the chemical composition and density of the material. The work was highlighted in the September 2014 issue of the *New Scientist* magazine.

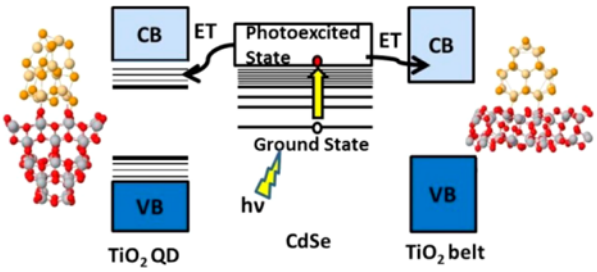

Dimensionality of nanoscale TiO_2 determines electron injection mechanism. We demonstrated that the mechanism of CT from a CdSe QD into nanoscale TiO_2 depends on TiO_2 dimensionality. The injection into a TiO_2 QD is adiabatic due to strong donor-acceptor coupling, arising from unsaturated chemical bonds on the QD surface, and low density of acceptor states. In contrast, the injection into a TiO_2 nanobelt is nonadiabatic, because the state density is high, the donor-acceptor coupling is weak, and multiple phonons accommodate changes in the electronic energy. Both mechanisms give efficient injection, but dependence on system properties is very different, demonstrating that the fundamental principles leading to efficient charge separation depend strongly on the type of nanoscale material.

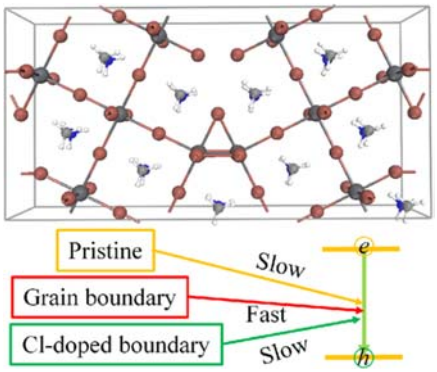

Grain boundary (GB) and doping in electron-hole recombination in perovskites. Electron-hole recombination constitutes a major pathway of energy and current losses. GBs are common in methylammonium lead iodine ($MAPbI_3$) perovskite polycrystalline films. Previous calculations suggested that GBs have little effect on the recombination; however, experiments defy this prediction. We showed that GBs notably accelerate the electron-hole recombination in $MAPbI_3$. First, GBs decrease the $MAPbI_3$ bandgap. Second, GBs enhance electron-phonon coupling by localizing electron and hole wave functions, and by creating additional phonon modes. Replacing iodines by chlorines at GBs reduces the electron-hole recombination. By pushing the HOMO density away from the boundary, chlorines restore the electron-phonon coupling close to the value observed in pristine $MAPbI_3$. By introducing higher-frequency phonons and increasing fluctuation of the electronic gap, chlorines shorten electronic coherence. Both factors compete successfully with the reduced bandgap relative to pristine $MAPbI_3$ and favor long excited-state lifetimes. The simulations suggest a route to increased photon-to-electron conversion efficiencies through rational GB passivation. The work was featured in a *JACS spotlight*.

DOE Sponsored Publications 2013-2016

Reviews

1. Akimov, A. V.; Neukirch, A. J.; Prezhdo, O. V., Theoretical Insights into Photoinduced Charge Transfer and Catalysis at Oxide Interfaces. *Chemical Reviews* **2013**, *113*, 4496-4565.
2. Jaeger, H. M.; Hyeon-Deuk, K.; Prezhdo, O. V., Exciton Multiplication from First Principles. *Accounts of Chemical Research* **2013**, *46*, 1280-1289.
3. Akimov, A. V.; Prezhdo, O. V., Large-Scale Computations in Chemistry: A Bird's Eye View of a Vibrant Field. *Chemical Reviews* **2015**, *115*, 5797-5890.
4. Neukirch, A. J.; Hyeon-Deuk, K.; Prezhdo, O. V., Time-Domain Ab Initio Modeling of Excitation Dynamics in Quantum Dots. *Coordination Chemistry Reviews* **2014**, *263*, 161-181.

Regular Articles

5. Akimov, A. V.; Muckerman, J. T.; Prezhdo, O. V., Nonadiabatic Dynamics of Positive Charge During Photocatalytic Water Splitting on Gan(10-10) Surface: Charge Localization Governs Splitting Efficiency. *Journal of the American Chemical Society* **2013**, *135*, 8682-8691.
6. Akimov, A. V.; Prezhdo, O. V., Persistent Electronic Coherence Despite Rapid Loss of Electron-Nuclear Correlation. *Journal of Physical Chemistry Letters* **2013**, *4*, 3857-3864.
7. Akimov, A. V.; Prezhdo, O. V., The Pyxaid Program for Non-Adiabatic Molecular Dynamics in Condensed Matter Systems. *Journal of Chemical Theory and Computation* **2013**, *9*, 4959-4972.
8. Kalugin, O. N.; Voroshylova, I. V.; Riabchunova, A. V.; Lukinova, E. V.; Chaban, V. V., Conductometric Study of Binary Systems Based on Ionic Liquids and Acetonitrile in a Wide Concentration Range. *Electrochimica Acta* **2013**, *105*, 188-199.
9. Kilina, S. V.; Neukirch, A. J.; Habenicht, B. F.; Kilin, D. S.; Prezhdo, O. V., Quantum Zeno Effect Rationalizes the Phonon Bottleneck in Semiconductor Quantum Dots. *Physical Review Letters* **2013**, *110*, 180404.
10. Liu, J.; Neukirch, A. J.; Prezhdo, O. V., Phonon-Induced Pure-Dephasing of Luminescence, Multiple Exciton Generation, and Fission in Silicon Clusters. *Journal of Chemical Physics* **2013**, *139*, 164303.
11. Long, R.; English, N. J.; Prezhdo, O. V., Defects Are Needed for Fast Photo-Induced Electron Transfer from a Nanocrystal to a Molecule: Time-Domain Ab Initio Analysis. *Journal of the American Chemical Society* **2013**, *135*, 18892-18900.
12. Prezhdo, O.; Drogosz, A.; Zubkova, V.; Prezhdo, V., On Viscosity of Selected Normal and Associated Liquids. *Journal of Molecular Liquids* **2013**, *182*, 32-38.
13. Wang, L. J.; Akimov, A. V.; Chen, L. P.; Prezhdo, O. V., Quantized Hamiltonian Dynamics Captures the Low-Temperature Regime of Charge Transport in Molecular Crystals. *Journal of Chemical Physics* **2013**, *139*.
14. Akimov, A. V.; Long, R.; Prezhdo, O. V., Coherence Penalty Functional: A Simple Method for Adding Decoherence in Ehrenfest Dynamics. *Journal of Chemical Physics* **2014**, *140*, 194107.
15. Akimov, A. V.; Prezhdo, O. V., Advanced Capabilities of the Pyxaid Program: Integration Schemes, Decoherence Effects, Multiexcitonic States, and Field-Matter Interaction. *Journal of Chemical Theory and Computation* **2014**, *10*, 789-804.
16. Chaban, V. V.; Maciel, C.; Fileti, E. E., Solvent Polarity Considerations Are Unable to

Describe Fullerene Solvation Behavior. *Journal of Physical Chemistry B* **2014**, *118*, 3378-3384.
17. Guo, Z. Y.; Prezhdo, O. V.; Hou, T. J.; Chen, X.; Lee, S. T.; Li, Y. Y., Fast Energy Relaxation by Trap States Decreases Electron Mobility in Tio2 Nanotubes: Time-Domain Ab Lnitio Analysis. *Journal of Physical Chemistry Letters* **2014**, *5*, 1642-1647.
18. Korsun, O. M.; Kalugin, O. N.; Prezhdo, O. V., Control of Carbon Nanotube Electronic Properties by Lithium Cation Intercalation. *Journal of Physical Chemistry Letters* **2014**, *5*, 4129-4133.
19. Liu, J.; Neukirch, A. J.; Prezhdo, O. V., Non-Radiative Electron-Hole Recombination in Silicon Clusters: Ab Initio Non-Adiabatic Molecular Dynamics. *Journal of Physical Chemistry C* **2014**, *118*, 20702-20709.
20. Neukirch, A. J.; Shamberger, L. C.; Abad, E.; Haycock, B. J.; Wang, H.; Ortega, J.; Prezhdo, O. V.; Lewis, J. P., Nonadiabatic Ensemble Simulations of Cis-Stilbene and Cis-Azobenzene Photoisomerization. *Journal of Chemical Theory and Computation* **2014**, *10*, 14-23.
21. Postupna, O.; Jaeger, H. M.; Prezhdo, O. V., Photoinduced Dynamics in Carbon Nanotube Aggregates Steered by Dark Excitons. *Journal of Physical Chemistry Letters* **2014**, *5*, 3872-3877.
22. Tafen, D. N.; Long, R.; Prezhdo, O. V., Dimensionality of Nanoscale Tio2 Determines the Mechanism of Photoinduced Electron Injection from a Cdse Nanoparticle. *Nano Letters* **2014**, *14*, 1790-1796.
23. Trimithioti, M.; Akimov, A. V.; Prezhdo, O. V.; Hayes, S. C., Analysis of Depolarization Ratios of Clno2 Dissolved in Methanol. *Journal of Chemical Physics* **2014**, *140*, 014301.
24. Zhu, H. M.; Yang, Y.; Hyeon-Deuk, K.; Califano, M.; Song, N. H.; Wang, Y. W.; Zhang, W. Q.; Prezhdo, O. V.; Lian, T. Q., Auger-Assisted Electron Transfer from Photoexcited Semiconductor Quantum Dots. *Nano Letters* **2014**, *14*, 1263-1269.
25. Akimov, A. V.; Jinnouchi, R.; Shirai, S.; Asahi, R.; Prezhdo, O. V., Theoretical Insights into the Impact of Ru Catalyst Anchors on the Efficiency of Photocatalytic CO2 Reduction on Ta2o5. *Journal of Physical Chemistry B* **2015**, *119*, 7186-7197.
26. Chaban, V. V.; Fileti, E. E.; Prezhdo, O. V., Buckybomb: Reactive Molecular Dynamics Simulation. *Journal of Physical Chemistry Letters* **2015**, *6*, 913-917.
27. Hyeon-Deuk, K.; Kim, J.; Prezhdo, O. V., Ab Initio Analysis of Auger-Assisted Electron Transfer. *Journal of Physical Chemistry Letters* **2015**, *6*, 244-249.
28. Neukirch, A. J.; Park, J.; Zobac, V.; Wang, H.; Jelinek, P.; Prezhdo, O. V.; Zhou, H. C.; Lewis, J. P., Calculated Photo-Isomerization Efficiencies of Functionalized Azobenzene Derivatives in Solar Energy Materials: Azo-Functional Organic Linkers for Porous Coordinated Polymers. *Journal of Physics-Condensed Matter* **2015**, *27*, 134208.
29. Prezhdo, V.; Olan, K.; Prezhdo, O.; Zubkova, V., Vapor-Phase Molar Kerr Constant Values from Solution Measurements. *Journal of Molecular Structure* **2015**, *1079*, 258-265.
30. Tafen, D.; Prezhdo, O. V., Size and Temperature Dependence of Electron Transfer between Cdse Quantum Dots and a Tio2 Nanobelt. *Journal of Physical Chemistry C* **2015**, *119*, 5639-5647.
31. Trivedi, D. J.; Wang, L. J.; Prezhdo, O. V., Auger-Mediated Electron Relaxation Is Robust to Deep Hole Traps: Time-Domain Ab Initio Study of Cdse Quantum Dots. *Nano Letters* **2015**, *15*, 2086-2091.
32. Wang, L. J.; Prezhdo, O. V.; Beljonne, D., Mixed Quantum-Classical Dynamics for Charge Transport in Organics. *Physical Chemistry Chemical Physics* **2015**, *17*, 12395-12406.

33. Chaban, V. V.; Prezhdo, O. V., Pressure-Driven Opening of Carbon Nanotubes. *Nanoscale* **2016**, DOI: 10.1039/c6nr00138f, Nanoscale Focus.
34. Long, R.; Liu, J.; Prezhdo, O. V., Unravelling the Effects of Grain Boundary and Chemical Doping on Electron−Hole Recombination in Ch3nh3pbi3 Perovskite by Time-Domain Atomistic Simulation. *Journal of the American Chemical Society* **2016**, in press.
35. Sowers, K. L.; Pal, S.; Hou, Z.; Peterson, J. J.; Swartz, B.; Prezhdo, O. V.; Krauss, T. D., Optical Properties of Cdse/Cds Core/Shell Qds with Tunable Surface Composition. *Chemical Physics* **2016**, in press.
36. Chaban, V. V.; Prezhdo, O. V., Ionic Vapor Composition in Pyridinium-Based Ionic Liquids. *Journal of Physical Chemistry B*, submitted.
37. Chaban, V. V.; Prezhdo, O. V., Ionic Vapor Composition in Critical and Supercritical States of Strongly Interacting Ionic *Journal of Physical Chemistry B*, submitted.
38. Chaban, V. V.; Prezhdo, O. V., Boron Doping of Graphene – Pushing the Limit. *Nanoscale Horizons*, submitted.
39. Chaban, V. V.; Prezhdo, O. V., The Haber Process Made Efficient by Hydroxylated Graphene. *Chemistry of Materials*, submitted.
40. Pal, S.; Prezhdo, O. V., Hollow Zno Cluster as a Promising Acceptor for D-Π-a Type Dye-Sensitized Solar Cells. *Journal of Physical Chemistry C*, submitted.
41. Chaban, V. V.; Prezhdo, O. V., Energy Storage in Cubane Derivatives and Their Real-Time Decomposition: Computational Molecular Dynamics and Thermodynamics, in preparation.
42. Loh, Z. H.; Pal, S.; Prezhdo, O. V., Auger Assisted Hole Trapping in Cdse/Cds Nanoplatelets, in preparation.
43. Pal, S.; Ninjar, P.; Prezhdo, O. V., Atomistic Study of Long-Lived Quantum Coherence in Two-Dimensional Cdse Nanostructures at Room Temperature, in preparation.

Book Chapter:

44. A. J. Neukirch and O. V. Prezhdo "Charge and exciton dynamics in semiconductor quantum dots: A time-domain, ab initio view" in Book *Dynamics of Electron Transfer in Solar Energy Conversion*, Edited by Piotr Piotrowiak, ISBN 978-1-84973-387-8 Royal Society of Chemistry, 2013.

Characterizing Singlet Fission in the Context of Exciton Migration and Dissociation

Justin Johnson,[†] Dylan Arias,[†] Natalie Pace,[†,‡] Joe Ryerson,[†,‡]Niels Damrauer,[‡] Garry Rumbles[†,‡]
†National Renewable Energy Laboratory, 15013 Denver West Pkwy, Golden, CO 80401
‡Dept. of Chemistry and Biochemistry, University of Colorado, Boulder, CO 80309

In ensembles of molecules expected to undergo singlet fission, it is often the case that relatively fast exciton migration occurs in parallel with the formation of two triplets from one photoexcited singlet. For situations in which this motion is similar in rate to the intrinsic singlet fission process, the dynamics are coupled and produce interesting effects. We have chosen to investigate polymorphs of tetracene and pentance, and their simple derivatives, using tools that can help us measure specifically exciton motion and dissociation in concert with singlet decay and triplet formation.

Tetracene is the best-known singlet fission molecule. In the common bulk crystalline form, the singlet fission rate constant is approximately 10 ns^{-1}. In thin films the rate can be faster, although the origin of the enhancement is unknown.[1] We have studied both the common tetracene polymorph (type I) and the less common one (type II) in thin film form by ultrafast transient absorption spectroscopy. The data clearly show a trend for the singlet fission rate constant with crystallite size in the type I film, but essentially no dependence in the type II film, which exhibits the fastest rate constant of about 40 ns^{-1} (Fig 1). Calculations suggest that the key interactions driving singlet fission are not responsible for this change in rate. However, it is clear that the overall density of molecules in the unit cell of type II crystals is higher than that of type I, and it is likely that the hastened migration of excitons to sites with preferred intermolecular orientation for singlet fission leads to the increased rate. The coupling of triplets to singlets via singlet fission and triplet fusion results in an effectively longer triplet exciton diffusion time, as the triplets can leverage the fast and long-range Förster energy transfer process while they remain in equilibrium with the singlet.

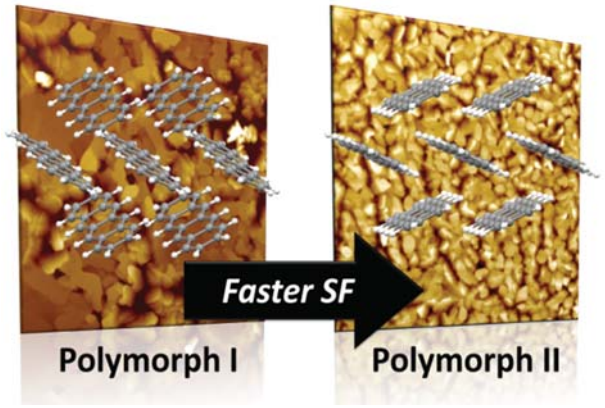

Figure 1. Thin film polymorphs of tetracene: atomic force microscopy images (background), structures (foreground) and their relative singlet fission rates.

Pentacene possesses a similar set of thin film polymorphs[2] as tetracene that have been investigated sparingly for their exciton dynamics properties. By careful control of the deposition conditions, we have produced two film types (called “thin film” and “bulk”) with high purity (Fig 2a). Despite a very similar variation in intermolecular arrangements as with the tetracene polymorphs, the kinetics associated with singlet fission in pentacene appear to be insensitive to the polymorph type (Fig 2b). The fast singlet fission rate, partially assisted by the net exoergicity of the process in pentacene, reduces any substantial migration of the singlet in the roughly 100-300 fs required for two triplets to form. The endothermicity of the process of triplet-triplet annihilation further lessens the opportunity for singlet exciton migration to play a

significant role.

In many manifestations of energy harvesting schemes involving singlet fission, charges need to be produced from the triplet excitons. Time-resolved microwave conductivity (TRMC) is a unique tool for monitoring the production and lifetime of mobile free carriers, which by itself enables the unique opportunity to observe the effects of singlet fission in a system designed to also separate charges. We have begun to investigate the singlet fission process using TRMC, finding that for both tetracene and pentacene, the TRMC signal is very large and long-lived in the neat films that lack an acceptor. In bilayers, the large hole mobility in the crystalline polyacenes complicates attempts to isolate the free electron signal that should occur upon interfacial electron transfer. Using diphenyltetracene, which can be fabricated as a quasi-amorphous layer,[3] we have been able to detect charges injected into mesoporous TiO_2 layers. Comparing the signal with that of a well-known MLCT dye injecting into TiO_2, we can quantify the charge carrier yield and its rise above 100% in the presence of efficient singlet fission.

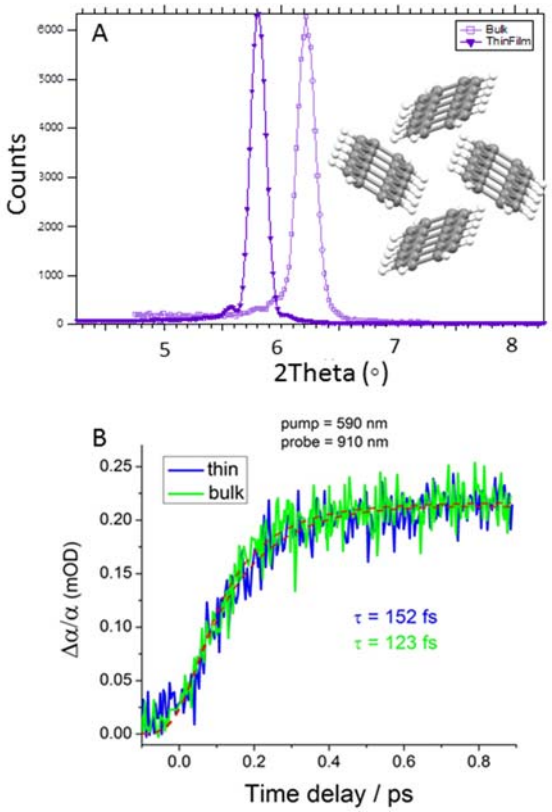

Figure 2. A) XRD scattering for bulk (light purple) and thin film(dark purple) pentacene samples. B) The singlet fission time, as observed as a rise in triplet absorption for both types of films.

Surprisingly, the signal from free charge carriers in neat pentacene films depends strongly on the excitation wavelength. Given our understanding that essentially all photoexcited singlets fission into triplets within 0.5 ps, the origin of this wavelength-dependent signal is puzzling. However, we find a connection between features in the TRMC action spectrum and those of charge-transfer (CT) states known to exist near and above the lowest singlet exciton.[4] The excitation of states that are strongly delocalized, many of which have high CT character, may lead to fast production of free charge carriers in competition with singlet fission, albeit in low yield (< 10%). The TRMC action spectrum can potentially reveal the character of these higher-lying exciton states that play a role not only in charge-generation but also in singlet fission. Further investigations are underway to measure the TRMC response from polyacene derivatives with varying degrees of intermolecular coupling in polycrystalline solids that influence the degree of delocalization in the initially photoexcited state. Correlation with transient absorption measurements of the singlet fission rate is also being pursued.

1. Piland, G.B.; Bardeen, C.J. *J. Phys. Chem. Lett.*, **2015**, *6*, 1841-1846.

2. Cheng. H-L.; Lin, J-W. *Cryst. Gr. Des.*. **2010**, *10*, 4501-4508.

3. S. T. Roberts, R. E. McAnally, J. N. Mastron, D. H. Webber, M. T. Whited, R. L. Brutchey, M. E. Thompson and S. E. Bradforth, *J. Am. Chem. Soc.*, **2012**, *134*, 6388-6400.

4. Coto, P; Sharifzadeh, S.; Neaton, J.B.; Thoss, M.; *J. Chem. Th. Comp*. **2015**, *11*, 147.

DOE Sponsored Publications 2013-2016

1. Schrauben, J.N.; Akdag, A.; Wen, J.; Ryerson, J.L.; Smith, M.; Havlas, Z.; Michl, J.; Johnson, J.C. "Excitation Localization/Delocalization Isomerism in Strongly Coupled Dimers of 1,3-Diphenylisobenzofuran," *J. Phys. Chem. A*, under revision.
2. Dowgiallo, A.; Mistry, K.S.; Johnson, J.C.; Reid, O.G., Blackburn, J.L. "Probing Exciton Diffusion and Dissociation in Single-Walled Carbon Nanotube-C_{60} Heterojunctions," *J. Phys. Chem. Lett*., under revision
3. Arias, D.; Ryerson, J.; Cook, J.; Damrauer, N.; Johnson, J. "Polymorphism influences singlet fission rates in tetracene thin films," *Chem. Sci.* **2016**, *7*, 1185.
4. Sagar, D.M.; Johnson, J.C.; Konold, P. Ullom, J.; Baddour, F.; Ruddy, D.; Jimenez, R. "Femtosecond Measurements of Size-Dependent Spin Crossover in $Fe^{II}(pyz)Pt(CN)_4$ nanocrystals," *J. Phys. Chem. Lett.* **2016**, *7*, 148-153**.**
5. Wan, Y.; Guo, Z.; Zhu, T.; Yan, S.; Johnson, J.C.; Huang, L. "Cooperative Singlet and Triplet Exciton Transport in Tetracene Crystals Visualized by Ultrafast Microscopy," *Nat. Chem.* **2015**, *7*, 785-792.
6. Beard, M.C.; Johnson, J.C.; Luther, J.M.; Nozik, A.J. "Multiple Exciton Generation in Quantum Dots vs. Singlet Fission in Molecules for Efficient Solar Photoconversion." *Phil.Trans. R. Soc. A*, **2015**, *373*, 2044.
7. Wheeler, L.M.; Anderson, N.C.; Palomaki, P.K.; Blackburn, J.B.; Johnson, J.C.; Neale, N.R. "Silyl Radical Abstraction in the Functionalization of Plasma-Synthesized Silicon Nanocrystals." *Chem. Mater.* **2015**, 27, 6869-6878.
8. Sagar, D.M.; Palomaki, P.K.; Neale, N.R.; Blackburn, J.L.; Johnson, J.C.; Beard, M.C. "Quantum Confined Electron-Phonon Interaction in Silicon Quantum Dots," *Nano Lett.* **2015**. 15, 1511.
9. Schrauben, J.N.; Zhao Y.; Mercado, C.; Ryerson, J.; Dron, P.; Michl, J.; Zhu, K.; Johnson, J.C. "Photocurrent Enhanced by Singlet Fission in a Dye-Sensitized Solar Cell," *ACS Appl. Mater. Interfaces*. **2015**. *7*, 2286-93.
10. Johnson, J.C.; Michl, J.; Chapter 10: "Singlet Fission and 1,3-Diphenylisobenzofuran as a Model Chromophore." **2014**, In *Advanced Concepts in Photovoltaics.* The Royal Society of Chemistry, p 324-344.
11. Anne-Marie Dowgiallo, Kevin S. Mistry, Justin C. Johnson and Jeffrey L. Blackburn. "Ultrafast Spectroscopic Signature of Charge Transfer between Single-Walled Carbon Nanotubes and C_{60}," *ACS Nano*, **2014** *8*, 8573.
12. Schrauben, J.N.; Ryerson, J.; Michl, J.; Johnson, Justin C. "The Mechanism of Singlet Fission in Thin Films of 1,3-Diphenylisobenzofuran," *J. Am. Chem. Soc.*, **2014**, *136*, 7363.
13. Ryerson, J.; Schrauben, J.N.; Ferguson, A.J.; Sahoo, S.C.; Naumov, P.; Havlas, Z.; Michl, J.; Nozik, A.J.; Johnson, J.C. "Two Thin Film Polymorphs of the Singlet Fission Compound 1,3-Diphenylisobenzofuran," *J. Phys. Chem. C*, **2014,** *118*, 12121-12132.
14. Crisp, R.W.; Schrauben, J.N.; Beard, M.C.; Luther, J.M.; Johnson, J.C. "Coherent Exciton Delocalization in Strongly Coupled Quantum Dot Arrays," *Nano Lett.* **2013,** 13, 4862.
15. Johnson, J.C.; Nozik, A.J.; Michl, J. "The Role of Chromophore Coupling in Singlet Fission," *Acc. Chem. Res.* **2013,** *46*, 1290-1296.
16. Johnson, J.C; Akdag, A.; Zamadar, M.; Chen, X.; Schwerin, A.F.; Paci, I.; Smith, M.B.; Havlas, Z.; Miller, J.R.; Ratner, M.A.; Nozik, A.J.; Michl, J. "Toward Designed Singlet Fission: Solution Photophysics of Two Indirectly Coupled Covalent Dimers of 1,3-Diphenylisobenzofuran," *J. Phys. Chem. B* **2013**, *117*, 4680.

Session IX

Heterogeneous Water Splitting

Modular Nanoscale and Biomimetic Systems for Photocatalytic Hydrogen Generation

Kara L. Bren, Richard Eisenberg, Todd D. Krauss
Department of Chemistry
University of Rochester
Rochester, NY14627-0216

The development of solar energy resources in the U.S. requires improved methods for the conversion of light energy into storable forms of energy. One approach is to perform artificial photosynthesis in which sunlight is used to drive the synthesis of a fuel. In this project, we are taking a multidisciplinary approach to developing systems that produce the energy carrier hydrogen (H_2) from water in a light-driven reaction. Our research team is drawing on synthetic chemistry, nanochemistry, and biochemistry to develop novel catalysts and assemble new integrated systems for reducing aqueous protons to hydrogen. By working as a multidisciplinary team, we can take advantage of the benefits offered by each of these approaches.

Systems performing the reductive side of water splitting to produce hydrogen require a photosensitizer and a compatible proton-reducing catalyst, as well as a source of electrons. Our work on colloidal semiconductor quantum dots (QDs) is toward developing robust and tunable photosensitizers. Earlier work in our labs demonstrated that dihydrolipoic acid (DHLA)-capped CdSe QDs paired with a simple Ni(II) catalyst produce H_2 in the presence of visible light with a turnover number (TON) > 600,000 with respect to catalyst. The robust nature of the QD photosensitizer is critical to the success of this system. More recently, we have been developing new QDs with improved properties. One attractive material in development is SnSe. SnSe QDs lack the toxic metal Cd. Furthermore, SnSe is an infrared absorber with a bulk bandgap of ~ 0.9 eV, and thus would absorb a significant portion of the solar spectrum that is not absorbed by wider bandgap semiconductors such as CdSe. Finally, for bulk SnSe the lowest energy optical transition at 0.9 eV is indirect, while the direct transition is at 1.3 eV; this electronic structure should result in a significantly longer excited-state lifetime for a SnSe QD compared to CdSe QD. In ongoing work, we have developed a synthesis for SnSe QDs based on our success using secondary phosphine selenides to programmably synthesize PbS and PbSe QDs. We found that SnSe QDs could be made with controlled size and size dispersion by regulating the Sn:Se precursor ratio and temperature. As shown in Fig. 1, SnSe QD diameters can be tuned from 5 to 7 nm, corresponding to an indirect bandgap measured using Tauc plots from 1.3 to 1.0 eV, respectively. In future work, the photophysical properties of these materials will be characterized and their activity as photosensitizers for synthetic and biomolecular proton-reducing catalysts will be tested.

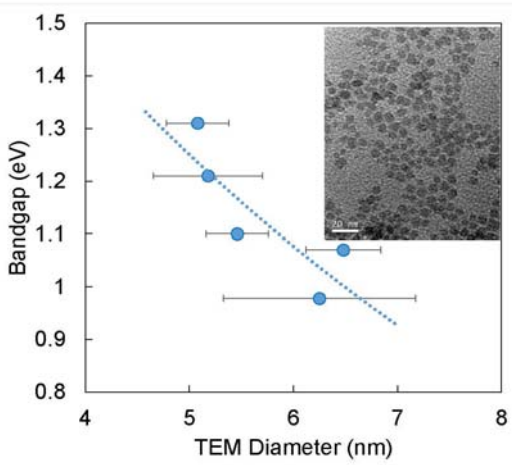

Figure 1: Correlation of SnSe QD bandgap fitted from Tauc plots with TEM determined diameter. The error bars represent the distribution of QD sizes within the sample. Inset is a TEM image of 5 nm SnSe QDs.

The development of catalysts for proton reduction has made use of both coordination complexes and biomolecular catalysts. For the former, we found that dissociation of the water-solubilizing bidentate DHLA capping agent led to DHLA substitution on the catalyst. To eliminate this problem, tridentate capping agents (S3; Fig. 2) are being employed, with the resultant QDs able to allow assessment of light-driven hydrogen production by different coordination complexes or biomolecular catalysts. Attention has also focused on complexes with redox-active ligands as possible catalysts since (a) such ligands provide additional sites for both proton stabilization and electron storage, and (b) such ligands are more resistant to hydrogenation that was a problem with other active catalysts having unsaturated ligands. Several classes of complexes have been examined in this context including Ni, Co and Fe bis(dithiolene) complexes and analogs with closely related ligands. Ongoing and future efforts are to pair these catalysts with new QD photosensitizers, and to use these catalysts in connection with photocathodes in order to produce hydrogen from aqueous protons without a sacrificial electron donor.

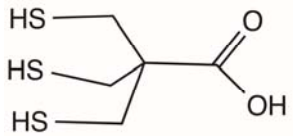

Figure 2. S3 capping ligand for CdSe quantum dots

Biomolecular hydrogen evolution catalysts offer a number of advantages. One is that they are usually soluble in water, which is the substrate and an environmentally friendly solvent. A second is their architectures facilitate the introduction of second-sphere interactions and proton relays that have been shown to greatly enhance efficiency in synthetic systems and in nature's hydrogenase enzymes. Ongoing work in our labs is toward developing robust and efficient biomolecular catalysts and characterizing proton reduction mechanism. Our first-generation semisynthetic catalyst, CoMP11-Ac, consists of an 11-mer peptide covalently bound to a cobalt porphyrin (Fig. 3, top) with a competitive turnover number (TON > 20,000 as an electrocatalyst) and rapid rate. In ongoing work, we are characterizing the role of buffering species in the catalytic mechanism and implementing CoMP11-Ac in photocatalytic systems by pairing with molecular photosensitizers, yielding preliminary TONs ~1000. New catalysts with more complex architectures also are in development. The cobalt-substituted protein variant, *Ht*-CoM61A (Fig. 3, middle) is significantly more robust than CoMP11-Ac, yielding a TON > 250,000 at a similar rate. A new system consists of a totally synthetic mini-protein with a cobalt porphyrin attached to two synthetic peptides (similar to Fig. 3, bottom). This cobalt "mimochrome" (CoMimVI) evolves hydrogen electrocatalytically with a preliminary TON of ~30,000 over 20 minutes. In future work, the synthetic protein offers the possibility of introducing unnatural amino acids as the axial Co ligand to test the effect of ligand donor strength on reactivity. Characterization of the effect of polypeptide folding on catalysis also is underway by altering pH and adding trifluoroethanol to alter polypeptide structure. Finally, all of these catalysts will be incorporated into photocatalytic systems using established (CdSe) and new (SnSe) QDs as photosensitizers. This work will be carried out in multicomponent systems and in integrated systems in which the biocatalyst is engineered to ligate the QD.

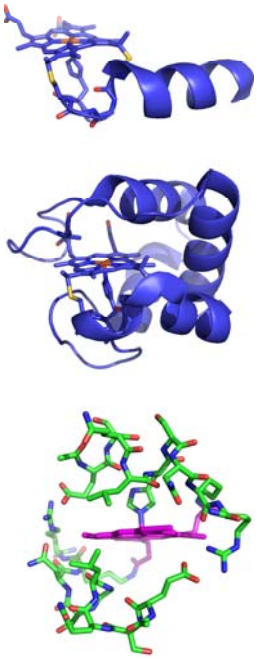

Figure 3. Models of biomolecular hydrogen evolution catalysts developed in this project. Top: CoMP11-Ac. Middle: *Ht*-CoM61A. Bottom: CoMimVI.

DOE Sponsored Publications 2013-2016

1. Cobalt Complexes as Artificial Hydrogenases for the Reductive Side of Water Splitting, Eckenhoff, W. T.; McNamara, W. R.; Du, P.; Eisenberg, R. *Biochim. Biophys. Acta* **2013**, *1827*, 958-973.
2. Photogeneration of Hydrogen from Water Using CdSe Nanocrystals: The Importance of Surface Exchange, Das, A.; Han, Z.; Haghighi, M. G.; Eisenberg, R., *Proc. Nat. Acad. Sci.* **2013**, *110*, 16716-16723.
3. Fuel from Water: The Photochemical Generation of Hydrogen from Water, Han, Z.; Eisenberg, R. *Acc. Chem. Res.* **2014**, *47*, 2537–2544.
4. Electron Conductive and Proton Permeable Vertically Aligned Carbon Nanotube Membranes, Pilgrim, G. A.; Leadbetter, J. W.; Qiu, F.; Siitonen, A. J.; Pilgrim, S. M.; Krauss, T. D. *Nano Lett*. **2014**, *14*, 1728–1733.
5. Hydrogen Evolution from Neutral Water Under Aerobic Conditions Catalyzed by Cobalt-microperoxidase-11, Kleingardner, J. G.; Kandemir, B., and Bren, K. L. *J. Am. Chem. Soc.* **2014**, 136, 4-7.
6. Multidisciplinary Approaches to Solar Hydrogen, Bren, K. L. *J. Royal Soc. Interface* **2015**, *5*, 1-12. ID: 20140091.
7. Biological Significance and Applications of Heme *c* Proteins and Peptides, Kleingardner, J. G.; Bren, K. L. *Acc. Chem. Res.* **2015**, *48*, 1845-1852.
8. Nickel Complexes for Robust Light-Driven and Electrocatalytic Hydrogen Production from Water, Das, A.; Han, Z.; Brennessel, W. W.; Holland, P. L.; Eisenberg, R., *ACS Catal.* **2015**, *5*, 1397–1406.
9. Photoelectrochemical Generation of Hydrogen from Water Using a CdSe Quantum Dot-Sensitized Photocathode, Ruberu, T. P. A.; Dong, Y.; Das, A.; Eisenberg, R. *ACS Catal.* **2015**, *5*, 2255–2259.
10. Semisynthetic and Biomolecular Hydrogen Evolution Catalysts, Kandamir, B.; Chakraborthy, S.; Guo, Y.; Bren, K. L. *Inorg. Chem.* **2016**, *55*, 467-477.
11. Single-Walled Carbon Nanotube/Protein Integrated Systems for Light Harvesting, Kubie, L.; Bren, K. L.; Krauss, T. D. (submitted, 2016).
12. Photocatalytic Hydrogen Generation by CdSe/CdS Nanoparticles, Qiu, F.; Han, Z.; Peterson, J. J.; Odoi, M. Y.; Sowers, K. L.; Krauss, T. D. (submitted, 2016).
13. Carbon Nanotube Based Membrane for Light-Driven Simultaneous Proton and Electron Transport, Pilgrim, G. A.; Amori, A. A.; Hou, Z.; Qiu, F.; Krauss, T. D. (submitted, 2016).
14. Catalysis of Light-driven Generation of Hydrogen from Water By Iron Dithiolene Complexes, Lv, H.; Ruberu, T. P. A.; Fleischauer, V.; Brennessel, W. W.; Neidig, M. L.; Eisenberg, R. (to be submitted, 2016).

DE-FG02-07ER15906

Solar energy-driven multi-electron-transfer catalysts for water splitting: robust and carbon-free nano-triads

Craig L. Hill, Tianquan Lian, Djamaladdin G. Musaev
Department of Chemistry, Emory University, Atlanta, GA 30322

The central thrust of this ongoing solar photochemistry research program is to conduct fundamental research on success-limiting factors in realizing more efficient and stable visible-light driven water oxidation/splitting systems. The hallmarks of this research project have been closely integrated experimental and computational research efforts targeting the synthetic, photophysical and photochemical properties of photo-driven water oxidation dyads and triads using our carbon-free, robust, soluble, fast and most significantly, tunable polyoxometalate (POM)-based water oxidation catalysts (WOCs), and semiconductor metal oxides (SMOs). Here, we summarize the main accomplishments relating to the general goals of our ongoing research.

A. Confirming key aspects of the stability and reactivity of the Co-POM WOC and development of new POM-based WOCs. After extensive analysis, our team re-confirmed the stability, reactivity and molecular nature (under homogeneous conditions) of our first POM WOC containing only earth-abundant elements, $[Co_4(H_2O)_2(PW_9O_{34})_2]^{10-}$ (**Co_4P_2**), (Figure 1). From a larger perspective, we developed an ensemble of techniques that allow the researcher not only to distinguish homogeneous versus heterogeneous catalytic water oxidation but also to quantify how much WOC activity comes from each type of catalyst, should both be present. We used our accumulated structural and other knowledge of POM WOCs to realize a second-generation molecular Co-POM WOC, namely, $[Co_4(H_2O)_2(VW_9O_{34})_2]^{10-}$ (**Co_4V_2**) which catalyzes water oxidation in both dark and visible-light-driven conditions. Under the same light-driven conditions **Co_4V_2** exhibits a superior reactivity and stability compared to **Co_4P_2**: the final O_2 yield by **Co_4V_2** is twice as high as that by **Co_4P_2**, and the quantum efficiency of O_2 formation at 6.0 μM **Co_4V_2** reaches *ca*. 68%. Multiple experimental results (e.g. UV-Vis absorption, FT-IR, ^{51}V NMR, dynamic light-scattering, tetra-*n*-heptylammonium nitrate ($THpANO_3$)-toluene extraction, effect of pH, buffer, and buffer concentration, etc.) all confirm that **Co_4V_2**, itself is the dominant active catalyst, and not Co^{2+}(aq) or cobalt oxide nanoparticles.[1] Subsequent computational studies have elucidated the mechanisms of the water oxidation by **Co_4P_2** and **Co_4V_2**, and have identified the factors impacting observed highest stability and reactivity of **Co_4V_2** relative to **Co_4P_2.**

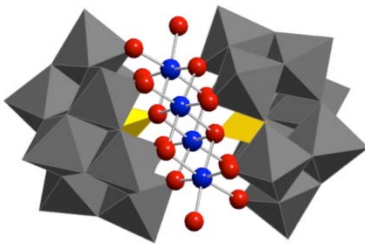

Figure 1. X-Ray structure of the $[Co_4(H_2O)_2(PW_9O_{34})_2]^{10-}$ (**Co_4P_2**) catalyst. Colors: Co, O, PO_4, WO_6.

Also, we developed several multi-Ni and multi-Sn-based POMs and analyzed their stabilities and WOC activities experimentally and computationally. Significantly, we just developed the first molecular WOCs (Cu-polyniobates) that are stable and very active in strong base (pH > 13).

B. Development of the POM-based molecular metal-to-metal charge transfer (MMCT) chromophores. We also prepared and characterized, both experimentally and computationally, robust POM-based molecular MMCT chromophores, including a POM-supported tri-rhenium carbonyl cluster complex, $[P_2W_{17}O_{61}\{Re(CO)_3\}_3\{ORb(H_2O)\}(\mu_3\text{-}OH)]^{9-}$, and intra-POM metal-

to-metal charge transfer (MMCT) chromophores, including a series of heterobimetallic transition-metal-substituted and Co^{II}-centered polyoxometalates (TMSPs) $[Co^{II}(M^xOH_y)W_{11}O_{39}]^{(12-x-y)-}$ (M^xOH_y = $V^{IV}O$, $Cr^{III}(OH_2)$, $Mn^{II}(OH_2)$, $Fe^{III}(OH_2)$, $Co^{II}(OH_2)$, $Ni^{II}(OH_2)$, $Cu^{II}(OH_2)$, and $Zn^{II}(OH_2)$). We evaluated the impact of the substituted transition metals on the photodynamics of the metal-to-POM charge transfer (MPCT) transitions. These complexes all show visible light absorption, but have relatively short excited state lifetimes.

C. Development of POM immobilization methodology and characterization of interfacial structures in POM-based dyads and triads. Because POMs are molecules it is challenging to immobilize them on photoelectrocatalytic surfaces. Our team recently achieved: (a) electrostatic immobilization of our very robust POM WOC, $[\{Ru_4O_4(OH)_2(H_2O)_4\}(\gamma\text{-}SiW_{10}O_{36})_2]^{10-}$ (**Ru_4Si**), on TiO_2 nano particles (NPs), and (b) preparation of a photocatalytic anode from the resulting TiO_2-Ru_4Si NPs (Figure 2). This electrode has successfully been used for 24 h of continual photocatalytic water oxidation and bulk electrolysis (Figure 2c) Most importantly, the increased surface area of NP-based photocatalytic electrodes facilitated the use of several techniques to establish the integrity of a molecular catalyst after use.

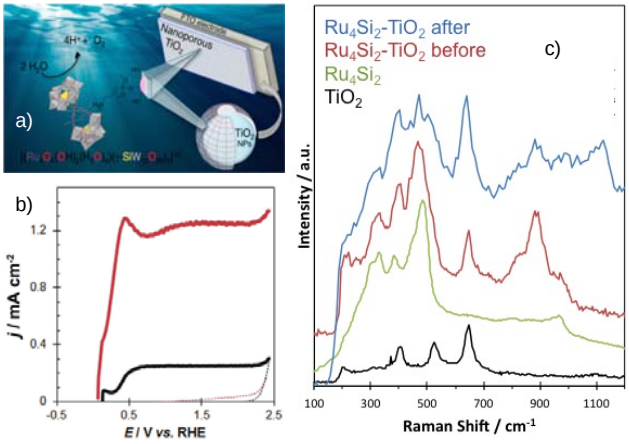

Figure 2. a) Schematic structure of TiO_2-Ru_4Si dyadic photoanode. b) Photocurrent as function of applied bias on Ru_4P_2-TiO_2 electrodes under UV illumination (solid red) and dark (dotted red) and TiO_2/FTO electrodes under 0.18 W/cm^2 UV illumination (solid black) and dark (dotted black) at pH 10. c) Raman spectra of the dyads before and after 24 hours of bulk electrolysis. Also shown for comparison are spectra of Ru_4Si and TiO_2

We also examined photoanodes consisted of POM WOCs attached to colored oxides. We focused our efforts on $BiVO_4$ and studied the I-V curve of a photoelectron-chemical cell using $BiVO_4$ as the photo-anode under different intensities of light illumination. The incident photon-to-current conversion efficiency (IPCE) increases with the applied bias, and its value decreases at higher illumination intensity. Transient spectra of $BiVO_4$ show a ground-state bleach at 500 nm. Transient kinetics of these samples show only minor bias dependence in < 20 microseconds. The data suggest that differences in carrier dynamics may occur at a much slower timescale. For this reason, we have constructed a transient absorption setup capable of extending the time resolution to seconds. Ongoing studies focus on following the carrier dynamics on femtosecond to second timescales as a function of illumination power.

D. Computational method/strategy development. During this grant period we developed two computational hybrid approaches applicable to the study interfacial electron/charge transfer dynamics in various dyads and triads. First, we extended the TCDM approach developed during the previous grant period, and used it to study the effect of hydration of the anatase (001), and rutile (001), (101) and (110) surfaces of TiO_2 on the rate of electron capture from an adsorbed graphene sheet. Second, we extended the conventional Fourier-grid discrete variable representation (DVR) approach to treat the bound state problem of a particle with a position dependent mass. We demonstrated that an infinite order representation, derived specifically to treat the case of a variable mass, can be used to electrostatically couple the electron with the hole by solving the generic Poisson equation in tandem with the Schrödinger equation. To our knowledge, this derivation of an infinite order DVR for Schrödinger-Poisson equation is novel.

DOE Sponsored Solar Photochemistry Publications 2013-2016

1. Xiang, X.; Fielden, J.; Rodriguez-Cordoba, W.; Huang, Z.; Zhang, N.; Luo, Z.; Musaev, D. G.; Lian, T.; Hill, C. L., Electron Transfer Dynamics in Semiconductor-Chromophore-Polyoxometalate Catalyst Photoanodes. *J. Phys. Chem. C* **2013,** *117*, 2013, 918-926.
2. Lv, H.; Rudd, J. A.; Zhuk, P. F.; Lee, J. Y.; Constable, E. C.; Housecroft, C. E.; Hill, C. L.; Musaev, D. G.; Geletii, Y. V., Bis(4'-(4-pyridyl)-2,2':6',2"-terpyridine)ruthenium(II) complexes and their N-alkylated derivatives in catalytic light-driven water oxidation. *RSC Adv.* **2013,** *3*, 20647-20654.
3. Zhao, C.; Rodríguez-Córdoba, W.; Kaledin, A. L.; Yang, Y.; Geletii, Y. V.; Lian, T.; Musaev, D. G.; Hill, C. L., An Inorganic Chromophore Based on a Molecular Oxide Supported Metal Carbonyl Cluster: $[P_2W_{17}O_{61}\{Re(CO)_3\}_3\{ORb(H_2O)\}(\mu_3\text{-}OH)]^{9-}$. *Inorg. Chem.* **2013,** *52*, 13490-13495.
4. Zhu, G.; Geletii, Y. V.; Song, J.; Zhao, C.; Glass, E. N.; Bacsa, J.; Hill, C. L., Di- and Tri-Cobalt Silicotungstates: Synthesis, Characterization, and Stability Studies. *Inorg. Chem.* **2013,** *52* (2), 1018-1024.
5. Matt, B.; Xiang, X.; Kaledin, A. L.; Han, N.; Moussa, J.; Amouri, H.; Alves, S.; Hill, C. L.; Lian, T.; Musaev, D. G.; Izzet, G.; Proust, A., Long lived charge separation in iridium(III)-photosensitized polyoxometalates: synthesis, photophysical and computational studies of organometallic-redox tunable oxide assemblies. *Chem. Sci.* **2013,** *4* (4), 1737-1745.
6. Vickers, J. W.; Lv, H.; Sumliner, J. M.; Zhu, G.; Luo, Z.; Musaev, D. G.; Geletii, Y. V.; Hill, C. L., Differentiating Homogeneous and Heterogeneous Water Oxidation Catalysis: Confirmation that $[Co_4(H_2O)_2(\alpha\text{-}PW_9O_{34})_2]^{10-}$ Is a Molecular Water Oxidation Catalyst. *J. Am. Chem. Soc.* **2013,** *135* (38), 14110-14118.
7. Sumliner, J. M.; Vickers, J. W.; Lv, H.; Geletii, Y. V.; Hill, C. L., Polyoxometalate Water Oxidation Catalytic Systems. In *Molecular Water Oxidation Catalysts: A Key Topic for New Sustainable Energy Conversion Schemes*, Llobet, A., Ed. John Wiley & Sons, Ltd.: **2014**; Vol. First Edition, pp 211-231.
8. Glass, E. N.; Fielden, J.; Kaledin, A. L.; Musaev, D. G.; Lian, T.; Hill, C. L., Extending Metal-to-Polyoxometalate Charge Transfer Lifetimes: The Effect of Heterometal Location. *Chem.- Eur. J.* **2014,** *20* (15), 4297-4307.
9. Sumliner, J. M.; Lv, H.; Fielden, J.; Geletii, Y. V.; Hill, C. L., Polyoxometalate multi-electron transfer catalytic systems for water splitting. *Eur. J. Inorg. Chem.* **2014**, 635-644.
10. Vickers, J. W.; Sumliner, J. M.; Lv, H.; Morris, M.; Geletii, Y. V.; Hill, C. L., Collecting meaningful early-time kinetic data in homogeneous catalytic water oxidation with a sacrificial oxidant. *Phys. Chem. Chem. Phys.* **2014,** *16*, 11942-11949.
11. Lv, H.; Song, J.; Geletii, Y. V.; Vickers, J. W.; Sumliner, J. M.; Musaev, D. G.; Kögerler, P.; Zhuk, P. F.; Bacsa, J.; Zhu, G.; Hill, C. L., An Exceptionally Fast Homogeneous Carbon-free Cobalt-based Water Oxidation Catalyst. *J. Am. Chem. Soc.* **2014,** *136* (26), 9268-9271.
12. Vickers, J. W.; Sumliner, J. M.; Lv, H.; Geletii, Y. V.; Hill, C. L., Importance of buffer in the design and study of solar fuel production systems. *ACS Division of Energy & Fuels 59(1).* **2014**, 162-163.
13. Vickers, J. W.; Sumliner, J. M.; Geletii, Y. V.; Morris, M.; Hill, C. L., Modular system for fast quantification of kinetics and oxygen yield of homogeneous water oxidation catalysts. *ACS, Division of Energy & Fuels 59(1).*. **2014**, 673-674.

14. Zhao, C.; Glass, E. N.; Chica, B.; Musaev, D. G.; Sumliner, J. M.; Dyer, R. B.; Lian, T.; Hill, C. L., All-inorganic Networks and Tetramer based on Tin(II)-containing Polyoxometalates: Tuning Structural and Spectral Properties with Lone-Pairs. *J. Am. Chem. Soc.* **2014,** *136* (34), 12085-12091.
15. Kaledin, A. L.; Lian, T.; Hill, C. L.; Musaev, D. G., An Infinite Order Discrete Variable Representation of an Effective Mass Hamiltonian: Application to Exciton Wave Functions in Quantum Confined Nanostructures. *J. Chem. Theory Comput.* **2014,** *10* (8), 3409-3416.
16. Lauinger, S. M.; Sumliner, J. M.; Yin, Q.; Xu, Z.; Liang, G.; Glass, E. N.; Lian, T.; Hill, C. L., High Stability of Immobilized Polyoxometalates on TiO_2 Nanoparticles and Nanoporous Films for Robust, Light-Induced Water Oxidation. *Chem. Mater.* **2015,** *27* (17), 5886-5891.
17. Kaledin, A. L.; Lian, T.; Hill, C. L.; Musaev, D. G., A Hybrid Quantum Mechanical Approach: Intimate Details of Electron Transfer Between Type I CdSe/ZnS Quantum Dots and an Anthraquinone Molecule. *J. Phys. Chem. B* **2015,** *119* (24), 7651-7658.
18. Fielden, J.; Sumliner, J. M.; Han, N.; Geletii, Y. V.; Xiang, X.; Musaev, D. G.; Lian, T.; Hill, C. L., Water splitting with polyoxometalate-treated photoanodes: enhancing performance through sensitizer design. *Chemical Science* **2015,** *6* (10), 5531-5543.
19. Guo, W.; Lv, H.; Chen, Z.; Lauinger, S. M.; Luo, Z.; Sumliner, J. M.; Lian, T.; Hill, C. L., Self-assembly of Polyoxometalates, Pt Nanoparticles and Metal-Organic Frameworks in a hybrid material for Synergistic Hydrogen Evolution. *J. Mater. Chem: A* **2016**, in press.
20. Glass, E. N.; Fielden, J.; Huang, Z.; Xiang, X.; Musaev, D. G.; Lian, T.; Hill, C. L., Transition Metal Substitution Effects on Metal-to-Polyoxometalate Charge Transfer. *Inorg. Chem.* **2016,** *55*, in minor revision.
21. Jia, Y.; Chen, J.; Wu, K.; Kaledin, A.; Musaev, J.; Xie, Z.; Lian, T., Enhancing Photo-reduction Quantum Efficiency Using Quasi-Type II Core/Shell Quantum Dots. *Chem. Sci.* **2016**, Published online 2 March **2016**.

Observing Nanoscale Photochemical Charge Separation with Surface Photovoltage Spectroscopy

Jing Zhao, Alexandra T. De Denko, Michael A. Holmes, Frank E. Osterloh
Department of Chemistry
University of California - Davis
Davis, CA 95616

The potential of nanostructures for photovoltaic and photoelectrochemical cells is currently limited by our understanding of photochemical charge transfer on the nanoscale. On the nanoscale, space charge layers are no longer effective for separating electrons and holes, and charge transfer and separation are controlled by structure and energetics of interfaces and by their defects. Recent work by the PI suggests that nanoscale photochemical charge transfer can be observed with Surface Photovoltage Spectroscopy (SPS). In SPS, changes of the surface potential of an illuminated sample film are recorded with a Kelvin Probe as a function of the incident light intensity and wavelength.

The purpose of this project is twofold. First it will evaluate the scope and limits of SPS for the observation of photochemical processes in a series of well-defined systems consisting of molecular, polymeric, and nanocrystalline light absorbers. Specific tasks will be to determine the dependence of the photovoltage signal on light intensity, ambient conditions, film thickness and other parameters. Secondly, the SPS data will be used to determine the main factors that control photochemical charge separation on the nanoscale, incl. the absorption cross-section, the built-in potential and spatial parameters of the donor/acceptor configurations.

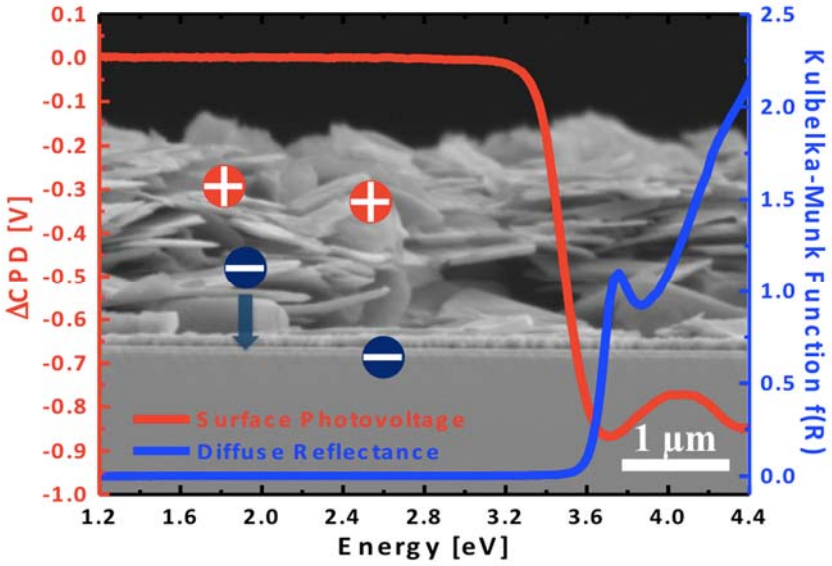

Surface photovoltage spectrum for $KCa_2Nb_3O_{10}$ nanoparticles on gold substrate. A -0.85 V photovoltage develops under illumination at > 3.5 eV, which is due to majority carrier injection into the gold substrate. From Zhao, J.; Osterloh, F. E., J. Phys. Chem. Lett. **2014**, 5, 782–786. http://dx.doi.org/10.1021/jz500136h

Session X

Photosystems for Fuel Production

Components of an Artificial Photosynthetic Solar Fuel System

Devens Gust, Ana L. Moore, and Thomas A. Moore
School of Molecular Sciences
Arizona State University
Tempe, AZ 85287

The artificial photosynthetic approach to solar fuel production involves gathering sunlight, using the light energy to carry out photoinduced electron transfer, and moving the charges from the initial charge separated state to catalysts for oxidation of one substrate and fuel production by using the resulting electrons for reduction of a second substrate. These components must be integrated into a single system. Our group has been carrying out fundamental research in all of these areas.

In the area of light harvesting, we have developed a method for synthesis of porphyrins with carboxylic acids at the *meso*-positions and used it to prepare a series of multiporphyrin arrays bearing up to 6 chromophores.[14] The porphyrins are coupled to a central benzene core via benzyl ester linkages. In the arrays, the porphyrins exist as twist-stacked dimers reminiscent of the special pairs of bacteriochlorophylls found in some photosynthetic bacteria. An example is hexad **1** (Fig. 1)**.** These dimers feature van der Waals contact between the macrocycles, and demonstrate excitonic splitting due to π-π interactions. The excitonic effects split and blue-shift the Soret absorptions, and slightly broaden the Q-band absorptions and shift them to longer wavelengths. The interactions also lower the first oxidation potentials by ca. 100 mV, and the arrays show evidence for delocalization of the radical cation over both porphyrins in the dimer. The hexad **1** features a trimer of dimers. The arrays demonstrate singlet-singlet energy transfer among the chromophores. Arrays of this type will be good models for some aspects of the interactions of photosynthetic pigments, including those of reaction center special pairs and possibly quantum coherence effects in antennas.

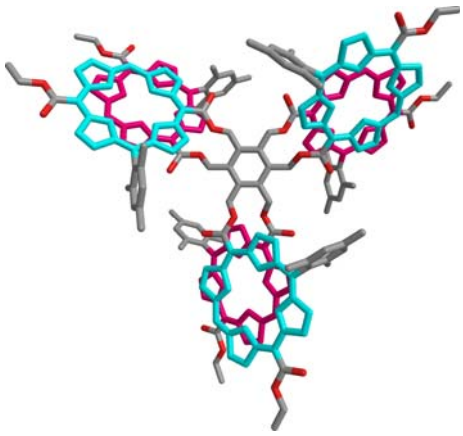

Fig. 1. Hexad **1**

In other research, a triad consisting of a fullerene (C_{60}) covalently linked to both a porphyrin energy and electron donor (P) and a β-tetracyanoporphyrin energy and electron acceptor (CyP) was synthesized in order to investigate the possibility of a fullerene acting as an electron and/or singlet energy relay.[24] A model for pH-regulated energy transfer in natural photosynthetic antennas was also synthesized and studied.

The transport of electrons from the water oxidizing complex of photosynthetic PSII to the oxidized reaction center chlorophyll is mediated by a Tyrz-His redox mediator. In 2012 in collaboration with T. E. Mallouk we showed that the use of a bioinspired redox relay between a high potential sensitizer and a heterogeneous water oxidation catalyst resulted in improved performance of a photoelectrochemical cell for water splitting. The redox relay consisted of a benzimidazole-phenol construct (BIP).[13] We are now preparing and studying other BIPs with

substitutions designed to mimic more fully the hydrogen bond network surrounding Tyr_Z.[17] Kinetic isotope effects were detected electrochemically and spectrochemically[20] and interpreted to provide mechanistic insight into the proton-coupled electron transfer (PCET) process that accompanies the oxidation of the phenol. Theoretical studies performed in collaboration with S. Hammes-Schiffer are guiding the design of the substituted BIPs with the main purpose of finding structures in which multiple proton transfers can be associated with a single electron transfer. Two new BIP derivatives, BIP-CH_2NH_2 and BIP-CH_2NEt_2, have been synthesized. Electrochemical studies of BIP-CH_2NH_2 indicate that the first oxidation potential (0.62 V vs. SCE in acetonitrile) is similar to the theoretically predicted value (0.66 V vs. SCE in acetonitrile) for the concerted electron transfer of the phenol coupled to two proton transfers. A similar value was obtained experimentally for BIP-CH_2NEt_2 (0.54 V vs. SCE in acetonitrile). These values are ca. 400 mV more negative than those of other BIPs where a second proton transfer is thermodynamically prohibited. Thus, we have electrochemical evidence that a concerted double proton transfer associated with a single electron transfer is taking place in these systems and consider this a starting point for the design and construction of biomimetic proton wires where the first step can be a photoinitiated PCET process.

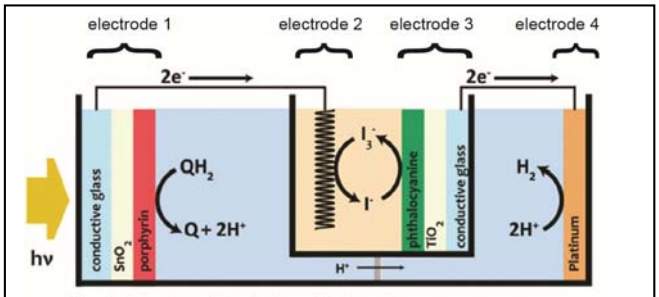

Fig. 2. A tandem photoelectrosynthetic cell

We have begun to investigate the fundamental processes and approaches necessary to design a complete photoelectrical system for solar fuel production. By using dyes that absorb different regions of the solar spectrum for sensitization by electron injection into the conduction band of appropriate wide band gap semiconductors, tandem photoelectrochemical cells can theoretically achieve far greater solar-to-fuel efficiencies than those relying on a single semiconductor. The efficacy of this design (Fig. 2) has been demonstrated by the production of H_2 using hydroquinone as an electron donor with the two photoelectrodes connected in series and light as the only energy driving this process.[23] The tandem cell architecture uses two *n*-type dye-sensitized photoanodes, with one junction consisting of a SnO_2-porphyrin interface (electrode 1) and the other a TiO_2-phthalocyanine interface (electrode 3). These semiconductors are well suited for sensitization with dyes having near the optimal band gaps for water redox to hydrogen and oxygen, 1.7 eV and 1.1 eV, taking into account an overpotential requirement of about 800 mV. The SnO_2 conduction band at about 0 V (vs. SHE) is positioned so that a high potential sensitizer (1.4 V vs. SHE), is able to inject an electron with a driving force of 300 mV. In operation, a free base porphyrin absorbing in the visible supplied adequate oxidation potential at electrode 1. The added voltage necessary for hydrogen production was provided by the TiO_2 semiconductor of electrode 2 sensitized by a low potential Si phthalocyanine absorbing in the near IR. This study demonstrates the utility of the tandem architecture. In future work we plan to provide electrode 1 with a high potential perfluoroporphyrin whose radical cation is capable of water oxidation, a BIP relay similar to that described above, and an iridium oxide catalyst in order to use water as a source of electrons rather than hydroquinone.

DOE Sponsored Publications 2013-2016

(1) "Separating Annihilation and Excitation Energy Transfer Dynamics in Light Harvesting Systems," Vengris, M.; Larsen, D. S.; Valkunas, L.; Kodis, G.; Herrero, C.; Gust, D.; Moore, T.; Moore, A.; van Grondelle, R. *J. Phys. Chem. B* **2013**, *117*, 11372.

(2) "Hole mobility in porphyrin- and porphyrin-fullerene electropolymers," Brennan, B. J.; Liddell, P. A.; Moore, T. A.; Moore, A. L.; Gust, D. *J. Phys. Chem. B* **2013**, *117*, 426.

(3) "Carotenoids as electron or excited-state energy donors in artificial photosynthesis: an ultrafast investigation of a carotenoporphyrin and a carotenofullerene dyad," Pillai, S.; Ravensbergen, J.; ntoniuk-Pablant, A.; Sherman, B. D.; van Grondelle, R.; Frese, R. N.; Moore, T. A.; Gust, D.; Moore, A. L.; Kennis, J. T. *Phys. Chem. Chem. Phys.* **2013**, *15*, 4775.

(4) "Selective oxidative synthesis of *meso*-beta fused porphyrin dimers," Brennan, B. J.; Arero, J.; Liddell, P. A.; Moore, T. A.; Moore, A. L.; Gust, D. *J. Porphyrins Phthalocyanines* **2013**, *17*, 247.

(5) "Artificial photosynthetic reaction center with a coumarin-based antenna system," Garg, V.; Kodis, G.; Liddell, P. A.; Terazono, Y.; Moore, T. A.; Moore, A. L.; Gust, D. *J. Phys. Chem. B* **2013**, *117*, 11299.

(6) "Comparison of silatrane, phosphonic acid, and carboxylic acid functional groups for attachment of porphyrin sensitizers to TiO_2 in photoelectrochemical cells," Brennan, B. J.; Llansola Portoles, M. J.; Liddell, P. A.; Moore, T. A.; Moore, A. L.; Gust, D. *Phys. Chem. Chem. Phys.* **2013**, *15*, 16605.

(7) "Artificial photosynthesis," Gust, D.; Moore, T. A.; Moore, A. L. *Theoretical and Experimental Plant Physiology* **2013**, *25*, 182.

(8) "Ultrafast energy transfer and excited state coupling in an artificial photosynthetic antenna," Maiuri, M.; Snellenburg, J. J.; van Stokkum, I. H. M.; Pillai, S.; Carter, K. W.; Gust, D.; Moore, T. A.; Moore, A. L.; van Grondelle, R.; Cerullo, G.; Polli, D. *J. Phys. Chem. B* **2013**, *117*, 14183.

(9) "Artificial photosynthesis combines biology with technology for sustainable energy transformation," Moore, T. A.; Moore, A. L.; Gust, D. *AIP Conf. Proc.* **2013**, *1519*, 68.

(10) "Evolution of reaction center mimics to systems capable of generating solar fuel," Sherman, B. D.; Vaughn, M. D.; Bergkamp, J. J.; Gust, D.; Moore, A. L.; Moore, T. A. *Photosynth. Res.* **2014**, *120*, 59.

(11) "Organosilatrane building blocks," Brennan, B. J.; Gust, D.; Brudvig, G. W. *Tetrahedron Lett.* **2014**, *55*, 1062.

(12) "Synthesis and spectroscopic properties of a soluble semiconducting porphyrin polymer," Schmitz, R. A.; Liddell, P. A.; Kodis, G.; Kenney, M. J.; Brennan, B. J.; Oster, N. V.; Moore, T. A.; Moore, A. L.; Gust, D. *Phys. Chem. Chem. Phys.* **2014**, *16*, 17569.

(13) "A bioinspired redox relay that mimics radical interactions of the Tyr–His pairs of photosystem II," Megiatto, J. D.; Mendez-Hernandez, D. D.; Tejeda-Ferrari, M. E.; Teillout, A.-L.; Llansola Portoles, M. J.; Kodis, G.; Poluektov, O. G.; Rajh, T.; Mujica, V.; Groy, T. L.; Gust, D.; Moore, T. A.; Moore, A. L. *Nature Chem.* **2014**, *6*, 423.

(14) "Multiporphyrin Arrays with pi-pi IT Interchromophore Interactions," Terazono, Y.; Kodis, G.; Chachisvilis, M.; Cherry, B. R.; Fournier, M.; Moore, A.; Moore, T. A.; Gust, D. *J. Am. Chem. Soc.* **2015**, *137*, 245.

(15) "Design, synthesis and photophysical studies of phenylethynyl-bridged phthalocyanine-

fullerene dyads," Arero, J.; Kodis, G.; Schmitz, R. A.; Mendez-Hernandez, D. D.; Moore, T. A.; Moore, A. L.; Gust, D. *J. Porphyrins Phthalocyanines* **2015**, *19*, 1.
(16) "Enhanced dye-sensitized solar cell photocurrent and efficiency using a Y-shaped, pyrazine-containing heteroaromatic sensitizer linkage," Watson, B. L.; Sherman, B. D.; Moore, A. L.; Moore, T. A.; Gust, D. *Phys. Chem. Chem. Phys* **2015**, *17*, 15788.
(17) "Spectroscopic Analysis of a Biomimetic Model of Tyr(z) Function in PSII," Ravensbergen, J.; Antoniuk-Pablant, A.; Sherman, B. D.; Kodis, G.; Megiatto, J. D., Jr.; Mendez-Hernandez, D. D.; Frese, R. N.; van Grondelle, R.; Moore, T. A.; Moore, A. L.; Gust, D.; Kennis, J. T. M. *J. Phys. Chem. B* **2015**, *119*, 12156.
(18) "Photoinjection of High Potential Holes into Cu5Ta11O30 Nanoparticles by Porphyrin Dyes," Sullivan, I.; Brown, C. L.; Llansola-Portoles, M. J.; Gervaldo, M.; Kodis, G.; Moore, T. A.; Gust, D.; Moore, A. L.; Maggard, P. A. *J. Phys. Chem. C* **2015**, *119*, 21294.
(19) "Supramolecular photochemistry applied to artificial photosynthesis and molecular logic devices," Gust, D. *Faraday Disc.* **2015**, *185*, 9.
(20) "Kinetic isotope effect of proton-coupled electron transfer in a hydrogen bonded phenol-pyrrolidino 60 fullerene," Ravensbergen, J.; Brown, C. L.; Moore, G. F.; Frese, R. N.; van Grondelle, R.; Gust, D.; Moore, T. A.; Moore, A. L.; Kennis, J. T. M. *Photochem. Photobiol. Sci.* **2015**, *14*, 2147.
(21) "Charge-Transfer Dynamics of Fluorescent Dye-Sensitized Electrodes under Applied Biases," Godin, R.; Sherman, B. D.; Bergkamp, J. J.; Chesta, C. A.; Moore, A. L.; Moore, T. A.; Palacios, R. E.; Cosa, G. *J. Phys. Chem. Lett.* **2015**, *6*, 2688.
(22) "A new method for the synthesis of β-cyano substituted porphyrins and their use as sensitizers in photoelectrochemical devices," Antoniuk-Pablant, A.; Terazono, Y.; Brennan, B., J, ; Sherman, B. D.; Megiatto, J. D.; Brudvig, G. W.; Moore, A. L.; Moore, T. A.; Gust, D. *J. Mater. Chem. A* **2016**, 2976.
(23) "A tandem dye-sensitized photoelectrochemical cell for light driven hydrogen production," Sherman, B. D.; Bergkamp, J. J.; Brown, C. L.; Moore, A. L.; Gust, D.; Moore, T. A. *Energy & Environ. Sci.* **2016**, DOI: 10.1039/C6EE00258G
(24) "Photoinduced electron and energy transfer in a molecular triad featuring a fullerene redox mediator," Antoniuk-Pablant, A.; Kodis, G.; Moore, A. L.; Moore, T. A.; Gust, D. *J. Phys. Chem. B* **2016**, *submitted for publication*.

Nanostructured Photocatalytic Water Splitting Systems

Nicholas S. McCool, Nella M. Vargas-Barbosa, Timothy P. Saunders, Pengtao Xu, Tyler J. Milstein, Yuguang C. Li, Christopher Gray, Zhifei Yan, and Thomas E. Mallouk

Department of Chemistry, The Pennsylvania State University, University Park, PA 16802
Ana L. Moore, Thomas A. Moore, and Devens Gust

Department of Chemistry and Biochemistry, Arizona State University, Tempe AZ 85281
John R. Swierk, Colleen T. Nemes, and Charles A. Schmuttenmaer
Department of Chemistry, Yale University, New Haven, CT 06520

Our DOE-supported work focuses on understanding the kinetics of electron transfer in water splitting photoelectrochemical cells made from dyes, oxide semiconductors, and colloidal water oxidation catalysts. Because of the importance of managing protons in these solar cells, our interests have broadened to understanding the role of protons in controlling electron transfer rates and to proton transport in membrane-based cells for water and CO_2 electrolysis.

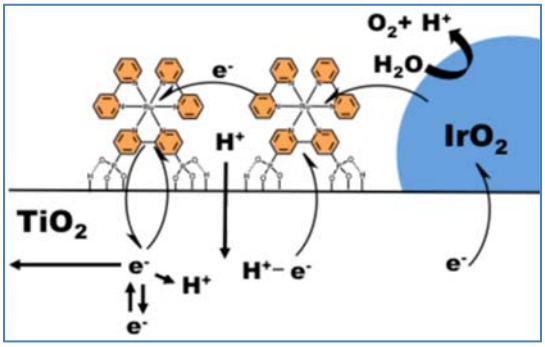

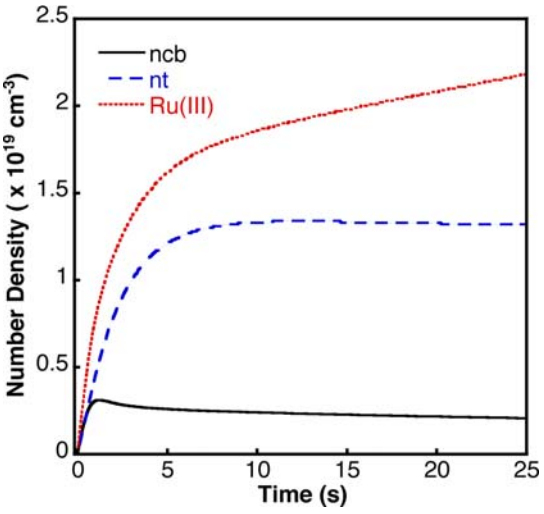

In water-splitting dye cells, ruthenium polypyridyl complexes or porphyrins are adsorbed onto a porous TiO_2 or core-shell anode. Several groups have studied different semiconductor-dye-catalyst combinations in this electrode architecture. Although the Faradaic efficiency of water oxidation is close to unity, the quantum efficiency is always low, typically 1-15%, and the photocurrent drops precipitously over a period of seconds. We have combined electrochemical and spectroscopic methods to measure the kinetics of electron transfer in these systems. Transient photovoltage measurements and chronopotentiometry were used to measure the rate of recombination between photoinjected electrons and the oxidized dye on the surface of the electrode, and spectroelectrochemical measurements gave the rate of charge transfer diffusion (D_{ct}) between dye molecules. Together these measurements enabled us to model the photocurrent and to understand the slow electrode polarization that is universally observed in terms of the slow accumulation of trapped electrons (n_t) and the buildup of oxidized sensitizer molecules (Ru(III)) on the electrode surface.

The photocurrent and the rate at which it decays were found to be sensitive to both the conditions of dye adsorption and electrode pre-treatment. Adsorption of dyes from protic solvents or exposure to acids gave low photocurrents, despite the fact that D_{ct} was faster. When these

electrodes were annealed (prior to dye adsorption) or heat-treated (after dye adsorption), higher photocurrents and slower polarization were observed. Spectroelectrochemical measurements suggested that these effects could be attributed to intercalated protons, which stabilized trapped electrons and thereby increased the rate of charge recombination with Ru(III). This hypothesis was confirmed by using terahertz spectroscopy in combination with nanosecond transient absorption spectroscopy to monitor the injection and trapping of electrons. Although the rate of charge injection is faster in acidic media, most of these electrons are injected into proton-stabilized trap states and are therefore invisible in the terahertz experiment.

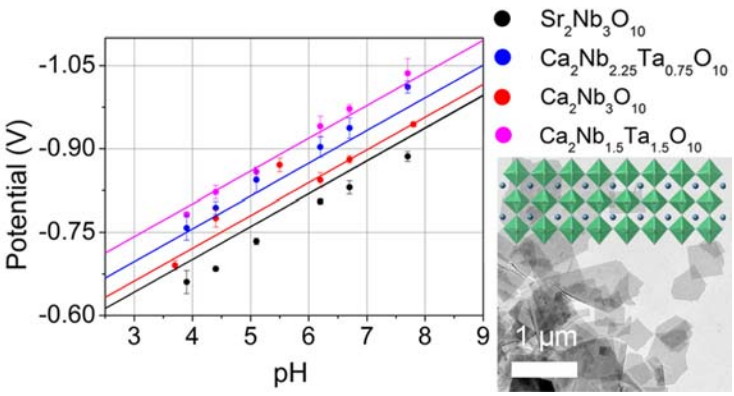

We are also studying molecular assemblies based on oxide semiconductor nanosheets for the photocathode of water-splitting cells. Multilayer electron transfer cascades are grown layer-by-layer on tranparent conductors. We have used the Mott-Schottky method to measure the flat-band potentials of layered niobates and tantalates. The relative conduction band edge potentials are consistent with DFT calculations.

Proton transport from the anode to the cathode is a system-level problem in water splitting cells. Ordinary cation- and anion-exchange membranes result in substantial energy losses in cells that operate near neutral pH. We have shown that bipolar membranes enable water electrolysis at low overpotential, in principle using only earth-abundant catalysts. In these electrolysis cells, water dissociates at the interface between anion- and cation-exchange layers (AEL and CEL in the figure at the right), and the anode and cathode reactions run in base and acid, respectively. The Nernstian shifts of electrode potentials compensate for the free energy needed to dissociate water at the AEL-CEL interface in the membrane.

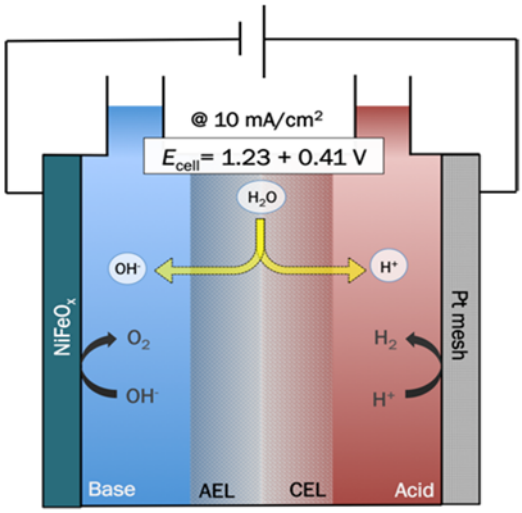

Proton management in a bipolar membrane water electrolysis cell.

Recent experiments by Masel, Rosenthal, and others have shown that CO_2 can be reduced to CO at high surface area Ag or Bi electrodes. These cathodes operate at relatively low overpotential in ionic liquids or in non-aqueous solutions that contain 1-alkyl-3-methylimidazolium cations. However, the issue of proton management in CO_2 electrolysis cells that oxidize water at the anode has not been addressed. We have studied this problem using bipolar membranes, with humidified gas-phase CO_2 at the cathode and aqueous strong base at the anode. Under these conditions, cells based Nafion membranes give high initial current density for CO_2 electrolysis but rapidly polarize. Bipolar membranes in the same cells give stable currents over periods of many hours.

DOE Sponsored Publications 2013-2016

1. N. S. McCool, J. R. Swierk, C. T. Nemes, T. P. Saunders, C. A. Schmuttenmaer, and T. E. Mallouk, “Proton-induced trap states, injection and recombination dynamics in water-splitting dye-sensitized photoelectrochemical cells,” submitted.

2. P. Xu, T. J. Milstein, and T. E. Mallouk, "Flat-band potentials of molecularly thin metal oxide nanosheets," submitted.

3. J. R. Swierk, N. S. McCool, C. T. Nemes, T. E. Mallouk, and C. A. Schmuttenmaer, "Ultrafast electron injection dynamics of photoanodes for water-splitting dye-sensitized photoelectrochemical cells," *J. Phys. Chem. C,* 120, 5940–5948 (2016).

4. C. Canales, F. Varas-Concha, T. E. Mallouk, and G. Ramirez, "Enhanced electrocatalytic hydrogen evolution reaction: supramolecular assemblies of metalloporhyrins on glassy carbon electrodes," *Appl. Catal. B: Environmental,* 188, 169-176 (2016).

5. Y. Zhao, N. Vargas-Barbosa, M. E. Strayer, N. S. McCool, M.-E. Pandelia, T. R. Saunders, J. R. Swierk, J. Callejas, L. Jensen, and T. E. Mallouk, "Understanding the effect of monomeric iridium(III/IV) aquo complexes on the photoelectrochemistry of $IrO_x.nH_2O$-catalyzed water-splitting systems," *J. Am. Chem. Soc.,* 137, 8749-8757 (2015).

6. J. R. Swierk, N. S. McCool, and T. E. Mallouk, "Dynamics of electron recombination and transport in water-splitting dye-sensitized photoelectrochemical cells," *J. Phys. Chem. C.* 119, 13858-13867 (2015).

7. D.-D. Qin, Y. Bi, X. Feng, W. Wang, G. D. Barber, T. Wang, Y. Song, and T. E. Mallouk, "Hydrothermal synthesis and photoelectrochemistry of highly oriented, crystalline anatase TiO_2 nanorods grown on transparent conductor electrodes," *Chem. Mater.,* 27, 4180-4183 (2015).

8. J. R. Swierk, D. D. Mendez-Hernandez, N. S. McCool, P. Liddell, Y. Terazono, I. Pahk, J. J. Tomlin, N. V. Oster, T. A. Moore, A. L. Moore, D. Gust, T. E. Mallouk, "Metal-free organic sensitizers for use in water-splitting dye-sensitized photoelectrochemical cells," *Proc. Natl. Acad. Sci. USA,* 112, 1681-1686 (2015).

9. N. M. Vargas-Barbosa, G. M. Geise, M. A. Hickner, and T. E. Mallouk, "Assessing the utility of bipolar membranes for photoelectrochemical water-splitting cells," *ChemSusChem,* 7, 3017-3020 (2014).

10. J. R. Swierk, N. S. McCool, T. P. Saunders, and T. E. Mallouk, "Effects of electron trapping and protonation on the efficiency of water-splitting dye-sensitized solar cells," *J. Am. Chem. Soc.,* 136, 10974-10982 (2014).

11. J. R. Swierk, N. S. McCool, T. P. Saunders, G. D.Barber, M. E. Strayer, N. M. Vargas-Barbosa, and T. E. Mallouk, "Photovoltage effects of sintered IrO_2 nanoparticle catalysts in

water-splitting dye-sensitized photoelectrochemical cells," *J. Phys. Chem. C.*, 118, 17046-17053 (2014).

12. T. E. Mallouk, "Water electrolysis: divide and conquer," *Nature Chem.*, 5, 362-363 (2013).

13. A. S. Hall, A. Kondo, K. Maeda, and T. E. Mallouk, "Microporous brookite-phase titania made by replication of a metal-organic framework" *J. Am. Chem. Soc.*, 135, 16276-16279 (2013).

14. J. R. Swierk and T. E. Mallouk, "Design and development of photoanodes for water-splitting dye-sensitized photoelectrochemical cells," *Chem. Soc. Rev.*, 42, 2357-87 (2013).

Posters

Excess Electron and Holes in Aliphatic Room Temperature Ionic Liquids

Francesc Molins i Domenech, Andrew T. Healy, Meghan Knutzon and David A. Blank
Department of Chemistry, University of Minnesota, Minneapolis, MN 55455

The rapid adoption of room temperature ionic liquids (RTILs) across a wide range of energy related applications that involve ionizing conditions, including solar energy conversion, motivates the need for better understanding of the production, reactivity, yield, relaxation, recombination, and structure of excess electrons and holes in these solvents. Our studies focus on the aliphatic cation series methyl-alkyl-pyrrolidinium [Py1,x^+], which has been demonstrated to be significantly more stable in the presence of excess electrons than similar aromatic cations.

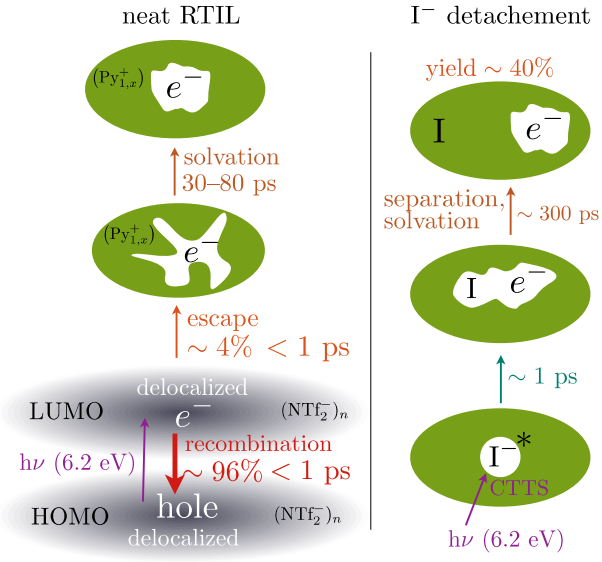

Fig 1. Diagram comparing photodetachment of neat [Py1,x^+] [NTf_2^-] to photodetachment of iodide in the same liquids, both at 6.2 eV.

When paired with the, bis(trifluoromethylsulfonyl)amide [NTf_2^-] anion, photo-excitation of the neat liquid initially creates a highly reactive electron that is delocalized over the anions. The geminate hole is also delocalized over the anions, and with the two in close proximity rapid recombination outcompetes electron escape resulting in relatively small (<5%) yields of free solvated electrons. Photodetachment from iodide in the same liquids proceeds differently, via a charge transfer to solvent (CTTS) intermediate that separates on a 300 ps time scale with a much higher yield (~40%) of free solvated electrons. The yield varies with the length of the alkyl tail on the cation. Figure 1 illustrates the different photodetachment mechanisms from the [NTf_2^-] anions and added iodide. In both cases the asymptotic solvated electron exhibits the same near-IR absorption spectrum. When paired with the dicyanoamide anion [$N(CN)_2^-$], photodetachment again appears to originate from the anions. Compared with the neat [NTf_2^-] liquids, the free electron yield is much higher (~30%) and cooling/solvation of the free electrons is more rapid. Figure 2 compares the transient visible absorption spectrum with the computational prediction for the absorption spectrum of an excess hole (dashed line). The high yields of relatively stable solvated electrons from iodide and [$N(CN)_2^-$] allow for more detailed interrogation of the local structure of these species using transient resonance enhance Raman spectroscopy.

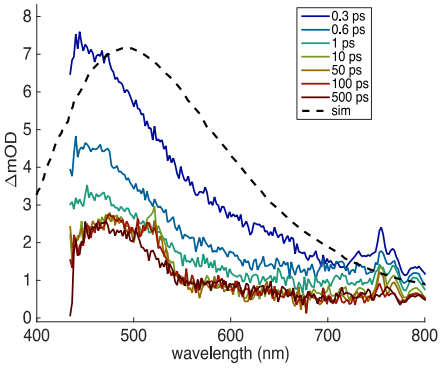

Fig 2. Transient absorption of the hole following photodetachement of neat [Py1,4^+] [$N(CN)_2^-$] at 4.65 eV

Carbon Dioxide Reduction to Organics in an Aqueous Photoelectrochemical Environment

James E. Park, Tao Zhang, Jessica J. Frick, Jason W. Krizan, Yuan Hu, Yong Yan, Jing Gu, Michael T. Kelly, Robert J. Cava and Andrew B. Bocarsly
Department of Chemistry
Frick Laboratory, Princeton University
Princeton, NJ 08544

Two distinct classes of p-type semiconductors have been investigated as photocathodes for the reduction of CO_2 in aqueous electrolyte: III-V materials and delafossite metal oxides. Studies using the first set of materials continue to focus on single crystal p-GaP based electrodes. This material was previously shown to be catalytic for the reduction of carbon dioxide to methanol in the presence of ~10mM pyridine, with ~95% faradaic efficiency at a ~200mV underpotential. Since our original report on this system it has been noted that CO_2 redox chemistry at the p-GaP interface should be crystal face sensitive. Therefore we have undertaken a consideration of the {111}, {110} and {100} planes as electroactive interfaces for CO_2 reduction. To allow a meaningful comparison of these surfaces a new etch procedure was developed that produced {110} planes starting from a [111] surface. Figure 1 shows the tripodal structures associated with the three-fold degenerate {110} planes, which run perpendicular to the [111] plane.

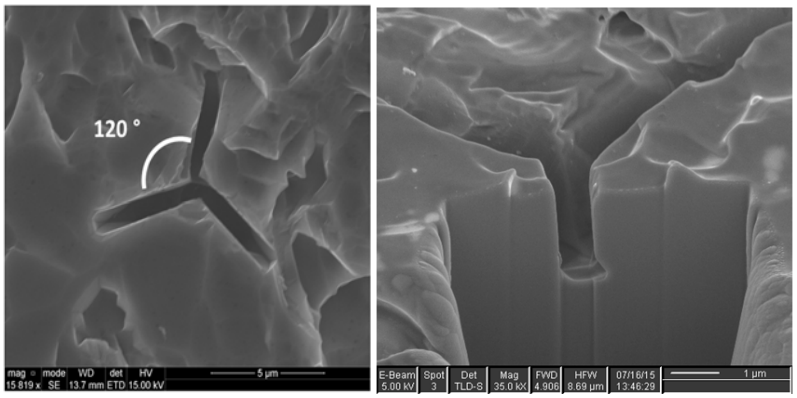

Figure 1: (Left) SEM of an etched [111] face of p-GaP showing a tripodal structure consisting of the three degenerate {110} planes. (Right) Milled image showing that the tripodal structure consists of planes that are perpendicular to the [111] surface, consistent with the geometric relationship between the {110} and {111} planes.

Given the geometric relationship between these two sets of planes, the etched structures do not significantly reduce the amount of [111] plane that is present. Thus, a study as function of etch time has allowed us to example CO_2 reduction chemistry on the GaP [110] surface, using the [111] surface as a control.

P-type delafossites of the form $MM'O_2$ (where M = Cu or Ag and M' = Fe or Rh) are found to form reasonably stable photocathodes in aqueous photoelectrochemical cells. When M' is Fe(III) then CO_2 is observed to be reduced under cell illumination to formate at an underpotential, with no need for a dissolved electrocatalyst. However, when Rh is employed (independent of whether M is Cu(I) or Ag(I)) CO_2 is not reduced; however, water is selectively reduced to H_2 in the presence of $CO_{2\,(aq)}$. The nature of the M site is found to be critical to the reductive stability of the cathode under illumination and is associated with the extent to which M atomic states mix with the conduction band of the semiconductor.

Fundamental Studies of Energy- and Hole/Electron Transfer in Hydroporphyrin Architectures

David F. Bocian,[1] Dewey Holten,[2] Christine Kirmaier,[2] and Jonathan S. Lindsey[3]
[1]Department of Chemistry, University of California, Riverside CA 92521-0403;
[2]Departments of Chemistry, Washington University, St. Louis, MO 63130-4889;
[3]Departments of Chemistry, North Carolina State University, Raleigh, NC 27695-8204

The long-term objective of our research program is to design, synthesize, and characterize tetrapyrrole-based molecular architectures that absorb sunlight, funnel energy, and separate charge with high efficiency and in a manner compatible with current and future solar-energy conversion schemes. This presentation focuses on two areas of progress over the past year.

(1) Efficient light harvesting for molecular-based solar-conversion systems requires absorbers that span the photon-rich red and near-infrared regions of the solar spectrum. We have achieved this goal with a palette of absorbers spanning five classes of tetrapyrroles: chlorins, chlorin–imides, bacteriochlorins, bacteriochlorin–imides and bacteriochlorin–bisimides (see figure at right). This objective has been achieved by advances in synthesis combined with in-depth characterization studies that provide a fundamental understanding of how molecular composition (macrocycle and substituents) dictates the electronic structure, redox potentials, and photophysical properties of tetrapyrroles. Almost all of the tetrapyrroles in these sets have excited-state lifetimes that are sufficiently long for use in solar-conversion systems, including the bacteriochlorin–bisimides that absorb near 900 nm (~1 ns).

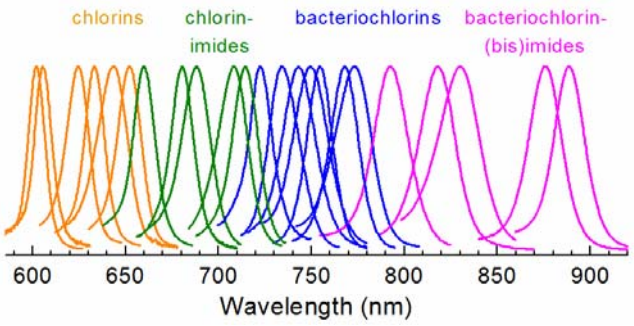

(2) Recently we have engineered and characterized panchromatic (near-UV to near-IR) absorbers based on one to four perylenes strongly coupled to a porphyrin. One architecture is a triad composed of a central porphyrin and two flanking perylene monoimides. The second figure shows such a triad denoted Per_2-Por, upon which we have elaborated (i) a perylene diimide (PDI; cyan diamond, bottom) that can serve as an excited-state electron acceptor, and (ii) a chlorin (green oval, top) that can serve as an excited-state hole trap. The PDI and chlorin can also serve as ancillary light-harvesting units to further enhance the panchromatic absorption. In addition to the pentad, we have prepared and characterized all the subunits (tetrads, triads, etc.). Studies reveal efficient and rapid (< 10 ps) energy transfer from the PDI or chlorin units to the Per_2-Por core, followed by charge separation in the tetrads and integrated pentad.

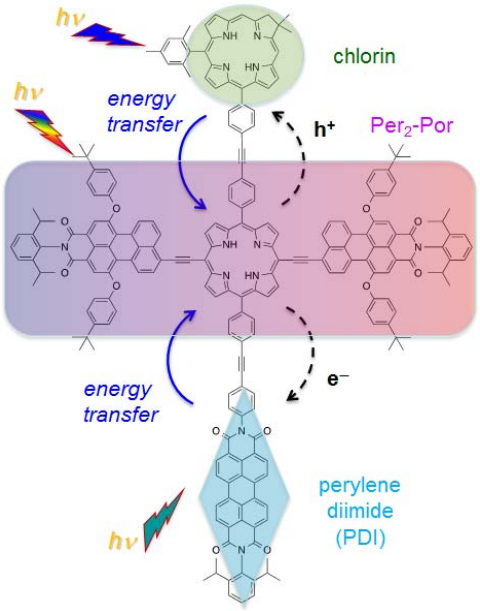

Extending Excited State Lifetimes in Cu(I) MLCT Excited States for Photochemical Upconversion

Catherine E. McCusker, Peter D. Crapps, and Felix N. Castellano*
Department of Chemistry
North Carolina State University
Raleigh, NC 27695-8204

Earth-abundant copper(I) diimine complexes are potential alternatives to the more familiar 2nd and 3rd row transition metal containing photosensitizers. Cu(I) diimine complexes feature metal-to-ligand charge transfer (MLCT) excited states similar to the benchmark $[Ru(bpy)_3]^{2+}$. However, upon photoexcitation these chromophores undergo a significant structural distortion, leading to excited states highly susceptible to exciplex formation that possess very short lifetimes. These properties limit their usefulness as photosensitizers, especially in donor solvents. Previous work from this laboratory has shown that methyl groups in the 3,8-positions of the phenanthroline ligand, combined with bulky *sec*-butyl groups in the 2,9-positions cooperatively restrict the degree of structural distortion in the Cu(I) MLCT excited state thereby extending its lifetime to the microseconds time scale. The long-lived $[Cu(dsbtmp)_2]^+$ (dsbtmp = 2,9-di(*sec*-butyl)-3,4,7,8-tetramethyl-1,10-phenanthroline) molecule has been demonstrated to sensitize visible-to-near UV upconversion in a series of anthracene derivatives. The upconversion quantum yields (λ_{ex} = 488 nm) of 9,10-diphenylanthracene (DPA) and 9,10-dimethylanthracene (DMA) sensitized by $[Cu(dsbtmp)_2]^+$ (17.8% and 9.2%, respectively) represent marked improvement over Ru(II) polypyridyl sensitized upconversion using the same acceptors.

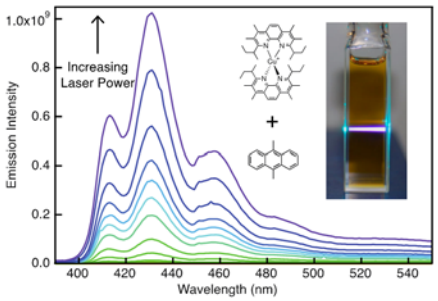

Given the success realized above, we are focused on expanding the inventory of long-lived Cu(I) MLCT chromophores. The 2,9-branched alkyl groups and the 3,8-methyl groups of the dsbtmp ligand both play an important role in restricting the excited state structural distortion in $[Cu(dsbtmp)_2]^+$, resulting in a long lived MLCT excited state. Changing the branched alkyl group in the 2,9-positions to isopropyl or cyclohexyl simplifies the structural characterization with respect to their chiral *sec*-butyl analogs. Varying the substituents at the 4,7-positions of the phenanthroline ring additionally permits modification of the photophysical, electrochemical, and solubility properties of the resultant Cu(I) complex, while maintaining the long lifetime of the parent $[Cu(dsbtmp)_2]^+$ chromophore. Two newly designed molecules will be described, $[Cu(diptmp)_2]^+$ and $[Cu(dsbdmdpep)_2]^+$ (diptmp = 2,9-diisopropyl-3,4,7,8-tetramethyl-1,10-phenanthroline; dsbdmdpep = 2,9-di(*sec*-butyl)-3,8-dimethyl-4,7-di(phenylethynyl)-1,10-phenanthroline), whose excited state lifetimes are on the microseconds time scale with strong MLCT photoluminescence and potent excited state reduction potentials. Investigations using these Cu(I) sensitizers in photochemical upconversion will be presented.

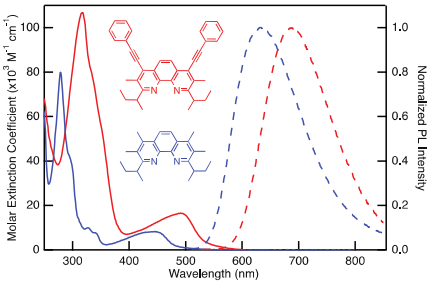

Can Cd chalcogenide clusters be covalently connected with other electron acceptors nanoparticles? And the relation between structure and electron dynamics in a series of substitutionaly doped TiO and Cd-chalcogenide clusters.

Philip Coppens, Yang Chen, Krishnayan Basuroy and Luis Velarde.
Chemistry Department, University at Buffalo, SUNY, Buffalo, NY, 14260-3000

The potential of Quantum Dot Sensitized Solar Cells (QDSSCs) has attracted considerable attention.[1] A number of articles have described the large effect of dicarbamate adsorption on the optical bandgaps of Cd chalcogenide quantum dots.[2] Watson *et al.* in a series of articles have described the electron transfer rates between CdS-Se QDs and TiO linked by mercaptoalkanoid acids (MAA) of different length and phenylene-briged linkers such as 4MBA and 4MPAA, and report that the electron injection yield decreases with increasing chain length, whereas the recombination rate is independent of MAA chain length.[3] Chen *et al*. have studied proton-coupled electron reduction (PCET) of 4,4' bipyridinium adsorbed on CdSe QD's in solutions prior to catalytic reduction of CO_2 to methanol.[4] As none of these studies are supported by diffraction evidence, we are exploring covalent linking of CdS-Se quantum dots. Our chemistry shows that only the three-coordinate Cd atoms are labile and can be substituted with pyridyl and bipyridyl substituents, leading to polymeric complexes, and to dimers, an example, linked by $Cd(dimethylformamide)_4$, is shown in figure a (Cd, teal; S, yellow; O, red; N, blue; C, grey, H atoms omitted). Such structures may be compared with infinite assemblies by Feng *et al*.[5]

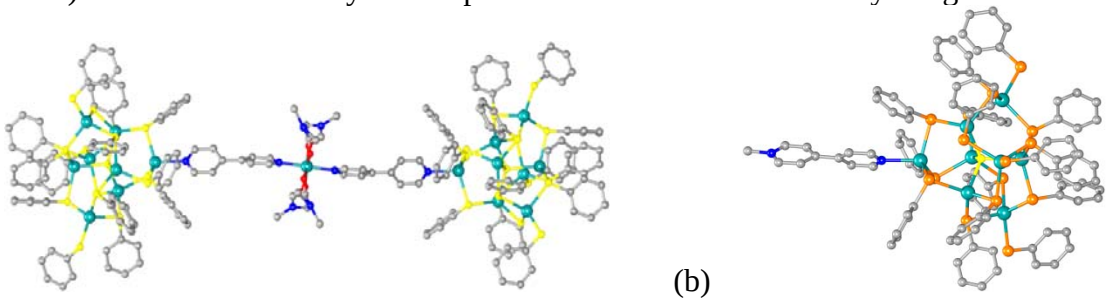

(a) (b)

A first example of substitution of a three-coordinate Cd atom was reported by Adams *et al*.[6] A solution of the tetraethyl ammonium salt of $Cd_8S(Sphenyl)_{15}$ is colorless, but turns orange when the complex is functionalized with *N*-methyl-4,4'-bipyridinium (MeQ) Se, orange). Our DFT calculations show that the excitation corresponds to a charge transfer of ~0.40e (b3pw91) from the cluster to the ligand and a shortening of the Cd-N and the C-C bonds, linking the two rings in the bipyridinium group, confirming the electron-donation properties of the quantum dots. A CdS-Se complex, $Cd_8S(SePh)_{15}(MeQ)$, from our recent studies is shown in figure b.
However, no covalent bridge has so far been found linking the Cd and TiO clusters.

In collaboration with Prof. Velarde of our Department we are developing the ability to perform TAS experiments on our TiO and Cd-chalcogenide clusters with the aim to correlate electron injection with precisely known structural features. First results will be reported.

(1) Kamat, P. V.. *et al. Proc. Natl. Acad. Sci. U. S. A.* **2011**, *108*, 29; *Phys. Chem. C* **2011**, *115*, 13511; *J. Phys. Chem. C* **2008**, *112*, 18737. (2) Frederick, M. T, Weiss, E. A. *et al. Nano Lett.* **2013**, *13*, 287; *Nano Lett.* **2011**, *11*, 5455; *ACS Nano* **2010**, *4*, 3195. . (3) Watson, D. F. et al. *Langmuir* **2014**, *30*, 13293; *ACS Appl. Mater. Interfaces* **2013**, *5*, 8649;. *ACS Appl. Mater. Interfaces* **2011**, *3*, 4242;. *J. Phys. Chem. C* **2009**, *113*, 18643. (4) Batista, V. S.; Lian, T. Q.*et al. J. Am. Chem. Soc.* **2016**, *138*, 884 (5) Zheng, N. F.; Feng, P. Y. *J. Am. Chem. Soc.* **2005**, *127*, 14990. (6) Fu, M. L.; Adams, R. D. *et al.; Eur. J. Inorg. Chem.* **2011**, 660.

Twisted Amides and their Relevance to Linker Design for Solar Applications

Robert H. Crabtree, Subhajyoti Chaudhuri, Brandon Q. Mercado, Victor S. Batista, Charles A. Schmuttenmaer and Gary W. Brudvig

Energy Sciences Institute, Yale University, 520 West Campus Drive, West Haven, CT, 06516, USA

Linkers that attach photosensitizers and water splitting catalysts to semiconductor oxide electrodes may be electrically conducting or not. The latter could prevent deleterious quenching of oxidized catalyst by ET from the semiconductor electrode.

For a nonconducting linker, the bicyclo[2.2.2]octane (BCO) unit provides sites for substituents at the opposing *tert*. positions, one for a surface-binding motif such as hydroxamate, the other for a catalyst or sensitizer. A BCO derivative containing both a tertiary amide and a methyl ester was shown crystallographically to adopt an abnormal cis configuration. This was fatal for solar applications, but we looked in more detail with a view to redesigning the system.

We now show that the cis conformation is sterically disfavored, but electronically favored. The steric strain leads to a big amide torsion (16°) that increases the solvolytic lability of the amide. Thus, we see competitive amide solvolysis in the presence of a normally more labile methyl ester also present. This is totally opposed to the standard reactivity order and has analogy with the enzymatic amide hydrolysis mechanism (e.g., urease), where amide twisting activates it for reaction. The scatterplot below shows the abnormal values in our compound versus the comparison set from the CSD. Class I (orthogonal-cis), Class II (coplanar-trans), Class III (orthogonal-trans), and Class IV (coplanar-cis) can be distinguished.

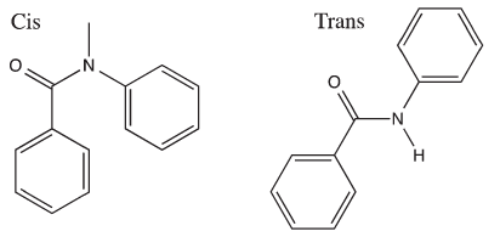

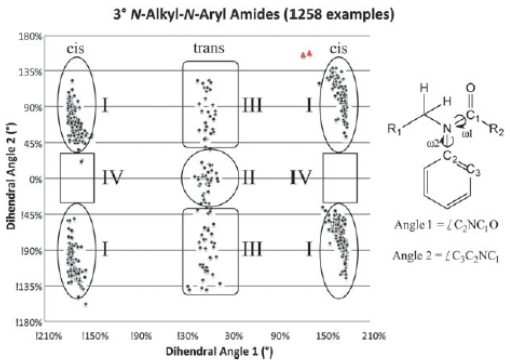

Thanks to extensive computational work, we were able to identify the main factor responsible for the effect. $A^{1,3}$ strain between the aryl and methyl substituents is arguably the factor that tips the aryl system out of conjugation with the amide. The resulting molecular orbitals are substantially higher in energy when the amide is in the trans conformation than in the cis conformation. The new designs will use -C≡C- linkers to avoid the problems encountered above.

Linear Free Energy Relationships in the Proton Transfer Steps Underpinning H_2 Evolution

Jillian L. Dempsey, Noémie Elgrishi, Daniel J. Martin, Brian D. McCarthy, Eric S. Rountree
Department of Chemistry
The University of North Carolina at Chapel Hill
Chapel Hill, NC 27599-3290

Proton-coupled electron transfer (PCET) reactions underpin the molecular transformations of consequence to solar fuel production. As such, this proton-electron reactivity must be carefully considered in the development of catalysts that mediate production of fuels like H_2. As molecular catalysts for the electrochemical reduction of acids to H_2 are often studied in non-aqueous solvents, it is imperative that the role of the acid source in the proton transfer (PT) component of these reactions is well understood. In recent work, we have utilized electrochemical and spectroscopic methods to elucidate the reaction mechanisms of several molecular catalysts and model systems for H_2 evolution and quantify the kinetics of PT reactions in acetonitrile.

Analysis of the $Co(dmgBF_2)_2(CH_3CN)_2$ ($dmgBF_2$ = difluoroboryl-dimethylglyoxime) catalyst with a series of para-substituted anilinium acids suggested an *ECEC* reaction pathway. Kinetics of the first PT step—protonation of a Co^{I} species—were evaluated with foot-of-the-wave analysis, while kinetics of the second PT step—protonation of a putative Co^{II}–H complex—were determined by analyzing the plateau current of the catalytic wave over a range of acid concentrations.[1] For each of these PT steps, the rate constants increase with acid strength and linear correlations were found between log(k_{PT}) and pK_a. In a related study, we examined the formation of a stable Co–H hydride complex, $[Co(Cp)(dppe)H]^+$, via cyclic voltammetry. Quantification of this *EC* reaction via peak shift analysis indicates PT rate constants increase with pK_a but plateau with stronger acids.

We have also studied the reactivity of a key Ni^{II}–H intermediate identified for the $[Ni(P_2^{Ph}N_2^{Ph})_2]^{2+}$ ($P_2^{Ph}N_2^{Ph}$ = 1,3,5,7-tetraphenyl-1,5-diaza-3,7-diphosphacyclooctane) catalyst. Kinetics analyses of the reaction between the Ni^{II}–H with acid to form H_2 were performed via stopped-flow spectroscopy.[2] Data collected for 15 different acids 1) reveal free energy relationships between the proton transfer rate constants and acid pK_a for a series of structurally related acids, 2) identify that an acid's tendency to homoconjugate, heteroconjugate, aggregate, and dimerize also influences its reactivity, and 3) show the addition of conjugate base and water can have profound effects on reaction kinetics. Together, these studies highlight the importance of acid selection for the study of proton transfer reactions and are revealing new opportunities to control and modulate PCET reaction pathways.

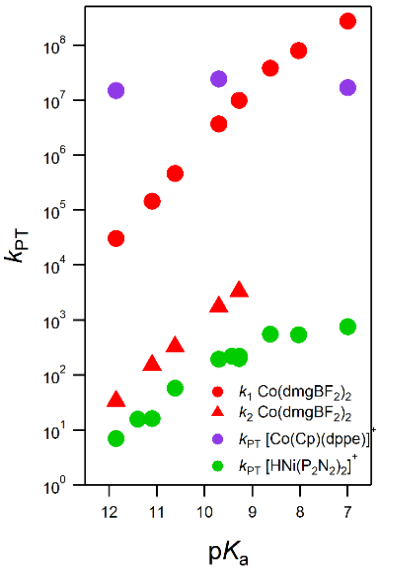

Figure 1. Linear free energy relationships have been observed between log(k_{PT}) and pK_a for proton transfer reactions in acetonitrile with p-substituted aniliniums.

(1) Rountree, E. S.; Martin, D. J.; McCarthy, B. D.; Dempsey, J. L. *ACS Catal.* **2016**, *Accepted*. (2) Rountree, E. S.; Dempsey, J. L. *Inorg. Chem.* **2016**. *Accepted.*

Two-Dimensional Electronic-Vibrational Spectroscopy of Light Harvesting Complexes

NHC Lewis, T.A.A. Oliver, N. Gruenke, Roberto Bassi*, M. Ballattori* and Graham R. Fleming
Department of Chemistry
University of California, Berkeley
and
Molecular Biophysics and Integrated Bioimaging Division
Lawrence Berkeley National Laboratory
Berkeley, CA 94720

** University of Verona*
Piazzetta Chiavica, 2, 37121, Verona VR Italy

We have developed a new spectroscopic technique, two-dimensional electronic-vibrational spectroscopy (2DEV) in which the excitation axis is at the optical frequency and the detection axis is at infrared frequencies. The experiment provides direct information on the correlation between the nuclear and electronic degrees of freedom [1-2]. It also, however, offers the potential to provide a direct experimental connection between the electronic states and the spatial location of the excitation within a light-harvesting complex [3]. It is possible, without assumptions, to calculate the site populations from these spectra for arbitrary values of the electronic coupling and the results are in precise agreement with the originally input quantum dynamical results [3].

Figure 1 shows 2DEV spectra for LHCII at 77K. The contributions from Chla and Chlb are readily distinguishable and it can be seen that Chlb to Chla energy transfer is apparent [4]. The spectra also show relaxation within the Chla manifold. By using a tensor decomposition method called PARAFAC three components can be identified, each of which fits to two exponential components ranging from 75fs to 16ps.

References

1. T.A.A. Oliver, et al, *PNAS*, 111, **28**, 10061 (2014)
2. H. Dong, et al, *J. Chem. Phys.* 142, 17420 (2015)
NHC Lewis, et al, *J. Chem. Phys.* 142, 174202 (2015)
3. NHC Lewis, et al, *J. Chem. Phys.*, 143, 124203 (2015)
4. NHC Lewis, et al, *J. Phys. Chem. Lett.*, 7, 831 (2016)

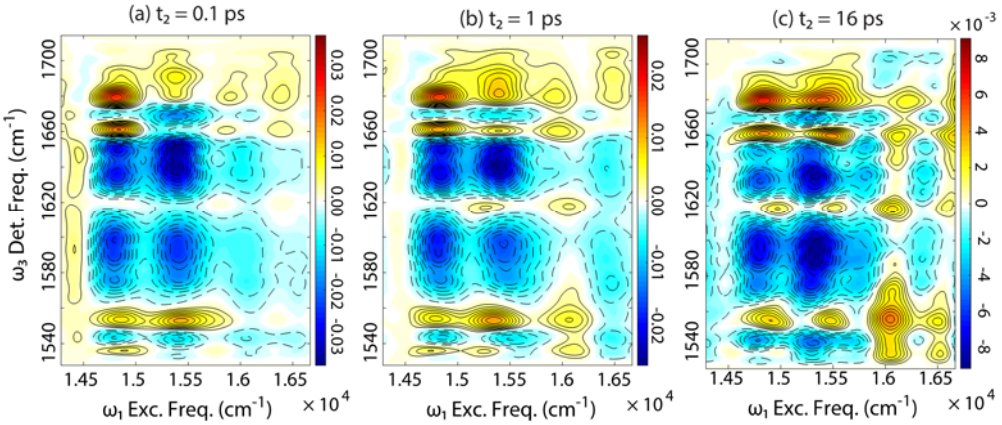

Figure 1 2DEV spectra of LHCII - The spectra show clear indications of Chlb to Chla energy transfer. Longer time relaxations are related to the Chla manifold. Some features suggest long-lived population on Chlb.

New Paradigms for Group IV Nanocrystal Surface Chemistry

Lance W. Wheeler, Nicholas C. Anderson, Peter K.B. Palomaki, Asa W. Nichols, Boris D. Chernomordik, Jeffrey L. Blackburn, Justin C. Johnson, Matthew C. Beard, and Nathan R. Neale
Chemistry & Nanoscience Center
National Renewable Energy Laboratory
Golden, CO 80401

We have been exploring the functionalization of group IV nanocrystals (NCs) to understand how surface chemistry influences fundamental photophysics and inter-NC charge transfer. Many silicon nanostructures exhibit favorable optical properties such as high emission quantum yield following surface functionalization with molecular groups through a Si–C bond. We show the mechanism of functionalization for Si NCs synthesized in a nonthermal radiofrequency plasma is fundamentally different than in other silicon systems. In contrast to hydrosilylation, where homolytic cleavage of Si−H surface bonds typically precede Si–C bond formation, we demonstrate the dominant initiation step for plasma-synthesized silicon nanocrystals is abstraction of a silyl radical, $\bullet SiH_3$, and generation of a radical at the Si NC surface. We experimentally trap the abstracted $\bullet SiH_3$ and show this initiation mechanism occurs for both radical- and thermally-initiated reactions of alkenes to give both alkyl and silylalkyl ligands (Fig. 1). These Si NCs exhibit size-dependent electron-phonon interactions, exciton formation dynamics, and absolute absorption cross-section.

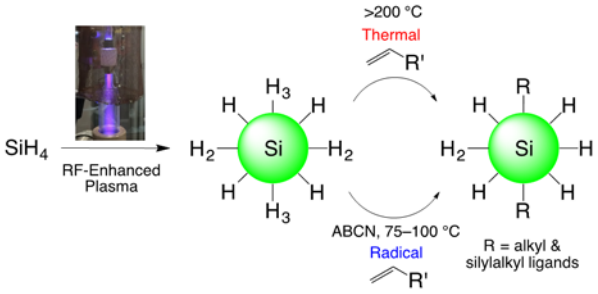

Figure 1. Silicon nanocrystals prepared by RF-enhanced plasma decomposition of silane (SiH_4) gas undergo surface functionalization reactions with alkenes via silyl ($\bullet SiH_3$) group abstraction to give both alkyl and silylalkyl ligands.

We additionally introduce a new paradigm for group IV NC surface chemistry based on surface activation that enables ionic ligand exchange. Germanium NCs synthesized in a gas-phase plasma reactor are functionalized with labile, cationic alkylammonium ligands rather than with traditional covalently bound groups. We demonstrate the alkylammonium ligands are freely exchanged on the Ge NC surface with a variety of cationic ligands, including short inorganic species such as ammonium and alkali metal cations (Fig. 2). This ionic ligand exchange chemistry is used to demonstrate enhanced transport in Ge NC films following ligand exchange. This new ligand chemistry should accelerate progress in utilizing Ge and other group IV NCs for optoelectronic applications.

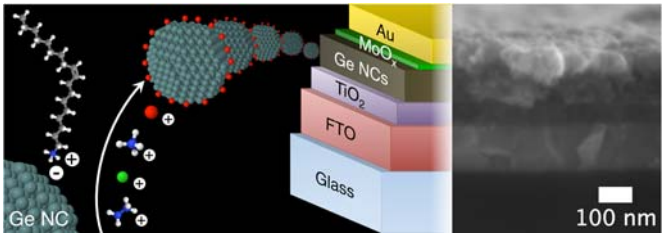

Figure 2. Surface activation of plasma-synthesized germanium nanocrystals yields negatively charged surfaces with weakly bound alkylammonium ligands that can be exchanged via simple solution chemistry using a variety of cationic groups including inorganic cations such as sodium (Na^+).

Charge Transport Across Molecular Wires embedded in Ultrathin Silica Separation Membrane

Eran Edri, Dirk Guldi, and Heinz Frei
Molecular Biophysics Division, Lawrence Berkeley National Laboratory
Berkeley, CA 94720

Photosynthetic units for closing the catalytic cycle of CO_2 reduction by H_2O on the nanoscale require the separation of the half reactions by an ultrathin proton transmitting, gas impermeable membrane. We are developing Co_3O_4-silica core-shell nanotube arrays (Figure) in which each nanotube operates as an independent photosynthetic unit by oxidizing water on the inside while reducing carbon dioxide on the outside. The spaces of O_2 evolution and reduced product are separated by the 2-3 nm thick dense phase silica shell. Charge transport across the silica layer is accomplished by embedded *p*-oligo(phenylenevinylene) molecular wires (OPPV, 3 aryl units).

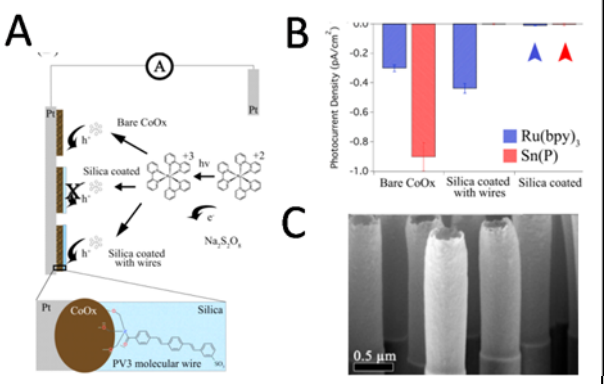

Figure: Photoelectrochemical measurements of charge transport across silica membrane with embedded wires. A) Schematic of visible light sensitized short circuit photocurrent measurement using Ru(bpy)$_3$-persulfate and Sn porphyrin (Sn(P))-triethylamine systems. B) Photocurrent observed for hole injection into bare Co oxide, Co oxide coated with SiO_2-PV3 membrane, and Co oxide coated with silica only. C) SEM of cm^2 sized Co_3O_4-SiO_2 core-shell nanotube array. Tube diameter, 500 nm. Co_3O_4 inner tube, 5 nm. Silica shell, 2 nm. Nanotube separation, 1 µm.

To quantify electron transport through the embedded OPPV molecules, we conducted visible light sensitized photo-electrochemical measurements using cm^2 sized planar Co_3O_4-silica/wire films pre-pared by atomic layer deposition on Pt.[1,2] STEM-EDX, XPS and grazing angle ATR-FT-IR showed covalent attachment of the wires to a 5 nm uniform Co_3O_4 layer at a density of 1 wire per nm^2. Measurement of visible light sensitized charge (hole) injection using sensitizer molecules with different redox potential revealed that the HOMO and LUMO energetics of the wire molecules controls electron flow and allowed us to quantify the flux.

To understand the detailed charge transfer pathway through this new nanoscale membrane for artificial photosynthesis, ultrafast optical spectroscopy was conducted using spherical Co_3O_4-silica/wire particles in aqueous solution. Femtosecond excitation of Zn porphyrin sensitizer adsorbed on the silica membrane revealed hole injection within a ps, which was monitored by the rise of the wire radical cation absorption band at 550 nm. Hole transfer from the embedded wire into Co_3O_4 catalyst occurred within 20 ns, directly monitored by the decay of the wire cation signal and rise of a characteristic absorption of Co_3O_4 at 800 nm. The observed charge transfer time between the visible light sensitizer and metal oxide water oxidation catalyst exceeds by a factor of 10^6 known transfer times for other molecular sensitizer - metal oxide nanoparticle catalyst systems.

1. Edri, E.; Frei, H. *J. Phys. Chem. C* **2015**, *119*, 28326.
2. Kim, W.; McClure, B. A.; Edri, E.; Frei, H. *Chem. Soc. Rev.* **2016**, *46*, 000.

Do Bases in the Second Coordination Sphere Aid CO_2 Reduction?

Etsuko Fujita, Mehmed Z. Ertem and James T. Muckerman
Chemistry Department
Brookhaven National Laboratory
Upton, NY 11973-5000

Proton responsive ligands offer control of catalytic reactions through modulation of pH-dependent properties, second coordination sphere stabilization of transition states, or by providing a local proton source for multi-proton, multi-electron reactions. We successfully used a series of Cp*Ir complexes with proton responsive ligands for CO_2 hydrogenation to formate (as an alternative to photochemical CO_2 reduction) and formic acid dehydrogenation under mild conditions in water.[1] Bases in the second coordination sphere especially accelerate H_2 heterolysis (RDS) of CO_2 hydrogenation by making a water bridge between Ir–H and O^- of the deprotonated ligand.

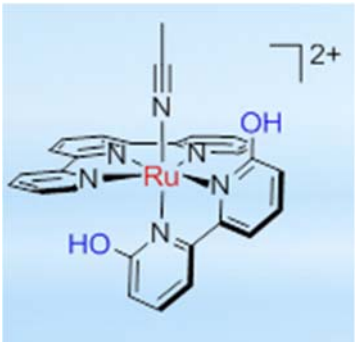

Ruthenium complexes with proton-responsive ligands $[Ru(tpy)(6DHBP)(NCCH_3)](CF_3SO_3)_2$ (tpy = 2,2′:6′,2″-terpyridine; 6DHBP = 6,6′-dihydroxy-2,2′-bipyridine) were examined for CO_2 reduction with our hypothesis that the proximity of 6,6′-OH groups to the Ru center might facilitate protonation of a putative metallocarboxylate intermediate or accelerate protonolysis of the metallocarboxylic acid.[2] However, electrochemical two-electron reduction of $[Ru(tpy)(6DHBP)(NCCH_3)]^{2+}$ unexcitingly generated the complex with a doubly-deprotonated ligand, 6,6′-dioxyl-2,2′-bipyridine ($6DHBP{-}2H^+$), through inter-ligand electron transfer in which the initially formed tpy radical anion reacts with a proton source to co-produce H_2. The complex is identical to that obtained by base titration. A third reduction (i.e., reduction of $[Ru(tpy)(6DHBP{-}2H^+)]^0$) triggers catalysis of CO_2 reduction; however, the catalytic efficiency is strikingly lower than that of unsubstituted $[Ru(tpy)(bpy)(NCCH_3)]^{2+}$. The Ru carbonyl formed by the intermediacy of a metallocarboxylic acid is stable against reduction, and mass spectrometric analysis of this product indicates the presence of two carbonates formed by the reaction of $DHBP{-}2H^+$ with CO_2.

We thank our collaborators Dr. Yuichiro Himeda (AIST, Tsukuba, Japan) and Prof. David J. Szalda (Baruch Coll. CUNY).

References:

1) (a) Hull, J. F.; Himeda, Y.; Wang, W.-H.; Hashiguchi, B.; Szalda, D. J.; Muckerman, J. T.; Fujita, E. *Nat. Chem.* **2012**, *4*, 383-388. (b) Wang, W.-H.; Muckerman, J. T.; Fujita, E.; Himeda, Y. *ACS Catal.* **2013**, *3*, 856-860. (c) Wang, W.-H.; Himeda, Y.; Muckerman, J. T.; Manbeck, G. F.; Fujita, E. *Chem. Rev.* **2015**, *115*, 12936-12973. (d) Ertem, M. Z; Himeda, Y.; Fujita, E.; Muckerman, J. T. *ACS Catal.* **2016**, *6*, 600-609. (e) Onishi, N.; Ertem, M. Z.; Xu, S.; Tsurusaki, A.; Manaka, Y.; Muckerman, J. T.; Fujita, E.; Himeda, Y. *Catal. Sci. Tech.* **2016**, *6*, 988-992,
2) Duan, L.; Manbeck, G. F.; Kowalczyk, M.; Szalda, D. J.; Muckerman, J. T.; Himeda, Y.; Fujita, E. *Inorg. Chem.* **2016**, Accepted.

Photoelectrochemical, Photophysical and Binding Studies of Chromophore-Linker-Anchor Compounds: the influence of interfacial dipoles

E. Galoppini,[a] R. A. Bartynski,[b] L. Gundlach,[c,d] J. Rochford[e]
A. Batarseh,[a] H. Fan,[a] S. Rangan,[b] J. Nieto-Pescador[c], B. Abraham[d], K. Ngo[e]

[a]Chemistry Department, Rutgers University, Newark, NJ 07102; [b]Department of Physics and Astronomy, Rutgers University, Piscataway, NJ 08854 [c]Department of Physics and [d]Department of Chemistry and Biochemistry, University of Delaware, Newark, DE 19716; [e]Chemistry Department, University of Massachusetts-Boston, Boston, MA 02125

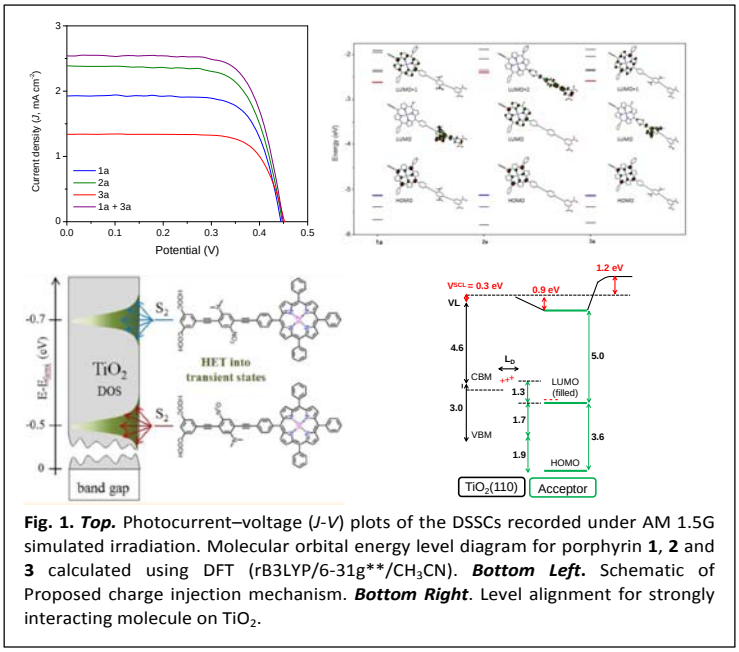

Fig. 1. ***Top.*** Photocurrent–voltage (*J-V*) plots of the DSSCs recorded under AM 1.5G simulated irradiation. Molecular orbital energy level diagram for porphyrin **1**, **2** and **3** calculated using DFT (rB3LYP/6-31g**/CH_3CN). ***Bottom Left.*** Schematic of Proposed charge injection mechanism. ***Bottom Right***. Level alignment for strongly interacting molecule on TiO_2.

The performance of dye sensitized solar cells is highly dependent upon the efficiency of photoinduced heterogeneous electron transfer and the energy level alignment of the dye/semiconductor interface. We are particularly interested in the dye/semiconductor interface where molecular design can be leveraged to optimize thermodynamic and kinetic properties of charge transfer.

A concept that is attracting increasing attention is that the energy level alignment of any interface at equilibrium is shifted, relative to its component native band edges, due to an interface dipole. In this poster we describe our progress in the following areas:

(A) The electrochemical, photoelectrochemical and surface properties of rigid-rod ZnTPP porphyrins with (**1** and **3)** or without (**2**) a Donor-Acceptor dipole in the bridge in solution (as esters, **1-3e**) and bound to nanostructured nanoparticle TiO_2 and ZrO_2 films (as acids, **1-3a**). Cyclic voltammetry confirmed that the presence or direction of the bridge dipole does not change the electronic properties of the ZnTPP ring, but DFT computations suggest that introduction of the DA/AD dipoles in the bridges lowers the energy of the bridge based π^* orbital. On nanostructured semiconductor films, the differences in packing that are caused by the bridge substitution override any electronic differences due to the presence of the small internal dipole. The effect of anchor group bonding on TiO_2 (110) is also discussed.

(B) The interfacial charge transfer kinetics**.** The poster will illustrate UV-Vis and steady state emission spectra as well as transient absorption spectra in solution and bound, and an analysis of the injection dynamics. Overall the intramolecular photo-dynamics of **1-3** resembled the well-known dynamics of ZnTPP, but the dipole carrying nitroaniline group gave rise to Dexter energy transfer from the excited state of the ZnTPP chromophore.

(C) Current work, devoted to address difference in surface packing and synthesize a new class of compounds with larger dipoles and improved chromophore.

Controlling Pathways of CO_2 Reduction with Manganese Precatalysts: Electrochemical and Transient Spectroscopic Investigations

David C. Grills
Chemistry Division, Brookhaven National Laboratory, Upton, NY 11973-5000

The current state of understanding of catalytic CO_2 reduction with molecular transition-metal-based electrocatalysts has progressed significantly in recent years, with Mn-based catalysts containing substituted bipyridine ligands having gained in popularity. However, many unanswered questions remain, and thus acquiring an advanced understanding of reaction intermediates will allow us to manipulate these species under non-equilibrium conditions to develop more efficient processes.

We recently studied[1] the Mn-based precatalysts, [*fac*-Mn(6,6'-R_2-bpy)$(CO)_3(CH_3CN)$](OTf) (**1**$^+$ and **2**$^+$), see right for identities of R, one of which was newly-synthesized (**1**$^+$), and the other (**2**$^+$) already established by Kubiak. While both **1**$^+$ and **2**$^+$ efficiently turn over the catalytic transformation of CO_2 to CO in acetonitrile in the presence of Brønsted acids, we found that the introduction of four pendant MeO groups into the second coordination sphere in **1**$^+$ provides local Brønsted base sites to facilitate directed protonation of the metallocarboxylic acid intermediate. This promotes CO_2 reduction at a lower applied potential via a so-called *protonation-first* pathway, in contrast to **2**$^+$, which predominantly follows a *reduction-first* pathway at more negative applied potential. This shows how self-assembly of a proton source in the outer coordination sphere can facilitate CO_2 reduction at lower overpotential.

1 R = 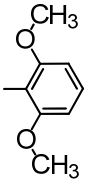

2 R = 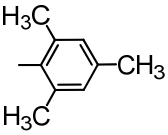

We are now investigating the mechanism of CO_2 reduction with **1**$^+$ and **2**$^+$ using a combination of IR spectroelectrochemistry and pulse radiolysis with time-resolved infrared detection (PR-TRIR).[2] In order to access the catalytic cycle, we must produce the two-electron reduced species, [*fac*-Mn(6,6'-R_2-bpy)$(CO)_3]^-$ ([**Mn**]$^-$). Although PR is a one-electron technique, our recent PR-TRIR investigations on **1**$^+$ and **2**$^+$ have revealed that **1**$^-$ and **2**$^-$ can be accessed after one-electron reduction of **1**$^+$ or **2**$^+$ via a disproportionation mechanism, e.g., **1**$^\bullet$ + **1**$^\bullet$ → **1**$^+$ + **1**$^-$. Such a mechanism is possible due to the steric bulk of the 6,6' substituents on the bipyridine ligand preventing dimerization[3] of the one-electron reduced [**Mn**]$^\bullet$ radicals. Our current goal is to prepare **1**$^-$ and **2**$^-$ by PR, and monitor their reactivity toward CO_2 and protons with TRIR detection. Other intermediates have also been and will be synthesized, e.g., the [**Mn**]-CO^+ tetracarbonyl species, and the [**Mn**]-COOH metallocarboxylic acid, allowing us to access the catalytic cycle at different points via PR to map out the kinetics and mechanism of CO_2 reduction by **1**$^+$ and **2**$^+$ in more detail.

1. Ngo, K. T.; Narayan, R.; Mahanti, B.; McKinnon, M.; Grills, D. C.; Rochford, J. manuscript in preparation.
2. Grills, D. C.; Farrington, J. A.; Layne, B. H.; Preses, J. M.; Bernstein, H. J.; Wishart, J. F. *Rev. Sci. Instrum.* **2015**, *86*, 044102.
3. Grills, D. C.; Farrington, J. A.; Layne, B. H.; Lymar, S. V.; Mello, B. A.; Preses, J. M.; Wishart, J. F. *J. Am. Chem. Soc.* **2014**, *136*, 5563-5566.

Acknowledgments: We thank our collaborator on this project, Prof. Jonathan Rochford (U. Mass, Boston) for the synthesis of the catalysts and the electrochemical studies.

Ultrafast microscopy of methylammonium lead iodide perovskite thin-films: heterogeneity of excited state spatial and temporal evolution

Andrew H. Hill, Eric S. Massaro, Kori E. Smyser, Erik M. Grumstrup
Department of Chemistry and Biochemistry
Montana State University
Bozeman, MT 59717

While organometal halide perovskites exhibit functional properties typically associated with high-performance, single-crystal inorganic semiconductors, the solution processing techniques used to fabricate the material can introduce significant heterogeneities in both structure and composition. To mitigate the influence of this variation, we utilize pump-probe microscopy to investigate the ultrafast dynamics of methylammonium lead iodide perovskite thin films. The high spatial resolution afforded by the technique reveals extensive spatial heterogeneity in excited state lifetime and mobility, both within and between individual domains. Our measurements suggest that in the first two picoseconds after photoexcitation, the band-edge transient kinetics are dominated by a dynamic competition between band-gap renormalization and band-filling as charge carriers cool from their initial photogenerated state. Once cooled to the band edge, charge carriers recombine via trap-mediated mechanisms on multiple timescales ranging from 100's of picoseconds to 10's of nanoseconds. These results highlight the role processing conditions play in determining the dominant recombination mechanism and lifetime of the excited state. We also directly image charge carrier diffusion in individual domains. While these results show the ambipolar charge carrier mobility varies by a factor of five from domain to domain, the thin film diffusivity can reach values that are comparable to those observed in single-crystalline nanostructure and bulk methylammonium lead iodide perovskite. Together, these results highlight the importance of precisely correlating measurements of optoelectronic functionality with specific structural and compositional properties so as to optimally design perovskite-based thin film photovoltaics.

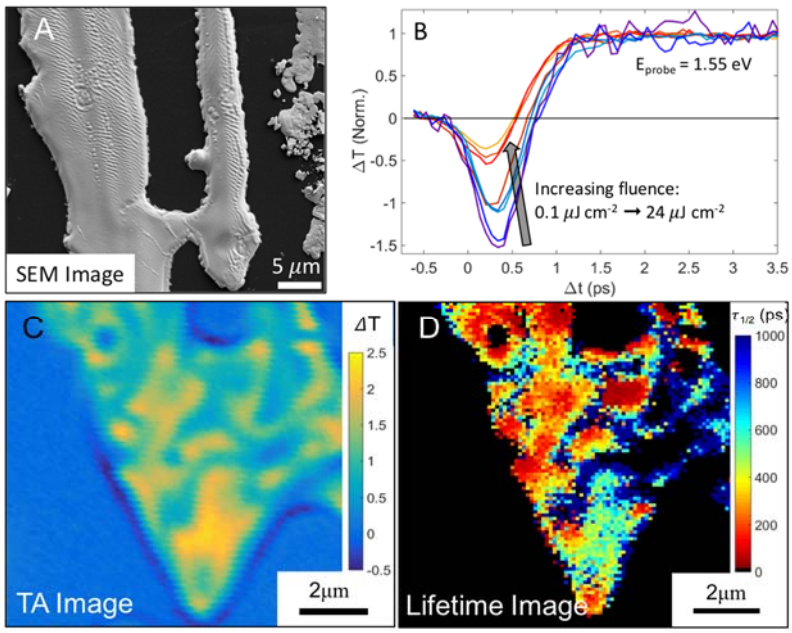

(A) Field-emission scanning electron micrograph of a single perovskite domain. (B) Early time band edge transient kinetics show a decrease in photoinduced absorption magnitude relative to the long lived transient bleach, suggesting fast band filling effects at high excitation densities. (C) Transient absorption image of a single perovskite domain at Δt = 2 ps. A series of such images are used to produce a lifetime image, shown in panel (D). The lifetime image shows an order of magnitude difference in charge carrier lifetime on length scales smaller than 1 μm.

Photoanode Energetics and Rate Limiting Processes in Dye-Sensitized Solar Cells with Cobalt-Based Redox Shuttles

Josh Baillargeon, Dhritabrata Mandal, Yuling Xie, Thomas W. Hamann
Department of Chemistry
Michigan State University
East Lansing, MI 48824

The general goal of this project is to understand the fundamental role of the relevant dye-sensitized solar cell, DSSC, components (photoanode, redox shuttle and sensitizer) involved in key efficiency-determining processes. This poster focuses on our dual efforts to determine the energy and concentration of both trapped and free conduction band (CB) electrons in photoanodes which can participate in recombination as well as elucidate and exploit the interplay of dye regeneration and recombination which control the charge collection with new outersphere redox shuttles.

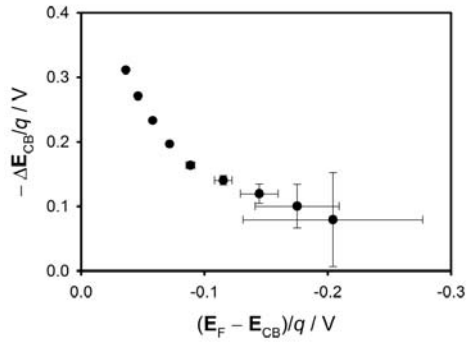

Figure 1. Conduction band shift as a function of the displacement of the Fermi level with respect to the conduction band.

We will present results from spectroelectrochemical measurements of the CB edge by monitoring the Burstein-Moss shift and free electron absorbance. From these measurements we were also to quantify the unpinning of band edges (ΔE_{CB}) due to charging electroactive surface states which causes a potential drop across the Helmholtz layer, shown in figure 1. The magnitude of band unpinning elucidates the nature of the potential dependence of conduction band electron absorbance and the measured trap state energy distribution. These results further allow estimation of the spatial location of the trap states in/on the nanoparticle which can control recombination.

Recent results comparing the dye regeneration efficiency and the electron diffusion length for DSSCs employing new cobalt-based redox shuttles will be presented. Self-exchange rate constants of the redox shuttles are determined from cross-exchange measurements. We find that we are able to tune the electron-transfer self-exchange rate constant by over eight orders of magnitude with cobalt redox shuttles through variation of the ligand framework. Application of Marcus theory allowed the difference in self-exchange rate constants to quantitatively account for the differences in regeneration efficiency and electron diffusion length of the redox shuttles measured. These results point to a new energy and kinetic space of redox shuttle which have the capability of achieving high efficiencies in next-generation DSSCs.

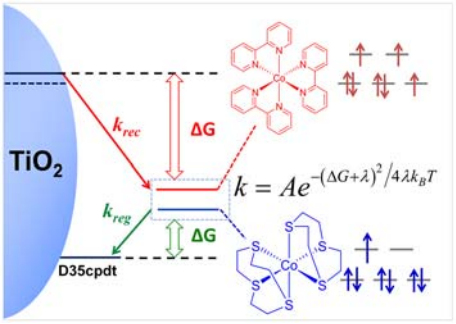

Figure 2. Scheme of recombination and regeneration reactions for two examples of cobalt-based redox shuttles described in a Marcus framework for electron transfer.

Understanding and Controlling Light Harvesting, Energy Transport, and Charge Transport within Chromophoric, Metal-Organic Framework based Electrode Films

Joseph T. Hupp
Department of Chemistry
Northwestern University
Evanston, IL 60093

By emulating key aspects of natural photosynthesis, molecule-based solar cells offer the prospect of tunable, inexpensive, and chemically benign light absorption and subsequent conversion to electrical or chemical energy. The best-known manifestations of this idea are dye-sensitized solar cells (DSCs), dye-sensitized photosynthetic cells, and organic photovoltaic (OPV) cells (more specifically, bulk-heterojunction type OPVs). Increasingly attractive as light absorbers are metal-organic frameworks (MOFs). These compounds constitute highly ordered and aligned assemblies of organic molecules (candidate chromophores) linked in well-defined fashion via coordination bonds to metal ions or clusters. Especially attractive for use in solar energy conversion are MOFs grown in thin-film form on transparent support electrodes. If MOF film synthesis is done via automated layer-by-layer (LBL) assembly, also termed liquid-phase epitaxy, film thicknesses can be controlled with close to single-molecular-layer precision. Furthermore, the chemical identity of the chromophore can be varied over the course of LBL film growth—in principle permitting panchromatic antenna-like structures to be grown, again with close to single-molecular-layer precision.

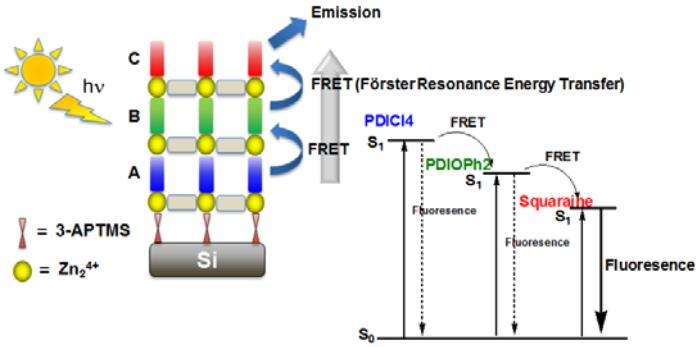

This poster will report on some of what we have learned about directional transport of: a) photo-generated molecular excitons, and b) redox-related charges (*i.e.* holes, electrons, ions), within thin-film MOFs. We find that rates of both can be varied over orders of magnitude and that the rate variations can be understood within the context of contemporary theory. We further find that we can capitalize on our understanding in predictive fashion to tune transport rates in ways that may make the associated structures more useful as components of molecule-based solar cells.

"Bias-switchable Permselectivity and Redox Catalytic Activity of a Ferrocene-Functionalized, Thin-Film Metal Organic Framework Compound," *J. Phys. Chem. Lett.*, **2015**, *6*, 586–591.

"Metal-organic framework materials for light-harvesting and energy transfer," *Chem. Commun.*, **2015**, *51*, 3501-3510.

"Modulating the Rate of Charge Transport in a Metal–Organic Framework Thin Film Using Host:Guest Interactions," *Chem. Commun.*, **2016**, *52*, 1705-1708.

"Layer-by-Layer Assembled Films of Perylene Diimide- and Squaraine-Containing Metal-Organic Frameworks: Solar Energy Capture and Directional Energy Transfer," **2016**, submitted (ID: am-2016-03307k)

Optical Inhomogeneity from 2D Spectra vs. TEM Size Dispersion in PbSe Nanocrystals

Samuel D. Park, Dmitry Baranov, Jisu Ryu, and David M. Jonas
Department of Chemistry and Biochemistry
University of Colorado
Boulder, CO 80309

Size dispersion is a fundamental property of an ensemble of quantum dots (QDs), and it is an important parameter in understanding the carrier dynamics because optical inhomogeneity broadens linewidths through the size dependent bandgap. A standard method for quantifying the size dispersion of a QD sample is by conventional transmission electron microscopy (CTEM). We used Two-Dimensional Fourier Transform spectroscopy in the short-wave infrared region to determine the optical inhomogeneity in a sample of colloidal PbSe QDs. This inhomogeneous linewidth is narrower than calculated from the static size dispersion obtained from CTEM and scanning transmission electron microscopy (STEM) images from the same sample.

For PbSe QDs, the 2D spectra at a waiting time of T = 1 ps contain a combination of signals that create a nodal line, in which the nodal line slope uniquely determines an upper bound on the static optical inhomogeneity. Using the nodal line slope method, we determine the inhomogeneous linewidth to be 85 ± 5 meV (FWHM). For comparison, the 1S-1S absorption linewidth is 145 meV (FWHM).

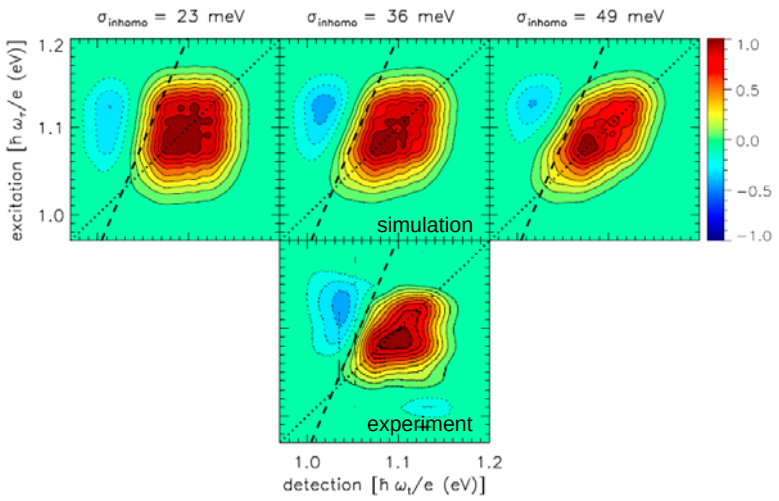

Figure 1: In 2D spectra, inhomogeneous broadening is parallel to the diagonal (dashed) and homogeneous broadening is perpendicular to the diagonal. The bottom panel shows experimental 2D spectra and the three upper panels show simulations for three different inhomogeneous linewidths. The dashed line marks the experimental nodal line in all 4 panels. The nodal line slope reflects optical inhomogeneity.

Static size dispersions were obtained by analyzing bright field CTEM images and annular dark field STEM images following published procedures, and were found to agree between two imaging modes and facilities. When using literature sizing curves to calculate the optical bandgap dispersion, assuming that all three QD dimensions have independent size dispersions leads to the smallest possible estimates of optical inhomogeneity, which range from 110-145 meV (FWHM). It is problematic that the lower bounds from TEM are greater than the upper bound from 2D spectra; either standard analyses of TEM images overestimate size dispersion or optical inhomogeneity does not directly reflect size dispersion. Factors that might contribute to overestimation of the static size dispersion obtained by standard analysis of TEM images are: noise, approximation of the QD shape as ellipsoidal in fitting, and QD contrast variations.

Bandgap versus Sub-bandgap Excitations in Cu-Deficient $CuInS_2$ Quantum Dots

Danilo H. Jara, Kevin G. Stamplecoskie, and Prashant V. Kamat
Radiation Laboratory and Department of Chemistry & Biochemistry
University of Notre Dame, Notre Dame, IN 46556

Ternary semiconductor quantum dots (QDs) such as $CuInS_2$ have recently emerged as a new class of light harvesting materials because of their well-matched bandgap with the solar spectrum And their composition of less toxic elements. Despite the increased interest in $CuInS_2$ QDs, its optical properties are yet to be understood fully. The difficulty in proposing a universal physical model for the charge carrier dynamics in $CuInS_2$ QDs arises from the uncertainties associated with the internal defect states located within the bandgap.

We have now elucidated excited state charge carrier dynamics of $CuInS_2$ QDs by varying the [Cu]:[In] ratio. The QD properties are influenced by the compositional changes and they can be tuned by varying the [Cu]:[In] ratio. Spectroscopic evidence points to two optical transitions contributing to the absorption properties of Cu_xInS_2 QDs (Figure 1). The bleaching of band edge absorption and broad tail absorption bands in the subpicosecond – nanosecond timescale provide further evidence to the dual optical transitions. The origin of the first and second transition were assigned to excitonic and Cu-related subbandgap state absorption, respectively. The photoluminescence lifetime measurements exhibit a wavelength-dependent decay, indicating a multi-state relaxation pathway. Understanding these photophysical mechanisms will help to control Cu_xInS_2 QDs properties, and aid in improving performance of photovoltaic and light-emitting devices.

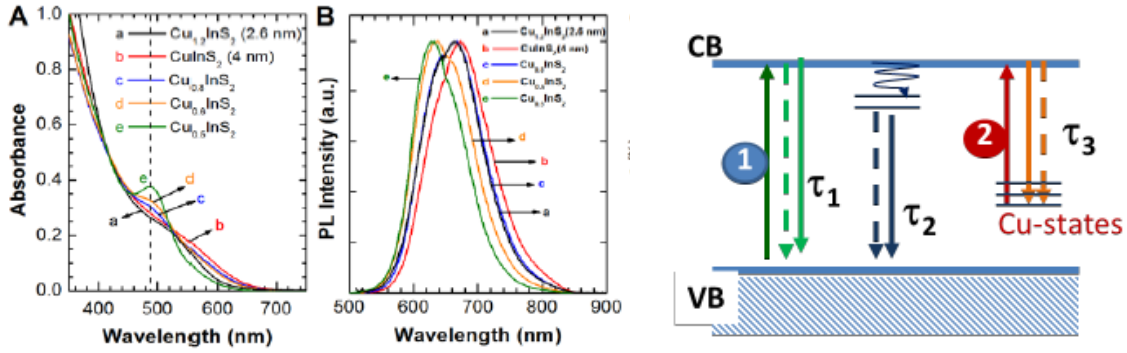

Figure 1: (A) Absorption spectra, and (B) emission spectra ($\lambda_{excitation}$ = 490 nm) of Cu_xInS_2 QDs with different [Cu]:[In] ratio, dispersed in chloroform. The scheme on the right shows two different optical transitions

Related Readings:

Jara, D. H.; Yoon, S. J.; Stamplecoskie, K. G.; Kamat, P. V., Size-Dependent Photovoltaic Performance of CuInS2 Quantum Dot-Sensitized Solar Cells. *Chemistry of Materials* **2014,** *26*, 7221–7228.

Jara, D. H.; Stamplecoskie, K. G.; Kamat, P. V., Two Distinct Transitions in Cu_xInS_2 Quantum Dots. Bandgap *Vs.* Sub-Bandgap Excitations in Cu-Deficient Structures. J. Phys. Chem. Lett., 2016, 7, 1452–1459

Hot Hole Photochemistry of CdSe Quantum Dots

Youhong Zeng, Ke Gong and David F. Kelley

Chemistry and Chemical Biology, University of California Merced,

5200 North Lake Road, Merced, CA 95343

CdSe quantum dots (QDs) have been shown to generate very high energy unrelaxed holes following one- or two-photon excitation. We find that upon irradiation, CdSe quantum dots that absorb two or more visible photons undergo photodarkening. The quantum yield for this process is on the order of 6% in chloroform and much smaller in nonpolar solvents, such as octane. An analysis of the energetics indicates that following two-photon excitation, the biexciton undergoes an Auger process producing a hot hole. This hot hole is ejected to a surface-bound TOP ligand, forming a QD^-/TOP^+ contact ion pair that separates in polar, but not non-polar solvents. The charged and deligated QD is dark, resulting in the overall photodarkening. A similar, Auger-induced hot hole ejection process can also occur following absorption of a single photon, by the mechanism indicated in figure 1.

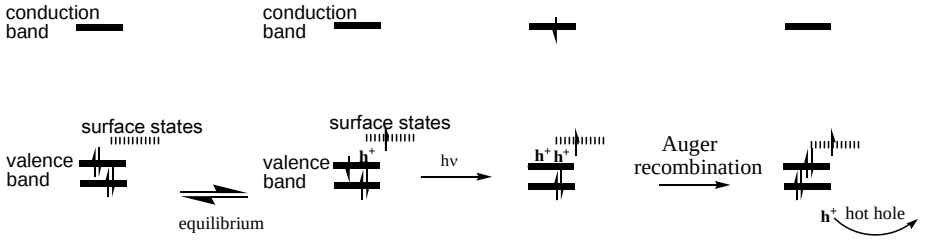

Figure 1. Mechanism of single-photon hot hole generation in solution-phase QDs.

In this case, only surface charged QDs (which are dark) dissociate, giving a ligand cation. The ligand cation subsequently undergoes charge transfer to another (bright) QD in solution , causing a delayed darkening on the minutes timescale, see figure 2.

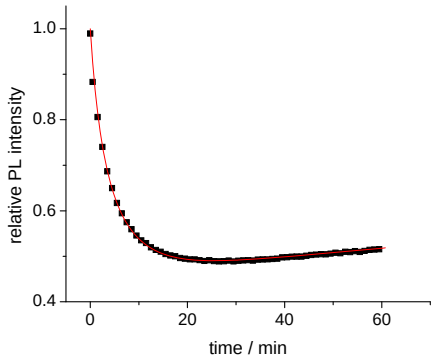

$$QD_L \xrightarrow{h\nu} QD^- + L^+$$

$$L^+ + QD(bright) \xrightarrow{k2} QD^+(dark) + L$$

$$QD^- + QD^+(dark) \xrightarrow{k3} 2QD(bright)$$

Figure 2. Luminescence intensity under steady-state illumination, following 30 seconds of irradiation. Also shown is a curve fit using kinetics based the indicated mechanism.

Charge recombination ultimately occurs on a longer timescale. Further studies of the hot hole production and ligand dissociation mechanisms are ongoing.

Establishing the Role of the Electrode Surface in Solar-Driven Pyridine-Catalyzed CO_2 Reduction

Coleman X. Kronawitter, Peng Zhao, Zhu Chen, and Bruce E. Koel
Department of Chemical and Biological Engineering
Princeton University
Princeton, NJ 08540

The design of new technologies that shift U.S. power consumption away from fossil fuels toward sustainable alternatives must take into account the nation's large-scale need for stored chemical fuels. Photoelectrocatalytic CO_2 reduction is one such technology, since it facilitates a process whereby solar energy is used to reduce CO_2, a combustion product, into chemical fuels that are compatible with the existing U.S. energy infrastructure. Our project involves experimental studies of well-defined surfaces to establish the role of the electrode surface in catalyzed heterogeneous CO_2 reduction. Specifically we investigate the role of the electrode surface in pyridine-catalyzed CO_2 reduction, which is reported to be associated with high yields for methanol and formic acid.

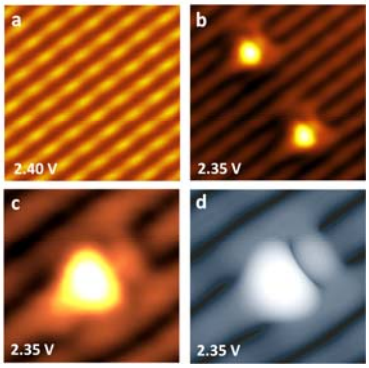

Figure 1. Top: Empty-state constant-current STM images of (a) the GaP(110) surface and (b) and pyridine/GaP(110). 35.8×35.8 Å^2. Individual pyridine molecule imaged by experimental (c) and DFT-calculated (d) constant-current STM. 15×15 Å^2.

Our recent work has reported the orbital-resolved adsorption state of pyridine on GaP(110), the most stable surface of GaP, using scanning tunneling microscopy (Fig. 1) [*J. Phys. Chem C*, **2015**, 119, 28917]. By examining the distribution of unoccupied molecular orbitals with high spatial and energetic resolution, we showed that scanning probe techniques can be used to positively identify the sites on pyridine susceptible to nucleophilic attack, consistent with frontier orbital theory. This technique can be used to explore the local reaction centers of adsorbed catalysts relevant to artificial photosynthesis. Our observations of the stable adsorption of both H [*J. Phys. Chem. C*, **2015**, 119, 17762] and pyridine on this surface is notable, because it characterizes the proposed precursor state for the formation of adsorbed dihydropyridine, which could be a key hydride-shuttling catalyst for heterogeneous CO_2 reduction.

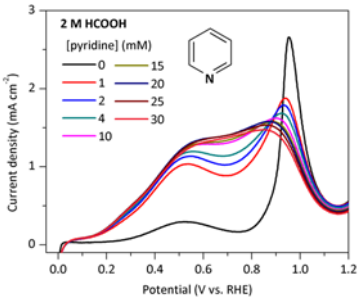

Figure 2. Anodic electrochemical response of polycrystalline Pt in 0.5 M H_2SO_4 and 2 M HCOOH, with (colored lines) and without (black lines) pyridine. 100 mV s^{-1}.

Through our investigation of the role of the electrode surface in this chemistry, we have recently explored the electrochemistry of Pt in the presence of pyridine. Specifically, to generate further mechanistic information for CO_2 conversion, we have investigated the *reverse reaction*, i.e., the oxidation of formic acid to CO_2 in the presence of dissolved pyridine. Our results show that the addition of pyridine to the electrolyte increases the formic acid oxidation rate at low applied potentials (Fig. 2) [**2016**, manuscript in preparation]. These data imply a reduction in the barrier for formic acid oxidation, a result we are in the process of interpreting in the context of the CO_2-to-methanol conversion pathway.

The Fate of Excitons in Single Walled Carbon Nanotubes

Amanda Amori, Zhentao Hou, Nicole M. B. Cogan, and Todd D. Krauss
Department of Chemistry
University of Rochester
Rochester, New York 14627-0216

Semiconducting single-walled carbon nanotubes (SWNTs) are fundamentally interesting and technologically relevant materials with size tunable absorption and emission across a range of visible and near infrared wavelengths. However, several important aspects of their photophysical properties are not known in enough depth to predict how SWNTs will behave as part of a larger integrated solar photochemical system. In particular, simple concepts such as the photoluminescence efficiency (PL QY) are not well understood for SWNTs.

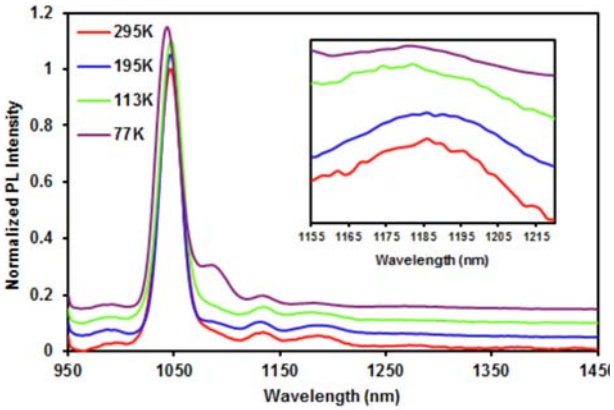

Figure 1: Normalized temperature dependent PL spectra of (*7*,*5*) SWNTs. Inset shows a zoom in of the PL sideband to the red of the bright E_{11} state.

In one experiment, variable temperature photoluminescence excitation (PLE) spectroscopy was performed for SWNTs in a glass-forming organic solvent to investigate the temperature dependence of several fundamental PL features related to the main E_{11} excitonic emission (Figure 1). We focused on a feature located to the red of the bright E_{11} exciton peak that is attributed to vibrationally assisted PL from the nominally forbidden *K*-momentum dark exciton (KDE) state. The temperature dependence of PL from the KDE state relative to E_{11} scales with the phonon occupation number and suggests the KDE state is populated through intervalley scattering of the E_{11} exciton by an optical phonon. For (*7*,*5*) chirality SWNTs at 295 K, we find that 88.5% of photoexcited excitons populate the bright E_{11} state, leaving an upper bound of 11.5% of the total exciton population to scatter into equivalent K-valleys.

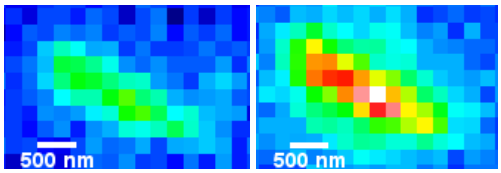

Figure 2. PL images from an individual ~ 1.5 µm long (6,5) SWNT before and after brightening with DTT (left and right, respectively).

Recently, we found that the SWNT PL QY can be increased substantially through the addition of small amounts of mildly reducing molecules such as dithiothreitol (DTT). In a second experiment, single molecule studies of brightened SWNTs longer than the diffraction limit reveal the surprising finding that upon adding the reductants, the SWNTs brightened uniformly, as determined from the PL image (Figure 2). The simplest picture suggests that non-uniform brightening would result from consecutive interactions with individual point defects. The single step brightening across the entire SWNT followed by a constant, nonblinking PL level suggests the brightening effect could be due to a single molecule interacting with the SWNT.

Dynamics of the Injection and Transport of Electrons in DNA

Frederick D. Lewis
Department of Chemistry
Northwestern University
Evanston, Illinois USA 60208

Charge transport in DNA can occur via the movement of either positive charge (holes) or negative charge (electrons) between bases, holes preferring to reside on bases of low electron affinity (purines and their derivatives) and electrons on bases of high electron affinity (pyrimidines and their derivatives). Our current knowledge of the dynamics of charge transport in DNA is derived mainly from experimental and theoretical studies of photoinduced injection and transport of holes. Much less is known about the dynamics and mechanism of electron injection transport in DNA. Whereas long-range e-transport has been detected by indirect means (e.g. loss of Br^- from reduced bromouracil), the dynamics of such processes have not been reported.

In collaboration with the Grozema laboratory in Delft, NL we have investigated the dynamics of electron injection from the singlet state of a stilbenediether hairpin linker (SD) into the adjacent base pairs in synthetic DNA hairpins (Chart 1a,b). Electron injection results in reduction of the neighboring pyrimidine base and formation of a $Sd^{-\bullet}B^{-\bullet}$ contact radical ion pair. Rate constants for electron injection (k_{inj}) increase with increasing pyrimidine reduction potential (Chart 1c); however, the rate constant for charge recombination (k_{r1}) is slower for thymine than either cytosine or chloro- or fluoro-uracil (Scheme 1, black). In the case of hairpins which possess a perylene-diimide (PDI) electron acceptor (Chart 1d) it is possible to determine the rate constants for e-transport to PDI (k_{et1}) for haripins **T4-PDI** and **F4-PDI**; however, the efficiency of e-transport is too low in the case of **C4-PDI** to allow measurement. Values of k_{et1} are strongly dependent upon the number of AT base pairs as was the case in our earlier studies of hole transport in DNA hairpins. Both the efficiency and rate constant for e-transport can be increased by the insertion of a single T-A base pair between a poly(F-A)base pair domain and PDI in the hairpins TF_n-PDI.

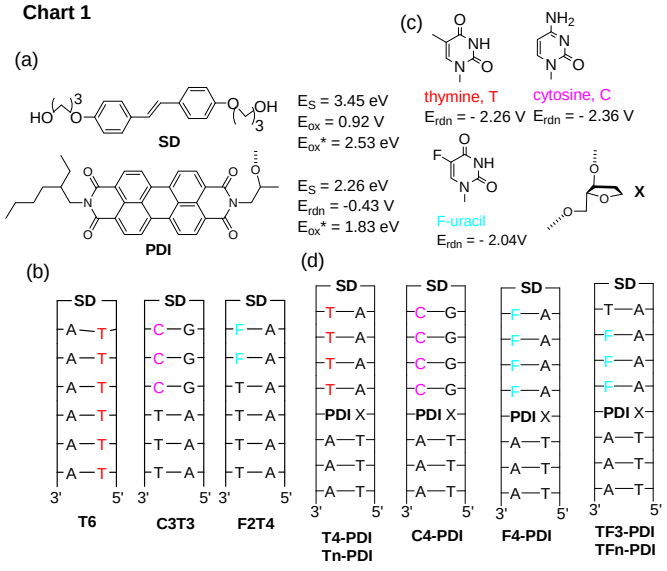

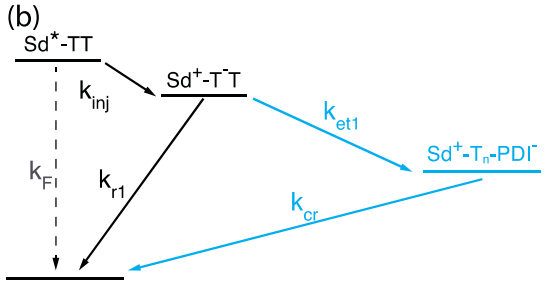

Scheme 1. Mechanism for e-injection and recombination in T6 (black) and for e-transport in Tn-PDI (blue).

Efficient Hot Electron Transer by a Plasmon Induced Interfacial Charge Transfer Transition in CdSe-Au Nanorod Heterostructures

Kaifeng Wu[1], Jinquan Chen[1], James B McBride[2] and Tianquan Lian[1]
[1]Department of Chemistry, Emory University, Atlanta, Georgia 30322
[2]Department of Chemistry, The Vanderbilt Institute of Nanoscale Science and Engineering, Vanderbilt University, Nashville, Tennessee 37235, USA

Surface plasmon resonance (SPR) has been used to improve the efficiency of photovoltaics and photocatalysis by either increasing light absorption through enhanced local fields near the metal nanostructures, or by plasmon-induced charge transfer from the excited metal. So far, all reported plasmon-induced charge-separation processes are believed to follow a conventional plasmon induced hot electron transfer (PHET) mechanism (Scheme 1A), in which the dephasing of the collective motion of many electrons in a plasmon leads to the formation hot electron-hole pairs within the metal (few to 10s femtosecond), which is followed by PHET into adjacent semiconductors or molecules. Unfortunately, the efficiency of PHET is small due to small hot electron population and competition of PHET with electron relaxation through rapid electron-electron scattering in the conduction band (CB) of metal (~100s fs).

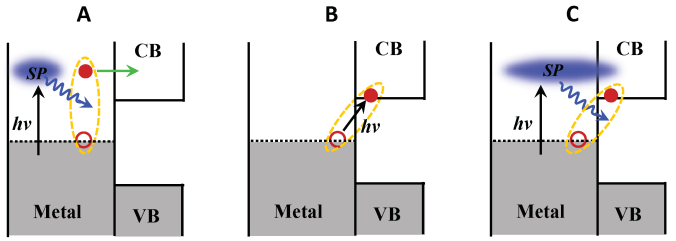

Scheme 1. Metal-to-semiconductor hot-electron transfer pathways. A) Convention plasmon induced hot electron transfer (PHET), B) Direct interfacial charge transfer transition (DICTT), C) Plasmon induced interfacial charge transfer transition (PICTT).

One approach to improve the metal-to-semiconductor hot-electron transfer efficiencies is to create a direct metal-to-semiconductor interfacial charge-transfer transition (DICTT) that can be directly excited to promote an electron from metal into semiconductor CB (Scheme 1B). However, these interfacial transitions are often too weak compared with bulk metal transitions or plasmon bands and cannot be an efficient light-harvesting pathway. Ideally, a desirable photoinduced hot-electron transfer pathway should combine the strong light absorbing power of plasmonic transitions with superior charge separation properties of direct interfacial charge transfer transition, as shown in Scheme 1C. In this plasmon-induced metal-to-semiconductor interfacial charge transfer transition (PICTT) pathway, the metal plasmon serves as a light absorber, but strong inter-domain coupling and mixing of the metal and semiconductor levels leads to a new plasmon decay pathway, the direct generation of an electron in the semiconductor and hole in the metal domains. We proposed and experimentally demonstrated this PICTT pathway in colloidal quantum confined CdSe-Au nanorod (NR) heterostructures, in which strong Au-CdSe interactions led to strong damping of the plasmon band of the Au tip and highly efficient plasmon induced Au-to-CdSe charge separation with > 24% quantum efficiencies.[1] In this poster, we will present data to support this model and discuss the requirement and generality of the PICTT pathway.

Reference. 1. K. Wu, J. Chen, J. R. McBride, T. Lian, "Efficient hot-electron transfer by a plasmon-induced interfacial charge-transfer transition", ***Science*** (2015), 349 (6248): 632.

Electron/Hole Selectivity in Organic Semiconductors for Solar Energy Conversion

Chris Weber, Colin Bradley, D. Westley Miller, and Mark C. Lonergan
Department of Chemistry and Biochemistry
University of Oregon
Eugene, OR 97403

The selective collection of electrons or holes at an interface with an absorber, either by chemical or electrical means, is a necessary step in the direct conversion of solar energy into fuels or electricity. Organic semiconductors are being widely investigated as carrier selective contacts in photovoltaics based on organic bulk heterojunction, methylammonium lead halide perovskite, and more traditional absorber materials (e.g. Si). The goal of our work is to develop fundamental understanding of selectivity, recombination, and related phenomena at organic semiconductor contacts (OSCs). The work is underpinned by a well-defined model of carrier selectivity and recombination, rooted in fundamental parameters of charge transfer at semiconductor interfaces, and the main experimental platform (Fig. 1) makes possible the simultaneous measurement of both electron and hole processes in exactly the same OSC under conditions relevant for solar energy conversion

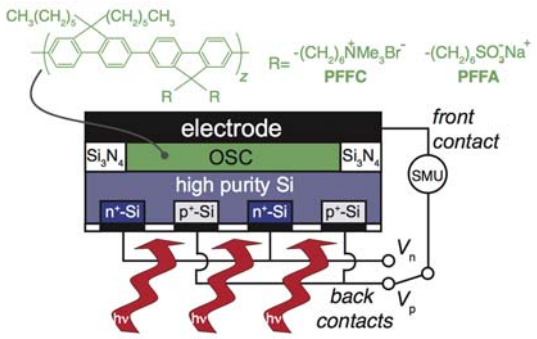

Figure 1 - Schematic of silicon interdigitated back contact solar cell, which is being used as a platform for studying the charge selectivity and recombination characteristics of organic semiconductor contacts such as the poly(fluorene) polyelectrolytes shown.

As one example of our work, we measured how thin interfacial layers of anionic versus cationic polyfluorenes (PFFA and PFFC) affect recombination and selectivity by using them as a third contact to the silicon interdigitated back contact (IBC) solar cell (Fig 1). The open-circuit voltage between the interfacial layer and either the n^+ or p^+ back contact of the IBC cell (V_N or V_P) are measured, also as a function of temperature. Changes in recombination at the interface cause the magnitudes of both V_N and V_P to either go up or down together while changes in selectivity cause one to go up and the other down. This can be quantified by comparing the sums and differences of V_N and V_P to numerical simulations to measure changes in a recombination parameter ($R = J_{on} J_{op}$) and selectivity parameter ($S = J_{op} / J_{on}$). Here, J_{on} and J_{op} are the exchange current densities for electrons and holes at the interface. These results demonstrate that PFFC (PFFA) modifies the PEDOT contact to silicon by lowering R four (six) orders of magnitude and the hole selectivity S by thirteen (five) orders magnitude with a 0.29 V (0.12 V) change in barrier height dominating any charge transfer velocity asymmetry in determining the selectivity.

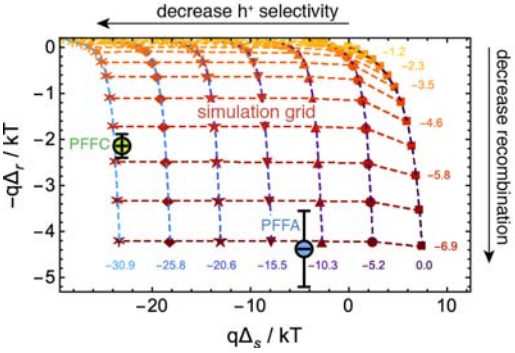

Figure 2 - Comparison of IBC solar cell measurements to COMSOL numerical simulations showing how interfacial layers of PFFA and PFFC modify the silicon / PEDOT interface.

Gains and Losses in PbS Quantum Dot Solar Cells with Submicron Periodic Grating Structures

Yukihiro Hara,† Abay Gadisa,† Yulan Fu,† Timothy Garvey,† Kristina T. Vrouwenvelder,‡ Chris W. Miller,† Jillian L. Dempsey,‡ Rene Lopez†

† Department of Physics and Astronomy University of North Carolina at Chapel Hill,
‡ Department of Chemistry, University of North Carolina at Chapel Hill,
Chapel Hill, NC 27599, USA

Corrugated structures are integral to many types of photo-electronic devices, used essentially for the manipulation of optical energy inputs. Here, we have investigated the gains and losses incurred by this microscale geometrical change. we have employed nanostructured electrode gratings of 600 nm pitch in PbS colloidal quantum dot (PbS-CQD) solar cells and investigated their effect on photovoltaic properties (fig1). Solar cells employing grating structure achieved a 32 % and 20 % increase in short-circuit current density (Jsc) and power conversion efficiency, respectively, compared to non-structured reference cells. The observed photocurrent increase of the structured devices mainly stems from the enhancement of photon absorption due to the trapping of optical energy by the grating structures. This optical absorption enhancement was particularly high in the near-infrared portion of the sun spectrum where PbS-based solar cells commonly present poor absorption. We have interestingly observed that the open-circuit voltage of all the devices increase with the increase in the absorbed photon energy (at a fixed light intensity), indicating a significant shift in fermi energy level due to localization of low photon energy generated-carriers in the tail of the density of states (fig 2). We elucidate the role of the grating structure on charge dynamics and discuss the feasibility of these structures for construction of cheap and efficient photovoltaic devices.

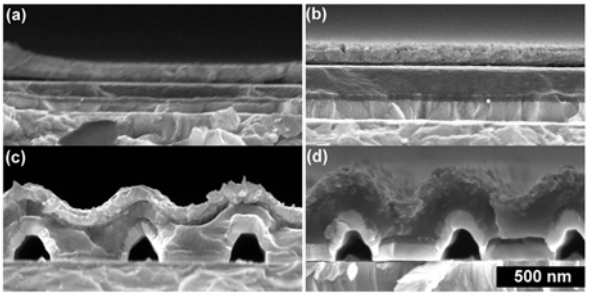

Fig. 1 SEM images of flat and grating devices with 70 nm (a and c) or 150 nm (b and d) PbS quantum dots think films

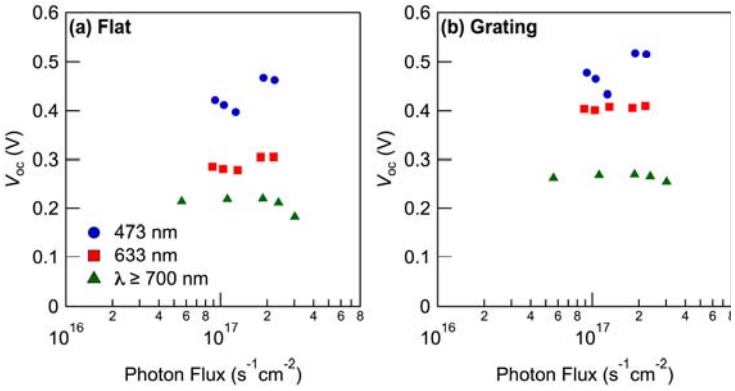

Fig. 1 Open circuit voltage (V_{oc}) as a function of photon flux with different light sources for (a) flat and (b) grating devices. Both samples have a 150 nm PbS quantum dot film.

Preparation of High Surface Area p-GaP Photocathodes and Covalent Attachment of Dyes on p-GaP(111)A: Towards a High Efficiency Sensitized Photocathode

Stephen Maldonado
Department of Chemistry
University of Michigan
Ann Arbor, MI 48109

The chief aim of this project is the development of a non-oxide, high-surface-area photocathode featuring an adsorbed sensitizer that extends the absorption bandwidth of the visible spectrum. In this capacity, this poster will present three advancements. First, we report a new step-wise preparation of p-type macroporous GaP films that allows separate control of the morphology and dopant density of the semiconductor material. Figure 1 summarizes the protocol we have developed. Intrinsic (lightly n-type) GaP is first anodically etched to create macroporous films with wall thicknesses matched to the width of the depletion region of GaP. Then a thin, continuous coating of ZnO is deposited by atomic layer deposition onto the macroporous film. An annealing step then selectively drives in Zn, thereby converting the film from n-type to p-type character. These macroporous p-GaP films represent the first high surface area platform that simultaneously possesses the abilities to operate under depletion conditions, retains high charge carrier mobilities (~100 cm^2 V^{-1} s^{-1}), and supports sensitized hole (h^+) injection from an organic chromophore. Second, we report on a chemical derivatization scheme that allows for molecular chromophores to be covalently attached to planar GaP(111)A surfaces that are free of native oxides and have a low density of electronic traps. The grafting scheme utilizes a dye featuring a pendant acyl chloride which is grafted to an oxide-free GaP surface previously functionalized with 'aniline' groups via a Grignard reaction sequence. The resultant surface demonstrates a model system to measure charge injection rates between the photoexcited chromophore and the valence band of GaP. Data will be shown that shows how the redox couple affects the efficacy of sensitized h^+ injection when the p-GaP electrode operates in depletion. Third, we present preliminary data on the sensitization of macroporous p-GaP by covalently attached organic dyes.

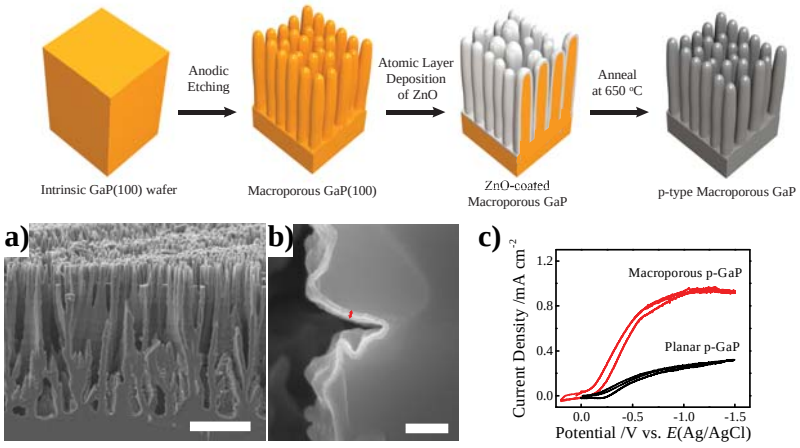

Figure 1. (top) Schematic depiction of the preparation of high aspect ratio, p-type GaP photoelectrode films via drive-in doping of a Zn-rich film deposited by atomic layer deposition. (bottom) (a) A cross-sectional electron micrograph of a macroporous n-GaP film prepared by anodic etching. Scale bar = 20 μm. (b) High magnification electron micrograph of n-GaP macropore wall coated with 50 nm ZnO film. Scale bar = 200 nm. (c) Steady-state photoelectrochemical responses of macroporous GaP film after thermal annealing to drive in Zn to convert material from n-type to p-type character.

Stiff and Soft Solvent Environments Result in Anomalous Dynamics in Ionic Liquids and Conventional Solvent Mixtures

J. C. Araque, J. Hettige, S. K. Yadav, M. Shadeck, M. Maroncelli, and C. J. Margulis
Department of Chemistry, University of Iowa, Iowa City, IA 52242

In more than one way, ionic liquids can be considered a two component system. One can think of cations and anions as subcomponents or alternatively, polar and apolar portions of the liquid can be thought of two distinct subcomponents. In a set of recent articles, we have described ionic

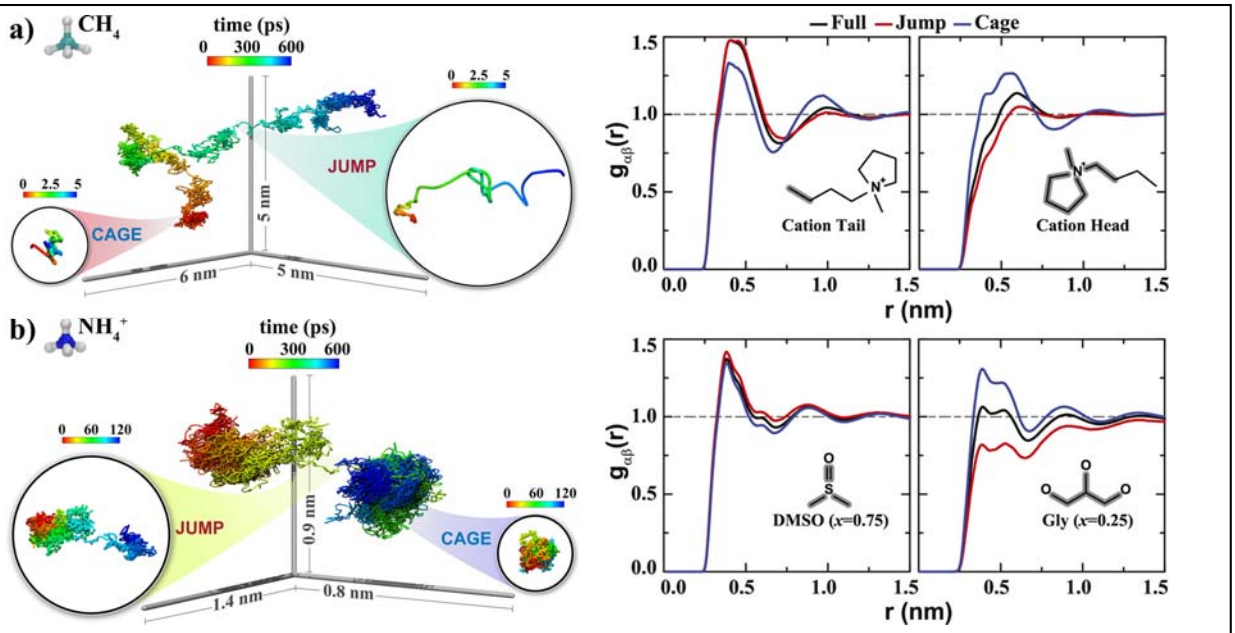

Figure 1: (Left) Translational motion in cage and jump regimes for neutral and charge solutes of small size in an ionic liquid. (Right) comparison between pair distribution functions in IL and a DMSO/Glycerol conventional solvent mixture. In both cases cages are associated with enhancement of the stiff solvent component and jump segments with its depletion. Left figures from reference J. Phys. Chem. B, 119 (40), 12727–12740, (2015) and right figures from J. Chem. Phys. 143, 134505 (2015)

liquids as composed of portions that are stiff (high electrostriction and number density) and soft (charge depleted) through which charged and neutral species must diffuse. Because of this frictional or energetic heterogeneity, the bulk viscosity is sometimes not a proper descriptor of friction and situations arise where Stokes-Einstein hydrodynamics fails. Interestingly we recently found the same phenomenon in classical mixtures of DMSO and glycerol. In this case, networks of hydrogen bonded glycerol act as the stiff solvent component whereas pockets of DMSO act as soft regions where diffusion is facile. Figure 1a (left) shows how for a small neutral molecule in IL cage and jump segments associated with stiff and soft environments occur resulting in large overall displacements. On the same time scale Fig. 1b (left) shows that a charged ion only undergoes a single jump transition. Figure 1 (right) shows that what happens in IL is not very different from the situation in the conventional solvent mixture. For a small neutral solute, jump segments are charge-depleted in the case of the IL and glycerol-depleted in the case of the conventional system. Instead, cage segments are charge enhanced in the case of IL and glycerol enhanced in the case of the conventional mixture.

Synthesis and Spectroscopy of Transition Metal-based Chromophores: Tailoring First-row Photophysics for Applications in Solar Energy Conversion

Monica Carey, Jonathan Yarranton, Sara Adelman, and James K. McCusker*
Department of Chemistry
Michigan State University
578 South Shaw Lane, East Lansing, MI 48824

Our research program continues to focus on the development of first-row transition metal-based chromophores for their use in solar energy conversions schemes. Past work has enabled the identification of a key problem associated with strongly absorbing compounds of metals such as Fe(II), namely the sub-100 fs lifetime of the metal-to-ligand charge transfer (MLCT) excited states that we believe must be accessed in order for these compounds to be useful as light harvesters in applications reliant on photo-induced electron transfer. Over the past year, we have made progress on two fronts pursuant to this goal.

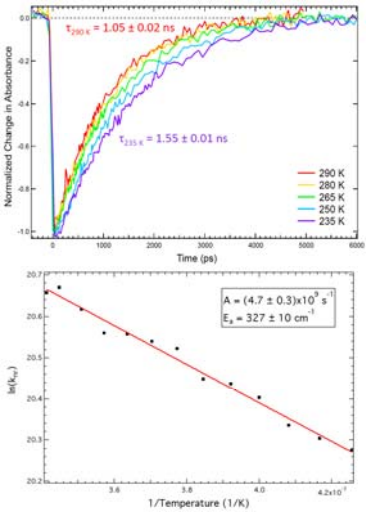

Figure 1. Variable-temperature time-resolved absorption kinetics (top) and the corresponding Arrhenius plot (bottom) for ground-state recovery acquired at 530nm on $[Fe(bpy)_3]^{2+}$ in CH_3CN solution following ^{1}MLCT excitation at 485nm.

1. Variable-temperature ultrafast time-resolved spectroscopy. As part of our effort to identify the nature of the reaction coordinate responsible for the rapid conversion from the MLCT to ligand-field (LF) state manifolds of Fe(II) chromophores, we have successfully incorporated a variable-temperature cryostat into our femtosecond time-resolved absorption spectrometer. The objective is to acquire variable-temperature relaxation rate data that will enable us to determine the reorganization energy associated with the MLCT-to-LF transition; when coupled with DFT and TD-DFT calculations, the vibrational modes associated with this conversion will be identified and that information used to synthetically reengineer the chromophore to interfere with excited-state evolution out of the charge-transfer state. The first data set acquired with this new set-up are shown in Figure 1 and represents ground-state recovery dynamics of $[Fe(bpy)_3]^{2+}$ following MLCT excitation and conversion to the lowest-energy, $^5T_2$ excited state. To our knowledge, this represents the first quantitative assessment of the activation energy associated with this process for this well-studied chromophore. Additional data acquired on synthetic variants of this and other systems will be presented.

2. Synthetic modification of $[Fe(dcpp)_2]^{2+}$: Inverting the LF and CT-state energies. On a second front, we have continued our efforts to modulate the electronic structure of the new compound we reported on previously, $[Fe(dcpp)_2]^{2+}$ (where dcpp is 2,6-(2-carboxypyridyl)-pyridine. This ligand presents a ligand-field strength to Fe(II) comparable to CN^-, yet exhibits a maximum in its MLCT absorption envelope at 610nm. The combination of these factors significantly reduced the energy gap between the lowest energy MLCT state and the lowest-energy ligand-field state. Recent progress in pushing this motif toward the desired energy inversion point (i.e., to where the relative energies of these two excited states are swapped) will be presented.

Electron Transfer Dynamics in Efficient Molecular Solar Cells

Ryan M. O'Donnell, Tim Barr, Brian DiMarco and Gerald J. Meyer
Department of Chemistry
University of North Carolina at Chapel Hill
Chapel Hill, NC 27599

An objective of this Department of Energy supported research is to provide new mechanistic insights into surface mediated photochemical reactions relevant to solar energy conversion. In this past three years this research has focused on iodide photo-redox chemistry and on the role surface electric fields play on such chemistry at molecular-semiconductor interfaces. The research is fundamental in nature with relevance to applications in dye-sensitized solar cells as well as the storage of solar energy in the form of chemical bonds.

This poster presentation will focus on electric fields generated at dye-sensitized TiO_2 interfaces by excited state injection and/or ion surface adsorption. To accomplish this the sensitizer $[Ru(dtb)_2(dcb)]^{2+}$, where dtb is 4,4'-di-*tert*-butyl-2,2'-bipyridine and dcb is 4,4'-dicarboxylic acid-2,2'-bipyridine, was anchored to mesoporous TiO_2 thin films and characterized by visible absorption and photoluminescence spectroscopies in 0.1 M Na^+, Li^+, Mg^{2+}, and Ca^{2+} perchlorate acetonitrile solutions on nanosecond and longer time scales. Relative to neat acetonitrile, the presence of these electrolyte cations induced a red shift in the metal-to-ligand charge transfer (MLCT) absorption of $Ru(dtb)_2(dcb)/TiO_2$, the magnitude of which increased with increasing valence of the metal cation. Global analysis, spectral modeling, and single wavelength kinetic analysis revealed that two dynamic processes were operative after excited state injection: 1) charge recombination, $Ru^{III}(dtb)_2(dcb)/TiO_2(e^-) \rightarrow Ru^{II}(dtb)_2(dcb)/TiO_2$, and 2) an electric field created by the injected electron. The ability of global analysis, specifically the decay-associated spectra, to kinetically and spectrally resolve these two processes was assessed. Interestingly, there was no evidence for charge screening of the electric field by electrolyte cations, behavior that is very different from that observed on the longer time scales of charge recombination to redox mediators in the external electrolyte.

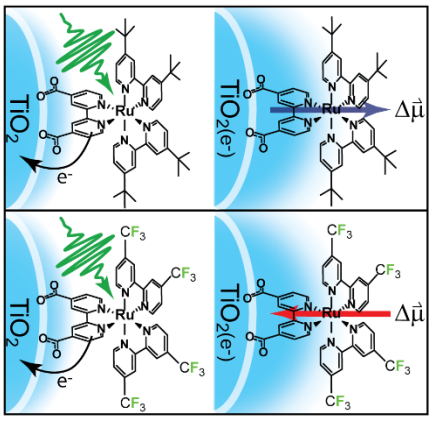

The studies of $Ru(dtb)_2(dcb)/TiO_2$ were complimented by a comparative analysis with $Ru(dfm)_2(dcb)/TiO_2$ where dfm is 4,4'-$(CF_3)_2$-2,2'-bipyridine. The ground state dipole of this sensitizer is parallel to the surface electric field resulting in spectral shifts that are in the opposite direction to that observed for $Ru(dtb)_2(dcb)/TiO_2$ as is shown schematically. Excited state behavior of these sensitizers was quantified in large > 10 MV/cm electric fields generated with a forward bias in photoelectrochemical cells. Interestingly, as the quasi-Fermi level of the sensitized TiO_2 was raised, the photoluminescence intensity from the sensitizers first increased and then decreased. To our knowledge, excited state quenching in large electric fields has not been previously observed at dye-sensitized TiO_2, but is known to occur in OLEDs. Possible mechanisms for this excited state reactivity will be proposed and discussed.

Self-Assembled Molecular p/n Junctions on Mesoporous *nano*ITO Electrodes

Byron H. Farnum, Kyung-Ryang Wee, Bing Shan, Thomas J. Meyer
Department of Chemistry, University of North Carolina at Chapel Hill, Chapel Hill, NC 27599

A novel strategy for long-lived photoinduced redox separation is presented in which self-assembled donor-chromophore-acceptor assemblies were prepared on the surfaces of mesoporous, transparent conducting indium tin oxide nanoparticle electrodes (*nano*ITO). Phosphonate-derivatized chromophores ($[Ru^{II}(4,4'\text{-}(PO_3H_2)_2\text{-}2,2'\text{-bipyridine})_2(2,2'\text{-bipyridine})]^{2+}$; RuP_2^{2+}), electron acceptors ($[N,N'\text{-}((CH_2)_2PO_3H_2)_2\text{-}4,4'\text{-bipyridinium}]^{2+}$; MV^{2+}), and electron donors ($N,N,N',N'\text{-}((CH_2)_3PO_3H_2)_4\text{-}4,4'\text{-dianiline}$; DA) were assembled by a layer-by-layer loading procedure in conjunction with $ZrOCl_2$ to generate Zr^{IV}-phosphonate linked molecular assemblies. By simply varying the order of addition of individual molecular units to the *nano*ITO surface, we have prepared a molecular photoanode (*nano*ITO|-MV^{2+}-RuP_2^{2+}-DA), with photoinduced electron transfer directed toward the electrode surface, and a molecular photocathode (*nano*ITO|-DA-RuP_2^{2+}-MV^{2+}), with photoinduced electron transfer directed away from the electrode surface. Nanosecond transient absorption and steady state photolysis measurements show that the electrodes function microscopically as molecular analogs of semiconductor p/n junctions with visible light excitation of the chromophore resulting in incredible redox separated lifetimes of milliseconds-to-seconds, depending on the applied potential.

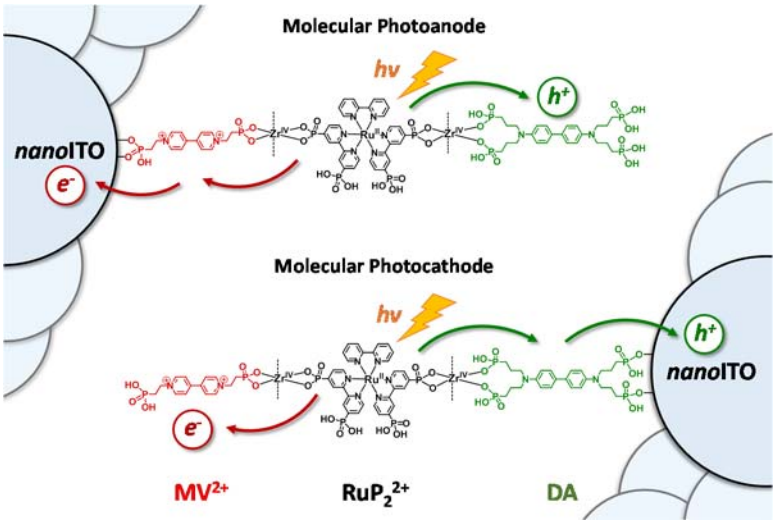

Photoanode:

*nano*ITO|-MV^{2+}-RuP_2^{2+}-DA + *hv* → *nano*ITO($\boldsymbol{e}^-$)|-MV^{2+}-RuP_2^{2+}-$DA^{+\bullet}$($\boldsymbol{h}^+$) φ = 16%

*nano*ITO($\boldsymbol{e}^-$)|-MV^{2+}-RuP_2^{2+}-$DA^{+\bullet}$($\boldsymbol{h}^+$) → *nano*ITO|-MV^{2+}-RuP_2^{2+}-DA τ = 5.6 s

Photocathode:

*nano*ITO|-DA-RuP_2^{2+}-MV^{2+} + *hv* → *nano*ITO($\boldsymbol{h}^+$)|-DA-RuP_2^{2+}-$MV^{+\bullet}$($\boldsymbol{e}^-$) φ = 9%

*nano*ITO($\boldsymbol{h}^+$)|-DA-RuP_2^{2+}-$MV^{+\bullet}$($\boldsymbol{e}^-$) → *nano*ITO|-DA-RuP_2^{2+}-MV^{2+} τ = 26 ms

These results build on our previous work of photoinduced electron transfer reactions at the surfaces of mesoporous conductive metal oxide electrodes to show that with a simple toolkit of molecular components, the direction of electron transfer, transiently stored redox potential, and lifetime of redox separate states can be tuned and controlled. Additionally, these results point to a new, molecular-based strategy for dye-sensitized solar energy conversion based on molecular excited states and electron transfer acceptors/donors on the surfaces of transparent conducting oxide nanoparticle electrodes rather than wide band gap, n-type or p-type semiconductors.

Singlet Fission

Josef Michl [b) a)], Thomas F. Magnera [b)], Paul I. Dron [b)], Eric A. Buchanan [b)], Jin Wen [a)], Zdeněk Havlas [a) b)]

a) Institute of Organic Chemistry and Biochemistry, ASCR, 166 10 Prague, Czech Republic
b) Department of Chemistry and Biochemistry, University of Colorado, Boulder, CO, USA

Our goal has been a first principles formulation of structural design rules for singlet fission sensitizers, both the chromophores and their mutual arrangement in space. At the outset of our work, we pointed out that biradicaloids such as isobenzofurans and indigoid heterocycles are likely candidates for isoergic or exoergic singlet fission. We have continued computational search for good candidates and followed it up with synthesis and photophysical studies (some of the latter in collaboration with Justin Johnson's group at NREL). In addition to isobenzofurans and cibalackrot (an indigoid), we have prepared and examined aminoquinones. We are looking for very small molecules, for which very high quality calculations of molecular dynamics of the singlet fission process would then be feasible, and for light-fast molecules that would be practically useful.

We have derived simplied formulas for the optimization of the spatial relation between two neighboring chromophores that involve both a maximization of the square of the electronic matrix element for singlet fission, $|T_{RP}|^2$, and a minimization of ΔE, the Davydov splitting induced reduction of its exothermicity. This was achieved by using the HOMO-LUMO model in which only the frontier orbitals on each chromophore are considered explicitly, and a series of physically justifiable approximations that have been numerically tested against an exact evaluation of $|T_{RP}|^2$ for dozens of favorable dimer geometries. The formulas are so simple that they permit an easy complete search of the full six-dimensional space of the mutual spatial relation between two rigid bodies. This involves an evaluation of $|T_{RP}|^2$ and ΔE at tens or hundreds of millions of dimer geometries. The most important ingredients needed for the evaluation are the molecular orbital coefficients for HOMO and LUMO and the overlaps between the atomic orbitals on one and the other chromophore. Qualitative results can often be guessed by inspection. Limiting cases, such as two identical chromophores, or one chromophore that is a strong electron donor and another that is a strong electron acceptor, yield particularly simple results. The number of significant local maxima for a pair of ethylene molecules, taken as a simple model, is in the hundreds. Additional chromophores are being tested now. Ultimately, a simultaneous consideration of a larger number of chromophores may be required, but has not yet been attempted.

Molecular Photoelectrocatalysts for Hydrogen Evolution

Matthew B. Chambers, Catherine L. Pitman, Alexander J. M. Miller
Department of Chemistry
University of North Carolina at Chapel Hill
Chapel Hill, NC 27599-3290

Molecular species that can directly couple visible light absorption and chemical catalysis offer an intriguing approach to solar fuel synthesis. We recently showed that $[Cp^*Ir(bpy)H]^+$ is a promising photoelectrocatalyst that evolves H_2 from water across a wide pH range with high Faradaic and quantum efficiency.[1] The key step is light-triggered release of H_2 from $[Cp^*Ir(bpy)H]^+$, either in water (Figure 1A) or in organic solvent with added acid. A mechanistic study of photochemical H_2 release has revealed a surprising, exceptionally efficient bimolecular excited state electron transfer (self-quenching) pathway, guiding the development of future catalysts.

Illumination of $[Cp^*Ir(bpy)H][PF_6]$ in the presence of excess CD_3CO_2D or $[Et_3ND][Cl]$ in CD_3CN with a 460 nm LED array initially produces *only* H_2, followed later by HD, indicating a bimetallic pathway wherein two Ir–H species couple to release H_2. The quantum yield is independent of acid strength and acid concentration, but shows a first order dependence on the concentration of $[Cp^*Ir(bpy)H]^+$, in accord with a bimetallic process. At hydride concentrations above 15 mM, photochemical H_2 release proceeds with essentially *unity quantum yield* (Figure 1B). Time-resolved fluorescence spectroscopy is consistent with a bimolecular self-quenching mechanism in which the excited state $[Cp^*Ir(bpy)H]^{+*}$ reacts with a ground state molecule of $[Cp^*Ir(bpy)H]^+$ with a rate constant, k_q = 3.8 x 10^9 M^{-1} s^{-1}. Self-quenching studies of $[Cp^*Ir(bpy)D]^+$ reveal no measureable kinetic isotope effect ($k_{q,H}/k_{q,D}$ = 1), suggesting that the Ir–H bond does not break during the self-quenching step. Furthermore, the self-quenching rate constant does not vary with acid concentration. Taken together, the data indicate that the excited state $[Cp^*Ir(bpy)H]^{+*}$ undergoes rate-limiting bimetallic electron transfer, followed by rapid bimetallic H_2 release (Figure 1C). The unusual photochemical H_2 release pathway is guiding photoelectrocatalyst design. For example, bimolecular electron transfer should be favored by polar media, and indeed the photochemical quantum yield is higher in the presence of 0.1 M electrolyte.

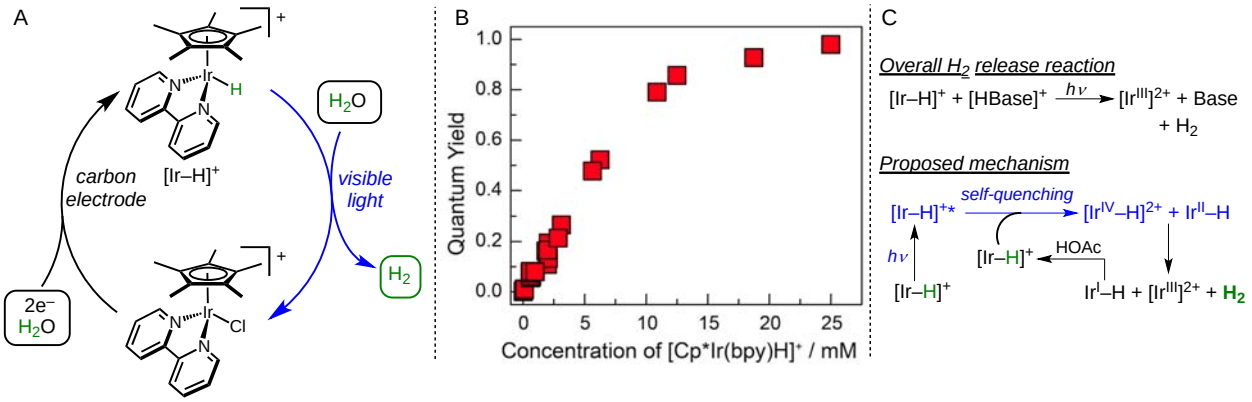

Figure 1. Photoelectrocatalytic H_2 evolution cycle (A), and quantum yield (B) of H_2 release (C).

[1] Pitman, C. L.; Miller, A. J. M. *ACS Catalysis* **2014**, *4*, 2727.

Toward Photochemical Water Oxidation in Metal Organic Frameworks

Maza, William A; Lin, Shaoyang; Ahrenholtz, S.R.; Zhu, J.; Usov, P.; Morris, A.J.
Chemistry
Virginia Tech
Blacksburg, VA 24060

My research program is centered on the exploration of metal organic framework (MOF) thin film assemblies capable of photo-induced heterogeneous water oxidation. Specifically, the proposed work aims to provide a fundamental understanding of MOF materials utilized in photo-induced electron transport processes to elucidate the design constraints of such catalysts. Current efforts focus on the study of two MOF catalyst candidates – (1) a Ru(terpy = terpyridine)(bpy = bipyridine)(dcbpy = 5,5′-dicarboxy-2,2′-bipyridine)-doped UiO-67 framework (zirconium nodes), and (2) PCN-224-Ni (a nickel porphyrin-based zirconium MOF). We also have an active program in the exploration of light harvesting and energy transfer in MOFs. Preliminary findings of each are provided below:

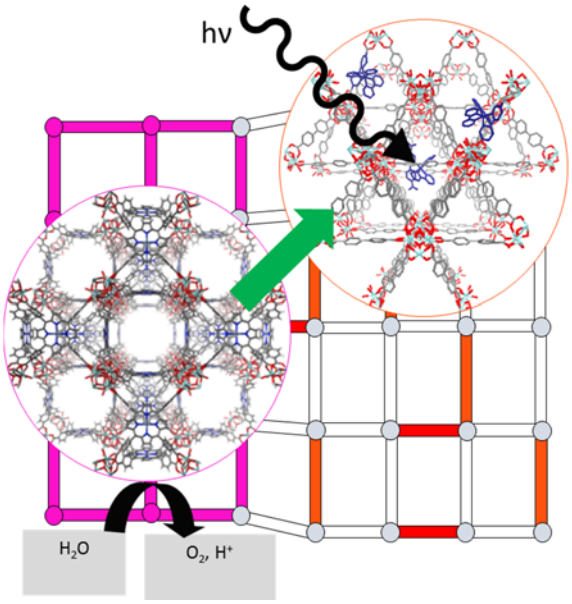

Ru(terpy)(bpy)(dcbpy)-doped UiO-67. A morphologically homologous Ru(terpy)(bpy)(dcbpy)-doped UiO-67 analog was synthesized and characterized. Interestingly, at low loading the observed current varies linearly with scan rate (similar to a surface adsorbed monolayer). However, at higher loadings, the current varies linearly with the square root of scan rate. We hypothesize that this is due to the creation of redox-hopping percolation pathways and may be a potential signature for electrochemical reactivity *in*-MOF.

PCN-224-Ni. Solvothermally deposited thin films of PCN-224-Ni were synthesized and characterized. The propensity of the films for catalytic water oxidation was confirmed. Cyclic voltammetry and bulk electrolysis confirm the oxidation of water by the thin film. The exchange current density as determined via Tafel analysis was ~10-11 A/cm^2. The TOF (assuming every porphyrin is catalytically active) was 5.94 h^{-1}. Interestingly, the Faradaic efficiency increased to 79% vs. 46% for the homogeneous catalyst in solution. Efforts are now directed to determination of mechanism (is molecular function conserved?) and electroactive porphyrin density.

Light Harvesting/Energy Transfer. The second component of the proposed work is to photo-initiate the aforementioned oxidative chemistry. To this end, we have explored MOFs composed of the water-stable UiO backbone with ruthenium polypyridyl ligands incorporated for light harvesting, energy transfer, and photo-induced charge separation at catalytic interfaces. Current efforts include the exploration of encapsulated solvent dielectric, Ru(dcbpy)(bpy) counter ion, degree of spin-orbit coupling (singlet character to triplet state), and lifetime on the efficiency of energy transfer.

Photocatalytic Water Oxidation at the Semiconductor-Aqueous Interface and Beyond…

James T. Muckerman
Chemistry Division
Brookhaven National Laboratory
Upton, NY 11973-5000

The GaN/ZnO alloy functions as a visible-light photocatalyst for splitting water into hydrogen and oxygen when coupled with a co-catalyst for proton reduction. We have investigated the microscopic structure of the aqueous interfaces of the of the $(10\bar{1}0)$ and $(1\bar{2}10)$ surfaces of the 1:1 GaN/ZnO alloy and compared them with the $(10\bar{1}0)$ aqueous interfaces of pure GaN and ZnO.[1] The calculations were carried out using first-principles density functional theory based molecular dynamics (DFT-MD). Water adsorption on all the surfaces is substantially dissociative through acid/base chemistry involving protonation of surface anions and hydroxylation of surface cations from dissociated water molecules. We further investigated the water oxidation mechanism on the prototypical GaN surface using a combined ab initio molecular dynamics and molecular cluster model approach taking into account the role of water dissociation and hydrogen bonding within the first solvation shell of the hydroxylated surface.[2] We further examined sequential PCETs, with the proton transfer (PT) following the electron transfer (ET), and found that photo-generated holes localize on surface –NH sites, and the calculated free-energy changes indicate that PCET through –NH sites is thermodynamically more favorable than –OH sites. However, proton transfer from –OH sites with subsequent localization of holes on oxygen atoms is kinetically favored owing to hydrogen bonding interactions at the GaN–water interface. The catalytic reaction proceeds through a sequence of four proton-coupled electron-transfer steps starting with *OH and then through $*O^{\bullet -}$, $*OOH^{-}$, and $*O_2^{\bullet -}$ before returning to the initial state by the elimination of O_2 and the addition of H_2O accompanied by the dissociation of a proton.

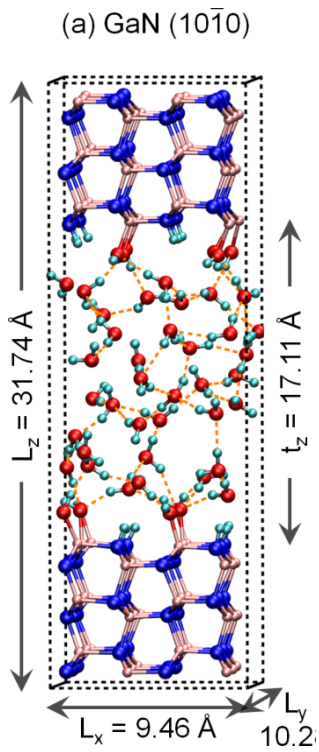

More recently, we have been exploring the analogous dissociation of water molecules at the rutile (110) and anatase (101) surfaces as well as hole trapping in the bulk semiconductor and at its aqueous interface. We find extensive water dissociation on both surfaces (ca. 30 to 40%) that involves either the direct or bridging-water mediated proton transfer from a Ti-bound water molecule to a bridging oxygen surface site. For rutile, the direct process dominates at room temperature, but both processes are triggered by a hydration layer fluctuation.

(1) Kharche, N.; Hybertsen, M. S.; Muckerman, J. T. "Computational Investigation of Structural and Electronic Properties of Aqueous Interfaces of GaN, ZnO, and GaN/ZnO Alloy," Phys. Chem. Chem. Phys. **2014**, 16, 12057-12066.

(2) Ertem, M. Z.; Kharche, N.; Batista, V. S.; Hybertsen, M. S.; Tully, J. C.; Muckerman, J. T. "Photo-induced water Oxidation at the Aqueous GaN (10$\bar{1}$0) Interface: Deprotonation Kinetics of the First Proton-Coupled Electron-Transfer Step," *ACS Catal.* **2015**, *5*, 2317-2323.

Unified Treatment of Electron Transfer Energetics and Coupling in Terms of Electron Detachment and Attachment

Marshall D. Newton
Department of Chemistry
Brookhaven National Laboratory
Upton, NY 11973

The nonadiabatic electron transfer (ET) rate constant can be expressed as the product of an electronic prefactor $(2\pi/\eta)$ $(H_{DA})^2$ and an activation factor (the so-called Franck-Condon Weighted Density of States (FCWD)). As shown previously (JPC B 119, 14728 (2015)), the FCWD for DA → D^+A^- can be expressed in terms of the vertical gaps (wrt the electron at infinity) for electron detachment, **d** (from D) and attachment, **a** (at A) at the ET transition state (TS). Here, we focus on a unifying feature: namely, that the same **d/a** TS picture yields the vertical TS gaps entailed in bridge-mediated (DBA) superexchange.

The electronic energies for the relevant states in the chosen example (initial [**1** (DA or DBA)], final [**2** (D^+A^-)] and intermediate virtual d and a states [**3** (D^+A) and **4** (DA^-) or **3'** (D^+B^-A) and **4'** (DB^+A^-)] are shown schematically in Figures 1 and 2 (below). The relevant state energies ($V^{\mathbf{i}}$) and vertical gaps ($\Delta V^{\mathbf{ij}}$) are expressed, respectively, as quadratic and linear functions of the two 'progress parameters' m_D and m_A (displayed in Figure 3), with the 'conventional' ET reaction coordinate given as $\Delta V^{\mathbf{12}}$. In evaluating the FCWD, due account must be taken of coulombic interactions between the sites (D, A, or B). This is carried out in terms of the normalized probability density of the initial state ($P^{\mathbf{1}}$) wrt to the independent coordinates ($\Delta V^{\mathbf{13}}$) and ($\Delta V^{\mathbf{32}}$) subject to 'resonance':

$$\mathrm{FCWD} = \int_{-\infty}^{+\infty} P^{\mathbf{1}}(\Delta V^{\mathbf{13}}, \Delta V^{32})\, \delta(\Delta V^{\mathbf{13}} + \Delta V^{\mathbf{32}})\, d(\Delta V^{\mathbf{13}})\, d(\Delta V^{\mathbf{32}})$$

In the classical limit this expression is found to yield the traditional Marcus expression.

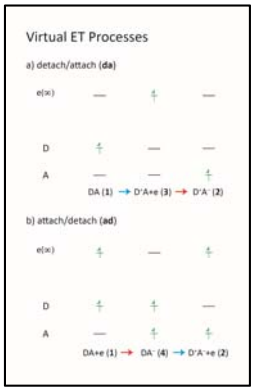

Fig. 1. D/A levels

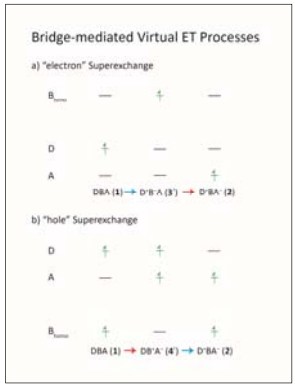

Fig. 2. DBA levels

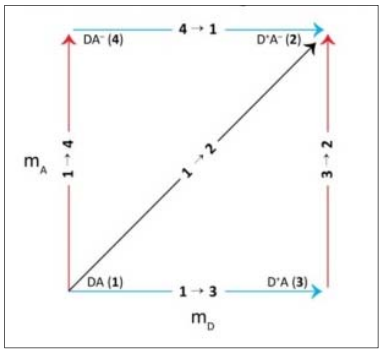

Fig. 3. D/A progress parameters

Unifying Heterogeneous and Homogeneous OER and ORR Catalysis

Casey Brodsky, Andrew M. Ullman and Daniel G. Nocera
Department of Chemistry and Chemical Biology
Harvard University
Cambridge, MA 02138

An experimental approach to begin unifying heterogeneous and homogeneous catalysis at the molecular level has been designed. Cobaltate clusters (Co-OEC) comprising a heterogeneous thin film are the linchpin between extended cobalt oxides and molecular cobalt oxides (Figure 1).

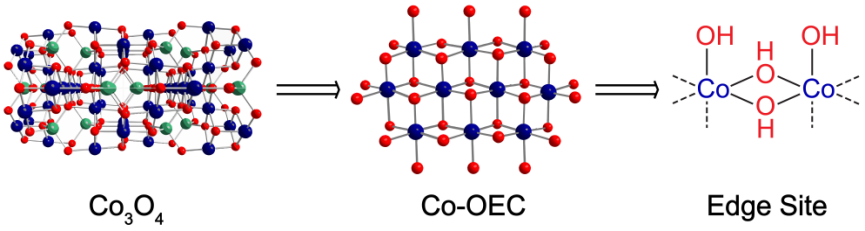

Figure 1. Dicobalt edge site is the dimensionally reduced active site of Co_3O_4 and Co-OEC.

A dogma of heterogeneous systems is that "edges" matter in promoting catalytic transformations. We provide a rationale for such dogma by showing that oxygen evolution reaction (OER) in cobaltic oxides likely occurs at a dimensionally reduced dicobalt edge site. Edge site reactivity is clearly revealed by differential electrochemical mass spectrometry (DEMS). This technique identifies the distribution of ^{18}O in evolved dioxygen from an ^{18}O labeled Co-OEC catalyst (in $H_2{}^{16}O$) under the exact electrochemically-driven conditions of OER as a function of applied potential. The observation of $^{36}O_2$ produced from an ^{18}O Co-OEC in ^{16}O H_2O can only occur from direct intramolecular coupling between terminal oxygen atoms ligated to cobalt at the edge sites. To more deeply address the nature of edge site chemistry, we have prepared a dicobalt complex wherein a diamond $Co_2(OH)_4$ core is stabilized by the six coordinate dipyridyl naphthyridine ligand (DPEN). We have identified edge site equilibrium reactions that deliver the open coordination sites needed for the intramolecular coupling reaction identified by the DEMS experiment. The kinetics of phosphate (P_i) and borate (B_i) binding to dicobalt centers of the DPEN complex differ by many orders of magnitude due to facile coordination chemistry between boric acid, $B(OH)_3$, and the edge of the cobalt dimer. Consistent with this observation, an inverse dependence of the activity of Co-OECs on [B_i] establishes the necessity of a syn configuration of the terminal hydroxo moieties of the diamond $Co_2(OH)_4$ core edge site. Together, the results of the authentic Co-OEC and dicobalt model compound demonstrate the important role of edge sites in controlling the OER activity of cobalt-oxide catalysts.

We have expanded our studies to also examine the microscopic reverse of OER, the oxygen reduction reaction (ORR). We derive a thermodynamic cycle that gives access to the standard potential of O_2 reduction to H_2O. The model shows that ORR selectivity at the Co edge site is largely dictated by the effective overpotential. The model is general and rationalizes the faradaic efficiencies reported for many ORR catalytic systems.

Design Principles for Colloidal Semiconductor Nanocrystals through Surface Chemistry Modification

Daniel M. Kroupa,[1,2] Márton Vörös,[3,4] Elisa M. Miller,[1] Brett McNichols,[5] Nicholas Brawand,[4] Greg Pach,[1,2] Alan Sellinger,[5] Giulia Galli,[3,4] Arthur J. Nozik,[1,2] Matthew C. Beard[1*]

1. Chemical and Material Sciences Center, National Renewable Energy Laboratory, Golden, Colorado 80401.

2. Department of Chemistry and Biochemistry, University of Colorado, Boulder, Colorado 80309

3. Materials Science Division, Argonne National Laboratory, Argonne, Illinois 60439

4. Institute for Molecular Engineering, University of Chicago, Chicago, Illinois 60637

5. Department of Physics, Colorado School of Mines, Golden, Colorado 80401

We present a robust solution phase ligand exchange procedure for PbS quantum dots (QDs) using an extensive library of small, aromatic molecules. These surface modified QDs serve as a model QD / ligand system to systematically study how specific surface-chemistry- related properties simultaneously affect three major QD design parameters, namely: i) broadband optical absorbance; ii) absolute band edge shifts; and iii) carrier type / doping level. During the course of this study, we establish specific QD design principles that allow us to enhance the QD broadband optical absorbance by a factor of two for a given ligand binding group, shift the absolute QD band edge energies well over 2.0 eV for a given ligand binding group, and change the carrier type of QD films from highly n-type to p-type through the modification of ligand binding group stoichiometry. Our design principles for QD / ligand material systems are supported by theoretical calculations, which can serve as a guide for future optimized material applications.

Photosensitization of Natural and Synthetic SnO_2 and ZnO Crystals with Dyes and Quantum Dots

Laurie A. King, Qian Yang, Michael L. Grossett, Zbigniew Galazka[2], Reinhard Uecker[2] and B. A. Parkinson[1]

[1]Department of Chemistry and School of Energy Resources, University of Wyoming, Laramie, Wyoming 82071, USA

[2] Leibniz Institute for Crystal Growth, Max-Born-Str. 2, 12489 Berlin, Germany

Abstract

The surface preparation and photosensitization of highly oriented natural and synthetic SnO_2 single crystals is investigated for the first time. Incident photon conversion efficiency (IPCE) spectra for SnO_2 single crystals sensitized with both CdSe quantum dots (QD) and a thiacyanine dye are measured and interpreted. We discuss the influence of crystal face and doping density on the IPCE spectral response and magnitude. Advantages of SnO_2 as a substrate for sensitization studies are also pointed out.

Lead selenide (PbSe) quantum dots (QDs) are an attractive material for application in both optoelectronic and photovoltaic devices due to the ability to tune their band gap, efficient multiple exciton generation and high extinction coefficients. Despite these attractive optical properties, PbSe QDs are quite unstable to oxidation in air. Recently there have been multiple studies detailing post-synthetic halide treatments to stabilize lead chalcogenide QDs. We exploit iodide stabilized capped PbSe QDs in a model quantum dot sensitized solar cell configuration where zinc oxide (ZnO) single crystals are sensitized using protonated cysteine as a bifunctional linker molecule. Sensitized photocurrents stable for > 1 hour can be measured in aqueous KI electrolyte that is usually corrosive to QDs. The spectral response of the sensitization extended out to 1700 nm, the farthest into the infrared yet observed. Hints of the existence of multiple exciton generation and collection as photocurrent, as would be expected in this system, are presented and discussed.

Electronic Structure of Charge Separated States in Organic Bulk-Heterojunctions: A Combined EPR and DFT Study

Oleg G. Poluektov, Jens Niklas, Lisa M. Utschig, Karen L. Mulfort, David M. Tiede
Argonne National Laboratory, Argonne, IL 60439
Kristy L. Mardis
Department of Chemistry & Physics, Chicago State University
Chicago, IL 60628

Our current research is aimed at resolving fundamental mechanisms of photochemical energy conversion and, as a long term goal, devise integrated systems that can capture, convert, and store solar energy. Solar-based technologies such as Organic Photovoltaics (OPV) convert captured photons to a useable electrochemical potential. These technologies could provide sufficient energy to satisfy the global energy demands in the near future. Understanding the charge separation and electronic structure at a molecular level is crucial for improving the efficiency of OPV materials.

To address these questions we are investigating the charge separation and stabilization mechanisms of semiconducting polymer-fullerene interfaces by employing a comprehensive suite of experimental and theoretical techniques, namely: multidimensional, multifrequency EPR spectroscopy in combination with Density Functional Theory (DFT) calculations and other computational methods. Under illumination, OPV active blends form two paramagnetic species due to photo-induced electron transfer between the conjugated polymer and the fullerene derivative. These species are the positive, P^+, and negative, P^-, polarons of the polymer and fullerene, respectively, also referred to as radical cations and radical anions. DFT calculations were used to determine the electronic structures of the fullerene anions and polymer cations (Figure 1). Magnetic resonance parameters were extracted from these calculations and the good agreement of the calculated parameters with those determined experimentally validates the DFT approach and justifies using the calculated spin density distributions of the charge separated species. Thus, we were able to obtain the delocalization length of the positive charge along the polymer chain for a number of different efficient OPV polymers, among them the high performing low bandgap polymers PCDTBT and PTB7.

In contrast to the positive polaron on the polymer, the negative polaron/charge is located on the cage of the fullerene and not delocalized between several molecules. For the first time, by the combined application of multifrequency EPR spectroscopy and DFT calculations we have acquired not only the principal values of the g-tensors for the widely used soluble derivatives of C_{60} and C_{70} fullerene ($PC_{61}BM$ and $PC_{71}BM$) but also the directions of the magnetic axes in the molecular frame. The relation of these data to the efficiency of the charge separation process in OPV is discussed.

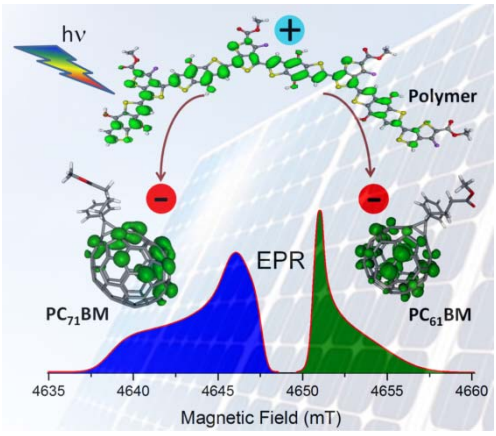

Figure 1. Delocalization of the spin densities along the polymer chain and on the soluble derivatives of fullerene as determined by high-frequency EPR and DFT calculations

Interfacial Processes at H_2O/III-V Semiconductor Surfaces under *Operando* Conditions

Xueqiang Zhang and Sylwia Ptasinska
Radiation Laboratory and Department of Physics
University of Notre Dame
Notre Dame, IN 46556

A photoelectrochemical (PEC) solar cell used for hydrogen production through water splitting offers an efficient approach to the future sustainable supply of energy. However, its performance is directly related to interfacial electronic and chemical properties of an electrolyte/photoelectrode.

III-V semiconductors exhibit many favorable properties that make them promising candidates for a photoelectrode of a PEC solar cell. Therefore our recent attention was focused on Ga- and In-based materials for photoelectrodes and their interactions with gas-phase H_2O molecules and other molecules [1-7]. We used ambient pressure X-ray photoelectron spectroscopy (AP-XPS) to track the physicochemical processes that occur on the III-V surfaces over wide ranges of pressure and temperature, thus approaching the operational conditions of PEC cells.

We were able to provide a better understanding of III-V surface chemistry at the molecular level and to observe the evolution of surface electrical properties that drive the performances of PEC devices with respect to work function, band bending, surface photovoltage effect, ionization energy, and electron affinity under *operando* conditions.

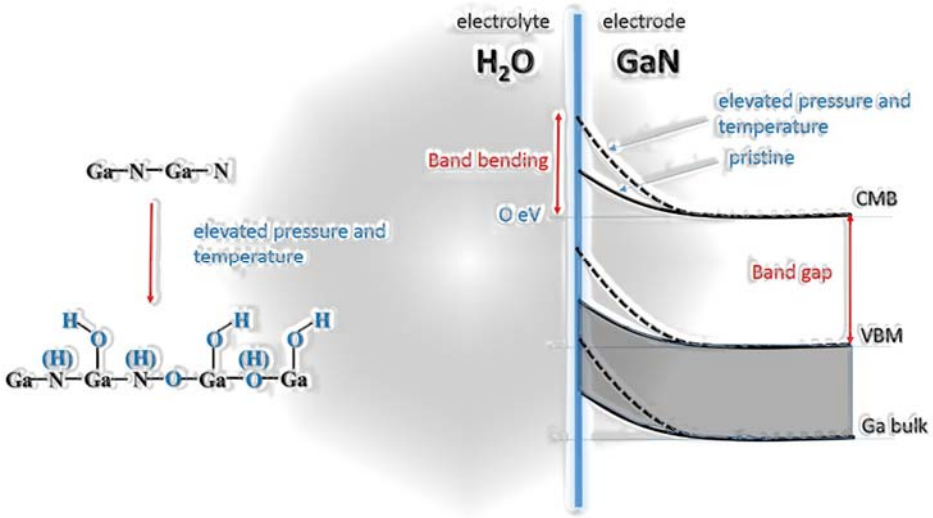

Figure. Correlation between chemical and electronic properties at the H_2O/GaN interface at the elevated pressures and tempertues.

1. X. Zhang, S. Ptasinska, Journal of Physical Chemistry C 118 (2014) 4259-4266
2. X. Zhang, E. Lamere, X. Liu, J.K. Furdyna, S. Ptasinska, Applied Physics Letters 104 (2014) 181602(1-4)
3. X. Zhang, E. Lamere, X. Liu, J.K. Furdyna, S. Ptasinska, Chemical Physics Letters 605-606 (2014) 51-55
4. X. Zhang, S. Ptasinska, Physical Chemistry Chemical Physics 17 (2015) 3909-3918
5. X. Zhang, S. Ptasińska, Journal of Physical Chemistry C 119 (2015) 262-270
6. X. Zhang, S. Ptasinska, Topics in Catalysis 59 (2016) 564-573
7. X. Zhang, S. Ptasinska, Scientific Reports (2016) accepted

Effect of Carrier Delocalization on Long-lived Free Carriers in Conjugated Polymers and Single-Walled Carbon Nanotubes

Garry Rumbles, Natalie Pace, Jessica Ramirez, Jaehong Park, Rachelle Ihly, Jeff Blackburn
Jesse Bergkamp[+], Devens Gust[+], and Obadiah Reid

Chemistry and Nanoscience Center,
National Renewable Energy Laboratory, Golden, Colorado, 80404
and
[+]Department of Chemistry and Biochemistry,
Arizona State University, Tempe, AZ 85287

An unusual, but useful, feature of electron acceptors dispersed in a conjugated polymer host is the photogeneration of high yields of charges that exhibit long lifetimes, while the initial photo-induced electron transfer step frequently occurs on a sub-100 femtosecond time-scale. An objective of this part of the solar photochemistry program at NREL is to understand these experimental observations, and to rationalize them with the photo-induced electron transfer processes of isolated molecular donor-acceptor pairs. To make these investigations we use a variety of spectroscopic techniques that includes time-resolved microwave conductivity, ultra-fast transient absorption spectroscopy, and time-resolved photoluminescence spectroscopy.

We report on two studies in media of low dielectric constant, where the long-lived nature of the separated carriers can be attributed to the delocalization of at least one of the charges. In the first system, which uses a substituted silicon phthalocyanine as the donor molecule, we show that the hole is transferred from the excited macrocycle to the crystalline region of a film of regioregular poly(3-hexylthiophene) and where it is delocalized leading to carrier yields of ~20% and lifetimes that exceed 500 ns. (Feier, H. M et al. *Advanced Energy Materials,* **2016**, DOI:10.1002/aenm.201502176)

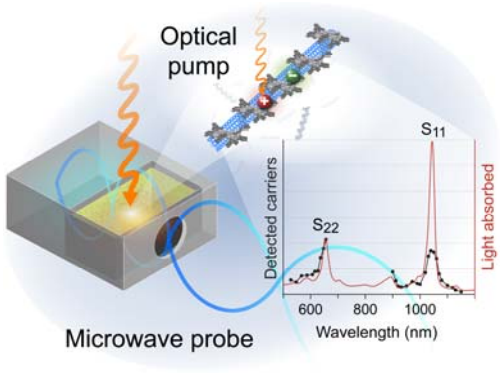

Figure – Photogenerated charges generated in a polymer-wrapped, SWCNTs dispersed in toluene, and detected using microwave absorption. Microwave abosprtion action spectrum shows a strong dependence on the excitation wavelength.

In a separate study, high yields of long-lived carriers in dilute toluene solutions of chiral-pure single-walled carbon nanotubes (SWCNTs) were again observed (Park, J. et al. *Nat. Comms.* **2015,** DOI: 10.1038/ncomms9809). The carriers were generated by direct photoexcitation of the carbon nanotube and exhibited a lifetime of ~160 ns, and an upper limit of yield of ~10%. The wavelength response of the carrier yield (see Figure) show a 3:1 ratio of charges generated by exciting the S_{22} transition relative to the S_{11} transition. The high yield of charges for this low energy exciton transition is unusual as the exciton binding energy is >> k_BT. Although the microwave conductivity experiment is unable to determine if electrons or holes are generated in this system, it is assumed that it is predominantly holes that are being detected. The long lifetime is attributed to the charge being delocalized along the nanotube length, and with the electrons being trapped at an as yet undetermined site.

Studying Carrier Dynamics and Solar Energy Conversion using THz Spectroscopy

Charles A. Schmuttenmaer, Kevin P. Regan, Coleen T. Nemes, Christopher Koenigsmann, Victor S. Batista, Robert H. Crabtree, and Gary W. Brudvig

Department of Chemistry and Energy Sciences Institute
Yale University
New Haven, CT 06520-8107

Terahertz spectroscopy has proven itself to be an excellent non-contact probe of transient conductivity with sub-picosecond time resolution. One may exploit this capability to study a wide variety of samples, and here we choose to probe the transient photoconductivity of dye-sensitized nanostructured wide band gap semiconductors, as well as lower band gap metal oxides such as WO_3. These systems are of interest in the area of renewable energy research and artificial photosynthesis.

Time-resolved terahertz (THz) spectroscopy and open circuit photovoltage measurements have been employed to examine the size-dependent charge carrier dynamics of tungsten oxide (WO_3) particles. Specifically, films of commercially available WO_3 nanoparticles (NPs) and granular particles (GPs) with diameters of 77 ± 34 nm and 390 ± 260 nm, respectively, were examined in air and also while immersed in 0.1 M Na_2SO_4 electrolyte. See Figure 1 for a SEM image of the two particle types. Examination of the frequency-dependent transient photoconductivity at short and long timescales indicates the presence of high mobility photoinduced charge carriers at early times, and in some cases low mobility ones at later times with comparable carrier densities. The presence of long-lived photoinduced charge carriers that contribute to surface chemistry are not detectable until the high-mobility carriers are trapped.

In addition, we have recently shown that it is possible to probe a fully functioning dye-sensitized solar cell by using patterned transparent conductive oxide (TCO) electrodes.[1] The standard TCO electrodes transmit visible light, but reflect THz light. Our results show that it is possible to probe a DSSC while applying a bias voltage and/or under steady state illumination. This new technique should be applicable to any type of devices used in solar energy conversion that uses transparent conducting electrodes.

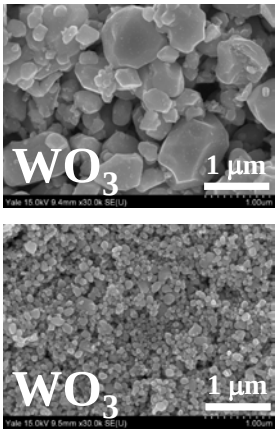

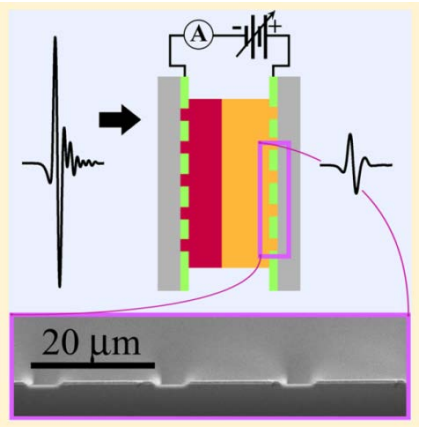

(1) Nemes, C. T.; Koenigsmann, C.; Schmuttenmaer, C. A., "Functioning Photoelectrochemical Devices Studied with Time-Resolved Terahertz Spectroscopy," *J. Phys. Chem. Lett.* **2015**, *6*, 3257.

Ultrafast Photo-induced Electron Transfer seen *via* Vibrationally Coherent Wavepackets

Shahnawaz Rafiq, Marius Koch, Gregory D. Scholes
Frick Chemistry Laboratory
Princeton University, NJ, 08544

One aim of this research program is to work out how to think about 'coherence' in electron transfer reactions. To this end we must ascertain different experimental windows to the underlying dynamical processes that govern electron transfer reactions. A particular motivation for such studies is to establish how chemical design at the molecular level influences, and induces the *interplay* among, electronic coupling between molecules, interactions with the environment, and intramolecular vibrations. The key point of the work is that we will investigate the *interplay* of factors, which is a hallmark of the attribute loosely called 'coherence'. Our essential approach is to revisit the insights concluded in seminal papers on the theory of electron transfer reactions and use new experimental probes based on multidimensional electronic spectroscopy to explore these fundamental aspects of electron transfer dynamics. Two advances will be reported:

(i) A coherent superposition of vibrational states (wavepacket) generated in the reactant state during an electron transfer (ET) reaction carries information about the reaction in the form of phase correlations. We have developed 12 fs broadband white-light probe experiments to detect simultaneously the excited initial states as well as photoproduct photoinduced absorptions. In studies of electron transfer systems comprising oxazine dyes in electron-donating solvents we observe abrupt loss of phase coherence in the vibrational wavepacket during the transition to the product state on a 200 fs time scale. Control experiments where the electron donating solvent is diluted with methanol show vibrational coherences of the excited state in the absence of the reaction dephase at a much slower rate (>1 ps). This rapid phase decoherence suggests that the population transfer from the reactant to the product state occurs strictly via curve crossing enabled by a collective vibrational coordinate involving intramolecular modes. Anharmonicity in the mixing region leads to fast wavepacket broadening. This observation contrasts with results (also to be reported) where the vibrational wavepacket survives the reaction—typical of spectator modes.

(ii) Generally speaking, photo-induced ET, including the above example, invokes a donor (D) and acceptor (A) molecule undergoing unidirectional transfer guided by free energy changes. A rigid hetero-molecular dyad synthesized by the Castellano group (NC State Univ) was studied using broad-band pump probe spectroscopy. In this system we discovered bidirectional electron transfer and subsequent stabilization of both ionic states, formally populating $D^{\bullet+}/A^{\bullet-}$ and $D^{\bullet-}/A^{\bullet+}$ simultaneously. Preliminary exploration suggests that design principles for such a new class of photoactive amphipolar molecules are related to the fine-tuned interplay of intra- and intermolecular couplings, whose information is embedded in the phase correlations of the wavepacket. Its exploration is thus the key for understanding this new area of photo-induced ET.

A multi-functional biphasic water splitting catalyst tailored for integration with high performance semiconductor photoanodes

Jinhui Yang,[1,2] Adam Schwartzberg,[3] Francesca M. Toma,[1,2] Jason K. Cooper,[1,2]
Marco Favaro,[1,2] Ethan Crumlin,[1,4] Christian Kisielowski,[3] Ian D. Sharp[1,2]
[1]Joint Center for Artificial Photosynthesis, [2]Chemical Sciences Division, [3]Molecular Foundry,
[4]Advanced Light Source
Lawrence Berkeley National Laboratory
Berkeley, CA 94720

To achieve efficient and durable artificial photosynthesis devices for solar water splitting, it is necessary to overcome thermodynamic limitations on material stability, integrate catalysts with light absorbers, and engineer interfaces to reduce recombination loss. Atomic layer deposition (ALD) has recently emerged as a powerful tool for integrating conformal thin film corrosion protection layers onto the surfaces of intrinsically unstable light absorbers, thereby enabling stable operation under the harsh aqueous conditions required for solar water splitting. Here, we show that plasma-enhanced ALD (PE-ALD) can be used to directly deposit a highly active cobalt oxide catalyst for the oxygen evolution reaction (OER) onto silicon.[1,2] However, the composition and structure of PE-ALD materials can differ significantly from those synthesized by other methods. Using a combination of transmission electron microscopy (TEM) and X-ray photoelectron spectroscopy (XPS), together with functional (photo)electrochemical testing, we show that multi-functional bilayer cobalt oxide coatings significantly enhance the performance of integrated semiconductor/catalyst assemblies, thereby enabling efficient and sustained photoelectrochemical water splitting under alkaline conditions.[1-3] These bilayers consist of nanocrystalline spinel Co_3O_4, which provides a stable interface, and a $Co(OH)_2$ surface layer, which can chemically transform to the catalytic phase with a high concentration of active sites (Fig. 1a). Chemical transformations of the coating are directly probed by operando electrochemical XPS. Application of this coating to photovoltaic p^+n-Si junctions yields best-reported performance characteristics for crystalline Si photoanodes (Fig. 1b). This work shows that engineering the catalyst and the semiconductor/catalyst interface at the nanoscale is essential for simultaneously achieving efficient charge extraction, catalytic activity, and chemical stability. Finally, plans for future studies aimed at identifying and overcoming charge transfer limitations in thin film metal oxide materials will be presented.

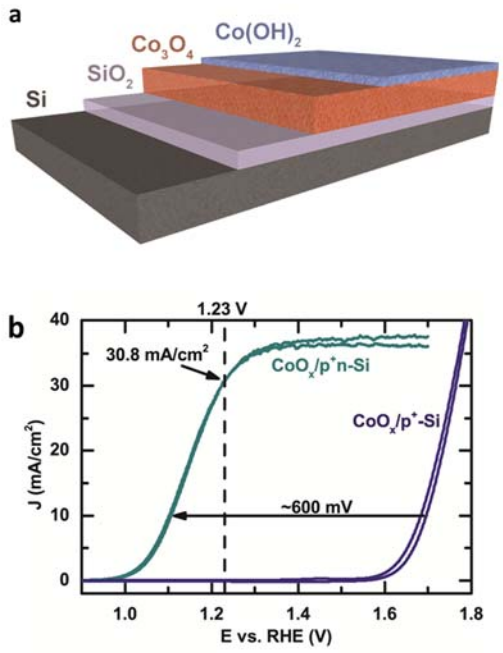

Fig. 1: (a) Schematic illustration of the biphasic catalyst coating that is engineered for integration with semiconductor light absorbers. (b) Photoelectrochemical performance characteristics obtained by integrating catalyst coating with p^+n-Si junctions.

[1] Yang *et al*. J. Am. Chem. Soc. **136**, 6191 (2014).
[2] Yang *et al*. submitted (2016).
[3] Kieselowski *et al*. submitted (2016).

The Synthesis and Chemistry of Molybdenum Complexes that Contain a Trianionic Calix[6]azacryptand Ligand Derived from 1,3,5-Trismethoxy-Calix[6]arene

Richard R. Schrock and Lasantha A. Wickramasinghe
Department of Chemistry
Massachusetts Institute of Technology 6-331
77 Massachusetts Avenue
Cambridge, Massachusetts 02139

A key requirement of catalytic nitrogen reduction to ammonia with protons and electrons at room temperature and pressure by molybdenum triamidoamine complexes is the development of a catalyst system in which the ligand is not removed from the metal under (acidic) catalytic conditions. A candidate, a new type of calix[6]azacryptand ligand (H_3CAC), has been prepared in six steps starting from 1,3,5-trismethoxy-calix[6]arene. An X-ray study shows that H_3CAC has a sterically protected tren-based binding site at the bottom of a polyaromatic bowl and methoxy (three plus three) groups around its rim. Zn^{2+} is bound in H_3CAC to give a $[Zn(H_3CAC)(H_2O)_3](triflate)_2$ complex in which Zn^{2+} is in a trigonal bipyramidal geometry with one water bound in one apical position and two additional waters hydrogen bonded to it within the cavity. We also have been able to prepare a C_{3v} symmetric Mo(VI) nitrido complex, [CAC]Mo(N) (see below), that contains the triply deprotonated ligand, $[CAC]^{3-}$. Nitrogen reductions and related studies that involve $[CAC]^{3-}$ complexes of Mo will be described.

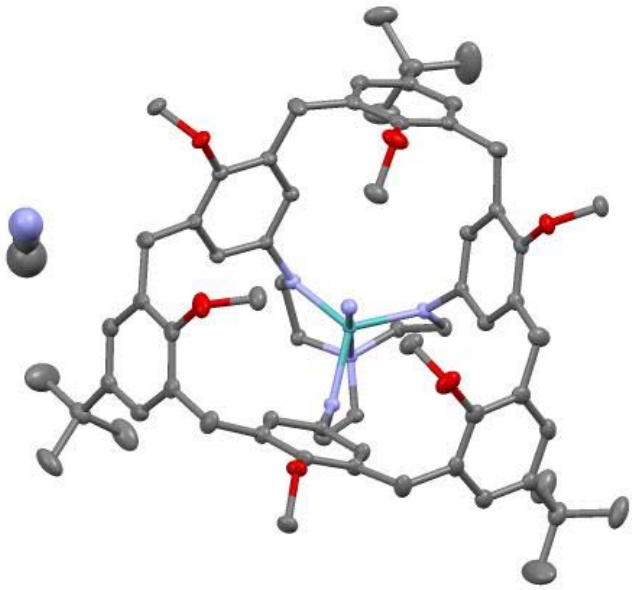

Photo-Induced Hole and Electron Transfer Reactions in Well-Defined Nanoscale Objects that Feature Electronically Homogeneous Single-Walled Carbon Nanotubes Wrapped by Redox Active Polymers

Jean-Hubert Olivier, Jaehong Park, Mary Glesner, Yusong Bai and Michael J. Therien

Department of Chemistry, French Family Science Center, 124 Science Drive, Duke University, Durham, NC 27708-0346, USA

Single-walled carbon nanotube (SWNT)-based nanohybrid compositions based on (6,5) chirality-enriched SWNTs ([(6,5) SWNTs]) and a chiral n-type polymer (**S-PBN(b)-Ph$_4$PDI**) that exploits a perylenediimide (PDI)-containing repeat unit are reported; **S-PBN(b)-Ph$_4$PDI-[(6,5) SWNT]** superstructures feature a PDI electron acceptor unit positioned at 3 nm intervals along the nanotube surface, thus controlling rigorously SWNT–electron acceptor stoichiometry and organization. Time-resolved pump–probe spectroscopic studies demonstrate that **S-PBN(b)-Ph$_4$PDI-[(6,5) SWNT]** electronic excitation generates PDI$^{\bullet-}$ via a photoinduced CS reaction (τ_{CS} = 0.4 ps, Φ_{CS} = 0.97). These experiments highlight the concomitant rise and decay of transient absorption spectroscopic signatures characteristic of the SWNT hole polaron and PDI$^{\bullet-}$ states. Multiwavelength global analysis of these data provide two charge-recombination time constants (τ_{CR} = 31.8 and 250 ps) that likely reflect CR dynamics involving both an intimately associated SWNT hole polaron and PDI$^{\bullet-}$ charge-separated state, and a related charge-separated state involving PDI$^{\bullet-}$ and a hole polaron site produced via hole migration along the SWNT backbone that occurs over this timescale.

In contrast to ***S*-PBN(b)-Ph$_4$PDI-[(6,5) SWNT]** nanohybrids, selective photoexcitation of a SWNT superstructure in which a (porphinato)zinc (PZn)-based polymer wraps the nanotube surface triggers the formation of SWNT electron polaron and PZn radical cation states. Despite the disparate driving forces for photoinduced CS and thermal CR reaction is ***S*-PBN(b)-Ph$_4$PDI-[(6,5) SWNT]** and ***S*-PBN-PZn-[(6,5) SWNT]** superstructures, similar magnitude τ_{CS} (τ_{CS} = 0.4ps) and bi-exponential τ_{CR} values (τ_{CR} = 22 and 307 ps) are determined in these experiments. These intriguing results provide mechanistic insights into the factors that govern photo-induced charge transfer reactions in these well-defined polymer-wrapped [(6,5) SWNT] superstructures.

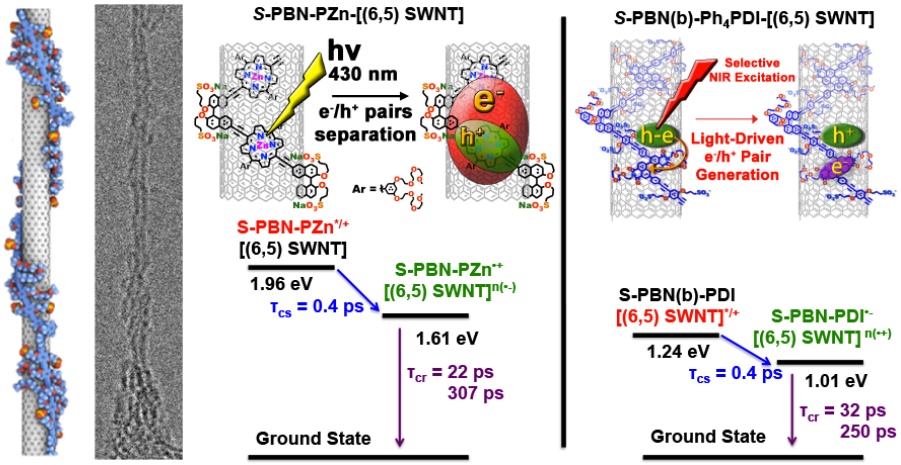

Photocatalysts for H_2 Evolution: Combination of the Light Absorbing Unit and Catalytic Center in a Single Molecule

Travis A. White, Suzanne E. Witt, Tyler J. Whittemore, Ryan P. Coll,
Kim R. Dunbar, and Claudia Turro

Department of Chemistry and Biochemistry, The Ohio State University, Columbus OH, 43210
Department of Chemistry, Texas A&M University, College Station, TX 77843

Solar-to-chemical energy conversion schemes to produce H_2 fuel from H_2O present an attractive alternative to our reliance on carbon-based fossil fuels. Typical photocatalytic systems rely on spatially-separated light absorbing subunits and catalytic centers whereby photoexcitation and subsequent charge transfer must compete with highly efficient charge recombination. In an effort to reduce this deactivating process and the number of required molecular components within the catalytic scheme, the Turro and Dunbar groups have developed formamidinate-bridged, dirhodium(II,II) half paddlewheel complexes of the formula *cis*-$[Rh_2(\mu\text{-form})_2(NN)_2]^{2+}$ (μ-form = bridging formamidinate, NN = diimine ligand) with the aim of single-component photocatalytic H_2O reduction. Our current research focuses on the enhancement of visible light spectral coverage, the electronic control of selective and rapid catalysis through careful ligand design, and excited state population and dynamics upon photoexcitation. Visible light absorption has been increased with the extended aromatic diimine ligand (1,12-diazaperylene, dap) and by modification of the diimine ligand coordination mode from a chelating κ^2 bidentate to μ bridging (1,8-naphthyridine, np), Figure 1. The catalytic nature of the $[Rh_2]^{4+}$ core and what electronic and steric factors drive selective and rapid catalysis towards either H^+ or CO_2 reduction have been investigated through the judicious choice of anionic bridging ligands to strongly modulate the electron density at the $[Rh_2]^{4+}$ core. We have discovered that the weaker electron-donating acetate bridges direct CO_2 reduction and the more electron-rich formamidinate bridging ligands direct H^+ reduction electrocatalytically. Ultrafast transient absorption and time-resolved infrared spectroscopies have provided insight into the excited state population and dynamics of the dirhodium(II,II) architecture.

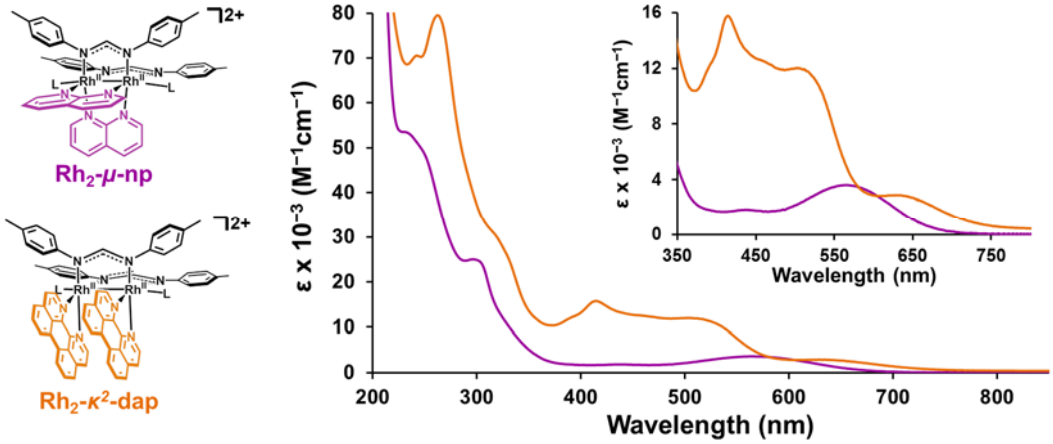

Figure 1. Structural representations of *cis*-$[Rh_2(\mu\text{-form})_2(NN)_2]^{2+}$ complexes and the corresponding electronic absorption spectra.

Size dependence of the band energetics of coupled PbS quantum dot films

Elisa M. Miller,[1] Daniel M. Kroupa,[1,2] Jianbing Zhang,[1] Philip Schulz,[1,3] Ashley R. Marshall,[1,2] Antoine Kahn,[3] Stephan Lany,[1] Joseph M. Luther,[1] Matthew C. Beard,[1] Craig L. Perkins,[1] and Jao van de Lagemaat[1]

[1]Chemical and Materials Sciences Center, NREL, Golden, CO 80401, USA
[2]Department of Chemistry and Biochemistry, University of Colorado, Boulder, CO 80309, USA
[3]Department of Electrical Engineering, Princeton University, Princeton, NJ 08544, USA

Films of colloidal quantum dots (QDs) can retain their quantum confinement and excitonic character even when the particles are coupled using short linker molecules, allowing them to become highly conductive. The band energetics and doping of such films are controlled by the surface chemistry, stoichiometry and other factors. This control potentially allows for their use in solar fuel generation as well as a solar absorber. Since knowledge of the precise energetic position of the hole and electron transport levels in QD films is essential to design energy conversion architectures, it is necessary to reliably determine the precise energetics.

Photoelectron spectroscopy (XPS and UPS) is regarded as the 'gold standard' for determining band energetics. In previous photoelectron spectroscopy reports, it was concluded that Fermi level and the valance band position do not move with the QD size but that only the conduction band moves. These results are in disagreement with results from scanning tunneling spectroscopy and theory, which indicate that both bands move with size.

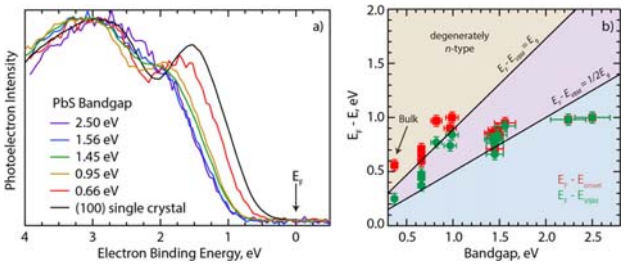

Fig. 1. XPS spectra of PbS QD and single-crystal PbS . (b) Values of $E_F - E_{onset}$ (red squares – traditional analysis) and $E_F - E_{VBM}$ (green circles – new analysis) as a function of the PbS band gap.

In this paper,* we show that this discrepancy is due to erroneous analysis of XPS/UPS data (Fig. 1) owing to these systems having a low density of states near the VB edge. Instead, we show that an alternative approach of analyzing the spectra of QD films based on a fit to a parabolic model and comparison with GW calculations of the density of states in bulk PbS and k•p theory for QDs (Fig 2). The analysis highlights the breakdown of the Brillioun zone representation for large bandgap, highly quantum-confined PbS QDs. We also show that in these systems the Fermi level position is dependent on QD size (se Fig. 1). In the smallest bandgap QD films the Fermi level is near the conduction band and the Fermi level moves away from the conduction band for larger bandgap PbS QD films. This change in Fermi level is likely due to changes in Pb:S ratio which are evident in XPS.

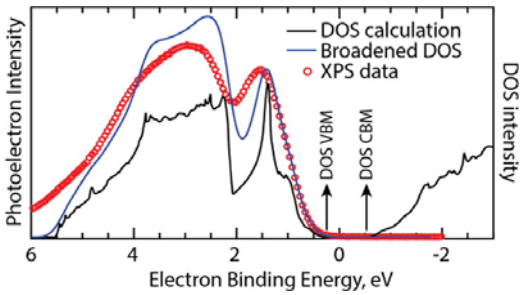

Fig. 2 Figure 3. Comparison of the XPS of bulk PbS experimental data with the GW-calculated DOS. The standard analysis would indicate that this material is degeneratively n-type which is not consistent with its conductivity.

* *ACS Nano* **2016** *10* (3), 3302-3311. doi: 10.1021/acsnano.5b06833

A Concerted Synthetic, Spectroscopic, and Computational Approach towards Water Splitting by Homo- and Hetero-metallic Complexes

Claudio Verani, H. Bernhard Schlegel, and John Endicott

Department of Chemistry
Wayne State University
Detroit, MI, 48202

In this poster the authors will present current understanding on novel photocatalytic water splitting systems based on Earth-abundant molecular catalysts that work in tandem with ruthenium photosensitizers. We investigate the criteria for mono- and bi-metallic species to become capable of effective electron transfer from the ruthenium to the metal for water reduction.

Verani and Schlegel will discuss work to elucidate the design criteria for modular cobalt, nickel, and copper catalysts for proton and water reduction. We will also discuss new ligand architectures to be used as mechanistic models and modules for the assembly of larger multimetallic species that target photocatalyzed processes. One such example is illustrated in **Figure 1**, where we demonstrate the mechanistic complexity of simple processes such as Co(III) to Co(I) reduction in simple heteroaxial Espenson catalysts capable of serving as modules for [RuCo] diads.

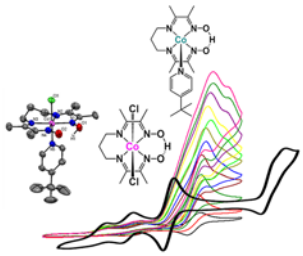

1. $[Co^{III}(oxH)(^{4tBu}py)(Cl)]^+ + e^- \rightarrow [Co^{II}(oxH)(^{4tBu}py)(Cl)]^o \rightarrow [Co^{II}(oxH)(^{4tBu}py)]^+ + Cl^-$
2. $[Co^{II}(oxH)(^{4tBu}py)]^+ + CH_3CN \rightarrow [Co^{II}(oxH)(^{4tBu}py)(CH_3CN)]^+$
3. $[Co^{III}(oxH)(^{4tBu}py)(Cl)]^+ + Cl^- \rightarrow [Co^{III}(oxH)(Cl)_2]^o + {}^{4tBu}py$
4. $[Co^{III}(oxH)(Cl)_2]^o + e^- \rightarrow [Co^{II}(oxH)(Cl)_2]^- \rightarrow [Co^{II}(oxH)(Cl)]^o + Cl^-$
5. $[Co^{II}(oxH)(Cl)]^o + CH_3CN \rightarrow [Co^{II}(oxH)(CH_3CN)(Cl)]^o$
6. $[Co^{II}(oxH)(CH_3CN)(Cl)]^o + {}^{4tBu}py \rightarrow [Co^{II}(oxH)(^{4tBu}py)(CH_3CN)]^+ + Cl^-$
7. $[Co^{II}(oxH)(^{4tBu}py)(CH_3CN)]^+ + e^- \rightarrow [Co^{I}(oxH)(^{4tBu}py)]^o + CH_3CN$

Figure 1. The procatalyst $[Co(III)(oxH)(^{4tBu}py)(Cl)]^+$ and its catalytic behavior (left) and each of the steps involved with Co(III)/Co(II)/Co(I) reduction to lead to the formation of the Co(I) catalyst involved in water splitting (right).

Schlegel and Endicott will discuss key properties governing electron transfer of ^{3}MLCT states in Ru-containing photosensitizing modules. We have studied the competing reactions such as radiative and non-radiative relaxation, emission quantum yield, and internal conversion that determine the efficiency of generation of the catalyst in the photoexcited state. The radiative lifetimes of Ru-bipyridine (Ru-bpy) chromophores show a strong emission energy dependence that is correlated with the configurational mixing between the emissive ^{3}MLCT and a higher energy $\pi\pi^*$ excited state. This feature is absent for analogous Ru-monodentate aromatic ligand (Ru-MDA) chromophores.

Enabling Singlet Fission by Controlling Intramolecular Charge Transfer

E. A. Margulies, C. E. Miller, Y. Wu, L. Ma, G. C. Schatz, R. M. Young, and M. R. Wasielewski
Department of Chemistry
Northwestern University
Evanston, IL 60208-3113

Singlet exciton fission (SF) in ensembles of molecular chromophores down-converts one singlet exciton (S_1) produced by single-photon absorption into two triplet excitons (T_1) provided that the overall process is exoergic, i.e. $E(S_1) > 2E(T_1)$. While there has been great interest in SF because of its potential for increasing the maximum efficiency of photovoltaics from the 32% Shockley-Queisser limit for single-junction devices to nearly 45%, important details of the SF photophysical mechanism remain unresolved. SF can occur by two general mechanisms: one that directly couples the initial $^1(S_1S_0)$ state to a multi-exciton $^1(T_1T_1)$ state by a two-electron process, and another that proceeds via a charge transfer (CT) state by two consecutive one-electron processes. In the latter process, photoexcitation of a chromophore that is electronically coupled to a second nearby chromophore creates an electronic superposition state involving $^1(S_1S_0)$, a virtual CT state, and $^1(T_1T_1)$. Electronic dephasing of this superposition state typically should occur on a sub-picosecond timescale leaving the spin-coherent $^1(T_1T_1)$ state, which is frequently referred to as a correlated triplet pair state. Spin dephasing is a much slower process, typically on the order of nanoseconds, so that spin dephasing in $^1(T_1T_1)$ may occur on a timescale comparable to spatial separation of the triplet states resulting in two independent triplet states.

We report here on a series of covalently-linked terrylene-3,4:11,12-bis(dicarboximide) (TDI) dimers in which triptycene spacers hold two TDI molecules in π-stacked geometries (Figure 1A). When dimer **2** in which the TDI chromophores are slip-stacked by 7.6 Å is dissolved in polar CH_2Cl_2, ultrafast symmetry-breaking charge separation occurs in τ = 8.1 ps to yield $TDI^{+\bullet}$-$TDI^{-\bullet}$. In contrast, when the same dimer is dissolved in non-polar toluene, rapid singlet fission is observed in τ = 2.2 ps, while the reverse triplet-triplet annihilation occurs in τ = 4.4 ps resulting in an excited state equilibrium giving an overall 133% triplet yield in steady state. Controlling the $TDI^{+\bullet}$-$TDI^{-\bullet}$ CT state energy relative to that of $^1(S_1S_0)$ results in the CT state serving as either a virtual state promoting singlet fission or a trap state inhibiting it (Figure 1B).

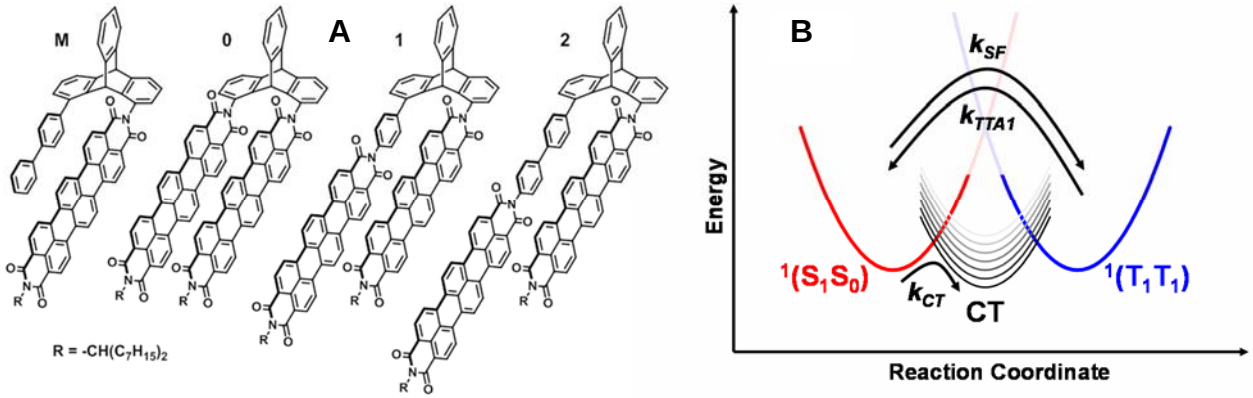

Figure 1. A) Structures of TDI derivatives. B) Proposed schematic potential energy surface of SF. The CT state serves either as a trap (k_{CT}) or as a virtual state through which SF (k_{SF}) or triplet-triplet annihilation (k_{TTA1}) may proceed along the reaction coordinate depending on how its energy level is affected by solvent polarity.

Photoinduced radical generation, cage escape and recombination in ionic liquids

James F. Wishart and Koji Osawa
Chemistry Department
Brookhaven National Laboratory
Upton, NY 11973

The early steps of photoinduced reactions often involve a competition between recombination and escape of the photoproducts, whether they are radicals or charge-separated states. This competition largely determines the quantum efficiency of energy capture and in some cases, photodegradation yields in catalytic systems. Ionic liquids (ILs) provide a great opportunity to probe the dynamics of caged transient species due to their slower relaxation dynamics and higher viscosity compared to molecular solvents. An excellent probe molecule for cage dynamics studies is *ortho*-chloro-hexaarylbisimidazole (*o*-Cl-HABI or HABI, Fig. 1) and related molecules, whose excited states cleave into two identical lophyl radicals, as shown in the figure. The HABI molecule is highly distorted into a sort-of "butterfly" shape due to the steric interactions between the six phenyl rings. Excitation causes HABI to split at the asymmetric N-C bond, and the resulting lophyl radicals relax to become completely planar. Recombination into stable HABI occurs, but it is slow because it requires significant distortion of the planar lophyl radicals. For this reason HABI and similar derivatives have been widely used in industry as radical photoinitiators. The lophyl radicals are also strongly colored (550 nm), which makes their formation and decay easy to detect and has led to their extensive development as photochromic materials.

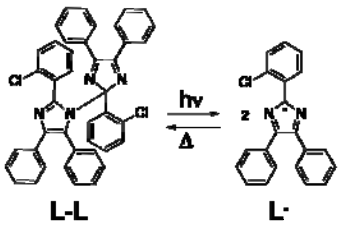

Fig. 3.3.9. Photolytic cleavage and thermal recombination of *o*-Cl-HABI.

In an earlier study we saw lower cage escape yields of lophyl radicals formed by photolysis of *o*-Cl-HABI in several ionic liquids compared to DMSO. This implied that there could be something different about the IL environment that reduces the yield of lophyl radicals. Low-temperature EPR work by Trifunac and Krongauz supports the mechanistic interpretation that dissociation from the HABI singlet excited state is in competition with intersystem crossing (ISC) to a nondissociative triplet state. Slow relaxation of the IL solvent cage can impede dissociation of the HABI singlet excited state, resulting in a longer time for ISC to occur and consequently a lower yield of lophyl radicals. We will present results exploring this effect using an informed selection of ionic liquids. Our earlier study also slowed that bimolecular diffusive recombination of lophyl radicals was faster in ILs than DMSO, even before accounting for viscosity. Those observations imply that something about the IL environment might actually stabilize the transition state for recombination. The generality and mechanism(s) of this effect will be explored using different types of ionic liquid cations and anions to test the range of potential transition-state stabilizing interactions.

Building a Toolbox of Singlet Fission Molecules for Solar Energy Conversion

Xiaoyang Zhu, Colin Nuckolls
Department of Chemistry
Columbia University
New York, NY 10027

The proposed research aims to build a large toolbox of molecular materials possessing efficient singlet fission yield for solar energy conversion, with power conversion efficiency potentially exceeding the Shockley-Queisser (SQ) limit. Achieving this goal requires the development of design principles based on mechanistic understanding, the synthesis of molecular materials with high singlet fission yields, and the implementation of singlet fission for efficient multi-charge harvesting. During the past year, we have focused our efforts on two fronts. The first focuses on the mechanism of singlet fission in the model system of crystalline hexacene and the second on the assembly of molecular chromophores to control singlet fission rates.

Singlet fission, the splitting of a singlet exciton (S_1) into two triplets ($2xT_1$), is believed to proceed through the correlated triplet pair ^{1}(TT). We probe the ^{1}(TT) state in crystalline hexacene using time-resolved two-photon photoemission and transient absorption spectroscopies. We find a distinctive ^{1}(TT) state which decays to $2xT_1$ with a time constant of 270 fs. However, the decay of S_1 and the formation of ^{1}(TT) occur on different time scales of 180 fs and <50 fs, respectively. Theoretical analysis suggests that a vibrationally excited ^{1}(TT) is resonant and forms an initial quantum superposition with S_1. Ultrafast dephasing of this quantum superposition leads to populations of S_1 and ^{1}(TT) states; the former is further converted to ^{1}(TT) in an incoherent rate process. Both coherent and incoherent singlet fission mechanisms likely coexist in crystalline hexacene and this may also reconcile different experimental observations in other acenes.

One of the most critical and least understood aspects of singlet fission is how singlet fission rates depend on inter-molecular interactions. We are exploring two approaches to direct probe this. In the first approach, in collaboration with Prof. Luis Campos' group, we have successfully developed block-copolymers with functional pentacene pendants. These block-copolymers self-assemble in the solution phase to form nanoscale domains of pentacene clusters. We find that efficient singlet fission occur in these nano-domains and, more interestingly, the rate of singlet fission can be systematically controlled by the solvent environment. This can be understood as systematic tuning of inter-pentacene distance in different solvent environment, leading to controllable electronic interactions. In the second approach, we have developed covalent organic frameworks (COFs) to determine the spatial arrangements of pentacene molecules. This material system allows us to probe not only how singlet fission rate depends on inter-molecular interaction but also how triplet diffusion can be directed and controlled in such the three dimensional network.

Chemical Control Over the Electrical Properties of GaAs and Group VI Dichalcogenide Semiconductor Surfaces and Photoelectrodes

Fan Yang, Joshua D. Wiensch, Ellen Yan and Nathan S. Lewis
Department of Chemistry and Chemical Engineering
California Institute of Technology
Pasadena, CA 91125

The goal of our work is to understand, and control, the interplay between often-competing factors that determine the behavior of photoelectrochemical systems designed to produce electricity or fuels from sunlight. During this period, our work has focused on photoelectrochemical systems based on GaAs or the Group VI layered dichalcogenides.

GaAs is a technologically important semiconducting material with a desirable direct band-gap energy of ~1.4 eV, and is used for creating high-efficiency solar cells. The direct band gap at higher energy than the indirect band gap of Si (1.14 eV) allows GaAs solar cells to absorb more light using less material and to operate more efficiently than Si solar cells. However, GaAs corrodes rapidly when operated electrochemically in the presence of water. To take advantage of the beneficial properties of GaAs in a photoelectrochemical fuel-forming system, surface passivation is required to prevent either the formation of an insulating oxide in the region of pH 4-10 or to prevent dissolution in strongly alkaline or acidic electrolytes.

Layered transition-metal dichalcogenides (MX_2s) are a very attractive class of materials for use in photoelectrochemical cells because due to their high stability relative to other semiconductors with comparable band gaps. Transition-metal dichalcogenides possess both indirect and direct band gaps which allow the direct band gap to be selected by transitioning from bulk crystals to single-layer samples.

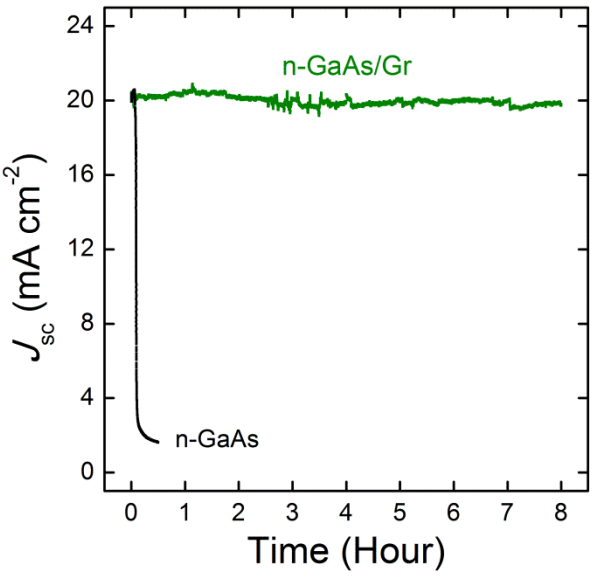

Figure 1. Comparison of the *J*-t behavior of potentiostatically controlled n-GaAs (black) and n-GaAs/Gr (green) electrodes (E = 0 V vs. solution) in contact with a CH_3CN-$Fc^{+/0}$ system containing a trace amount of water (H_2O concentration 0.1%, v/v) under AM1.5 illumination.

We have demonstrated a method to substantially increase the stability of n-GaAs toward passivation in non-aqueous electrolytes containing a trace amount of water. Additionally, limited protection against corrosion was observed when n-GaAs photoanodes were in contact with an aqueous solution containing $K_3[Fe(CN)_6]$/ $K_4[Fe(CN)_6]$. Under simulated 1 Sun illumination, the graphene-coated electrodes produced a stable short-circuit photocurrent density of 20 mA cm^{-2} for up to 8 hours of continuous operation in nonaqueous electrolytes with a trace amount of water. In contrast, under the same conditions, bare n-GaAs in contact with a CH_3CN-$Fc^{+/0}$ solution gave an initially high

short-circuit current density before rapidly decaying within 400 s (Figure 1). In aqueous $Fe(CN)_6^{3-/4-}$ solution bare n-GaAs photoanodes showed effects of corrosion immediately upon operation and provided very little output power; however a single layer of graphene allowed significant initial power generation with a slow decline in current density over a matter of hours.

Fermi-level pinning at the GaAs/Gr/liquid interface in 1.0 M $LiClO_4/CH_3CN$ was indistinguishable from an uncoated GaAs electrode (Figure 2). For n-GaAs/CH_3CN contacts, the open-circuit voltage varied by only ~300 mV, while the change in $E_{eff}(A/A^-)$ was in excess of 1.0 V. If the semiconductor/liquid junction behaved ideally, V_{oc} should change linearly with $E_{eff}(A/A^-)$ with a slope of unity. What was observed instead was evidence of partial Fermi-level pinning over the range of solution potentials that were explored. Partial Fermi-level pinning is also observed for n-GaAs samples that were not coated by a single layer of graphene.

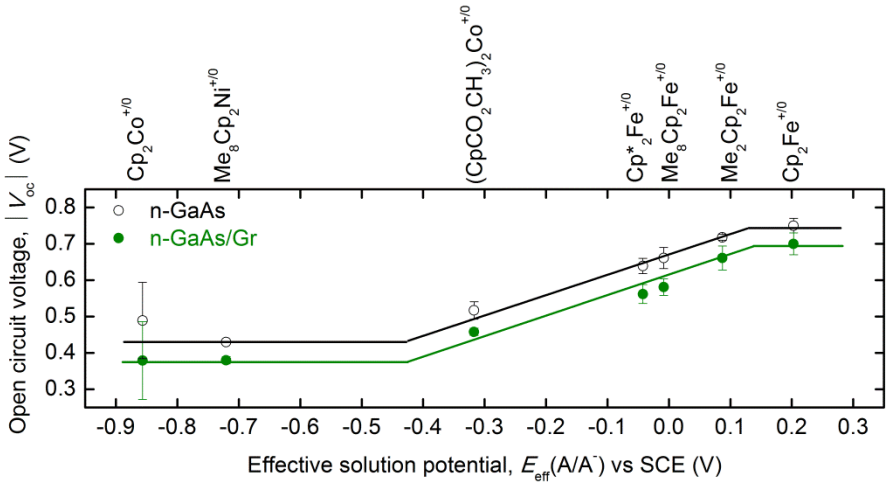

Figure 2. Open-circuit voltage, V_{oc}, vs the effective solution redox potential, $E_{eff}(A/A^-)$, in 1.0 M $LiClO_4/CH_3CN$ for n-GaAs (black, open circles) and n-GaAs/Gr (green, filled circles). The corresponding lines serve as guides to indicate the observed trends in the different regions of V_{oc}, vs. $E_{eff}(A/A^-)$

We also studied MX_2 (M = Mo; X = S, Se) surface functionalization on exfoliated single crystals and polycrystalline thin films. MX_2 single-crystal samples used in this study were grown by chemical-vapor transport from elemental molybdenum and the respective chalcogenide. Polycrystalline thin-film $MoSe_2$ samples were prepared by selenization of elemental molybdenum in a custom-built chemical-vapor-deposition system. We have compared the behavior of covalently functionalized single-crystal MX_2 samples with polycrystalline thin films. Our studies have shown differences in small molecule binding for ligands on single-crystal versus polycrystalline thin-film samples of $MoSe_2$. Edge-site rich polycrystalline thin-film samples fail to bind bidentate disulfide ligands under identical conditions under which single-crystal samples selectively bind ligands to macroscale edges. Ongoing studies are exploring the root-cause of this differential reactivity.

Further studies of the protection of graphene-coated p-GaAs and other III-V and II-VI semiconductors will advance the understanding of the extent of the graphene-imparted stability. Additionally, we are exploring the covalent functionalization of the terrace sites of transition metal dichalcogenides to allow for monolayer self-assembly. We wish to determine the effects of functionalization on electronic properties such as band-edge positions and behavior in contact with solution-based redox couples.

Organic Macromolecular Materials for Long-Range and Efficient Transport Properties in Light Energy Conversion Applications

Goodson III, T.
Department of Chemistry, Department of Macromolecular Science and Engineering, University of Michigan, Ann Arbor, Michigan 48109

In this investigation the approach is directed toward gaining information about the fundamental excitation dynamics and the energy migration process in particular organic macromolecules in solution and in the solid state. By combining oligothiophene properties with a cyclic topology we are able to gain a novel perspective in the development of efficient light conversion devices that utilize strong coupling in synthetic macrocycles. It was recently found that 8-mer thienylene-ethynylene–vinylene macrocycle provides the best geometrical match for the C_{60} inclusion and these new complexes demonstrate formation of supramolecular structures with C_{60} incorporated within the planar ring. This system showed high stability in the solid state. To study the excitation energy transport in supramolecular nanostructures we have built the near-field scanning microscope (NSOM) excited with the femtosecond pulse sequence to combine femtosecond time resolution with the spatial resolution of tens of nanometers. We have investigated local dynamics of optical excitations in the aggregates of cyclic oligothiophene-C_{60} complexes.[1] These dynamics are associated with the fact that chromophore is coupled to the rest of the aggregate. The energy from the excited donor group is transferred to the acceptor molecules in the aggregate resulting in the pulse pair separation dependence. Observed exponential profile of the NSOM inter-pulse interval dependence (Figure 1) corresponds to the energy transfer from the donor at the tip of the fiber along the fiber away from the tip with the energy transfer rate of 1/ 585 fs^{-1}.[1]

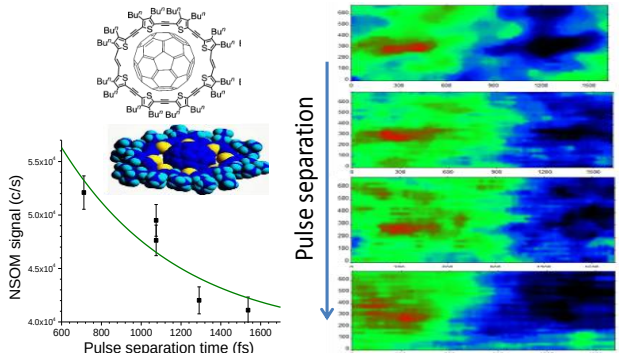

Figure 1 *Phase-locked pulse pair near-field microscopy experiments with cyclic oligothiophene - C_{60} aggregated system.*[1]

New low bandgap electron-accepting polymers have been also investigated to probe the structure–function relationships important to highly efficient solar cells. We probed the dynamics of a set of novel bithiophene donor and acceptor systems.[2] The effect of heteroatoms on the properties important to highly efficient solar cells has been studied in low bandgap polymers featuring benzodifuran (BDF).[3]

1. Varnavski, O.P.; Abeyasinghe, N.; Iyoda, M.; Goodson III, T. Excitation Energy Transport in Small Aggregates of Cyclic Oligotiophene-C_{60} Complexes Measured by Pulse Pair Microscopy *Nature* **2016,** submitted for publication.
2. Vázquez, R.J.; Yau, S. H., Cai, Z. Goodson III, T., Yu, L.P. Ladder-Type Thienoacenes Fully Conjugated with Perylene-Diimide and Their Electronic and Optical Properties *J.Am. Chem. Soc.* **2016,** submitted for publication.
3. Vázquez, R.J.; Adegoke, O.O.; Jeffries-EL, M.; Goodson lll, T. Influence of the Heteroatom on Optical Properties in Conjugated Donor-Acceptor Copolymers Based on 2,6 di(thiophen-2-yl)benzo[1,2-b:4,5-b′]difurans and Diketopyrrolopyrrole *J. Phys. Chem.* **2016**, submitted for publication.

New Paradigms for Group IV Nanocrystal Surface Chemistry

Lance W. Wheeler, Nicholas C. Anderson, Peter K.B. Palomaki, Asa W. Nichols, Boris D. Chernomordik, Jeffrey L. Blackburn, Justin C. Johnson, Matthew C. Beard, and Nathan R. Neale
Chemistry & Nanoscience Center
National Renewable Energy Laboratory
Golden, CO 80401

We have been exploring the functionalization of group IV nanocrystals (NCs) to understand how surface chemistry influences fundamental photophysics and inter-NC charge transfer. Many silicon nanostructures exhibit favorable optical properties such as high emission quantum yield following surface functionalization with molecular groups through a Si–C bond. We show the mechanism of functionalization for Si NCs synthesized in a nonthermal radiofrequency plasma is fundamentally different than in other silicon systems. In contrast to hydrosilylation, where homolytic cleavage of Si−H surface bonds typically precede Si–C bond formation, we demonstrate the dominant initiation step for plasma-synthesized silicon nanocrystals is abstraction of a silyl radical, $\bullet SiH_3$, and generation of a radical at the Si NC surface. We experimentally trap the abstracted $\bullet SiH_3$ and show this initiation mechanism occurs for both radical- and thermally-initiated reactions of alkenes to give both alkyl and silylalkyl ligands (Fig. 1). These Si NCs exhibit size-dependent electron-phonon interactions, exciton formation dynamics, and absolute absorption cross-section.

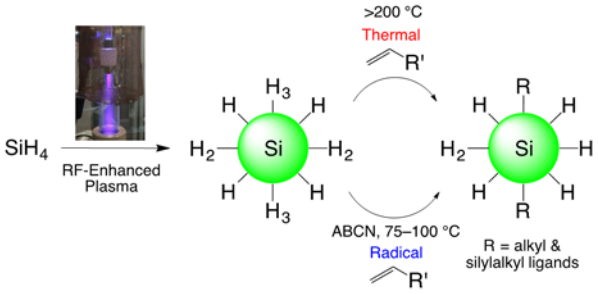

Figure 1. Silicon nanocrystals prepared by RF-enhanced plasma decomposition of silane (SiH_4) gas undergo surface functionalization reactions with alkenes via silyl ($\bullet SiH_3$) group abstraction to give both alkyl and silylalkyl ligands.

We additionally introduce a new paradigm for group IV NC surface chemistry based on surface activation that enables ionic ligand exchange. Germanium NCs synthesized in a gas-phase plasma reactor are functionalized with labile, cationic alkylammonium ligands rather than with traditional covalently bound groups. We demonstrate the alkylammonium ligands are freely exchanged on the Ge NC surface with a variety of cationic ligands, including short inorganic species such as ammonium and alkali metal cations (Fig. 2). This ionic ligand exchange chemistry is used to demonstrate enhanced transport in Ge NC films following ligand exchange. This new ligand chemistry should accelerate progress in utilizing Ge and other group IV NCs for optoelectronic applications.

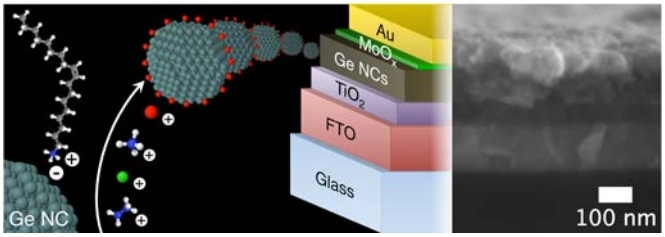

Figure 2. Surface activation of plasma-synthesized germanium nanocrystals yields negatively charged surfaces with weakly bound alkylammonium ligands that can be exchanged via simple solution chemistry using a variety of cationic groups including inorganic cations such as sodium (Na^+).

List of Participants

Participants List – 38th Solar Photochemistry P.I. Meeting

John Asbury
Pennsylvania State University
Department of Chemistry
University Park, PA 16801
814-863-6309
jba11@psu.edu

Allen Bard
University of Texas at Austin
105 E. 24th St., Stop A5300
Austin, TX 78712-1224
512-471-3761
ajbard@mail.utexas.edu

Robert Bartynski
Rutgers University
136 Frelinghuysen Rd.
Piscataway, NJ 08854
732-445-5500
bart@physics.rutgers.edu

Victor Batista
Yale University
P.O. Box 208107
New Haven, CT 06477
203-432-6672
victor.batista@yale.edu

Matt Beard
National Renewable Energy Laboratory
15013 Denver West Pkwy.
Golden, CO 80401
303-384-6781
Matt.beard@nrel.gov

Jeff Blackburn
National Renewable Energy Laboratory
15013 Denver West Pkwy.
Golden, CO
80401303-384-6649
jeffrey.blackburn@nrel.gov

David Blank
University of Minnesota
207 Pleasant St. SE
Minneapolis, MN 55455
612-624-0571
blank@umn.edu

Andrew Bocarsly
Princeton University
Frick Laboratory
Princeton, NJ 08544
609-258-3888
bocarsly@princeton.edu

David Bocian
University of California, Riverside
Department of Chemistry
Riverside, CA 92521
951-827-3660
David.Bocian@ucr.edu

Shannon Boettcher
University of Oregon
Department of Chemistry
Eugene, OR 97403
541-346-2543
swb@uoregon.edu

Kara Bren
University of Rochester
120 Trustee Rd.
Rochester, NY 14627-0216
585-275-4335
bren@chem.rochester.edu

Gary Brudvig
Yale University
P.O. Box 208107
New Haven, CT 06477
203-432-5202
gary.brudvig@yale.edu

Emilio Bunel
Argonne National Laboratory
9700 S. Cass Ave.
Argonne, IL 60439
630-252-4309
ebunel@anl. gov

Ian Carmichael
University of Notre Dame
223 Radiation Laboratory
Notre Dame, IN 46556
574-631-4502
carmichael.1@nd.edu

Participants List – 38th Solar Photochemistry P.I. Meeting

Felix N. Castellano
North Carolina State University
2620 Yarbrough Dr.
Raleigh, NC 27695
919-515-3021
fncastel@ncsu.edu

Lin Chen
Argonne National Lab/Northwestern Univ.
9700 S. Cass Ave.
Argonne, IL 60439
630-252-3533
lchen@anl.gov

Kyoung-Shin Choi
University of Wisconsin, Medison
1101 University Ave.
Madison, WI 53706
608-262-5859
kschoi@chem.wisc.edu

Javier Concepcion
Brookhaven National Laboratory
Chemistry Department
Upton, NY 11973-5000
631-344-4369
jconcepc@bnl.gov

Philip Coppens
University at Buffalo SUNY Buffalo
732 NSC Complex
Buffalo, NY 14260-3000
716-645-4273
coppens@buffalo.edu

Robert Crabtree
Yale University
225 Prospect St.
New Haven, CT 06520
203-432-3925
robert.crabtree@yale.edu

Jillian Dempsey
University of North Carolina
Department of Chemistry
Chapel Hill, NC 27599-3290
919-962-4617
dempseyj@email.unc.edu

Kim Dunbar
Texas A&M University
Department of Chemistry
College Station, TX 77843-3255
979-845-5235
dunbar@mail.chem.tamu.edu

James Durrant
Imperial College, London
United Kingdom
44 7590 250596
j.durrant@imperial.ac.uk

Richard Eisenberg
University of Rochester
Department of Chemistry
Rochester, NY 14627-0216
585-275-5573
eisenberg@chem.rochester.edu

Graham Fleming
Lawrence Berkeley National Laboratory
One Cyclotron Rd.
Berkeley, CA 94720
510-643-2735
grfleming@lbl.gov

Christopher Fecko
U.S. Department of Energy
1000 Independence Ave., SW
Washington, DC 20585
301-903-1303
Christopher.Fecko@science.doe.gov

Heinz Frei
Lawrence Berkeley National Laboratory
One Cyclotron Rd.
Berkeley, CA 94720
510-486-4325
HMFrei@lbl.gov

Etsuko Fujita
Brookhaven National Laboratory
Chemistry Department
Upton, NY 11973-5000
631-344-4356
fujita@bnl.gov

Participants List – 38th Solar Photochemistry P.I. Meeting

Elena Galoppini
Rutgers University
73 Warren St.
Newark, NJ 07041
973-353-5317
galoppin@rutgers.edu

Theodore Goodson III
University of Michigan at Ann Arbor
930 N. University Ave.
Ann Arbor, MI 48109-1055
734-647-0274
tgoodson@umich.edu

David Grills
Brookhaven National Laboratory
Chemistry Department
Upton, NY 11973-5000
631-344-4332
dcgrills@bnl.gov

Erik Grumstrup
Montana State University
240 Gaines Hall
Bozeman, MT 59717
406-994-2988
erik.grumstrup@montana.edu

Devens Gust
Arizona State University
Dept. Chemistry and Biochemistry
Tempe, AZ 85287
480-965-4547
gust@asu.edu

Thomas Hamann
Michigan State University
578 S. Shaw Ln., RM 411
East Lansing, MI 48824
517-355-9715
hamann@chemistry.msu.edu

Alexander Harris
Brookhaven National Laboratory
Chemistry Department
Upton, NY 11973-5000
631-344-4301
alexh@bnl.gov

Craig Hill
Emory University
1515 Dickey Dr., NE
Atlanta, GA 30322
404-727-6611
chill@emory.edu

Russ Hille
University of California, Riverside
Department of Biochemistry
Riverside, CA 92521
951-827-6354
russ.hille@ucr.edu

Dewey Holten
Washington University
Chemistry Department
St. Louis, MO 63130
314-93 5-6502
holten@wustl.edu

Joseph Hupp
Northwestern University
2145 Sheridan Rd.
Evanston, IL 60208
847-441-0136
j-hupp@northwestern.edu

Justin Johnson
National Renewable Energy Laboratory
15013 Denver West Pkwy.
Golden, CO 80401
303-384-6190
justin.johnson@nrel.gov

David Jonas
University of Colorado
215 UCB
Boulder, CO 80309-0215
303-492-3818
david.jonas@colorado.edu

Prashant Kamat
University of Notre Dame
223 Radiation Laboratory
Notre Dame, IN 46556
574-631-5411
pkamat@nd.edu

Participants List – 38th Solar Photochemistry P.I. Meeting

David Kelley
University of California, Merced
5200 N. Lake Rd.
Merced, CA 95343
209-228-4354
dfkelley@ucmerced.edu

Cheryl Kerfeld
Department of Plant and Microbial Biology
Michigan State University
East Lansing, MI 48824
517-432-4371
ckerfeld@lbl.gov

Christine Kirmaier
Washington University
Dept. of Chemistry, Box 1134
St. Louis, MO 63130
314-725-6157
kirmaier@wustl.edu

Bruce Koel
Princeton University
Dept. Chem. & Biol. Eng.
Princeton, NJ 08544
609-258-4524
bkoel@princeton.edu

Todd Krauss
University of Rochester
120 Trustee Rd.
Rochester, NY 14627-0216
585-275-5093
krauss@chem.rochester.edu

Frederick Lewis
Northwestern University
2145 Sheridan Rd.
Evanston, IL 60208
847-491-3441
fdl@northwestem.edu

Nathan Lewis
California Institute of Technology
1200 E. California Blvd.
Pasadena, CA 91125
626-395-6335
nslewis@caltech.edu

Xiaosong Li
Department of Chemistry
University of Washington
206-696-8118
xiaosongli@gmail.com

Tianquan Lian
Emory University
1515 Dickey Dr. NE
Atlanta, GA 30322
404-727-6649
tlian@emory.edu

Jonathan Lindsey
North Carolina State University
CB8204, 2620 Yarbrough Dr.
Raleigh, NC 27695-8204
919-5 15-6406
jlindsey@ncsu.edu

Elisa Miller Link
National Renewable Energy Laboratory
15013 Denver West Pkwy.
Golden, CO 80401
elisa.miller@nrel.gov

Mark Lonergan
University of Oregon
1253 Department of Chemistry
Eugene, OR 97403
541-346-4748
lonergan@uoregon.edu

Rene Lopez
University of North Carolina
343 Chapman Hall, Physics Dept.
Chapel Hill, NC 27713
919-962-7216
rln@physics.unc.edu

Stephen Maldonado
University of Michigan at Ann Arbor
930 N. University Ave.
Ann Arbor, MI 48109-1055
734-647-4750
smald@umich.edu

Participants List – 38th Solar Photochemistry P.I. Meeting

Thomas Mallouk
Pennsylvania State University
Department of Chemistry
University Park, P A 16801
814-863-9637
tom@chem.psu.edu

Diane Marceau
U.S. Department of Energy
1000 Independence Ave., SW
Washington, DC 20585
301-903-0235
Diane.Marceau@science.doe.gov

Claudio Margulis
University of Iowa
118 TATL
Iowa City, IA 52242
319-335-0615
claudio-margulis@uiowa.edu

James McCusker
Michigan State University
578 South Shaw Ln.
East Lansing, MI 48824-1322
517-355-9715
jkm@chemistry.msu.edu

Gail McLean
U.S. Department of Energy
1000 Independence Ave., SW
Washington, DC 20585
301- 903-7807
Gail.Mclean@science.doe.gov

Gerald Meyer
University of North Carolina
Department of Chemistry
Chapel Hill, NC 27599-3290
919-962- 6320
gjmeyer@email.unc.edu

Thomas Meyer
University of North Carolina
Department of Chemistry
Chapel Hill, NC 27599-3290
919-843-8313
tjmeyer@unc.edu

Josef Michl
University of Colorado
Dept. Chem. and Biochem., 215 UCB
Boulder, CO 80309-0215
303-492-6519
michl@eefus.colorado.edu

Alexander Miller
University of North Carolina
Department of Chemistry
Chapel Hill, NC 27599-3290
919-962-4618
ajmm@email.unc.edu

John Miller
Brookhaven National Laboratory
Chemistry Department
Upton, NY 11973
631-344-4354
jrmiller@bnl.gov

Ana Moore
Arizona State University
Dept. Chemistry and Biochemistry
Tempe, AZ 85287-1604
480-965-2747
amoore@asu.edu

Thomas Moore
Arizona State University
Dept. Chemistry and Biochemistry
Tempe, AZ 85287-1604
480-965-3308
tmoore@asu.edu

Amanda Morris
Virginia Polytechnic Institute
Department of Chemistry
Blacksburg, VA 24061-0212
540-231-5585
ajmorris@vt.edu

James Muckerman
Brookhaven National Laboratory
Chemistry Department
Upton, NY 11973-5000
631-344-4368
muckerma@bnl.gov

Participants List – 38th Solar Photochemistry P.I. Meeting

Karen Mulfort
Argonne National Laboratory
9700 S. Cass Ave.
Argonne, IL 60439
630-252-3545
mulfort@anl.gov

Charles Mullins
University of Texas at Austin
Dept. of Chemical Eng. C0400
Austin, TX 78712
512-471-5817
mullins@che.utexas.edu

Djamaladdin Musaev
Emory University
1515 Dickey Dr.
Atlanta, GA 30322
404-727-2382
dmusaev@emory.edu

Nathan Neale
National Renewable Energy Laboratory
15013 Denver West Pkwy.
Golden, CO 8040 1
303-384-6165
nathan.neale@nrel.gov

Marshall Newton
Brookhaven National Laboratory
Chemistry Department
Upton, NY 11973
631-344-4366
newton@bnl.gov

Daniel Nocera
Harvard University
12 Oxford St.
Cambridge, MA 02138
617-495-8904
dnocera@fas.harvard.edu

Arthur Nozik
University of Colorado
215 UCB
Boulder, CO 80309
303-384-6603
arthur.nozik@colorado.edu

Colin Nuckolls
Department of Chemistry
Columbia University
New York, NY 10027
212-854-6289
cn37@columbia.edu

Frank Osterloh
University of California, Davis
Department of Chemistry
Davis, CA
530-754-6242
fosterloh@ucdavis.edu

Bruce Parkinson
University of Wyoming
1000 E. University Ave.
Laramie, WY 82071
303-766-9891
bparkin1@uwyo.edu

Oleg Poluektov
Argonne National Laboratory
9700 S. Cass Ave.
Argonne, IL 60439
630-252-3546
Oleg@anl.gov

Dmitry Polyansky
Brookhaven National Laboratory
Chemistry Department
Upton, NY 11973-5000
631-344-4315
dmitriyp@bnl.gov

Oleg Prezhdo
University of Southern California
Department of Chemistry
Los Angeles, CA 90089
213-821-3116
prezhdo@usc.edu

Sylwia Ptasinska
University of Notre Dame
223 Radiation Laboratory
Notre Dame, IN 46556
574-631-1846
sptasins@nd.edu

Participants List – 38th Solar Photochemistry P.I. Meeting

Yulia Pushkar
Purdue University
525 Northwestern Ave.
West Lafayette, IN 97407
765-496-3279
ypushkar@purdue.edu

Garry Rumbles
National Renewable Energy Laboratory
15013 Denver West Pkwy.
Golden, CO 80401
303-384-6502
garry.rumbles@nrel.gov

Richard Schaller
Argonne National Laboratory
9700 S. Cass Ave.
Argonne, IL 60439
630-252- 1423
schaller@anl. gov

Bernhard Schlegel
Wayne State University
Department of Chemistry
Detroit, MI 48202
313-577-2562
hbs@chem.wayne.edu

Charles Schmuttenmaer
Yale University
225 Prospect St.
New Haven, CT 06520-8107
203-432-5049
charles.schmuttenmaer@yale.edu

Gregory Scholes
Princeton University
Department of Chemistry
Princeton, NJ 08544
6092580729
gscholes@princeton.edu

Richard Schrock
Massachusetts Institute of Technology
Department of Chemistry
Cambridge, MA
617-253-1596
rrs@mit.edu

Ian Sharp
Lawrence Berkeley Laboratory
One Cyclotron Rd.
Berkeley, CA 94720
510-495-8715
idsharp@lbl.gov

Mark Spitler
U.S. Department of Energy
1000 Independence Ave., SW
Washington, DC 20585
301-903-4568
mark.spitler@science.doe.gov

Michael Therien
Duke University
124 Science Dr. 5330 FFSC
Durham, NC 27708-0346
919-660-1670
michael.therien@duke.edu

Randolph Thummel
University of Houston
Chemistry Department
Houston, TX 77204-5003
713-743-2734
thummel@uh.edu

David Tiede
Argonne National Laboratory
9700 S. Cass Ave.
Argonne, IL 60439
630-252-3539
tiede@anl. gov

William Tumas
National Renewable Energy Laboratory
15013 Denver West Pkwy.
Golden, CO 80401
303-384-7955
bill.tumas@nrel.gov

John Turner
National Renewable Energy Laboratory
15013 Denver West Pkwy.
Golden, CO 80401-3393
303-275-4270
John.Turner@nrel.gov

Claudia Turro
Ohio State University
100 W. 18th Ave.
Columbus, OH 43210
614-292-6708
turro@chemistry.ohio-state.edu

Jao van de Lagemaat
National Renewable Energy Laboratory
15013 Denver West Pkwy.
Golden, CO 80401
303-384-6143
jao.vandelagemaat@nrel.gov

Claudio Verani
Wayne State University
5101 Cass Ave.
Detroit, MI 48202
311-577-1076
cnverani@chem.wayne.edu

Michael Wasielewski
Northwestern University
2145 Sheridan Rd.
Evanston, IL 60208
847-467-1423
m-wasielewski@northwestem.edu

James Wishart
Brookhaven National Laboratory
Chemistry Department
Upton, NY 11973-5000
631-344-4327
wishart@bnl.gov

Xiaoyang Zhu
Department of Chemistry
Columbia University
New York, NY 10027
212-851-7768
xyzhu@columbia.edu

P.I. Author Index

Author Index

Asbury, J. 26
Bard, A. 5
Bartynski, R. 36
Batista, V. 31, 120
Beard, M. 14, 19, 156, 162
Blackburn, J. 39, 51, 155
Blank, D. 115
Bocarsly, A. 116
Bocian, D. 117
Boettcher, S. 23
Bren, K. 95
Brudvig, G. 31, 120, 156
Castellano, F. 81, 118
Chen, L. 48, 75, 81
Choi, K.S. 11
Concepcion, J. 59, 69
Coppens, P. 119
Crabtree, R. 31, 120, 156
Dempsey, J. 121, 139
Dunbar, K. 161
Durrant, J. 1
Eisenberg, R. 95
Endicott, J. 163
Fleming, G. 122
Frei, H. 124
Fujita, E. 59, 125
Galoppini, E. 36, 126
Goodson, T. 169
Grills, D. 39, 59, 127
Grumstrup, E. 128
Gust, D. 105, 109, 155
Hamann, T. 129
Hill, C. 98
Hille, R. 57
Holten, D. 117
Hupp, J. 130
Johnson, J. 51, 89
Jonas, D. 131
Kamat, P. 132
Kelley, D. 133
Kirmaier, C. 117
Kerfeld, C. 45
Koel, B. 134
Krauss, T. 95, 135
Lewis, F. 136
Lewis, N. 167
Lian, T. 98, 137
Lindsey, J. 117
Lonergan, M. 138
Lopez, R. 139
Maldonado, S. 140
Mallouk, T. 109
Margulis, C. 141
Maroncelli, M. 141
McCusker, J. 142
Meyer, G. 143
Meyer, T. 144
Michl, J. 145
Miller, J. 39
Miller, A. 146
Moore, A. 105, 109
Moore, T. 105, 109
Muckerman, J. 59, 125, 148
Mulfort, K. 48, 75, 81, 153
Mullins, C. 5
Musaev, J. 98
Neale, N. 14, 19, 123,170
Newton, M. 39, 149
Nocera, D. 150
Nozik, A. 151
Nuckolls, C. 166
Osterloh, F. 102
Parkinson, B. 152
Poluektov, O. 48, 75, 153
Polyansky, D. 59
Prezhdo, O. 84
Ptasinska, S. 154
Pushkar, Y. 72
Rumbles, G. 39, 51, 89, 155
Schaller, R. 81
Schlegel, B. 163
Schmuttenmaer, C. 31, 109, 120, 156
Scholes, G. 157
Sharp, I. 158
Therien, M. 160
Thummel, R. 63
Tiede, D. 48, 75, 87, 153
Turner, J. 14, 19
Turro, C. 161
Van de Lagemaat, J. 19, 162
Verani, C. 163
Wasielewski, M. 164

Author Index

Wishart, J. 165
Zhu, X. 166